

PERFORMANCE OF DRILLED SHAFT FOUNDATIONS SUPPORTING COASTAL
MAST ARM TRAFFIC SIGNAL AND HIGHWAY SIGN STRUCTURES

by

Carlos M. Rodriguez

A thesis submitted to the faculty of
The University of North Carolina at Charlotte
in partial fulfillment of the requirements
for the degree of Master of Science in
Civil Engineering

Charlotte

2019

Approved by:

Dr. Miguel A. Pando

Dr. Rajaram Janardhanam

Dr. Matthew J. Whelan

© 2019
Carlos M. Rodriguez
ALL RIGHTS RESERVED

ABSTRACT

CARLOS MAURICIO RODRIGUEZ GUEVARA. Performance of drilled shaft foundations supporting coastal mast arm traffic signal and highway sign structures.
(Under the direction of Dr. MIGUEL A. PANDO)

Mast arm traffic signals and cantilever highway signs have an inverted L-shaped structure and this geometry results in high loading demand to their support foundations when subjected to high wind loading. This MS thesis is motivated by an NCDOT research need statement related to design and construction challenges inherent in inverted L-shaped traffic signal structures located in coastal environments. For these coastal structures wind loading demand can be very high associated to design wind speeds in the order of 209 KMH (130 MPH) or higher. These high design wind speeds result in high loading demand to the foundation system particularly for traffic signal structures with long mast arms lengths (e.g., lengths of 25 m or greater), and the high surface areas exposed to wind in highway signal structures with areas of 20 m² or greater. Exacerbating the design challenge, these coastal projects often involve a small right-of-way resulting in a small footprint for the foundation system and often involve sites with poor geotechnical conditions such a loose sand deposits with a high-water table.

The first part of this thesis includes a state of practice (SOP) and literature review study performed as part of the NCDOT project. The SOP component of the study involved a survey questionnaire with follow-up phone interviews to 12 coastal U.S departments of transportation to document the foundation systems commonly used for supporting coastal mast arm traffic signal structures, as well as typical dimensions, and design procedures. The SOP also involved review and comparison of current design procedures used by the

participating DOTs. The SOP study found that the most commonly used foundation system to support these structures are single drilled shafts with diameter typically ranging from 0.6 to 1.5 m (2 and 5 ft). Additional to the SOP study the NCDOT project involved a literature review related to foundation systems under high loading demand of inverted L-shaped structures that involve a complex load combination that includes lateral loading, lateral bending moment, and torsion. The literature review identified a few studies that investigated the effect of combined lateral loading and torsion. For example, Hu (2003) and Thiyyakkandi (2016) reported significant capacity reduction in the lateral resistance of single drilled shafts when subjected to coupled torsion loading. This topic warrants additional research. This SOP study shows that coastal DOTs have a challenging task to design safe and cost-effective foundations systems for coastal mast arm traffic signals due to the loading demand associated to the high winds and long mast arm lengths, and the poor geotechnical conditions often encountered in coastal environments. The selection of the commonly used drilled shaft option often results in large diameters (up to 1.5 m) and long embedment depth (up to 11 m).

The second part of this MSCE thesis reports on three failure case studies of inverted L-shaped highway sign structures in Puerto Rico affected by the 2017 Hurricane Maria. For each case history the details of the cantilever signal structures are provided and the geotechnical conditions as well as the failure mechanism is described. All three cantilevered highway signal structures rotated significantly about their zenith as result of high wind pressures applied to the structure. The load capacity of the drilled shafts for each case history are predicted using different design methodologies reported in the SOP study. The analyses performed for the three failure case histories revealed that the ultimate load

method based on Broms (1964 a and b) predicts lateral loading short-pile type for all 3 cases. This suggests this method is conservative as only one of the three case histories showed some lateral rotation and the main failure mode was torsional rotation. The Broms method, as originally published (Broms 1964), is considered conservative also due to the neglect of lateral resistance of the upper 1.5 diameters of the drilled shaft for clayey foundation soils. The use of p-y models to analyze the lateral load and bending moment loading condition was found to be more realistic as it did not predict failure under this type of loading which is consistent with the field observations for these three foundation failure case histories. The torsion capacity predictions, using different methods, were all lower than the estimated torsion loading demand experienced by the different drilled shafts, thus predicting correctly the observed main mode of failure for these three foundation failure case histories.

ACKNOWLEDGMENTS

This MS thesis includes the practice and literature review report study supported by the North Carolina Department of Transportation (NCDOT) under Project No. 2018. The author would like to acknowledge the funding received in the form of a research assistantship from this research project. The author would also like to thank financial support received from the graduated School of UNC Charlotte in the form of a GASP tuition and health insurance awards during the initial two years of this project when the scope of the project was at the doctoral level.

The author would also like to thank the guidance and support of Dr. Miguel Pando as my thesis advisor and the principal investigator of the NCDOT project that was the basis of the state or practice study presented in this thesis. The support and feedback received from committee members Dr. Matthew Whelan and Dr. J are also greatly appreciated.

Finally, but not least, I would like to express my greatest gratitude and love to my family and my wife for their constant support during my time as a graduate student at UNC Charlotte.

TABLE OF CONTENTS

LIST OF TABLES	xiii
LIST OF FIGURES	xv
LIST OF SYMBOLS AND ABBREVIATIONS	xxii
CHAPTER 1: INTRODUCTION	1
1.1. Background and motivation.....	1
1.2. Objectives	2
1.3. Thesis organization	3
CHAPTER 2: BACKGROUND AND DEFINITIONS	6
2.1. Introduction.....	6
2.2. Typical structures to support traffic signals and highway signs	6
2.2.1. Mast arms traffic signals (MATS) structures.....	9
2.2.2. Cantilever sign (CS) structures	10
2.3. Loading demand for inverted L-Shaped structures.....	12
2.3.1. Gravitational load.....	12
2.3.2. Wind loading.....	13
2.3.3. Wind loading demand on inverted L-Shape structure	16
2.4. Typical foundation systems	19
2.5. Summary	23

CHAPTER 3: STATE OF PRACTICE STUDY ON FOUNDATIONS FOR COASTAL TRAFFIC SIGNAL MAST ARM STRUCTURES.....	24
3.1. Introduction.....	24
3.2. Methodology of the SOP study.....	25
3.3. Summary of Results of SOP study	26
3.3.1. Dimensions of mast arms structures	26
3.3.2. Design wind speed values used for design	27
3.3.3. Foundation types used for coastal traffic signal structures	30
3.3.4. Drilled shafts.....	32
3.3.4.1. Range of dimensions reported by SOP participants	32
3.3.4.2. Design procedures used by SOP participants	34
3.4. Summary	35
CHAPTER 4: LITERATURE REVIEW	36
4.1. Introduction.....	36
4.2. Overview of recent research on drilled shafts under combined loading	36
4.3. Centrifuge testing at UF by Hu et al. (2006)	38
4.4. Study by Qiang et al. (2017) involving torsion loading.....	40
4.5. Study by Qiang et al. (2017) involving combined loading	46
4.6. Method by Duncan et al. (1995) for lateral and torsion loading.....	47
4.7. Alternative Foundation Systems	49

4.8.	Summary	51
CHAPTER 5: HURRICANE MARIA ACROSS PUERTO RICO		53
5.1.	Introduction.....	53
5.2.	Natural Storm Maria 2017	53
5.3.	Hurricane Maria event in Puerto Rico	55
5.4.	Summary	57
CHAPTER 6: FAILURE CASE HISTORIES HIGHWAY SIGN STRUCTURES IN PUERTO RICO DURING THE 2017 HURRICANE MARIA		58
6.1.	Introduction.....	58
6.2.	Select highways and traffic signal failures	58
6.2.1.	Failure at Site-1	59
6.2.1.1.	Description of the failure at Site-1	59
6.2.1.2.	Geotechnical properties of the soil at Site-1	62
6.2.1.3.	Characteristics of the drilled shaft foundation at Site-1.....	64
6.2.1.4.	Soil-structure interaction after Hurricane Maria at Site-1	67
6.2.1.5.	Summary of findings at Site-1	68
6.2.2.	Failure at Site-2.....	69
6.2.2.1.	Description of the failure at Site-2.....	69
6.2.2.2.	Geotechnical properties of the soil at Site-2.....	71
6.2.2.3.	Characteristics of the drilled shaft foundation at Site-2.....	73
6.2.2.4.	Soil-structure interaction after Hurricane Maria at Site-2	75

6.2.2.5.	Summary of findings at Site-2	77
6.2.3.	Failure at Site-3	77
6.2.3.1.	Description of the failure at Site-3	77
6.2.3.2.	Geotechnical properties of the soil at Site-3	80
6.2.3.3.	Characteristics of the drilled shaft foundation at Site-3	83
6.2.3.4.	Soil-structure interaction after Hurricane Maria at Site-3	83
6.2.3.5.	Summary of findings at Site-3	84
6.3.	Summary	85
CHAPTER 7: ANALYSIS		86
7.1.	Introduction	86
7.2.	Methodology	86
7.3.	Analysis of failure sites	87
7.3.1.	Failure study of Site-1	88
7.3.1.1.	Predicted lateral loads	89
7.3.1.2.	Predicted torsional moments	93
7.3.1.3.	Summary of results	94
7.3.1.4.	Discussion of results	94
7.3.2.	Failure study of Site-2	96
7.3.2.1.	Predicted lateral loads	96
7.3.2.2.	Predicted torsional moments	100
7.3.2.3.	Summary of results	101
7.3.2.4.	Discussion of results	101

7.3.3. Failure study of Site-3.....	103
7.3.3.1. Predicted embedment depth due to lateral loads.....	103
7.3.3.2. Predicted embedment depth due to torsional loads.....	105
7.3.3.3. Predicted embedment depth due to combined loading	105
7.3.3.4. Summary of predicted embedment depth	106
7.3.3.5. Discussion of results	107
7.4. Summary	107
CHAPTER 8: CONCLUSIONS	108
8.1. State of practice.....	108
8.2. Literature review	108
8.3. Case studies.....	109
REFERENCES	113
APPENDIX A: GEOTECHNICAL INFORMATION FOUND IN SITES 1, 2 AND 3	119
APPENDIX B: LOADING DEMAND OF CS-1, CS-2, AND CS-3 STRUCTURES ..	126
APPENDIX C: DESCRIPTION OF METHODS FOR PREDICT LATERAL, TORSIONAL AND COUPLED RESISTANCES	132
APPENDIX D: WEBSITES USED TO COMPILE DESIGN AND CONSTRUCTION INFORMATION.....	139
APPENDIX E: SUMMARYTABLES WITH SUMMARY OF SURVEY QUESTIONNAIRE AND FOLLOW-UP CONFERENCE	142
APPENDIX F: SUMMARY OF STANDARD DESIGNS	154

APPENDIX G: COPY OF SURVEY QUESTIONNAIRES RESPONSES FROM	
COASTAL DOTS.....	171
APPENDIX H: RESULTS OF PILE INTEGRITY TESTS.....	194

LIST OF TABLES

TABLE 3-1: Standards used for selection of design wind speeds for mast arm traffic signal structures	28
TABLE 3-2: Standards used for selection of design wind speeds for mast arm traffic signal structures	29
TABLE 3-3: Typical foundation system used by the SOP participants	30
TABLE 3-4: Summary of design procedures for drilled shaft foundations.....	34
TABLE 4-1: Summary of test conditions (Hu et al. 2006).....	38
TABLE 4-2: Summary of test conditions (Qiang et al. 2017 & Poulos 1975).....	41
TABLE 4-3: β skin friction static method for drilled shafts based in SPT	45
TABLE 4-4: Summary of Model Test Information (Duncan et al. 1995).	47
TABLE 6-1: Information of the select geotechnical failure sites	59
TABLE 6-2: Summary of Index test results at Site-1	62
TABLE 6-3: Summary of undrained shear strength results at Site-1	63
TABLE 6-4: Parameters used in lateral and torsional analysis at Site-1	64
TABLE 6-5: Summary of Index test results at Site-2.....	72
TABLE 6-6: Summary of comparison between geotechnical parameters in Sites-1 & 2	72
TABLE 6-7: Geotechnical parameters used in lateral and torsional analysis at Site-2	73
TABLE 6-8: Soil classification summary.....	81

TABLE 6-9: Summary of undrained shear strength results.....	81
TABLE 6-10: Summary of undrained shear strength results at Site-3	82
TABLE 6-11: Summary of geotechnical correlations at Site-3.....	82
TABLE 7-1: Summary of analytical methods for cohesive soils considered.....	87
TABLE 7-2: Summary of analytical methods for cohesionless soils considered.....	87
TABLE 7-3: Resultant moments, bending moment and shear	88
TABLE 7-4: Required S_u and FS computed following (Broms, 1964a) assumptions.....	90
TABLE 7-5: Summary of loads and moments predicted using p-y curves	92
TABLE 7-6: Summary of predicted torsional moments results	93
TABLE 7-7: Summary of FS computed for different prediction failures	94
TABLE 7-8: Resultant moments, bending moment and shear	96
TABLE 7-9: Required S_u and FS computed following (Broms, 1964a) assumptions.....	97
TABLE 7-10: Summary of loads and moments predicted using p-y curves	99
TABLE 7-11: Summary of predicted torsional moments results	100
TABLE 7-12: Summary of FS computed for different prediction failures	101
TABLE 7-13: Resultant moments, bending moment and shear	103
TABLE 8-1: Rotation and tilts measurements after Hurricane Maria.....	110

LIST OF FIGURES

FIGURE 2-1: Typical traffic signal structures.....	7
FIGURE 2-2: Typical highway traffic structures.	8
FIGURE 2-3: Photos of typical MATS structures	9
FIGURE 2-4: Schematic of a typical MATS structure	10
FIGURE 2-5: Photos of CS structures.....	11
FIGURE 2-6: Schematic of a typical CS structure	11
FIGURE 2-7: Schematic showing gravitational loads on an L-shaped structure	12
FIGURE 2-8: Wind speed and direction of the Hurricane Irma.....	14
FIGURE 2-9: Wind pressure graphical representation	16
FIGURE 2-10: Resultant lateral forces associated with wind about the x-axis.....	16
FIGURE 2-11: Graphical representation of the wind resultant force shear acting on the top of the foundation system.....	17
FIGURE 2-12: Graphical representation of combined bending moment	18
FIGURE 2-13: Resultant lateral forces associated with wind about y-axis.....	19
FIGURE 2-14: Graphical representation of the resultant torsional moment	19
FIGURE 2-15: Typical sections of drilled shafts foundation	20
FIGURE 2-16: Typical section of a spread footing foundation.....	21
FIGURE 2-17: Typical grade beam.....	21

FIGURE 2-18: Typical micro piles with pile cap	22
FIGURE 2-19: Typical drilled shaft with wing walls.....	22
FIGURE 3-1: Map showing participants of SOP study.....	25
FIGURE 3-2: Range of mast arm lengths reported by SOP participants.	27
FIGURE 3-3: Isotach wind speed map for continental USA by ASCE (2009).....	28
FIGURE 3-4: Summary map of maximum coastal wind speeds.	29
FIGURE 3-5: Examples design drawings for drilled shafts with wingwalls.....	31
FIGURE 3-6: Example of group of micropiles and cap.	32
FIGURE 3-7: Range of dimensions of drilled shafts reported by SOP participants.	33
FIGURE 4-1: Summary of recent research on drilled shaft foundations subjected to lateral and torsional loading.....	37
FIGURE 4-2: Photos of the centrifuge model testing (Hu et al., 2006).	38
FIGURE 4-3: Experimental versus predicted lateral failure loads from Hu et al. (2006).	39
FIGURE 4-4: Combined lateral and torsion loading centrifuge study by (Hu 2006).....	40
FIGURE 4-5: Subsurface profile at test and field test photo (Qiang et al. 2017).....	41
FIGURE 4-6: Experimental versus predicted torsion failure loads in clays.....	42
FIGURE 4-7: Subsurface profile at test and test details (Qiang et al. 2017).....	42
FIGURE 4-8: Experimental versus predicted torsion failure loads in sands.	43
FIGURE 4-9: β method predictions vs field test (McVay et al. 2014).....	44
FIGURE 4-10: Skin friction factors as a function of depth for fictitious sand site.	46

FIGURE 4-11: Subsurface profile at test and test details (Qiang et al. 2017 & Thiyyakkandi et al. 1975)	46
FIGURE 4-12: Lateral and torsion coupled loading.....	47
FIGURE 4-13: Schematic foundation under torsion loading (Duncan et al. 1995).....	48
FIGURE 4-14: Results of models shafts.....	49
FIGURE 4-15: Photos of grouted precast pile reported by Herrera et al. (2017).	50
FIGURE 4-16: Photo of SPINFIN finned pipe pile.....	51
FIGURE 5-1: Hurricane Maria meteorological recap.	54
FIGURE 5-2: Variation of wind speed and pressure during hurricane Maria.....	54
FIGURE 5-3: Track of hurricane Maria in Puerto Rico.	55
FIGURE 5-4: Thermal satellite image of Hurricane Maria after landfall in PR	56
FIGURE 5-5: Maximum wind gust in MPH during Hurricane Maria.....	56
FIGURE 6-1: Locations of select failures	58
FIGURE 6-2: Location of the geotechnical failure at Site-1	59
FIGURE 6-3: Front and back photos of CS structure at Site-1 before Hurricane Maria..	60
FIGURE 6-4: Photos of CS structure rotated after hurricane Maria at Site-1	60
FIGURE 6-5: Photo of the initial CS structure position and graphical representation of the CS structure rotated at Site-1. (Adapted from Google earth)	61
FIGURE 6-6: Graphical representation of the failure top view at Site-1	61
FIGURE 6-7: Generalized soil profile at Site-1	63

FIGURE 6-8: Ultrasonic pulse velocity test at Site-1	64
FIGURE 6-9: Ultrasonic pulse velocity results at Site-1	65
FIGURE 6-10: Drilled shaft location of the PIT test	65
FIGURE 6-11 PIT test configurations	66
FIGURE 6-12 PIT results at Site-1	66
FIGURE 6-13: Characteristics and dimension of foundation system (DS) at Site-1	67
FIGURE 6-14: Schematic of the gap between soil and DS at Site-1	68
FIGURE 6-15: Summary of geotechnical and structural information at Site-1	68
FIGURE 6-16: Location of the geotechnical failure at Site-2	69
FIGURE 6-17: Front and back photos of CS structure at Site-2 before Hurricane Maria.	69
FIGURE 6-18: Photos of CS structure at Site-2 after Hurricane Maria	70
FIGURE 6-19: Photo of the initial CS structure position and graphical representation of rotate CS structure at Site-2.	71
FIGURE 6-20: Graphical representation of the failure top view at Site-2	71
FIGURE 6-21: Generalized soil profile at Site-2	73
FIGURE 6-22: Ultrasonic pulse velocity results at Site-1	74
FIGURE 6-23: Ultrasonic pulse velocity results at Site-1	74
FIGURE 6-24: Characteristics and dimension of foundation system (DS) at Site-2	75
FIGURE 6-25: Photos of the gap between soil and DS at Site-2	76
FIGURE 6-26: Schematic of the gap top view between soil and DS at Site-2	76

FIGURE 6-27: Summary of geotechnical and structural information at Site-2	77
FIGURE 6-28: Location of the geotechnical failure at Site 3	78
FIGURE 6-29: Front and back photos of CS structure at Site-3 before Hurricane.	78
FIGURE 6-30: Photos of CS structure at Site-3	79
FIGURE 6-31: Photo of the initial CS structure position and graphical representation of rotate CS structure Site-3.	80
FIGURE 6-32: Graphical representation of failure top view at Site-3	80
FIGURE 6-33: Generalized soil profile at Site-3	82
FIGURE 6-34: Characteristics and dimension of foundation system (DS) at Site-3	83
FIGURE 6-35: Photos of the gap between soil and DS at Site-3	84
FIGURE 6-36: Schematic of the gap top view between soil and DS at Site-3.....	84
FIGURE 6-37: Summary of geotechnical and structural information at Site-3	85
FIGURE 7-1: Schematic loading demand of an inverted L-shape CS structure	88
FIGURE 7-2: Predicted undrained shear strength and factor of safety using (Broms, 1964a)	90
FIGURE 7-3: Predicted deflection of a drilled shaft with length of 2.44 m and diameter of 0.91 m using Reese and Welch's (1975) model	91
FIGURE 7-4: Predicted deflection of a drilled shaft with length of 2.44 m and diameter of 0.91 m using API model	92
FIGURE 7-5: Relationship between the embedment depth and factor of safety	94

FIGURE 7-6: Schematic of the comparison of minimum embedment depths required to carry lateral and torsional load demand	95
FIGURE 7-7: Lateral and torsional loadings in a CS with ratio pole height to arm length of 0.64	96
FIGURE 7-8: Predicted undrained shear strength and factor of safety using (Broms, 1964a)	97
FIGURE 7-9: Predicted deflection of a drilled shaft with length of 1.8 m and diameter of 0.91 m using Reese and Welch's (1975) model	98
FIGURE 7-10: Predicted deflection of a drilled shaft with length of 1.8 m and diameter of 0.91 m using API model	99
FIGURE 7-11: Relationship between the embedment depth and factor of safety.....	101
FIGURE 7-12: FS comparison between shaft resistance in SITE-1 and SITE-2	102
FIGURE 7-13: Computed factors of safety using predicted results	102
FIGURE 7-14: Required embedment depth as a function of bending moment according to (Broms, 1964)	104
FIGURE 7-15: Required embedment depth as a function of lateral loading and bending moment according to (API)	104
FIGURE 7-16: Required embedment depth as a function of lateral loading and bending moment according to (Sand O'Neill, 1984).....	105
FIGURE 7-17: Required embedment depth as a function of torsion moment	105
FIGURE 7-18: Required embedment depth as a function of coupled loading demand .	106

FIGURE 7-19: Required embedment depth for lateral, torsional and coupled analysis	106
FIGURE 8-1: Comparison between lateral and torsional loading demand on inverted L- Shape structures varying L/r	111
FIGURE 8-2: Schematic of the failures rotation direction	112

LIST OF SYMBOLS AND ABBREVIATIONS

A_s	Area of the highway sing
AASHTO	American Association of State Highway and Transportation Officials
AASHTO-LTS	Standard Specifications for Structural Supports for Highway Signs, Luminaires, and Traffic Signals
ALDOT	Alabama Department of Transportation
ASCE	American Society of Civil Engineers
ASD	Allowable Strength Design
c'	Effective cohesion
C_d	Drag coefficient
CS	Cantilever signal
D	Diameter
DS	Drilled Shaft
FDOT	Florida Department of Transportation
f_s	Unit side friction
ft	Feet
G	Gust effect factor
GDOT	Georgia Department of Transportation
I_r	Wind importance factor
KPH	Kilometer per hour
K_d	Directionality factor

K_z	Height and exposure factor
L	Embedment depth of drilled shaft
L_a	Mast arm length
LaDOT	Louisiana Department of Transportation
LRFD	Load & Resistance Factor Design
M	Moment
M_T	Bending moment
MassDOT	Massachusetts Department of Transportation
MATS	Mast arm traffic signal
MDOT	Mississippi Department of Transportation
m	meter
MPH	Miles per hour
MRI	Mean Recurrence Interval
M_g	Gravitational moment
M_w	Moment due to wind
N_{60}	SPT blow counts corrected for a hammer energy efficiency of 60%
NCDOT	North Carolina Department of Transportation
ODOT	Oregon Department of Transportation
P_{wz}	Wind pressure
P_{wi}	Shear force due to wind
PIT	Pile integrity test
PR	Puerto Rico
Q_s	Drilled shaft axial capacity associated to side resistance

Q_t	Drilled shaft axial capacity associated to Tip tip resistance
Q_u	Ultimate axial capacity of drilled shafts (Bored Pile)
SOP	State of practice
SCDOT	South Carolina Department of Transportation
SPT	Standard Penetration Test
T	Torsion
TCP	Texas Cone Penetrometer
TxDOT	Texas Department of Transportation
V	Wind speed
VDOT	Virginia Department of Transportation
W_{pile}	Pile weight
W_p	Wind pressure
W_g	Gravitational load
WSDOT	Washington Department of Transportation
α	Torsion side friction coefficient resistance factor
β	Torsion side friction coefficient resistance factor
ϕ'	Effective friction angle
γ	Total unit weight
γ'	Effective unit weight
γ_{sat}	Saturated unit weight
γ_w	Water uUnit weight of water
ω_{FDOT}	FDOT torsional side friction coefficient

CHAPTER 1: INTRODUCTION

1.1. Background and motivation

This MS thesis investigates the performance of drilled shaft foundations supporting coastal mast arm traffic signs and cantilevered highway signs. These two structures have an inverted L-shape geometry that basically consists of a horizontal arm attached to a vertical pole, that in turn is supported by a foundation system that often consists of a single drilled shaft but other foundation types are also used. The loading demand considered for design includes gravity and wind loading. For these loading types an inverted L-shaped structure will transmit to the top of foundation system a vertical load (V_L), a shear force (P_W), a lateral bending moment (M_T), and a torsional moment (T_W). These four resultants constitute a complex loading demand that for some U.S. coastal environments can be very demanding if the structure is exposed to very high wind speeds. The loading demand on the supporting foundation increases with increasing mast arm length (or cantilever arm for highway cantilevered signs). The focus of this MS thesis is on the performance of drilled shafts of coastal inverted L-shaped structures under this complex loading demand.

This MS thesis also documented the state of practice of coastal U.S departments of transportation regarding the different foundation systems used to support these inverted-L shaped structures. typically. As described in the state of practice (SOP) chapter, other foundation systems considered for the support of these types of structures including: a group of two drilled shafts with a connecting cap, a shallow spread footings (if loading is not too high and geotechnical conditions are favorable), groups of micropiles with a connecting cap, and single drilled shafts with wing walls to primarily increase the foundation system torsion resistance.

The motivation of this study is related to the design and construction challenges inherent to inverted L-shaped structures located in coastal environments. Particularly the focus was for cases where these structures are exposed to very high wind loading demand such as locations where design wind speeds are 130 MPH or higher and have considerable mast arm lengths (e.g., $L_a > 70$ ft). Or for the case of cantilevered highway signs high loading demand is associated to large exposed area of the highway sign (e.g., $A_s > 20$ m²). It should be noted, that the complexity of the foundation system design challenge is further exacerbated due to a small footprint availability for the foundation system (associated to limited right-of-way) and poor geotechnical conditions, such a loose sand deposits with a high-water table, that are often present at coastal sites.

Economically and constructively, the inverted L-shaped structures have resulted great solution in order to support highway signs and traffic signals. Therefore, in recent years the North Carolina Department of Transportation NCDOT have shown interest in studying with more detail financial and technical implications of foundations for this type of structures. This thesis will conduct a comprehensive review of the national state of practice of foundation systems being considered for traffic and sign structures that are subject to high and complex loading demand coupled with poor foundation soil conditions. The analysis of three cantilever signal structure failures due to the complex loading demand mentioned also will be include in this thesis.

1.2. Objectives

The main objectives of this thesis are:

- Detailed literature review and detailed survey of the state of current practice followed by other U.S. DOTs facing similar challenges e.g., high loading demand and poor foundation conditions.
- Detailed geotechnical analysis of the drilled shaft foundation system failure due to complex loading demand used to support cantilever signal structures located in Puerto Rico in Hurricane Maria.

1.3. Thesis organization

The first part of this thesis presents a summary of the state of practice (SOP) study performed as part of a recent NCDOT funded project that reviewed foundation systems used to support mast arm traffic signals in coastal environments. The state of practice study also summarizes design procedure commonly used by coastal USDOTs. It will be shown that most coastal DOTs use a decoupled approach for the design of drilled shafts supporting mast arm traffic signal structures. In other words, the torsional loading demand is considered separately from lateral load and bending. Although this is a commonly used design approach, recent studies supported by the Florida Department of Transportation (e.g., Hu et al. 2006; Thuyyakkandi, et al. 2016) show that there is significant reduction of the lateral resistance of the drilled shaft foundation when subjected to combined lateral and torsional loading.

The SOP study include a survey questionnaire and detailed follow-up phone interviews to 12 coastal U.S Departments of Transportation. The main objective of the survey was to find out their construction and design practice related to foundation systems used to support traffic signal mast arm structures in coastal environments where they are often exposed to high wind loads and poor geotechnical conditions. The SOP summarizes

information such as type of foundations used, design methodologies and procedures, design wind loading, and scope of geotechnical investigation typically used for these structures in coastal environments. The survey found that the most common foundation system used is a conventional drilled shaft without wing walls. Wingwalls in drilled shafts were only found to be used by NCDOT, VDOT, and ALDOT, however, VDOT and ALDOT reported that the trend is not to use wing walls due to construction with installation difficulties. The study also found that FDOT has similar wind loading demand and mast arm dimensions used by NCDOT. This agency is using conventional drilled shafts without wing walls with a similar range of diameters as NCDOT.

The second part of this Master thesis presents failure case histories of several coastal highway cantilevered structures that occurred during the 2017 Hurricane Maria that devastated a large extent of the island of Puerto Rico. The failure case histories were identified during an NSF funded GEER reconnaissance mission by Silva-Tulla et al. (2018). The thesis will provide details of the failure of three drilled shaft supported inverted L-shape cantilever highway sign structures that failed by torsional rotation with some lateral tilt. The information obtained for these three structures also includes field testing performed based on two trips to the island in February 2018 and June 2019. During these two field visits to Puerto Rico, the failure mechanism and characteristics were documented for the three structures. Additionally, field work entailed assessment of the geometry of structure and foundation, collection of additional geotechnical information through sampling, dynamic cone testing, and field vane testing. The drilled shaft foundations were tested using the pile integrity testing (PIT) and complemented with ultrasound testing of the exposed concrete of the foundation drilled shafts.

In addition to documenting the failure of the three case histories, this thesis presents analyses of the foundation of the three sites to assess whether the observed failure can be adequately predicted using the conventional design approaches reported by USDOT participants in the SOP. For example, many USDOTs reported using the ultimate load procedure proposed by Broms (1964) for the design of the drilled shaft against laterally loads. The application of Broms method to the three failure case histories in PR predicts failure of all three structures under the high lateral loading demand associated with the wind speeds generated by Hurricane Maria. However, the field observations indicate that the main failure mechanism was rotation associated with the high torsional loading. The application of a decoupled approach also predicts failure of the drilled shaft foundations due to torsional loading. The study of these three failure case histories confirms the complexity of the soil-structure interaction under this loading demand and highlights the need to continue to investigate this problem. The SOP study highlighted the challenges that coastal USDOTs have when dealing with these structures where often budget and personnel limitations influence the level of risk that is accepted for the potential failure of the foundation of some of these structures.

CHAPTER 2: BACKGROUND AND DEFINITIONS

2.1. Introduction

This chapter presents background in foundation engineering and definitions that are related to this research project. Specifically, the followings main topics are covered:

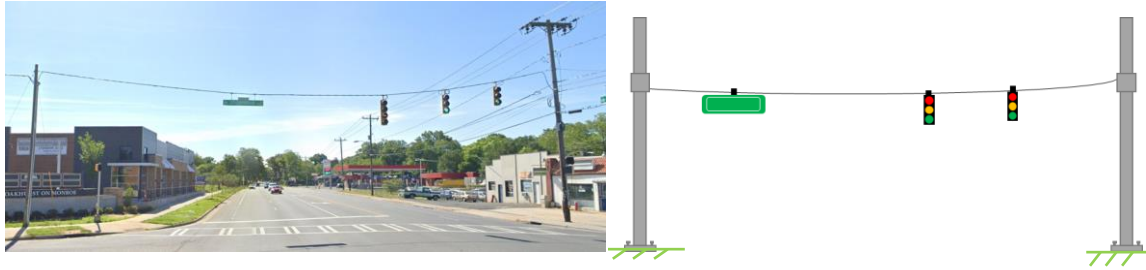
- typical structures used to support traffic signals and highway signs,
- wind loading generalities including computation,
- loading demand of selected structures (mast arms traffic signals and cantilever sign structures).

The reader familiar with this information may opt to skip this chapter.

2.2. Typical structures to support traffic signals and highway signs

This research project involved investigation of the foundation systems that support inverted L-shaped structures commonly used to support traffic signals and highway signs. The focus is on inverted L-shaped structures located in coastal environments where typically there is a higher exposure due to high wind speeds and often less competent geotechnical conditions associated with coastal soils and hurricane conditions.

Traffic signal structures are assemblies used for supporting traffic signals, as shown in Figure 2-1. This figure shows photographs of traffic signal structures located in a Charlotte intersection and maintained by NCDOT. (Figure 2-1a) shows a strain pole system where the traffic signals are attached to cables. (Figure 2-1b) shows a traffic signal mast arm that is composed of a horizontal arm attached to a vertical pole. This mast arm traffic signal (MATS) structure has an inverted L-shaped configuration and is that is part of the focus of this thesis.



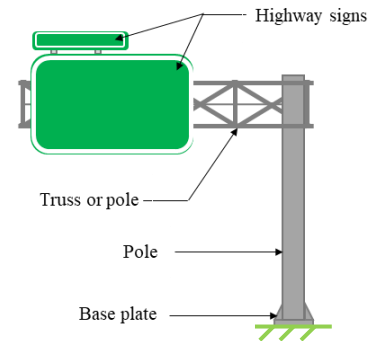
a. Photo of a strain pole structure and its schematic representation



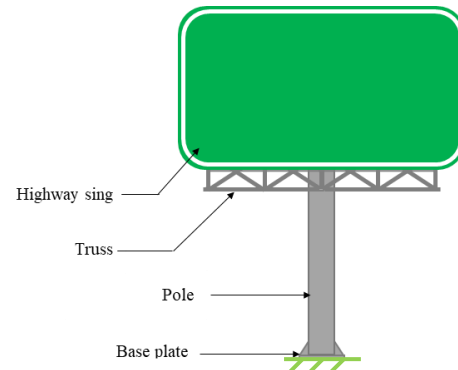
b. Photo of a mast arm structure (MATS) and its schematic representation

Figure 2-1: Typical traffic signal structures. (Photos from Google Earth, earth.google.com/web/)

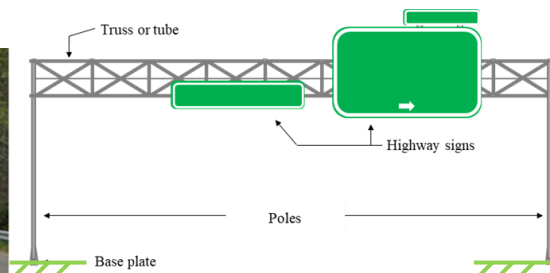
Highway sign structures are structures used for supporting highway signs, that are commonly located on the side of highways to show important information about routes. Figure 2-2 shows some examples of commonly used highway signs. The photographs shown in this figure correspond to a cantilever sign CS structure (Figure 2-2a), a balanced tee (Figure 2-2b), and a bridge span structure (Figure 2-2c).



a. Photo of a cantilever sign (CS) structure and its schematic representation



b. Photo of a balanced tee structure and its schematic representation



c. Bridge span structure and its schematic representation

Figure 2-2: Typical highway traffic structures. (Photos from Google Earth, earth.google.com/web/)

For this research, the main focus was on the mast arm traffic signal (MATS) structures and the cantilever sign (CS) structures. Both of these two structures have a configuration of an inverted L-Shape structure (cantilever) that will result in a similar loading demand to the supporting foundation system.

Under wind loading, the foundation system of an inverted L-shape structure will be subjected to:

Vertical compression load, horizontal lateral load, biaxial bending moment, and torsion. More details of the two main types of structures investigated in this project are provided in the following subsections.

2.2.1. Mast arms traffic signals (MATS) structures

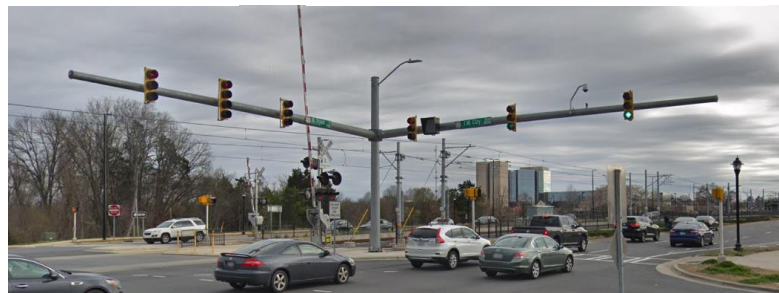
In current USDOT practice, there are several types of MATS structures. These structures are commonly made of aluminum, steel, or timber. Vertical elements are poles, columns, tapered tubes, or posts. The pole is usually supports one or two arms that could be either straight or curved elements, as shown in Figure 2-3. In some cases, the structure can be used to support luminaires and small signs in addition to traffic signals.



a. Typical MATS with luminaire



b. Typical curved MATS



c. Typical dual MATS

Figure 2-3: Photos of typical MATS structures. (Photos from Google Earth, earth.google.com/web/)

The horizontal arm is usually attached to the vertical pole using either a flange plate or with a fill-welled socket connections (NCDOT 2016). The arm should be able to support

traffic elements as: traffic signals, traffic signs, cameras, sensors, among others. Figure 2-4 shows a schematic of a typical MATS structure that shows the main elements of these types of structures.

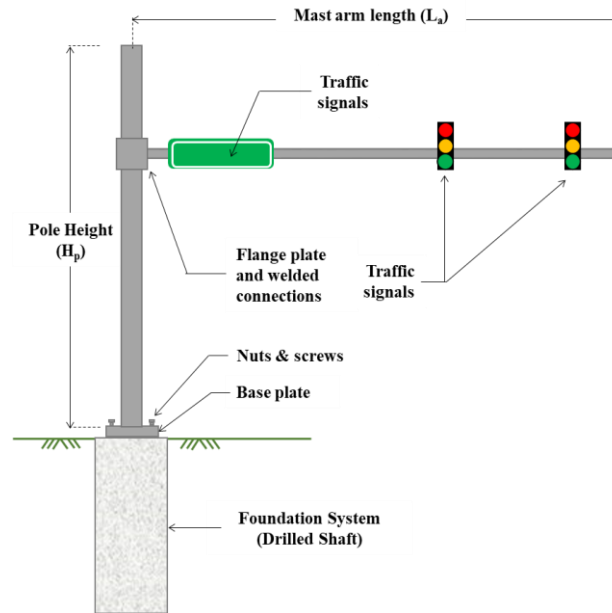


Figure 2-4: Schematic of a typical MATS structure.

2.2.2. Cantilever sign (CS) structures

As MATS, there are different types of CS structures frequently used by many USDOTs. The difference is mainly the number of elements forming the structure. The first type of structures corresponds to single cantilever sign structure, which is composed of only one element (monotube). When the CS structures is composed of a horizontal arm attached to a vertical pole, the structure corresponds to a dual CS structure. Figure 2-5 (a) and (b) shown a picture of single and dual CS structures, respectively.



a. Typical single CS



b. Typical dual CS

Figure 2-5: Photos of CS structures. (Photos from Google Earth, earth.google.com/web/)

The pole of dual CS structures could correspond either to a cylindrical or a tapered tube. The pole height varies between 6.0 meters and 12.0 meters depending of the traffic type in the highway. The diameter of the poles varies from 0.15 meters to 1.20 meters. The tube or the truss used as arm is connected to the pole either using a flange plate or with a fill-welled socket connection. The length of the arm of the CS structure usually varies from 5.0 to 12.0 meters. The arm length will depend on the lanes of the road or highway. Figure 2-5 shows a schematic of a typical CS structure.

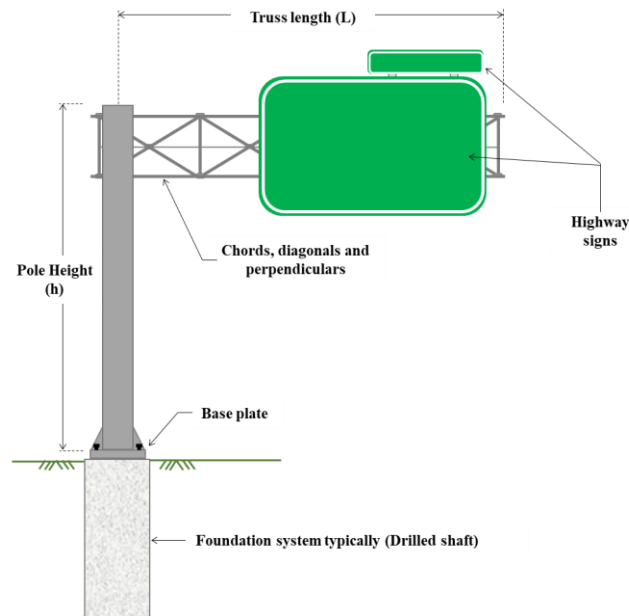


Figure 2-6: Schematic of a typical CS structure

2.3. Loading demand for inverted L-Shaped structures

The loading demand for the foundation system of inverted L-shaped structures are associated primarily to gravity and wind. The following subsections describe these main sources of loading demand.

2.3.1. Gravitational load

The gravitational loads that these structures transmit to the foundation system will result in an axial compression load and a bending moment, as shown Figure 2-7.

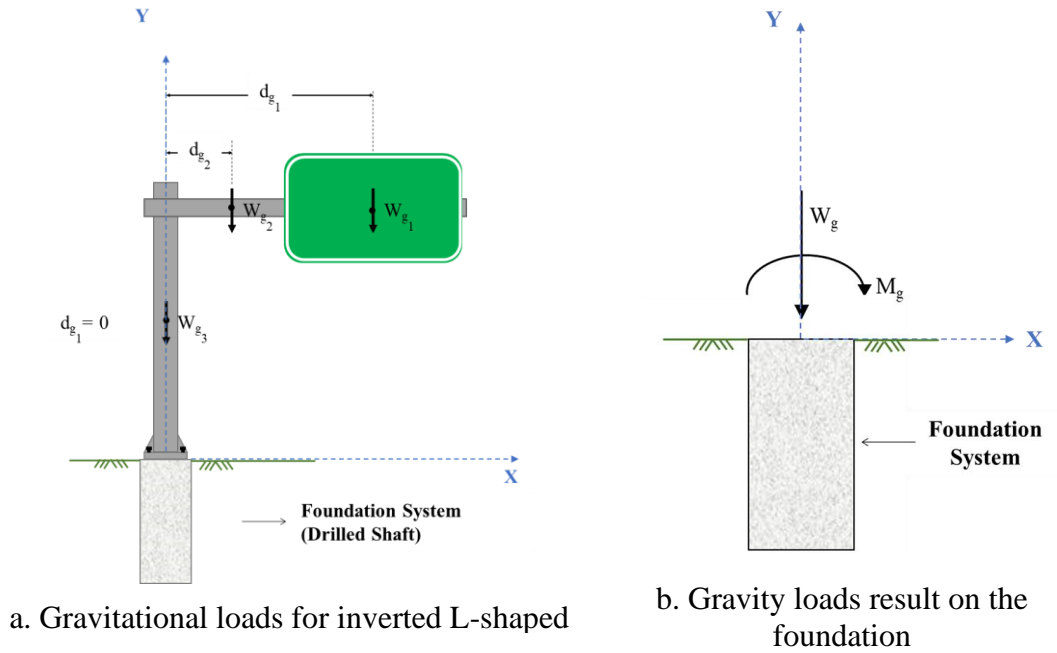


Figure 2-7: Schematic showing gravitational loads on an L-shaped structure

Figure 2-7(a) shows several W_g forces (W_{gi}) that correspond to gravitational loads associated to the weight of the signs, truss or tube, pole, etcetera. The three gravitational loads shown in the Figure 2-7(a), W_{gi} , result in the following resultant axial compression load acting on the foundation system:

$$W_g = \sum_{i=1}^3 W_{gi} \quad (2.1)$$

The resultant bending moment acting on the top of the foundation system is:

$$M_g = \sum_{i=1}^3 W_{gi} \cdot d_{gi} \quad (2.2)$$

where, d_{gi} are the moment arm distances of the respective gravitational loads W_{gi} to the centroid of the foundation cross section.

2.3.2. Wind loading

The loading associated with the action of wind is a complex phenomenon that is difficult to model and predict. The wind-structure interaction can be modeled using computational fluid dynamics to estimate the loading demand on the structure associated to wind action. However, the complex drag forces are often estimated using a simplified approach that is based on estimating an equivalent pressure acting on the surface of the structure as a function of the wind speed, gust coefficient, and other factors. The detailed computation of hurricane wind loading is a phenomenon outside of the scope of this research. For this thesis the wind loading is computed using the approach suggested in highway codes and standards developed by AASHTO (2009). A brief description of the simplified approach used in highway codes is provided below.

The basic wind and gust speeds vary during hurricane events and could be measured using weather instruments known as anemometers (i.e., ultrasonic, laser, vane or cup anemometers). The average wind speeds over a period of time is known as basic wind speed, while the wind gust speeds are caused by variation of the direction and velocity of the wind flow. In most cases, the basic wind and the wind gust speeds are represented in biaxial graphs, as depicted in

Figure 2-8. This figure shows a representation of the basic wind and gust wind speed measured at the Georgia Regional airport during Hurricane Irma, data from (NWS, 2017).

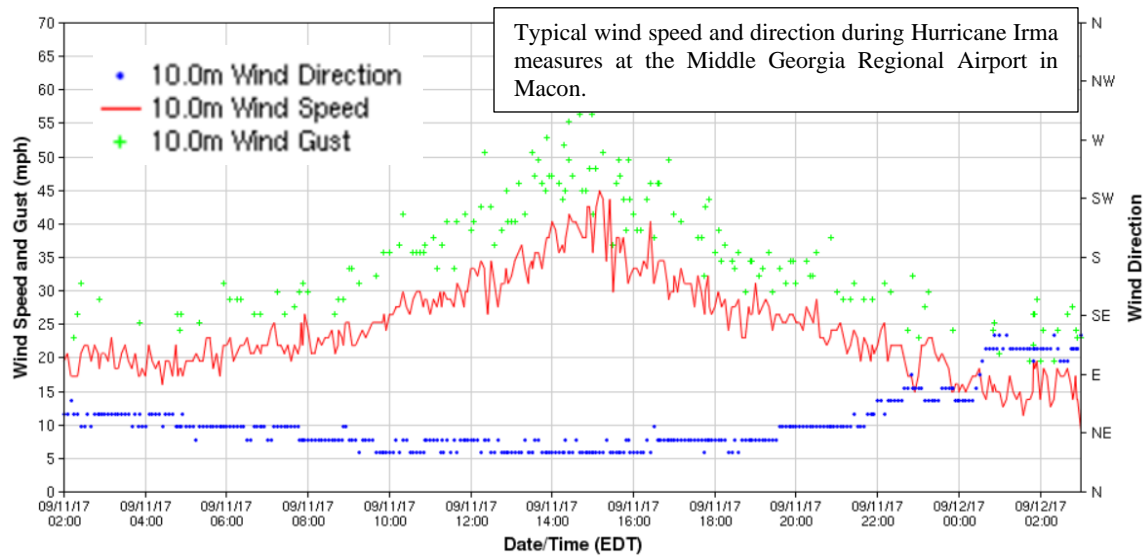


Figure 2-8: Wind speed and direction of the Hurricane Irma (From NWS, 2017)

The data shown in Figure 2-8 exhibits the complexity of the wind loading during a hurricane event. This figure shows wind speed data for a period of 24 hours recorded primarily on September 11, 2017. On this date and at this station, Hurricane Irma was a tropical storm. The figure shows the average wind speed using the red solid line, and during the hurricane event it fluctuates rapidly with sudden jumps and drops in the order of 5 MPH or more. Furthermore, this figure illustrates how the wind speed magnitude and the velocity can change considerably during a hurricane event making the associated wind loading demand on an affected structure equally complex with variable magnitude and direction as a function of time.

Due to the complexity of wind loading, a more simplified approach is recommended in codes to estimate the wind load demand. For MATS and CS structures, the wind load is computed based on an estimated wind pressure acting horizontally in the

exposed structures based on a fundamental fluid-flow approach. The following expression is adopted by the AASHTO code specification for structural supports for highway signs, luminaires, and traffic signals, (AASHTO, 2009):

$$P_{wz} = 0.00256 \cdot K_z \cdot I_r \cdot G \cdot V^2 \cdot C_d \quad (2.3)$$

where, the constant 0.00256 comes from results of typical values for air density and gravitational acceleration, V is the basic design wind speed for the structure, K_z is the coefficient for height and exposure factor, I_r is the importance factor, G is the gust effect factor, and C_d is the drag coefficient factor. According to AASHTO (2009), the factor K_z can be computed as:

$$K_z = 2.0 \left(\frac{z}{z_g} \right)^{\frac{2}{\alpha}} \quad (2.4)$$

where, z is the height above the ground where pressure P_{wz} is calculated, z_g is taken to be 9.2 and α is a constant that can be taken to be 900 for structural supports for high signs, luminaires, and traffic signals. For different support types, AASHTO (2009) has recommended different values for the wind importance factors I_r based... The directionality factor depends of the recurrence interval year and varies between 0.71 to 1.15.

The recurrence interval year recommended for overhead signs structures corresponds to 50 years. AASHTO (2009) indicates that drag coefficients C_d and the gust effect factor G should be computed using procedures outlined in Sections 3.8.5 and 3.8.6 of this reference respectively. Wind drag coefficients depend on the element geometry. And vary between 0.45 and 1.30.

2.3.3. Wind loading demand on inverted L-Shape structure

As discussed in the previous section, the wind acting on the exposed surfaces of the structure will result in complex drag forces that are often computed as equivalent pressures, as shown in Figure 2-9.

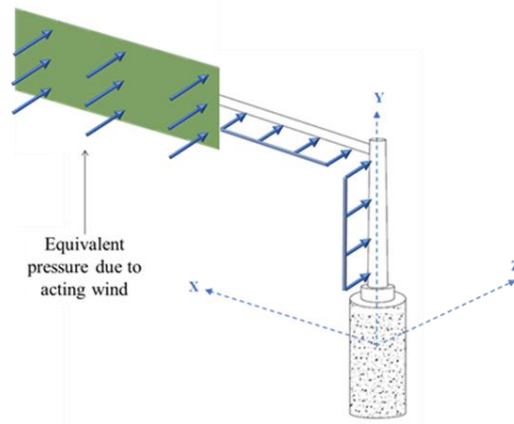


Figure 2-9: Wind pressure graphical representation

The pressure distributions shown in Figure 2-9 will result in the resultant lateral forces shown in Figure 2-10.

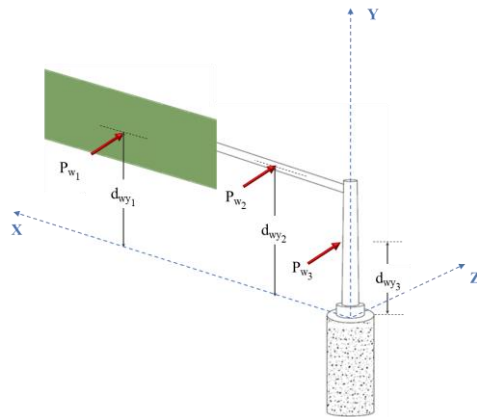


Figure 2-10: Resultant lateral forces associated with wind about the x-axis

The three lateral forces shown in Figure 2-10 will result in a lateral load demand acting of the top of foundation system equal to:

$$P_W = \sum P_{Wi} \quad (2.5)$$

where, P_{wi} are the wind related resultant lateral forces. The resultant force P_{wi} corresponds to a lateral force acting on the top of the foundation system Figure 2-11. Additionally, there will be a bending moment associated with the wind lateral forces that will act about x-axis with a magnitude:

$$M_W = \sum_{i=1}^3 P_{wi} \cdot d_{wi} \quad (2.6)$$

where, P_{wi} are the wind related lateral forces defined above and d_{wi} is the vertical distance of each lateral force to the foundation system top (i.e. where the reference system is located). The resultant bending moment, from the combination of gravitational M_g and wind loads M_w , can be computed as:

$$M_T = \sqrt{M_g^2 + M_w^2} \quad (2.7)$$

where, M_T is the resultant bending moment, and M_g and M_w as defined above.

The resultant force P_{wi} can be translated to the top of the drilled shaft (DS) as follows:

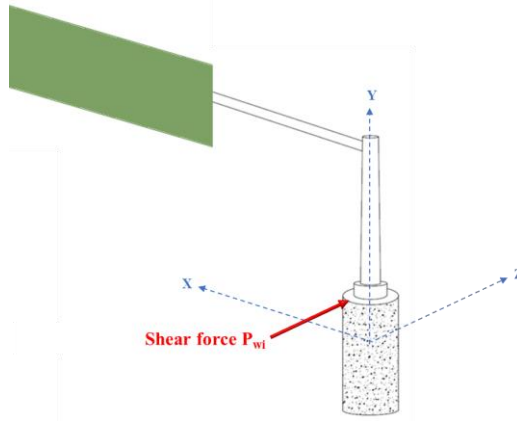


Figure 2-11: Graphical representation of the wind resultant force shear acting on the top of the foundation system

A graphical representation of the bending moment acting on the foundation system is shown in red in Figure 2-12.

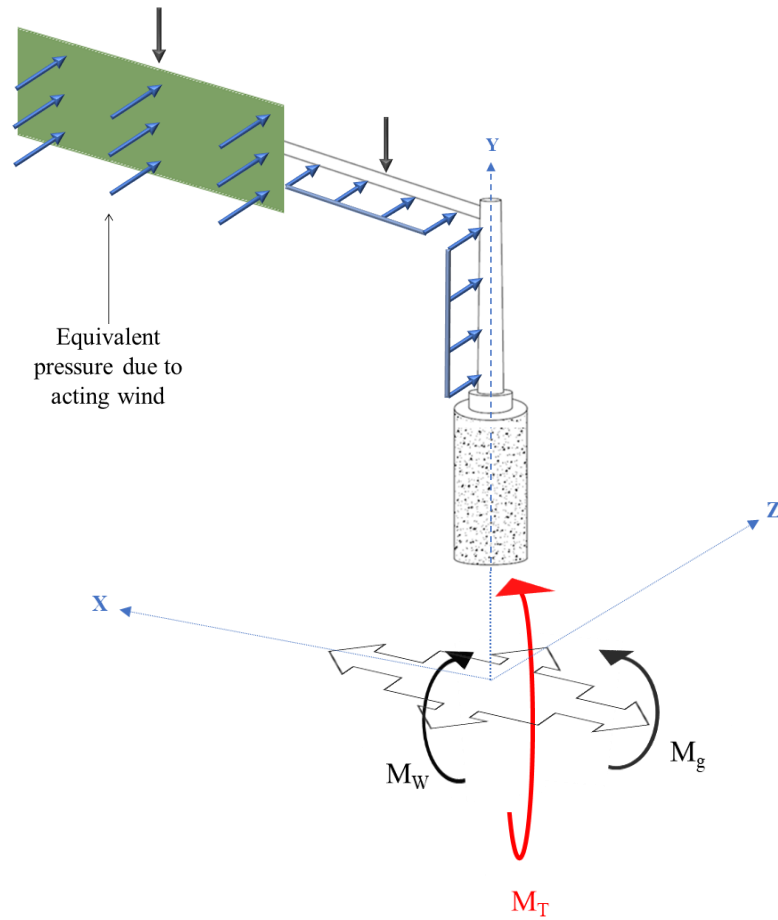


Figure 2-12: Graphical representation of combined bending moment

There is also a torsional loading demand associated with wind loading. The resultant lateral forces produced by the wind pressure distributions are shown again with their horizontal distances with respect to the x-axis in Figure 2-13.

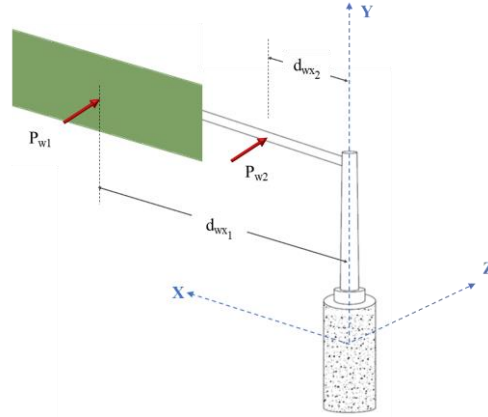


Figure 2-13: Resultant lateral forces associated with wind about y-axis

The torsion loading demand on the foundation system can be computed as:

$$T_W = \sum_{i=1}^3 P_i \cdot d_{xwi} \quad (2.8)$$

where, T_W is the resultant torsion loading demand, P_i as defined above, and d_{xwi} is the horizontal distance of each P_i component to the foundation centroid. A graphical representation is shown in Figure 2-14.

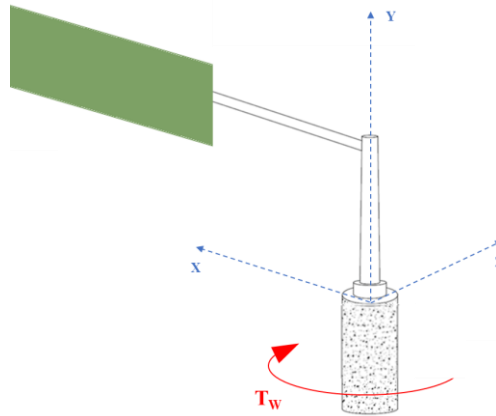


Figure 2-14: Graphical representation of the resultant torsional moment

2.4. Typical foundation systems

The MATS and CS structures are commonly constructed on one of two conventional types of foundations. The first one corresponds to drilled shaft (DS) structures, which are deep structures with cylindrical shapes made in concrete. The

advantage of using deep foundations for traffic signal structures is the small shallow footprint needed. Figure 2-15 shows the generalities of different types of drilled shafts (Das, 2014).

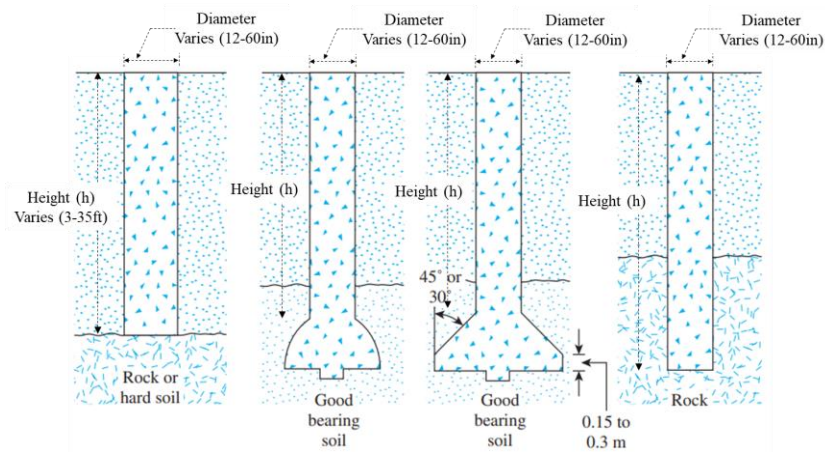


Figure 2-15: Typical sections of drilled shafts foundations. (Adapted from Das, 2014)

The second most common type of foundation for traffic signal and overhead highway structures is a spread footing. In cases where the shallow soil layers are competent enough to support high loads with low displacements and settlements, the best foundation option corresponds to a shallow foundation. According to Rodriguez, C., et al. (2019), most of the departments of transportation in the U.S consider shallow foundations as a method to withstand traffic signals and overhead highway structures. However, in most cases a space limitation can preclude the use of a spread footing. Figure 2-16 shows a schematic of a shallow foundation.

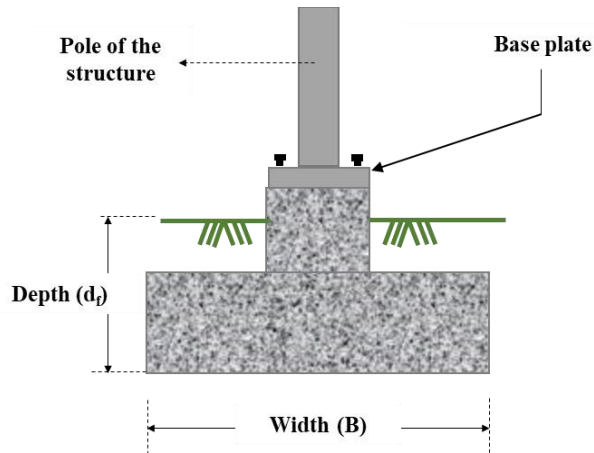


Figure 2-16: Typical section of a spread footing foundation

Figure 2-17 and Figure 2-18 shows other types of foundation systems used to support CS and MATS structures. This information was primarily obtained by the UNC Charlotte Research team in the project on the effects of torsion and moment on traffic signals structures. As shown in Figure 2-17, one type of alternative foundation system consists of a reinforced concrete beam capable of transmitting the load from the grade beam to another type of foundation (i.e. pile caps, aggregate piers, etc).

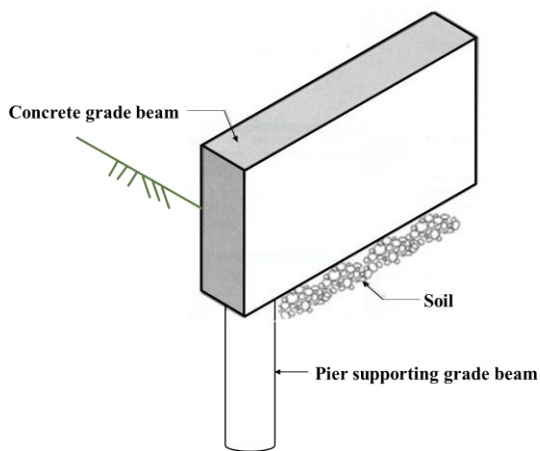


Figure 2-17: Typical grade beam

Another alternative foundation system consists of micro piles with a pile cap that transfers loads from the structure to a group of micro piles. Figure 2-18 shows a typical foundation system constituted by caps and piles elements.

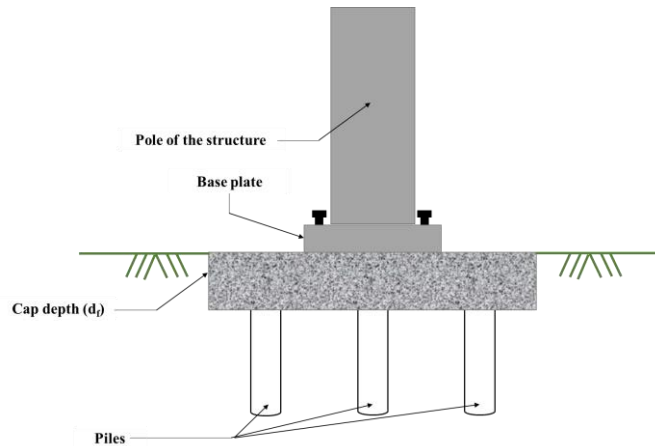


Figure 2-18: Typical micro piles with pile cap

In both cases of grade beam and micro piles with pile cap, the greatest limitation corresponds to footprint size in the site of installation. Another less used alternative, due to constructive challenges in cohesionless soils is a drilled shaft with single or dual wing wall. This system is composed of a drilled shaft with one or two lateral reinforced concrete walls as shown in Figure 2-19.

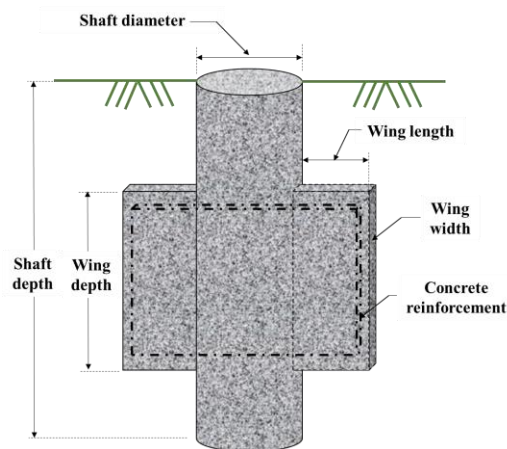


Figure 2-19: Typical drilled shaft with wing walls

2.5. Summary

This chapter described the characteristics and loading demand of inverted L-shaped structures i.e., MATS & CS. In this chapter, the most common foundation systems used to support inverted L-shaped structures were described. The most common foundation type was found to be single drilled shafts.

CHAPTER 3: STATE OF PRACTICE STUDY ON FOUNDATIONS FOR COASTAL TRAFFIC SIGNAL MAST ARM STRUCTURES

3.1. Introduction

This chapter presents a synthesis of a state of practice (SOP) study that was carried out as part of a research project funded by the North Carolina Department of Transportation. The SOP focused on documenting design and construction practices followed by participant USDOTs related to foundation systems for coastal mast arm traffic signal structures. Specific information gathered included: typical range of dimensions of mast arm structures, types of foundation systems used, range of dimensions (i.e., embedment depth and diameter) for DS foundations, design used by DOTs to estimate loading demand, and process for the geotechnical design of DS foundations.

A copy of the survey questionnaire used for the SOP study is provided in Appendix G. The SOP survey questionnaire was completed by the 12 coastal DOTs shown in Figure 3-1. In addition to the survey questionnaire, the SOP study included follow-up virtual interviews with participants to confirm responses and obtain additional information. The follow-up virtual interviews were performed using the Zoom platform and included participants of several members of the NCDOT research project Steering and Implementation Committee.

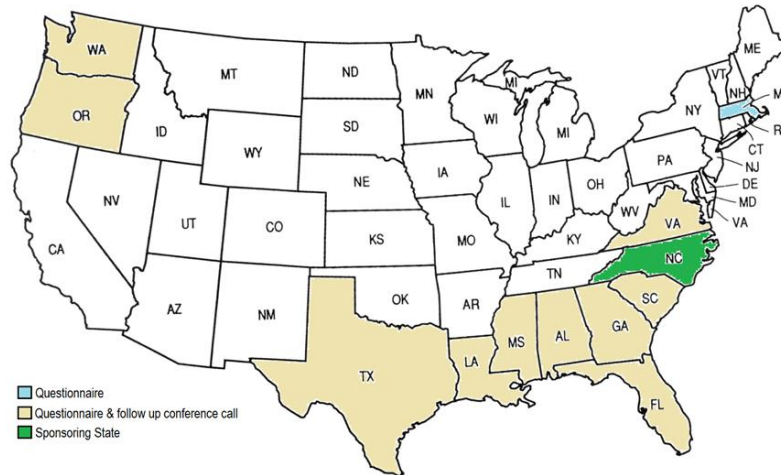


Figure 3-1: Map showing participants of SOP study.

3.2. Methodology of the SOP study

The methodology followed in this SOP study consisted of the following steps:

- (i) Review of online information (manuals, design drawings, etc.), as well as review of available online design resources (e.g. spreadsheets, software) used by individual DOTs;
- (ii) design of a survey questionnaire to collect information not readily available online;
- (iii) distribution of survey questionnaire to participants;
- (iv) compilation of survey response; progress meeting on July 2018 with members of Steering and Implementation Committee (SIC) of NCDOT to provide an update on the SOP synthesis and survey responses received to date, as well as to receive feedback;
- (v) follow-up conference calls to survey respondents (performed between July to October 2018);
- (vi) compilation of survey questionnaire results and information compiled during follow-up conference calls;
- (vii) and presentation and delivery of final draft of SOP Report to NCDOT (Rodriguez et al. 2019).

3.3. Summary of Results of SOP study

The following subsections summarize the main result of the SOP study.

Specifically, the following information is summarized:

- dimensions of mast arm structures (Sect. 3.3.1),
- wind speed values used for design (Sect. 3.3.2),
- foundation types used for coastal traffic signal structures (Sect. 3.3.3),
- information about drilled shaft (Sect. 3.3.4).

3.3.1. Dimensions of mast arms structures

The SOP study found that the dimensions for mast arms used by coastal DOTs vary greatly from state to state. For example, in North Carolina, based on the NCDOT ITS Mast Arm Standard (dated 12/14/11), the maximum pole height used is 26 feet, the range of mast arm lengths is from 10 to 75 feet, and the diameter of the support pole base ranged from 12 to 26 inches. The range of mast arm lengths reported by the SOP survey participants are summarized in Figure 3-2.

This figure shows for each participant the typical range and for some states (e.g., South Carolina, Georgia, Mississippi, Oregon, and Washington) the figure also shows the longest mast arm reported by DOT personnel based on follow-up conference calls. DOT's that have standards that allow use of mast arm lengths of 70 feet or longer include North Carolina, Florida, and Virginia.

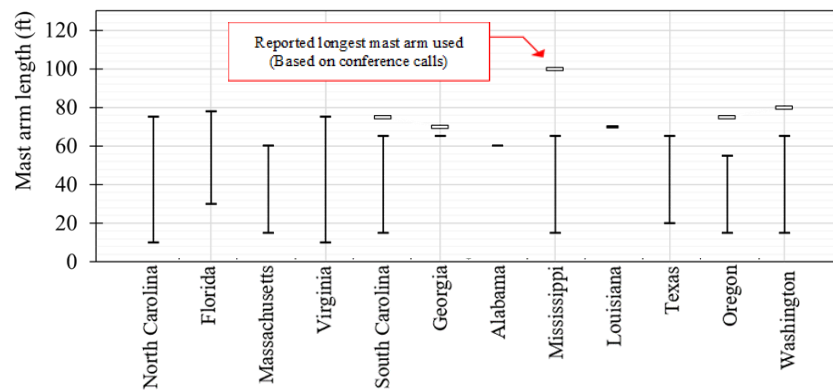


Figure 3-2: Range of mast arm lengths reported by SOP participants.

3.3.2. Design wind speed values used for design

The loading demand on the foundation system is greatly influenced by the design wind speed. A review of design wind speeds is not part of the scope of this study, but a summary of the design wind speeds was included as part of the SOP study. Since the load factors and wind speed maps have changed significantly over the past several revisions of ASCE 7, the associated specifications on specific ASCE wind speed map uses by the survey respondent was also requested. Most state DOTs obtain design wind speeds from isotach wind zone maps, such as the one shown in Figure 3-3. This figure shows that the design wind speed values vary based on the geographic location of the structure. Wind speed maps like this one have been periodically updated by ASCE such as ASCE 7-93, 7-98, 7-05, 7-10, and 7-16. The wind speed maps included in these different ASCE versions look similar but have important differences. An important difference is that ASCE 7-05 and earlier versions were ASD based maps and in 2010, starting with ASCE 7-10 the load factors changed and the wind speed maps were developed base on risk category. The periodic updating of wind maps is a challenge for many state DOT agencies, since this

requires revision and updating of design standards often with limited personnel or resources.

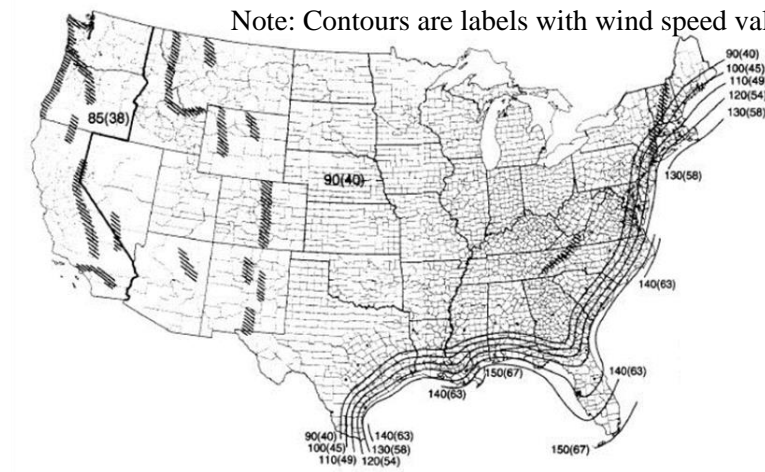


Figure 3-3: Isotach wind speed map for continental USA by ASCE (2009).

A summary of the AASHTO specifications, design wind speed source, and design philosophy, used by the SOP participants for design of mast arm structures is presented in Table 3-1 and Table 3-2.

Table 3-1: Standards used for selection of design wind speeds for mast arm traffic signal structures

AASHTO Standard	Year (Edition)	Wind Map Source	Comments
LTS 3	1994 (3 rd Ed)	ASCE 7-93	ASD. Wind map based on wind speed at 10m elevation. 3-s gust.
LTS 4	2001 (4 th Ed)	ASCE 7-98	ASD. Wind map based on wind speed at 10m elevation. 3-s gust.
LTS 5	2009 (5 th Ed)	ASCE 7-05	ASD. Wind map based on wind speed at 10m elevation. 3-s gust.
LTS 6	2013 (6 th Ed)	ASCE 7-10	ASD. Wind map based on wind speed at 10m elevation. 3-s gust.
LRFDLTS 1	2015 (1 st Ed)	ASCE 7-10	LRFD. Design wind map depends on risk level defined by MRI. Wind maps based on 3-s gust at 10m elevation

Notes: LTS: AASHTO Standard Specifications for Structural Supports for Highway Signs, Luminaires, and Traffic Signals.
 ASD: Allowable stress design; LRFD: Load and Resistance Factor Design; MRI: Mean Recurrence Interval;
 LRFDLTS: AASHTO LRFD Specifications for Structural Supports for Highway Signs, Luminaires, and Traffic Signals.

Table 3-2: Standards used for selection of design wind speeds for mast arm traffic signal structures

AASHTO LTS	Comments
LTS 3-1994	Texas, Alabama, Georgia
LTS 4-2001	Oregon, Mississippi,
LTS 5-2009	Louisiana, North Carolina
LTS 6-2013	South Carolina, Virginia, and Massachusetts
LRFDLTS 1-2015	Florida and Washington

Figure 3-4 shows a map summarizing the maximum coastal wind speed reported by the SOP participants. This figure also reports the current design standard being used by the participants for the design of coastal mast arm structures. Several participants indicated that foundation design for mast arm traffic signal structures had not yet been updated to the latest AASHTO standards due to personnel or other limitations. In contrast, most SOP participants reported having structural design standards updated to comply with the latest AASHTO edition. Figure 3-4 also is showing the maximum mast arm used by each DOT.

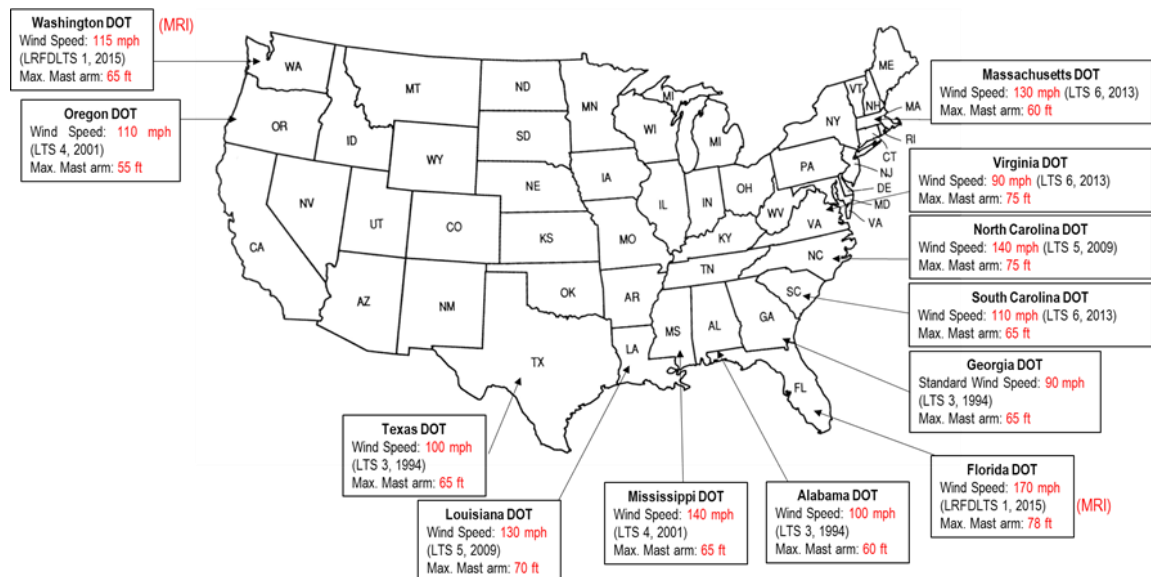


Figure 3-4: Summary map of maximum coastal wind speeds.

3.3.3. Foundation types used for coastal traffic signal structures

A summary of foundations used by the participants is shown in Table 3-3

Table 3-3: Typical foundation system used by the SOP participants

DOT Participant	Drilled Shaft	Drilled Shaft & Wingwalls	Spread Footings	Group of micropiles
WSDOT	Reported	No-reported	Reported	Reported
ODOT	Reported	Reported	No-reported	No-reported
TxDOT	Reported	Reported	No-reported	No-reported
LA DOT	Reported	No-reported	Reported	No-reported
MDOT	Reported	No-reported	No-reported	No-reported
ALDOT	Reported	Reported	No-reported	No-reported
FDOT	Reported	No-reported	No-reported	No-reported
GDOT	Reported	No-reported	No-reported	No-reported
SCDOT	Reported	Reported	No-reported	No-reported
NCDOT	Reported	No-reported	Reported	Reported
VDOT	Reported	No-reported	Reported	No-reported
MADOT	Reported	Reported	No-reported	No-reported

The most popular foundation system used by coastal DOTs for supporting coastal mast arm traffic signal structures is the drilled shaft. All 12 SOP respondents indicated that drilled shafts are the most commonly used foundation system used to support these structures. Occasional use of spread footings reported by Washington, Massachusetts, South Carolina, Oregon, Texas, and Alabama DOTs. However, spread footings were used only for projects with small mast arms located at sites with competent soil conditions. For sites with very poor geotechnical conditions, e.g., sites with low SPT blow counts and high water table, the DOTs from North Carolina, Virginia, and Louisiana reported having used drilled shafts with wingwalls. The use of drilled shafts with wingwalls features a conventional drilled shaft integrated with two reinforced concrete walls, where the steel reinforcement in the wingwalls is tied to the drilled shaft, as shown in Figure 3-5. The wingwalls are typically installed in the upper 3 to 6 feet of the drilled shaft, with the main

purpose being to increase the torsional capacity of the foundation. Virginia and Louisiana indicated that they are abandoning use of wingwalls due to constructability issues.

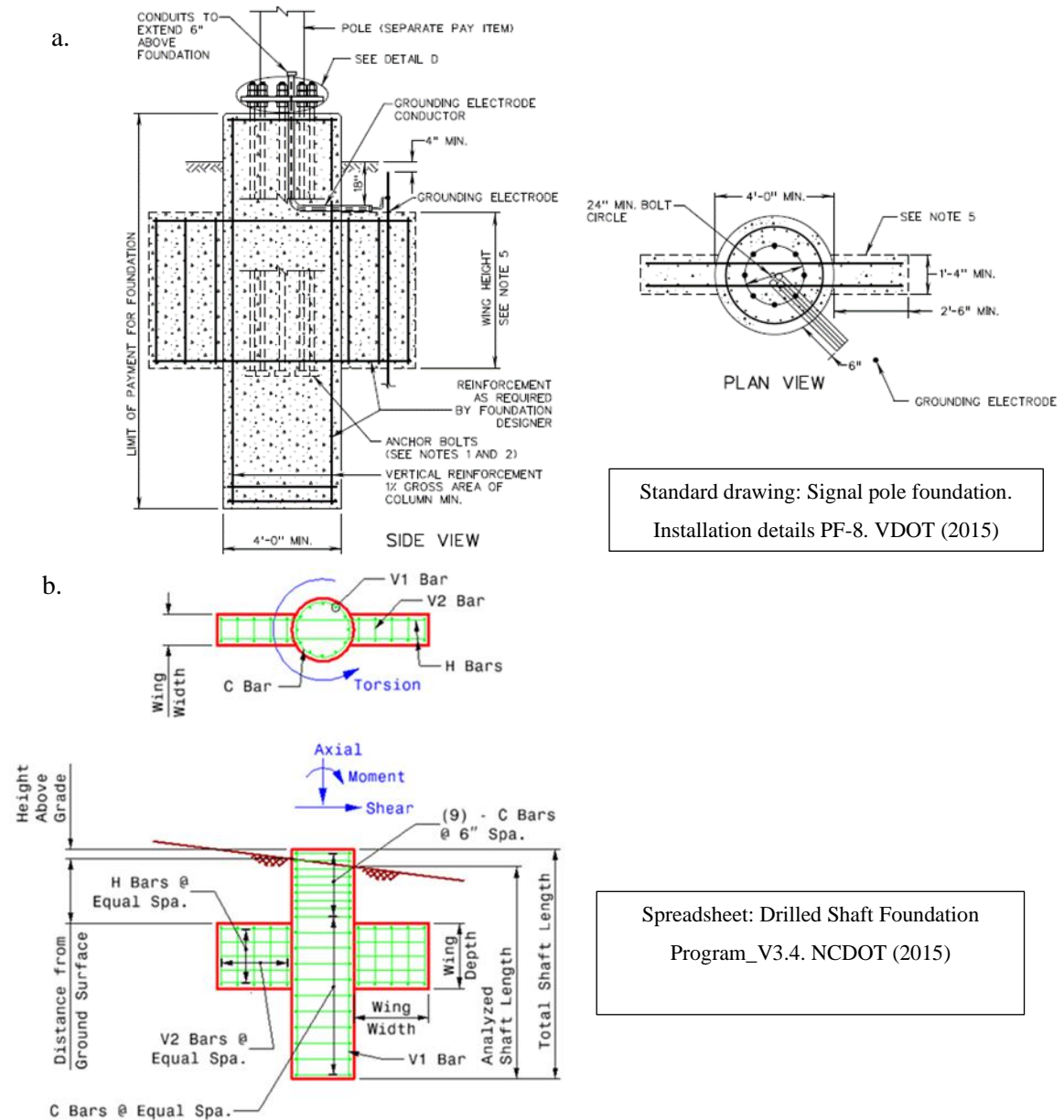


Figure 3-5: Examples design drawings for drilled shafts with wingwalls.

NCDOT and WSDOT reported using a foundation system consisting of a group of micropiles with a pile cap for sites with very poor geotechnical conditions (e.g., $SPT\ N \leq$

4). However, this type of solution usually requires a project specific design. Figure 3-6 shows a schematic of a micropile design used by NCDOT at a specific coastal project.

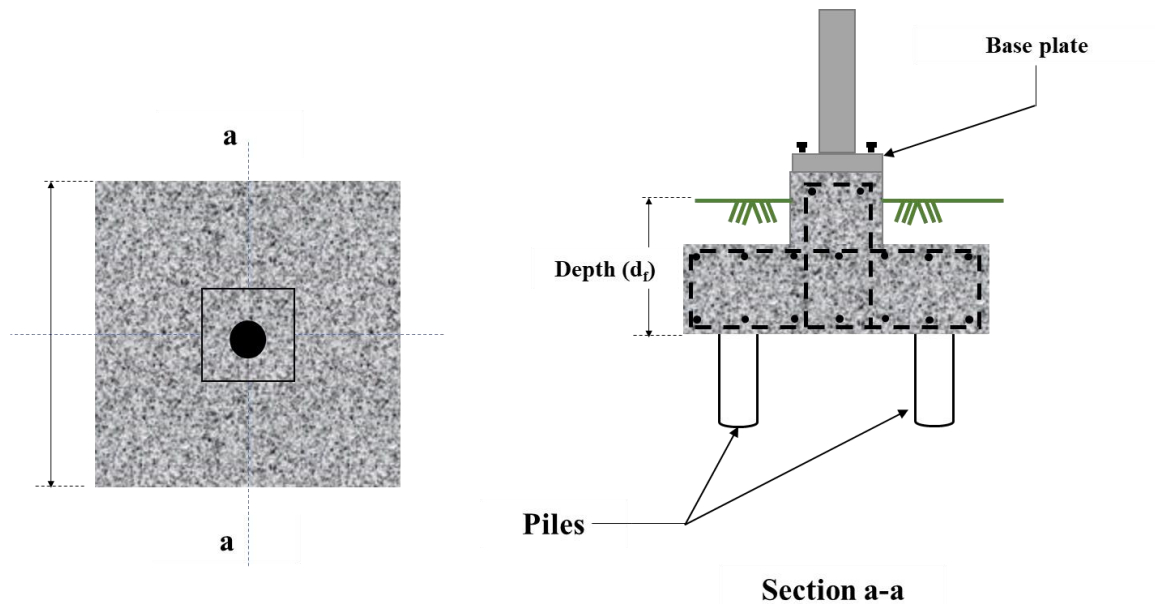


Figure 3-6: Example of group of micropiles and cap.

3.3.4. Drilled shafts

The SOP survey responses confirmed that drilled shafts are the most common foundation system used by participants for supporting mast arm traffic signal structures. This section summarizes dimensions and design procedures used across the states included in the survey.

3.3.4.1. Range of dimensions reported by SOP participants

As discussed earlier, the dimensions of the drilled shaft foundations will depend on the loading demand that in turn depends on the mast arm dimensions (primarily mast arm length) and design wind speed. The dimensions will also greatly depend on the geotechnical conditions of the site. Most DOTs use the Standard Penetration Test (SPT) as the main field test to characterize the geotechnical conditions at the site of mast arm traffic

signal structures. The range of embedment depths and diameters reported by the SOP participants are summarized in Figure 3-7. From this figure, it can be seen that the embedment depth of drilled shafts used in NCDOT projects ranges from 9 to 21 ft. and diameters range from 3.5 to 5 ft. These values are similar to the ones reported by FDOT that uses mast arms of similar dimensions and has a similar design wind speed. FDOT reported embedment lengths between 12 and 20 ft (with the deepest installation being 25 ft) and drilled shaft diameters typically between 4 and 4.5 ft.

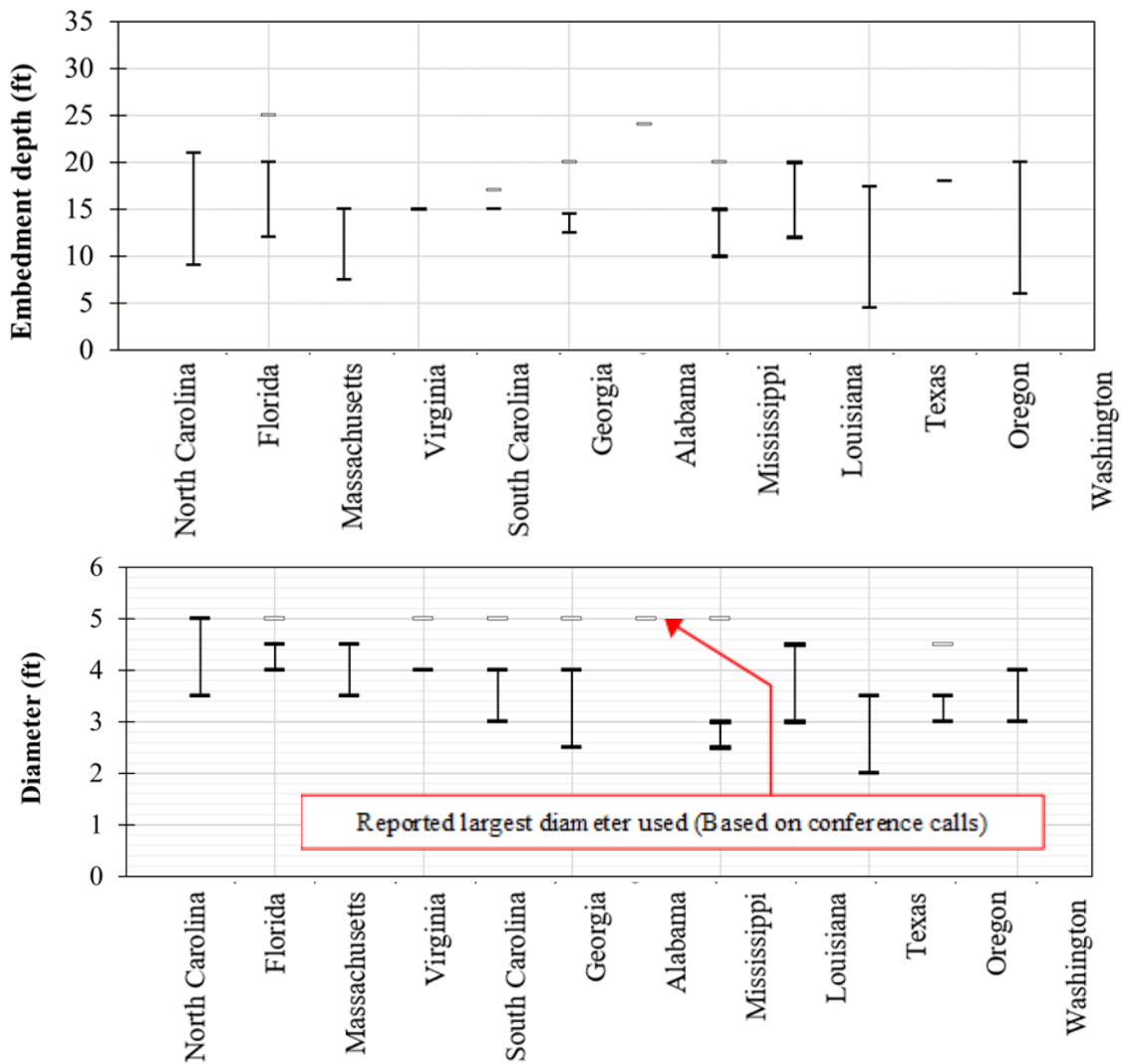


Figure 3-7: Range of dimensions of drilled shafts reported by SOP participants.

3.3.4.2. Design procedures used by SOP participants

As mentioned before, the loading demand for foundation systems of mast arm traffic signal structures involves combined lateral loading (producing shear and bending moment) and torsion. However, all SOP participants reported analyzing the problem using a decoupled approach where the effects of the lateral loading are considered separately from the torsion loading. Table 3-4 shows a summary of the design procedures used by the different DOTs to analyze the two loading conditions. For lateral loading, the ultimate load calculated by Broms (1964a, 1964b, 1965) is used by many DOTs. The other approach is to analyze the drilled shaft using non-linear p-y curves and a software such as L-Pile (Ensoft, 2015).

Table 3-4: Summary of design procedures for drilled shaft foundations.

STATE	Lateral Loading and Bending			Torsion Loading		Torsion is considered coupled with bending or separately
	Broms	L-Pile	Other	Skin	Other	
WSDOT	x				(1)	Separately
ODOT		x		(2)		Separately
TxDOT	x	x	(3)			Separately
LA DOT		x	Ensoft Shaft	(2)		Separately
MDOT	x	x		(2)		Separately
ALDOT		x		(2)		Separately
FDOT	x			(4)		Separately
GDOT	x	x		(2)		Separately
SCDOT		x		(2)		Separately
NCDOT		x		(2)		Separately
VDOT	x	x	COM624P	(2)		Separately
MADOT	x					Separately

Notes: (1): Washington Bridge design manual.
(2): β -method or α -method (FHWA, 2010).
(3): Texas cone penetrometer (FHWA, 2010).
(4): ω -FDOT uses a modified β -method that removes depth factor.

3.4. Summary

This chapter summarized the most relevant findings from the SOP study performed for the NCDOT research project on foundation systems of mast arm traffic signals (MATS). The study involved input and support of 12 coastal U.S. DOTs. A survey questionnaire was designed and issued with a focus on collecting range of dimensions of mast arm structures, wind speed values used for design purposes, design procedures used, and generalities of the foundation used to support MATS. The SOP survey revealed that most coastal DOTs use single drill shaft foundations to support MATS. The detailed SOP Report to NCDOT can be found in Rodriguez et al. (2019).

CHAPTER 4: LITERATURE REVIEW

4.1. Introduction

This chapter presents the literature review on research related to drilled shafts supporting inverted-L structures (i.e., MATS and CS structures). Most existing studies have focused on prediction of failure of drilled shafts under lateral loading (i.e., lateral load with associated bending moment) or torsion loading independently. The literature review presents a summary on the following main topics:

- Studies on capacity of torsional loading
- Studies on combined torsion and lateral loading
- Static methods to estimate torsional resistance skin friction

The literature review presented in the following sections reveals a need for additional research investigating the problem of drilled shafts under combined lateral and torsion loading. Only a few studies were identified that investigated the performance of a drilled shaft under combined lateral and torsion loading. The majority of these few studies that investigated the effects of combined loading were based on model testing and showed that the lateral load capacity decreases for a drilled shaft when torsion is present compared to the same drilled shaft under lateral loading alone. There are also important knowledge gaps in terms of static methods for predicting the required unit skin friction for torsion loading capacity.

4.2. Overview of recent research on drilled shafts under combined loading

A timeline of research related to drilled shaft foundations under lateral and torsion loading is presented in Figure 4-1. This figure summarizes the main research from 2000 and groups the references into: technical reports, thesis and dissertations, and scientific

papers. Most of the research summarized in this figure is from Florida (i.e., FDOT funded research performed by researchers from the University of Florida. The motivation of FDOT funded research is the high wind loads and long mast arm lengths used in this state and the need for safe and reliable design procedures. The timeline shows in the year 2000 early research on torsional capacity by Tawfiq (2000). The UF researchers then focused on combined torsion and lateral loads (e.g., Herrera 2001, and McVay et al. 2003). The UF group more recently looked at the feasibility of using post-grouted drilled shafts to enhance the capacity of the drilled shafts under combined loading.

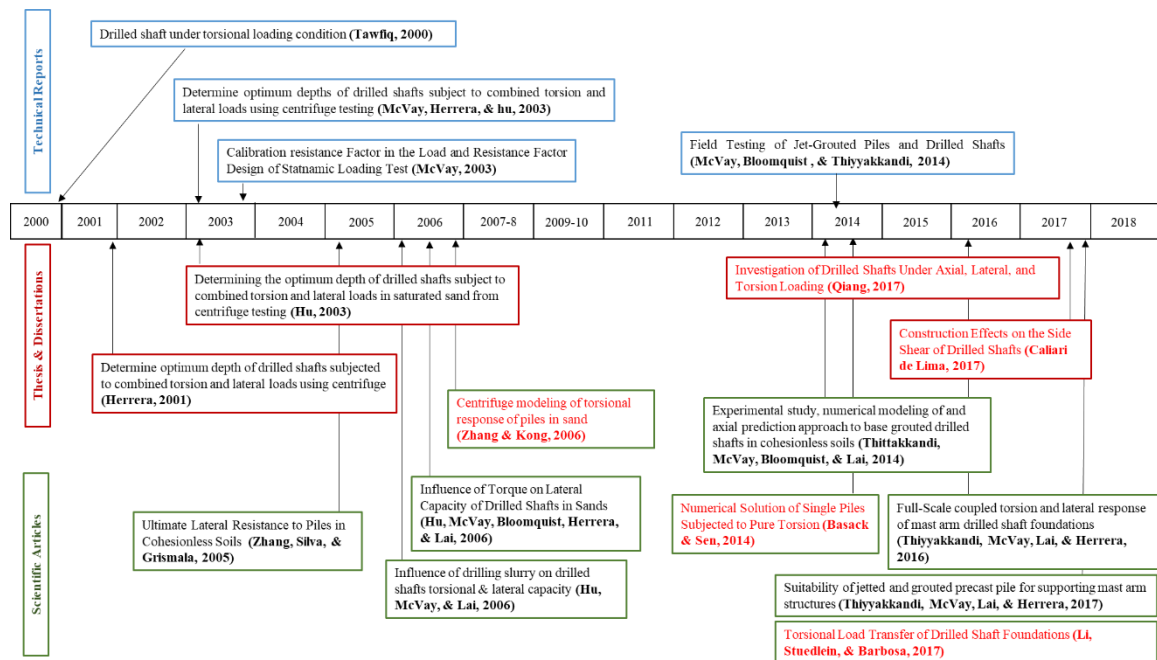


Figure 4-1: Summary of recent research on drilled shaft foundations subjected to lateral and torsional loading.

Sections 4.3 to 4.5 present more detailed information on some of the studies shown in the above figure. In particular research involving drilled shafts under combined lateral and torsional loading.

4.3. Centrifuge testing at UF by Hu et al. (2006)

Hu et al. (2006) performed 91 centrifuge tests on model drilled shafts under combined loading. The study considered three values of embedment to diameter (L/D) ratios, namely: 3, 5, and 7. Table 4-1 summarizes the test conditions used in the 91 centrifuge tests performed by the University of Florida (UF). As can be seen, tests considered three relative density levels (loose, medium, and dense) and dry and saturated soil conditions.

Table 4-1: Summary of test conditions (Hu et al. 2006).

Type of tests	Number of tests	Conditions	Embedment depth L/D	Load Application
Centrifuge	54	Loose, medium and dense dry sand	3, 5 and 7	Pole, mid-mast and dense.
Centrifuge	37	Loose and dense saturated Sand	5 and 7	

Figure 4-2 presents images that show the experimental setup used for the centrifuge tests. At the left, the image shows the test setup that includes elements such as the drilled shaft, mast arm, test sand, LVDTs and the loading piston. In the image to the right the mast arm and drilled shaft model is shown.

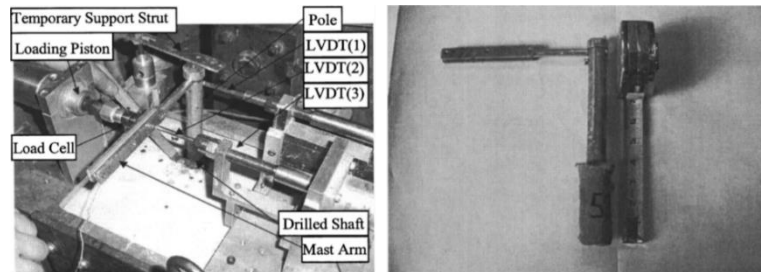


Figure 4-2: Photos of the centrifuge model testing (Hu et al., 2006).

The majority of the tests involved combined lateral loading and torsion, but some tests were performed without torsion by aligning the loading piston so that the lateral load

is applied centered with the axis of the sign vertical post. A summary of results obtained from centrifuge model lateral load tests (without torsion) are shown in Figure 4-3. This Hu et al. (2006), where the vertical axis represents the predicted failure calculated by Broms theory, while the horizontal axis represents the measured failure load from the centrifuge tests. The graph demonstrates that for $L/D < 5$ the prediction made with Broms overpredicts the measured response by about 35 %, while results from $L/D = 7$ show good agreement.

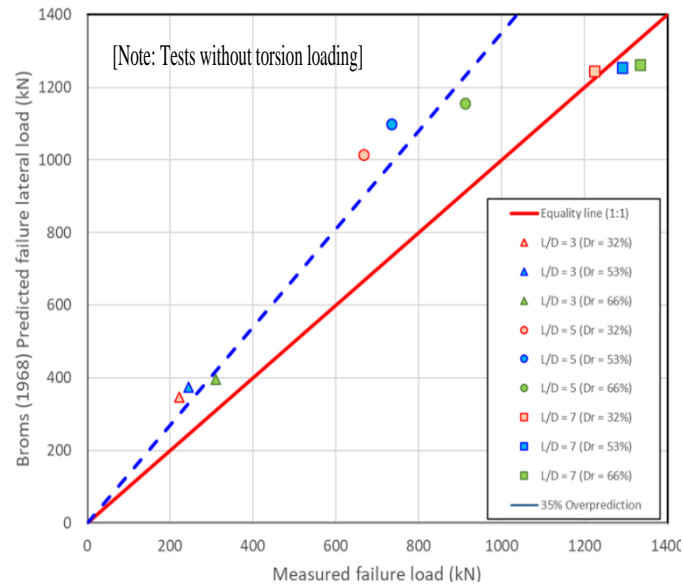


Figure 4-3: Experimental versus predicted lateral failure loads from Hu et al. (2006).

The centrifuge test results presented in terms of lateral load versus lateral deflection are presented in Figure 4-4. From this figure it can be concluded that: i) there is an evident reduction of the lateral load resistance when the load applied is producing torsion loading demand into the foundation; ii) and the resistance of the foundation is being increased as the L/D is increased. The second conclusion is as expected from conventional lateral load behavior of single piles. However, the first conclusion is one that can have important design

implications and needs to be incorporated by US DOTs that are currently analyzing this problem in a decoupled way.

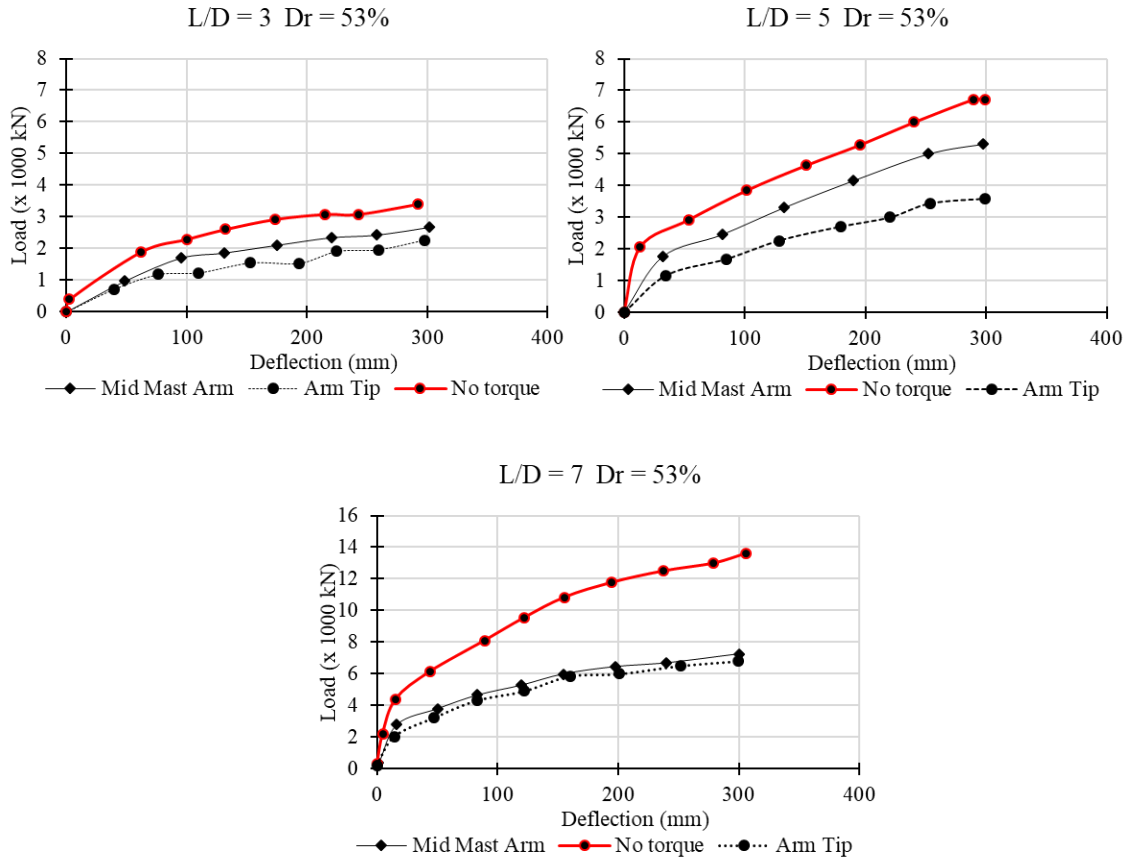


Figure 4-4: Combined lateral and torsion loading centrifuge study by (Hu 2006).

4.4. Study by Qiang et al. (2017) involving torsion loading

Qiang et al. (2017) performed a full-scale field test at a test site involving a saturated silty clay foundation soil. These authors also reviewed 21 torsion model tests performed by Poulos (1975) involving model piles installed in kaolinite. Table 4-2 summarizes the L/D embedment to diameter ratio values considered in all these tests.

Table 4-2: Summary of test conditions (Qiang et al. 2017 & Poulos 1975)

Type of tests	Number of tests	Conditions	Embedment depth L/D
Loading Test	21	Kaolinite	6 to 28
Field Test	1	Saturated silty clay	4.55

The field test performed by Qiang et al. (2017) is shown in Figure 4-5. This figure presents the soil profile at the test site and a photo of the drilled shaft tested in the field under torsional loading. The experimental values of failure torsion loading, for the model tests reported by Poulos (1975) and the field test by Qiang et al. (2017), are compared to predicted torsion loads using the α method proposed by Reese and O'Neil (1988) in Figure 4-6.

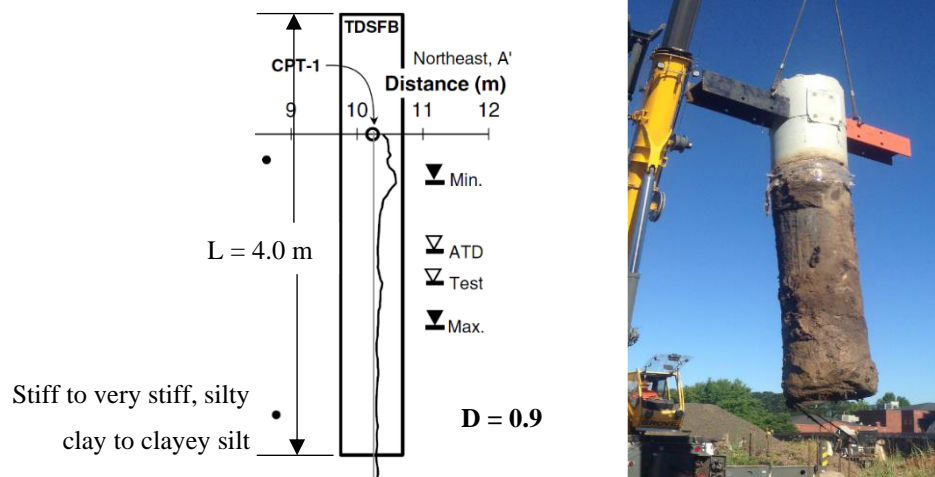


Figure 4-5: Subsurface profile at test and field test photo (Qiang et al. 2017)

[Torsion loading only; Data adapted from Qiang et al. (2017); and Poulos (1975)]

[Predictions using α method for axially loaded drilled shafts by Reese and O'Neil (1988)]

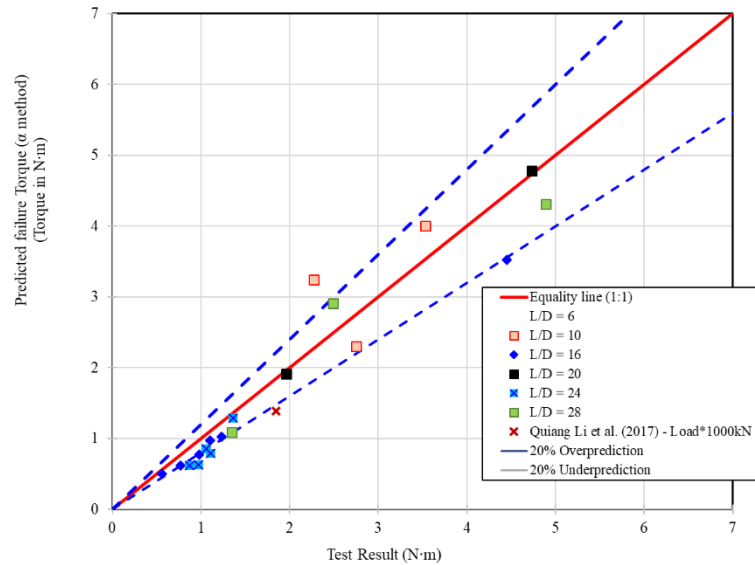


Figure 4-6: Experimental versus predicted torsion failure loads in clays.

Qiang et al. (2017) performed additional field tests at a test site involving cohesionless soils as shown in Figure 4-7. The embedment length (L) to diameter (D) ratio (L/D) was about 4.5.

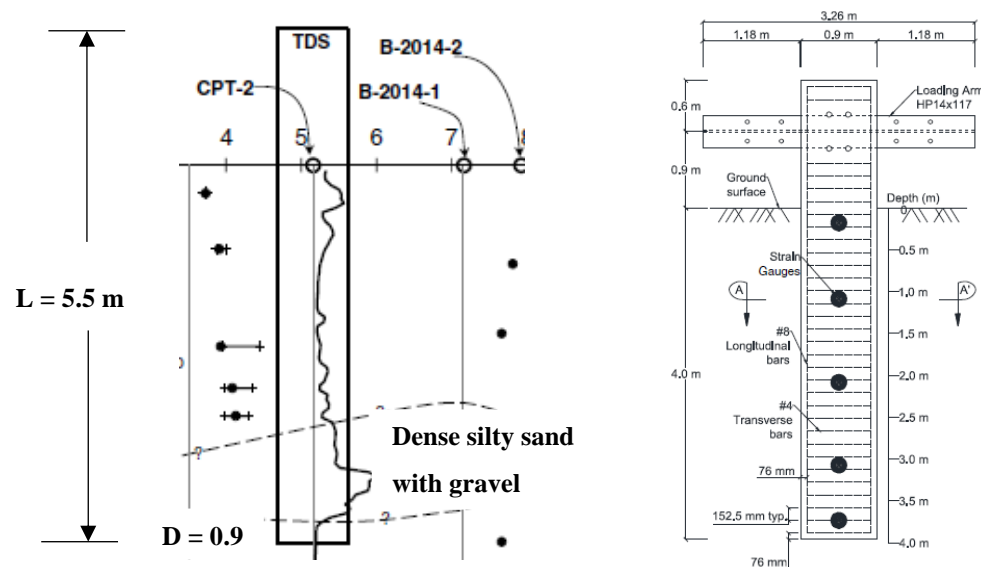


Figure 4-7: Subsurface profile at test and test details (Qiang et al. 2017)

The test results were reported also in McVay et al. (2014) under the test IDs: TS1, TS2 and TS3. A comparison of the experimental values of the measured failure torsion loads and the predicted torsion loads using the effective stress β -method for axially loaded drilled shafts proposed by Reese and O’Neil (1988) is shown in Figure 4-8

[Torsion loading only; Data adapted from McVay et al. (2014) and Qiang et al. (2017)]

[Predictions using β method for axially loaded drilled shafts by O’Neill & Reese (1999)]

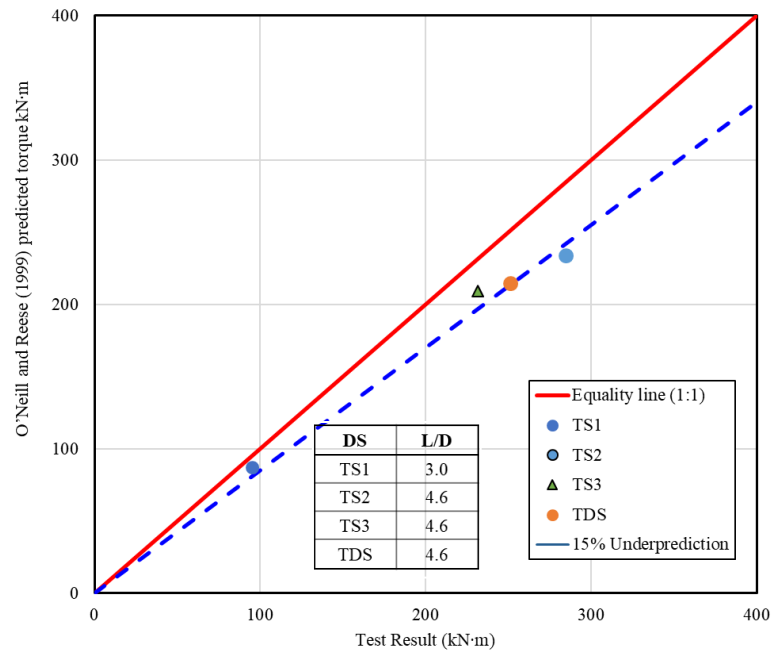


Figure 4-8: Experimental versus predicted torsion failure loads in sands.

The figure above presents the comparison with predictions using the β method by O’Neill and Reese (1999). The measured torsion failure load for test drilled shaft TS2 was compared with other commonly used static methods to estimate drilled shaft skin friction as shown in Figure 4-9. From this figure, it can be seen that the most accurate method for this estimate done with the SPT-based β -Method reported in FHWA-10 (Brown et al., 2010).

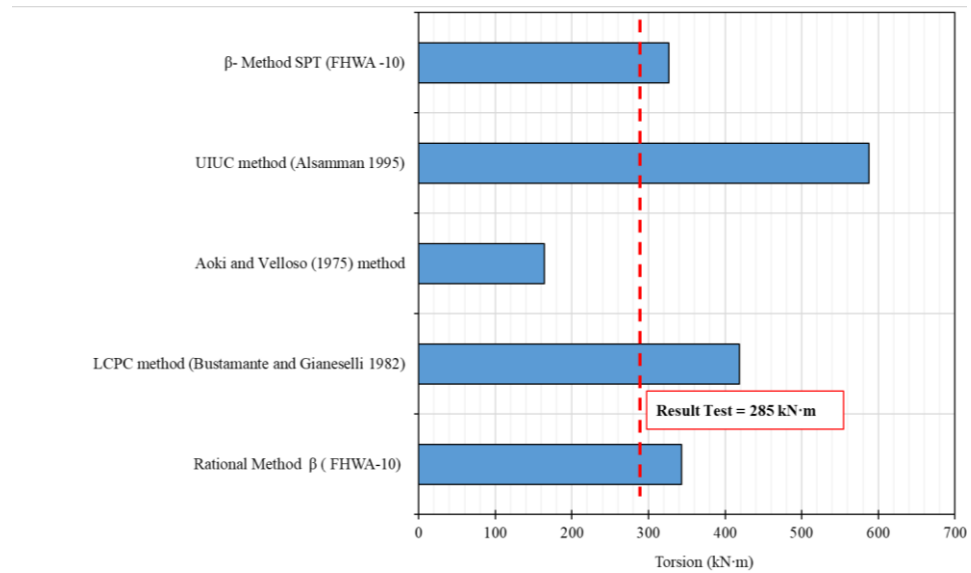


Figure 4-9: β method predictions vs field test (McVay et al. 2014)

Table 4-3 presents a summary of different skin friction static methods commonly used for drilled shafts based on SPT results. All static methods are based axial load tests. FDOT adapted the FHWA β -method by removing the depth influence and called this new effective beta factor omega, i.e., the ω for torsion prediction skin friction for FDOT. Table 4-3 also presents information about authors and the range of depths available for each method.

Table 4-3: β skin friction static method for drilled shafts based in SPT

β values used by FHWA and FDOT			
Manual	Equation	Reference	Comments
FHWA-99 (O'Neill and Reese, 1999)	$\beta = \frac{N_{field}}{15} \cdot (1.5 - 0.245 \cdot \sqrt{Z})$ Depth z in meters.	O'Neill and Hassan (1994)	Depth dependent. $0.25 \leq \beta \leq 1.20$ SPT Nfield ≤ 15 blows/0.3m
FHWA-10 Brown et al. (2010)	$\beta = \frac{N_{60}}{15} \cdot (1.5 - 0.135 \cdot \sqrt{Z})$ Depth z in meters.	Based on O'Neill and Hassan (1994)	Depth dependent. SPT N60 ≤ 15 blows/0.3m
FDOT Manual (ω)	$\omega = \frac{N_{field}}{15} \cdot (1.5)$ (Note: parenthesis doesn't have depth term).	FDOT Manual (modification of O'Neill and Reese, 1999)	$\omega = b$. Failure defined if shaft rotation exceeds 10 degrees. FDOT removed depth (z) dependency. (Depth independent).
Rational Method (FHWA-10)	$\beta = K_o \cdot \tan \phi'$ ($K_o = 1 - \sin \phi' \times OCR^{\sin \phi'}$)	FHWA-10 (Brown et al., 2010)	Limiting value: $b \leq K_p \cdot \tan \phi'$

The depth independency of the FDOT omega (ω) static method can be observed graphically in Figure 4-10. This graph shows the skin friction coefficient as a function of depth for a fictitious uniform sandy site with the following conditions:

- γ_{sat} total unit weight = 120 pcf,
- γ_{water} unit weight of water = 62.4 pcf,
- N_{60} standard penetration test = 5,
- N_{70} standard penetration test corrected = 5.83,
- ϕ' normally consolidated sand with $\phi' = 30^\circ$ and GWL at ground surface,
- OCR Over-consolidation pressure = 1.

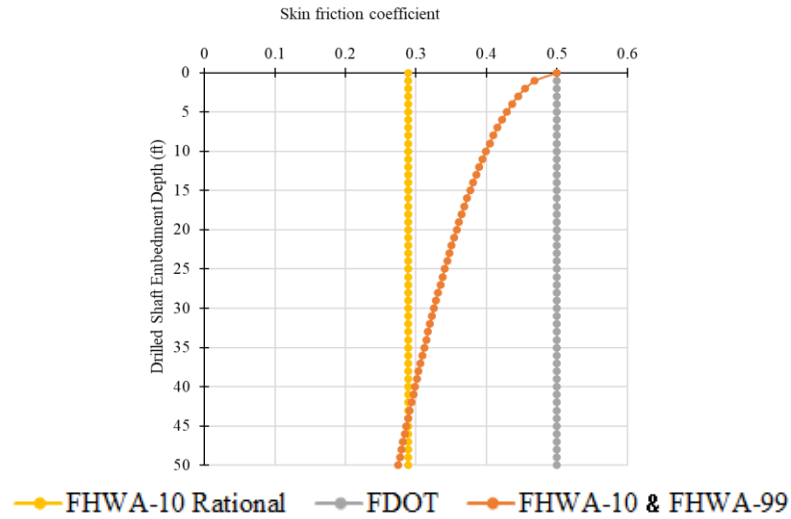


Figure 4-10: Skin friction factors as a function of depth for fictitious sand site.

4.5. Study by Qiang et al. (2017) involving combined loading

Qiang et al. (2017) also performed a field test under combined loading as shown in Figure 4-11.

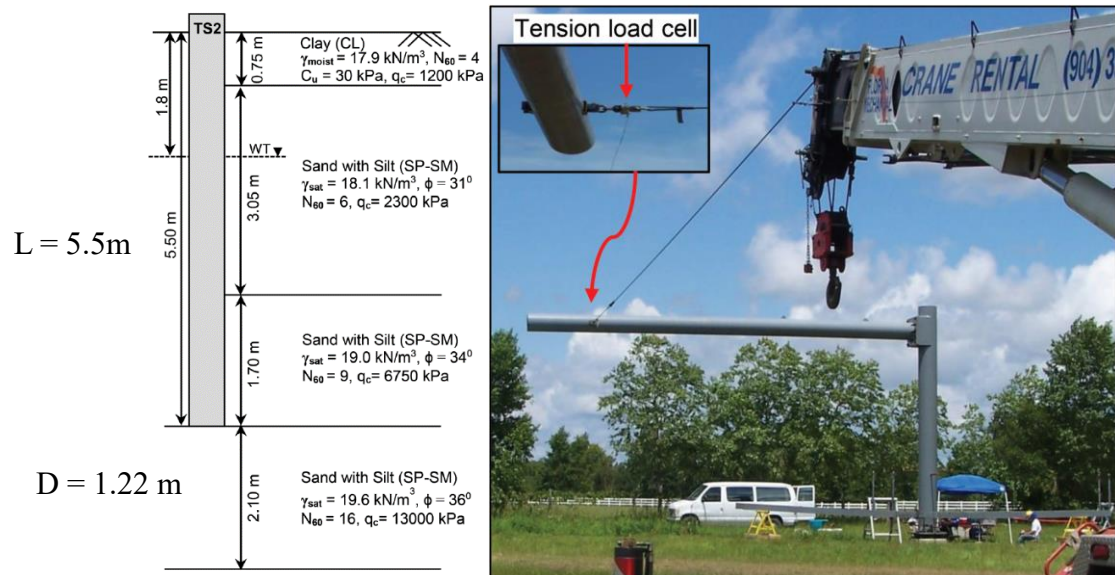


Figure 4-11: Subsurface profile at test and test details (Qiang et al. 2017 & Thiyyakkandi et al. 1975)

4.6. Method by Duncan et al. (1995) for lateral and torsion loading

Duncan et al. (1995) performed model tests using the geometry shown in Figure 4-12. A total of 24 tests were performed in shafts made with PVC which was covered with coarse sandpaper. The torsion loading was applied using cross-arm that was attached to the aluminum rod that extended upward from the pile foundation.

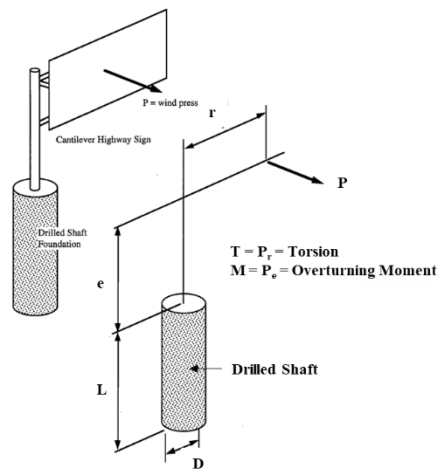


Figure 4-12: Lateral and torsion coupled loading. (Adapted from Duncan et al. 1995)

The key test variables used for the different model tests are summarized in Table 4-4. All tests were performed using sand as the test soil.

Table 4-4: Summary of Model Test Information (Duncan et al. 1995).

Dimension of the model shafts	
Diameter of the shaft (D)	1.98, 2.45, and 3.57 millimeters
Embedment Depth (L)	Variates from 6.13 to 15.3 millimeters
Distance from the pole to the applied load (r)	Variates from 0 to 20.40 millimeters
Distance from the drilled shaft top to the applied load (e)	Variates from 0 to 25.38 millimeters

The soil used was sand. The stress distribution along the drilled shaft for the uncoupled case (i.e., torsion only) is shown in Figure 4-13. The tests with pure lateral loading (and associated lateral bending moment) had distance to pole (r) equal to zero (referred to by the authors as pure overturning). The authors also performed tests where (e)

was restrained from lateral movement to produce pure torsion, and a third set of tests involved combined torsion and overturning.

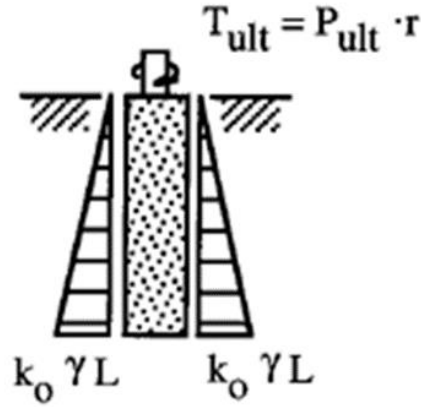


Figure 4-13: Schematic foundation under torsion loading. (Duncan et al. 1995)

Duncan et al. proposed the following general expression for the prediction of the ultimate applied load (P_{ult}):

$$P_{ult} = \frac{\alpha \frac{\pi}{4} k_o \gamma L^2 D \tan \delta}{\left[\frac{r}{D} - \beta (2.5 + 3e/L) \tan \delta \right]} \quad (4.1)$$

where:

- P_{ult} ultimate load capacity,
- L embedded length of drilled shaft,
- δ interface friction between drilled shaft and soil,
- K_o Rankine coefficient of earth pressure at rest = $(1 - \sin \phi')$,
- γ unit weight sand of sand,
- D diameter of drilled shaft (m),
- e vertical distance from ground surface to point of load application,
- α fraction of the component torsion capacity due to at-rest earth pressures that is effective at failure, $0 < \alpha < 1$, (1 was used by authors of study),
- β fraction of the component torsion capacity due to passive ground reactions to P that is effective at failure, $0 < \beta < 1$, (1 in this study),

A comparison of the measured failure load (from the model tests) and the predicted P_{ult} using the equation above is shown in Figure 4-14. In this figure the diagonal line represents the 1:1 line corresponding to a perfect agreement between measured and predicted. The circles in this figure correspond to torsion only tests, and the crosses represent the tests with combined loading performed by Duncan et al. (1995). Overall the predictions are quite good at least for the model piles considered.

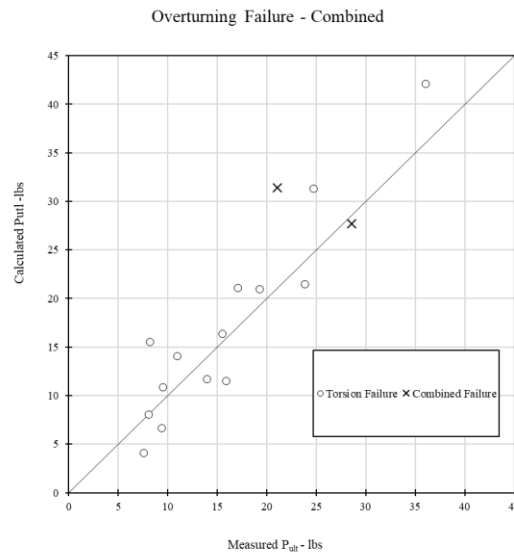


Figure 4-14: Results of models shafts (Duncan et al. 1995)

4.7. Alternative Foundation Systems

A new grouted precast driven pile was investigated by researchers at the University of Florida for FDOT (Herrera et al. 2017). The precast pile is driven into place and the grouted post installation to increase side and tip resistances. Photos of the pile are shown in Figure 4-15. The authors showed that this post-installation grouted pile results in similar or higher lateral and torsion load capacities compared to a drilled shaft of similar dimensions (embedment depth and width). Research regarding the feasibility of the pile is still ongoing, but results published by Herrera et al. (2017) suggest this pile has great

potential as an alternative foundation system to support coastal traffic signal mast arm structures. The study did not comment on any design or construction issues associated with possible vibrations induced during pile driving at sites located in urban environments.



Figure 4-15: Photos of grouted precast pile reported by Herrera et al. (2017).

An additional alternative foundation system that has been reported as having potential to support traffic infrastructure, included coastal traffic signal mast arm structures, are large diameter open ended driven steel pipe piles, as reported in the NCHRP study by Brown and Thompson (2015). However, for the specific application of this report a challenging issue is the often limited space or footprint right-of-way available for the installation of the foundations of traffic signal mast arms, particularly in urban settings.

A steel pipe pile with helical plate fins has been recently developed by PND Engineers Inc, as shown in Figure 4-16. These piles are proprietary based on the helical fin configuration near the tip and are marketed under the trade name SPIN FINTM piles (PND Engineers, 2018). The available information on these piles indicates they are utilized for sites with soft soils primarily to increase the axial capacity in compression and tension. No information was found related to torsional capacity for these piles.



Figure 4-16: Photo of SPINFIN finned pipe pile (Image from PND Engineers).

4.8. Summary

The literature review study shows that there is a need for more research that investigates the problem of drilled shafts under combined lateral and torsion loading. Most existing studies found focused on prediction of failure loads for lateral load and torsion separately. The few existing studies that involved combined lateral and torsion loading are useful but involved model testing under uniform, homogeneous soil conditions. There is a need for additional testing in particular full-scale field tests that involved combined lateral and torsion loading. Available experimental data shows the lateral load capacity of piles under combined torsion and lateral loading is significantly decreased and thus could become the controlling design consideration.

The literature review also revealed an important gap related to the need for static methods for predicting unit skin friction under torsion loading, or even better for combined torsion with axial and bending. The current methods are based on recent FHWA drilled shaft manuals (FHWA 2000 and 2010) that report different static methods based on axial

load testing so their applicability to the complex loading involved in traffic signal mast arms is questionable.

In terms of alternative foundation systems that could be used for supporting coastal traffic signal mast arm structures at sites with poor geotechnical conditions FDOT has reported research looking at driven post-grouted concrete piles. Other alternatives identified in this study include driven pipe piles (open or closed ended) and finned pipe piles.

CHAPTER 5: HURRICANE MARIA ACROSS PUERTO RICO

5.1. Introduction

This chapter provides a brief description of the hurricane Maria track across Puerto Rico. The chapter describes the event primarily from landfall to exit in Puerto Rico, i.e., from September 20, 2017 at about 6 am to September 21, 2017. This chapter also presents information on the wind speeds based on available data and reports. This is relevant to the failure case histories presented later in Chapter 6.

5.2. Natural Storm Maria 2017

The extended path of hurricane Maria reported by Banfield (2018) is shown in Figure 5-1. This figure shows the path of Hurricane Maria from September 16 when it was a tropical storm up to becoming a Category 5 hurricane. This figure also provides graphically the location of event landfalls with the respective wind speed as well as the peak gust intensity. The path of hurricane Maria affected many Caribbean islands including the Dominican Republic, the U.S Virgin Islands, and Puerto Rico. Hurricane Maria has been reported as the costliest Category 5 hurricane registered in the Caribbean, as well as the deadliest since Hurricane Mitch in 1999 (Banfield, 2018). One-minute sustained highest winds of 280 kph (175 MPH) were recorded, 3050 fatalities and an estimated damage of \$91.61 billion of dollars in the year 2017 (Banfield, 2018).

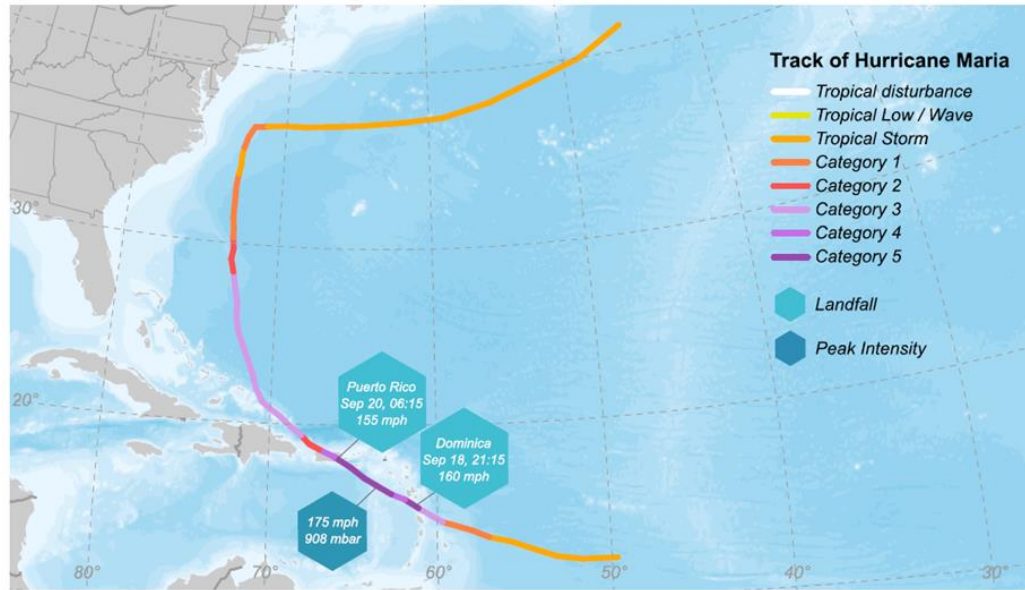


Figure 5-1: Hurricane Maria meteorological recap. (Adapted from Benfield, 2018)

Figure 5-2 is showing the variation of the wind speed and pressure during hurricane Maria along its path from September 14, 2017 to October 1, 2017. It can be observed in Figure 5-2 that the wind speed varied from about 20 MPH at the early stages of the path to a peak on September 19th of 180 MPH, and close to October 1, 2017 it drops to about 50 MPH sustained wind.

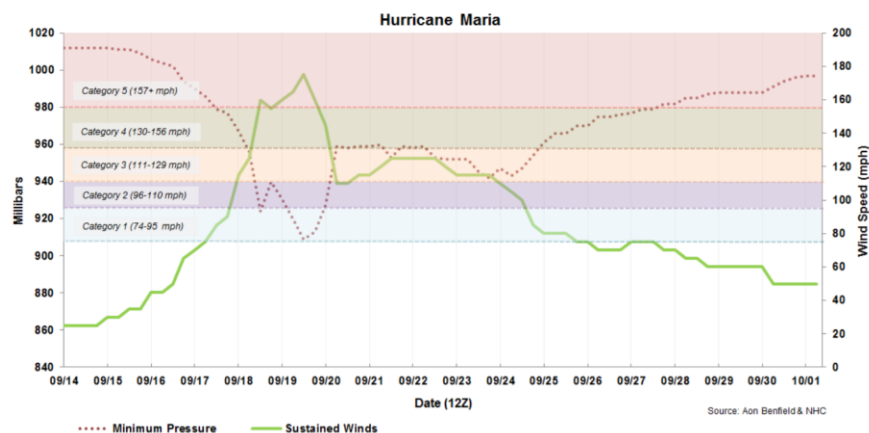


Figure 5-2: Variation of wind speed and pressure during hurricane Maria. (from Benfield, 2018)

5.3. Hurricane Maria event in Puerto Rico

At 10:15 UTC on September 20, 2017, hurricane Maria made landfall to the island of Puerto Rico near the town of Yabucoa as a hurricane Category 4 in the Saffir-Simpson hurricane wind speed scale with reported sustained winds of 250 km/h (155 MPH) (Benfield, 2018)). The storm made landfall in the southeastern region of the main island, then it followed a diagonal path across following a northwestern route as shown in Figure 5-3. After approximately eight hours, the hurricane emerged into the Atlantic on September 21, 2017 with reported sustained wind speeds of 175 km/h (109 MPH) sustained winds. Figure 5-3 shown the track hurricane in Puerto Rico, (Pasch, 2019).

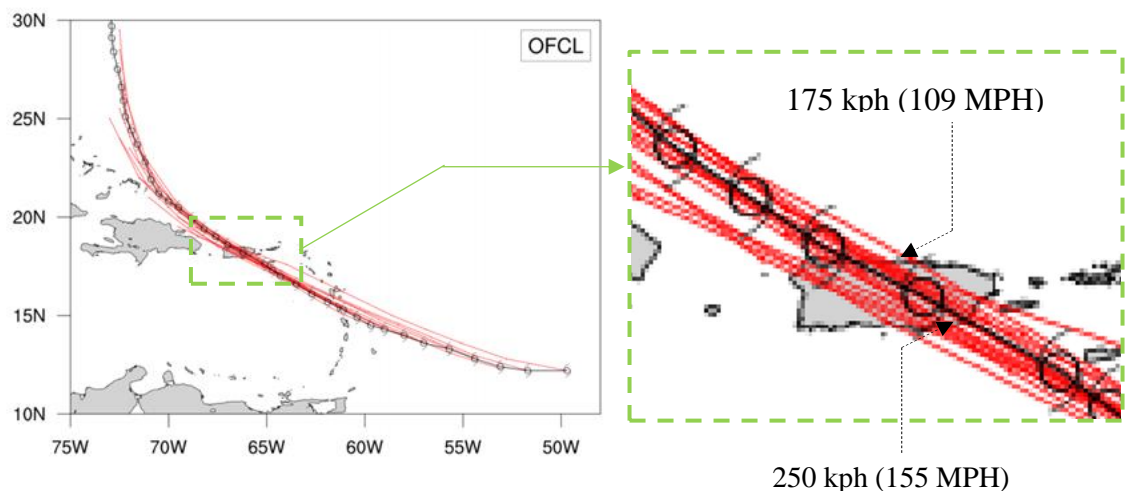


Figure 5-3: Track of hurricane Maria in Puerto Rico. (Adapted from Pasch, 2019)

Figure 5-4 shows a thermal satellite image of the hurricane Maria after landfall in Puerto Rico.

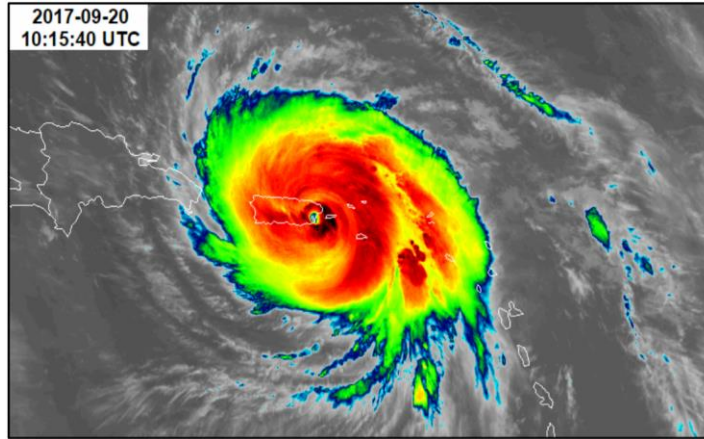


Figure 5-4: Thermal satellite image of Hurricane Maria after landfall in PR . (from Benfield, 2018)

Unfortunately, there is scarcity of wind speed data during the passing of Hurricane Maria across Puerto Rico. Most of the measuring equipment was designed to be capable of withstanding winds of up to 216 km/h (134 MPH) (Benfield, 2018). Figure 5-5 shows the maximum wind gust speeds measured during hurricane Maria. As could be observed, one of the stations shown in Figure 5-5 registered a wind gust of 112 MPH, this station is located at Arecibo 23 miles far away from the location of the zone that will be part of a case study performed and explained in following chapters.



Figure 5-5: Maximum wind gust in MPH during Hurricane Maria. (Adapted from Benfield, 2018)

5.4. Summary

The summary presented in this chapter shows that hurricane Maria was a Category 4 hurricane when it made landfall in the SE corner of PR on September 20, 2017 with sustained wind speeds of 250 KMH (155 MPH), and emerged near Arecibo in the NW of PR as Category 3 hurricane with sustained wind speeds of 185 KMH (109 MPH). The few wind speed data available indicates wind gust speeds as high as 180 KMH (112 MPH).

CHAPTER 6: FAILURE CASE HISTORIES HIGHWAY SIGN STRUCTURES IN PUERTO RICO DURING THE 2017 HURRICANE MARIA

6.1. Introduction

This chapter describes select failures of highways sign structures and one traffic signal structure that occurred during the 2017 Hurricane Maria. Six sites were identified during the GEER reconnaissance mission co-led by Dr. Francisco Silva-Tulla and Dr. Miguel Pando (Silva-Tulla et al., 2018).

6.2. Select highways and traffic signal failures

A total of six inverted L-shape highway and traffic signal structures are described in this chapter. The location of the selected structures is shown in Figure 6-1. The sites involved geotechnical failure of five inverted-L highway signs and one inverted-L mast arm traffic signal structure.

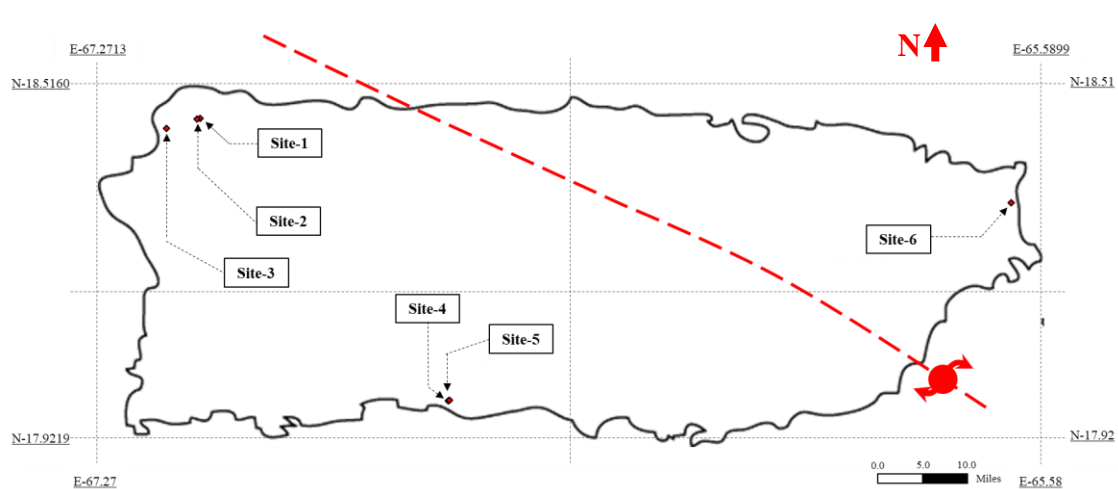


Figure 6-1: Locations of select failures

Three case studies were performed using information from Site 1, 2, and 3. The following sections describe the location, failure mode, among other findings for each site. The location and details of these three structures are provided in Table 6-1.

Table 6-1: Information of the select geotechnical failure sites

Site	Coordinates		Height of the pole (m)	Length of the arm (m)
	Longitude	Latitude		
1	18.4536	67.0891	9.2	9.5
2	18.4522	67.0938	9.2	9.5
3	18.4366	67.1478	9.2	9.5

6.2.1. Failure at Site-1

6.2.1.1. Description of the failure at Site-1

Figure 6-2 is showing the exact geographic location of the structure. As could be observed in this figure, the failure occurred in the northwest of the island, on westbound between Aguadilla and La Isabela.

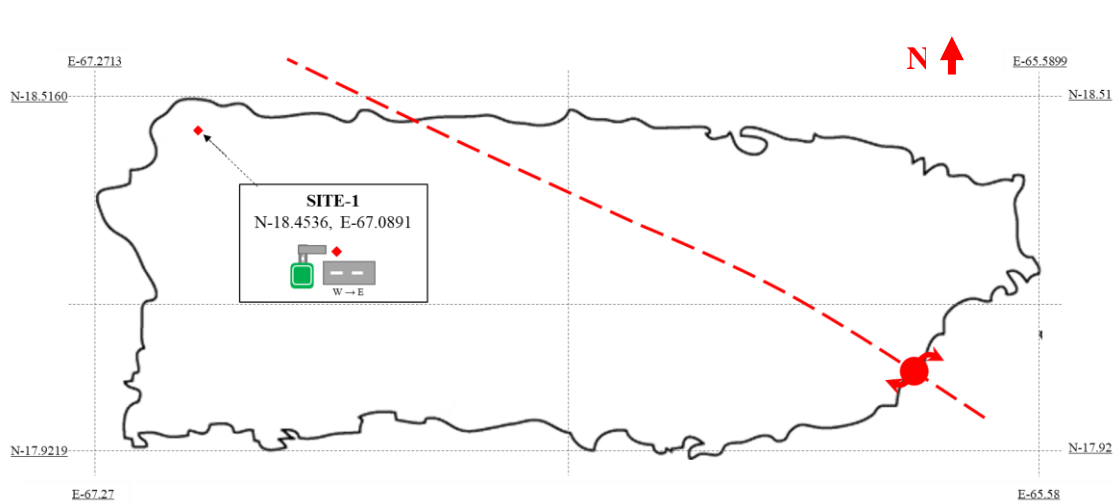


Figure 6-2: Location of the geotechnical failure at Site-1

Figure 6-3 shows front and back pictures of the CS structure at this site. The inverted L-shape structure is composed of a vertical pole, a horizontal truss with two chords and diagonals, and two highway signs.

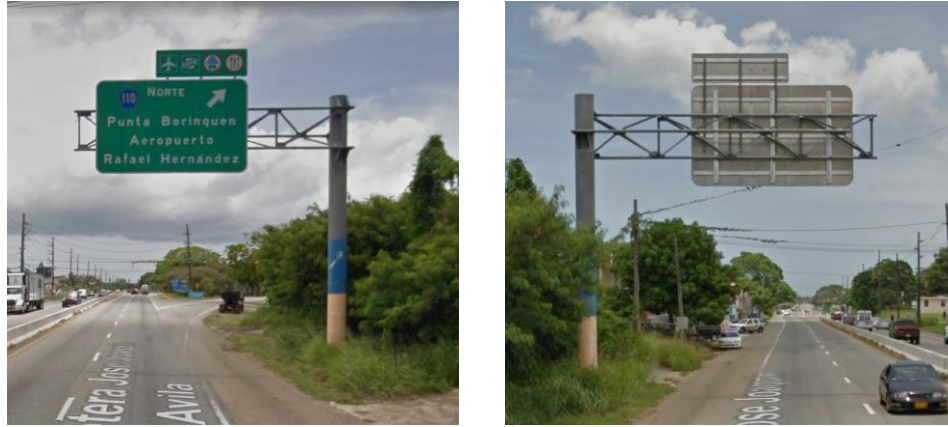


Figure 6-3: Front and back photos of CS structure at Site-1 before Hurricane Maria.
(from Google earth)

Figure 6-4 shows photos of the CS structure at Site-1 after the passing of Hurricane Maria. The photos show a significant rotation of the structure due to the high winds pressures associated with Hurricane Maria. The photos in Figure 6-4 show the inverted L-shape structure after the event. The photo in (Figure 6-4c) shows the pronounced gap that formed around the upper portion of the drilled shaft foundation that supports this structure.



Figure 6-4: Photos of CS structure rotated after hurricane Maria at Site-1. Figure 6-4(a)
(Silva-Tulla et al. 2018)

A graphical representation, using a photo before the hurricane from google maps, combined with photos after the event is shown in Figure 6-5. The final position of the CS structure shown in Figure 6-5 indicates a substantial rotational failure about the vertical axis (Y-axis as shown in figure inset).



Figure 6-5: Photo of the initial CS structure position and graphical representation of the CS structure rotated at Site-1. (Adapted from Google earth)

A similar figure shows a top view of the failure is shown in Figure 6-6. The final rotation showed in this figure is representing a counterclockwise rotation of about 135° . An approximate tilt of about 2 degrees of the pole with respect to the Zenith was also observed in its final failed position.

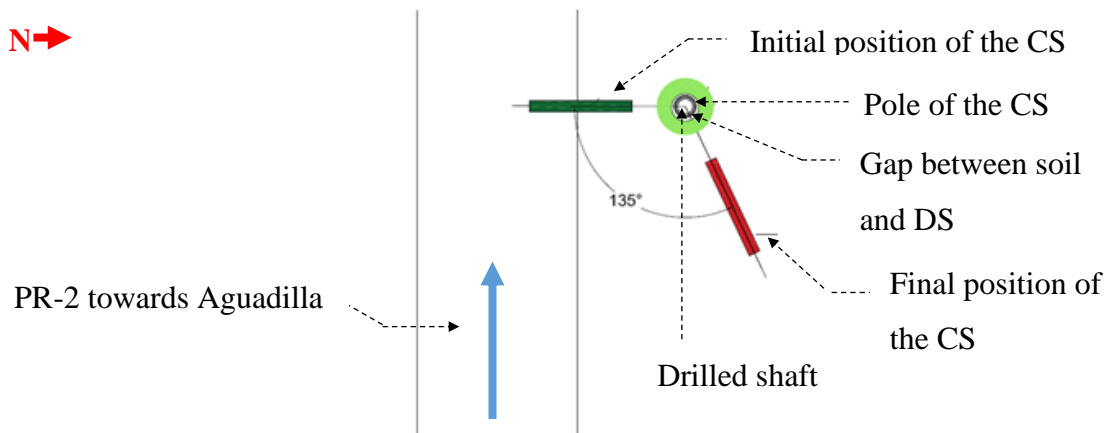


Figure 6-6: Graphical representation of the failure top view at Site-1

6.2.1.2. Geotechnical properties of the soil at Site-1

In order to obtain geotechnical soil information in this site, a hand boring 1.10 meters deep and 0.05 meters in diameter was performed. During the February 2018 field visit, shear vane tests were performed and samples were collected and retrieved to the lab. A grass and organic black soil layer of 0.10 meters was found and removed, then the soil in Site-1 was classified as sandy clay with some gravels, light yellowish. A full boring log of Site-1 is provided in Appendix A. Using three disturbed samples located at 0.38 (Sample-1.1), 0.40 (Sample-1.2), and 0.52 (Sample-1.3) meters, the tests listed in column 1 of Table 6-2 were performed.

Table 6-2: Summary of Index test results at Site-1

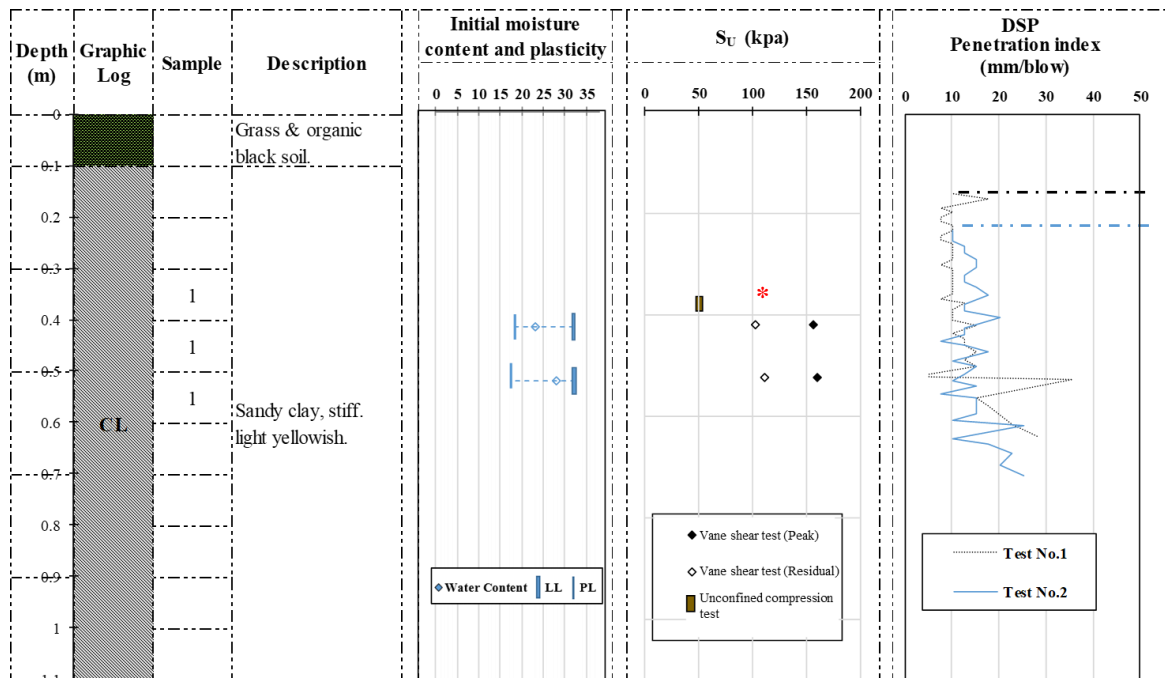
Test	Sample-1.1	Sample-1.2	Sample-1.3	Standard
Initial moisture content	20.34	23 %	28 %	ASTM D2216
Specific gravity	-	2.72	2.70	ASTM D854
Organic matter content	-	0.33 %	0.15 %	ASTM D2974
Plasticity index	-	13.5 %	14.09 %	ASTM D4318-
Unit weight	19.6 kN/m³	-	-	-
Gravel	7 %			ASTM D7928
Sand	34 %			
Fines	59 %			

The shear strength for the soil located in this site was obtained based on two vane shear tests located at 0.4 and 0.52 meters, as well as an unconfined compression performed on an undisturbed sample that was collected at 0.38 meters. Table 6-3 shows the shear strength results obtained.

Table 6-3: Summary of undrained shear strength results at Site-1

Depth	Sample-1.1	Sample-1.2	Sample-1.3	Standard
Undrained shear strength by Vane shear test (Peak)	-	156. kPa	160.0 kPa	ASTM D2573
Undrained shear strength by Vane shear test (Residual)	-	102.5 kPa	111 kPa	
Undrained shear strength by Unconfined Compression	53.8 kPa	-	-	ASTM D2166

Figure 6-7 shows a schematic representation of the soil profile in Site-1, this profile includes soil properties obtained from the geotechnical investigation. Properties displayed in this figure will be used in order to classify the soil, as well as correlate it with other properties needed in analysis design.



* The shear strength results obtained from the unconfined compression test was not considered because the sample had multiple vertical discontinuities and fissures. This sample and test were used in order to calculate, unit total weight $\gamma = 20 \text{ kN/m}^3$ and the initial degree of the saturation $S = 82.5\%$.

Figure 6-7: Generalized soil profile at Site-1

Table 6-4 lists geotechnical parameters that will be used in the followings chapters in order to predict the ultimate lateral and torsional soil capacity of the foundation using design methods.

Table 6-4: Parameters used in lateral and torsional analysis at Site-1

Test	Site-1	Source
Unit total weight kN/m ³	20	Unconfined compression
Undrained shear strength kPa	155	One of the results obtained by shear vane test
Type of soil/Soil classification	CL	By results from plasticity and size grain distribution

6.2.1.3. Characteristics of the drilled shaft foundation at Site-1

The drilled shaft embedment depth in Site-1 was obtained from the results of pile integrity test (PIT). Before performing PIT, an ultrasonic pulse velocity test (UPVT) on concrete was carried out using the Pulse Velocity Tester (James Instruments V-METER Mk II). Ten direct transmission readings were taken across the diameter of the DS at 0.15 meters from the top of DS as is shown in (Figure 6-8a). Five tests were performed from North to South DS direction, while the rest of the tests were performed perpendicular.

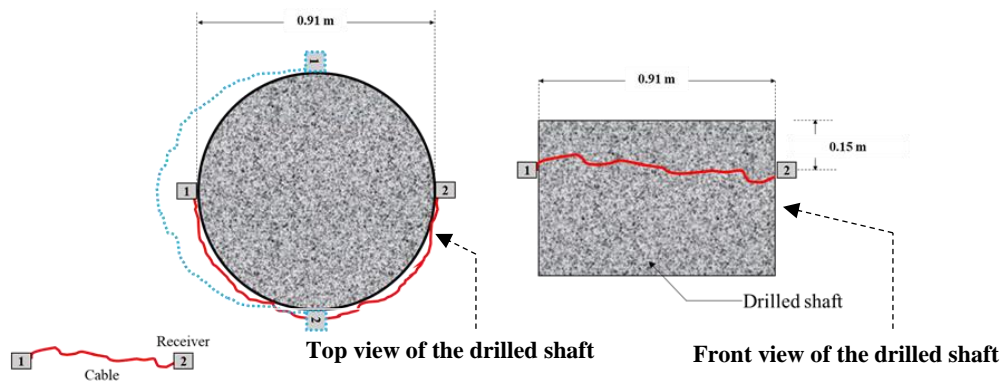


Figure 6-8: Ultrasonic pulse velocity test at Site-1

Figure 6-9 shows the results of the ultrasonic pulse velocity tests for this site. The average of the results from UPVT was calculated using is $2.49\text{E-}04$ s.

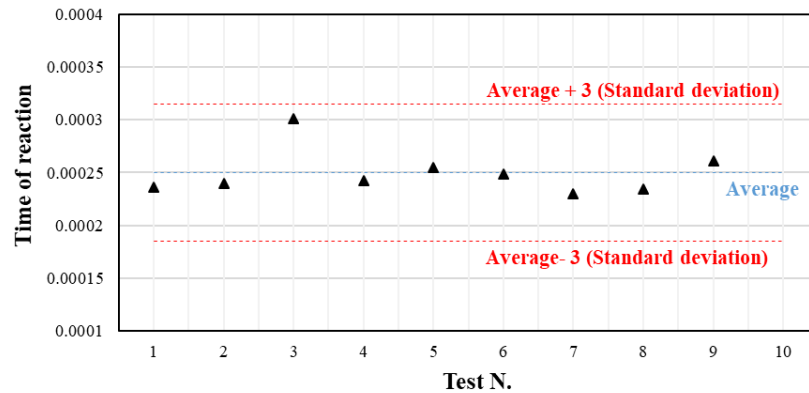


Figure 6-9: Ultrasonic pulse velocity results at Site-1

Before performing PIT tests, the top of the drilled shaft in Site-1 was cleaned. Some aggregate pieces which were stuck with cement to the surface were also found, these were removed using a driller. The surface was dried, grinded, rubbed and cleaned prior to performing the test as is shown in Figure 6-10.



Figure 6-10: Drilled shaft location of the PIT test

Figure 6-11 is showing the receptor and hammer position with respect to the drilled shaft top during tests at Site-1. In order to obtain good data quality, three different test configurations were used. Four, six, and twelve tests were performed following the first, second and, third configuration in this figure.

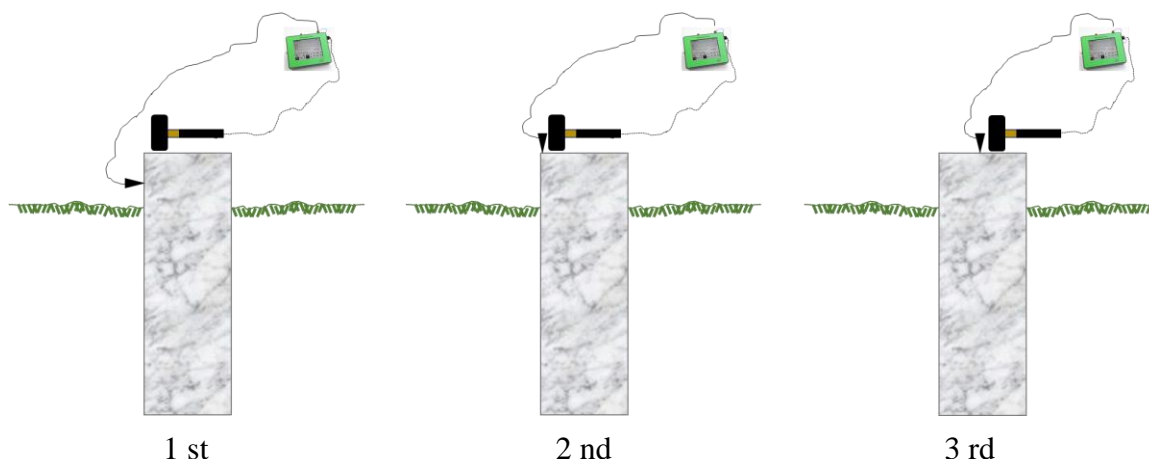


Figure 6-11 PIT test configurations

The results are shown using biaxial graphs in which the vertical and horizontal axis correspond to velocity and drilled shaft depth respectively. Figure 6-12 is showing the results obtained from a test performed using the third configuration in the figure above. The rest of the results obtained at this site can be observed in Appendix H.

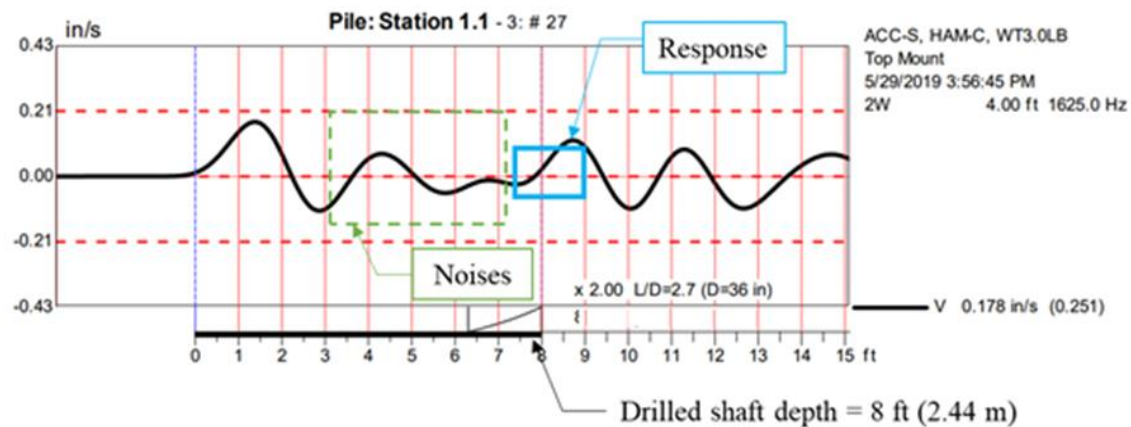


Figure 6-12 PIT results at Site-1

From this figure, the drilled shaft depth was determined as 2.44 m (8 ft).

Figure 6-13 shown a graphical representation with the dimensions of the drilled shaft encountered in Site-1. During February 2018 visit, the CS structure was still attached to the DS, however, in June 2019 visit the CS structure has been removed from the DS.

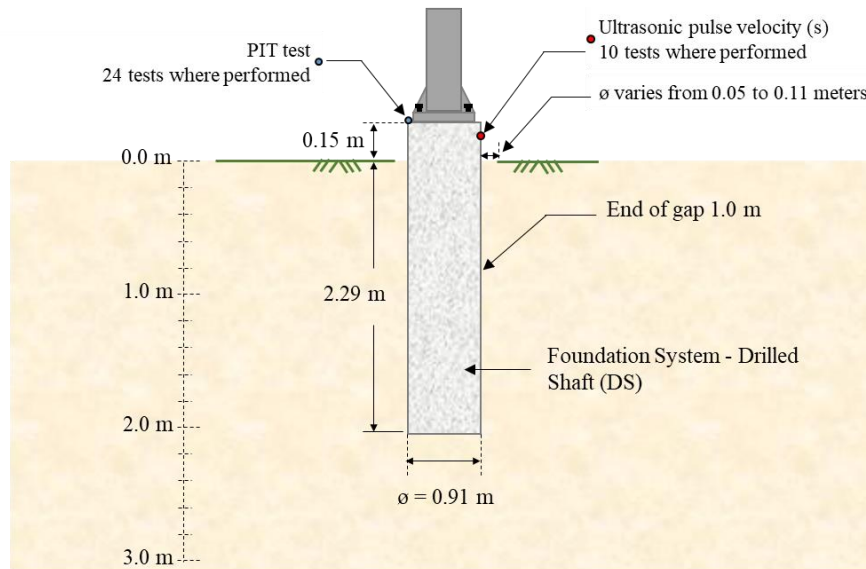


Figure 6-13: Characteristics and dimension of foundation system (Drilled shaft) at Site-1

6.2.1.4. Soil-structure interaction after Hurricane Maria at Site-1

A gap around the drilled shaft was formed as result of the soil deformations caused by the drilled shaft movements. In this case, the soil deformations encountered do not have a lot of variation. Figure 6-14 left shows a picture of the gap formed between DS foundation and the soil surround. The same figure also is showing a schematic top view of the soil-DS gap. Eight horizontal measures from the soil edge to the DS were taken using an engineering tape. The depth of the gap was obtained taking verticals readings in each location where the horizontal were taken.

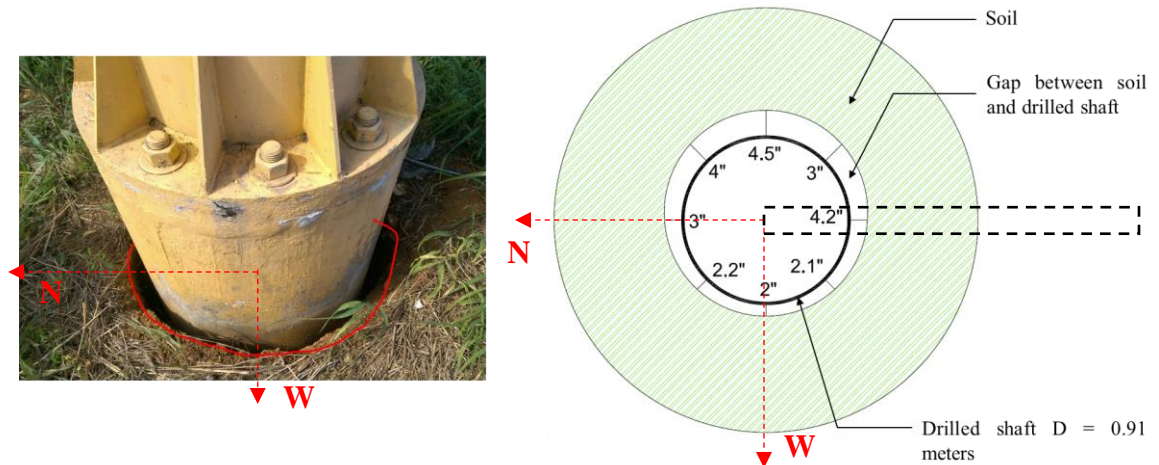


Figure 6-14: Schematic of the gap between soil and DS at Site-1

6.2.1.5. Summary of findings at Site-1

Figure 6-15 shows a schematic summary of soil, drilled shaft and inverted L-Shape characteristics found during the in this Site. Most of the results shown in this figure were obtained from the test performed in the field visit as well as in the geotechnical lab.

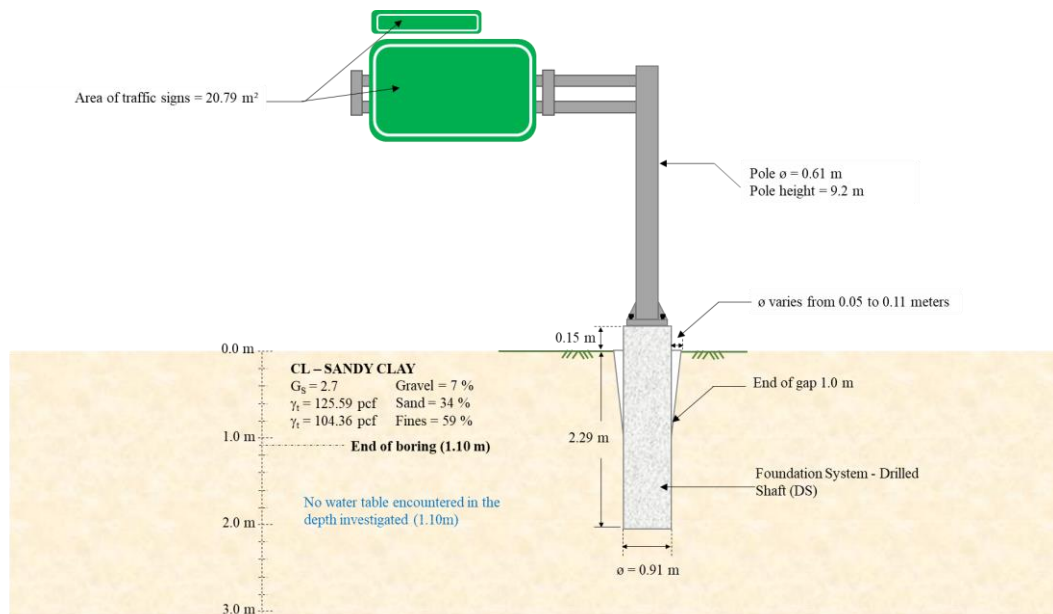


Figure 6-15: Summary of geotechnical and structural information at Site-1

6.2.2. Failure at Site-2

6.2.2.1. Description of the failure at Site-2

Figure 6-16 shows the exact geographic location of the structure. As could be observed in this figure, the failure occurred in the northwest of the Island, on westbound between Aguadilla and La Isabela.

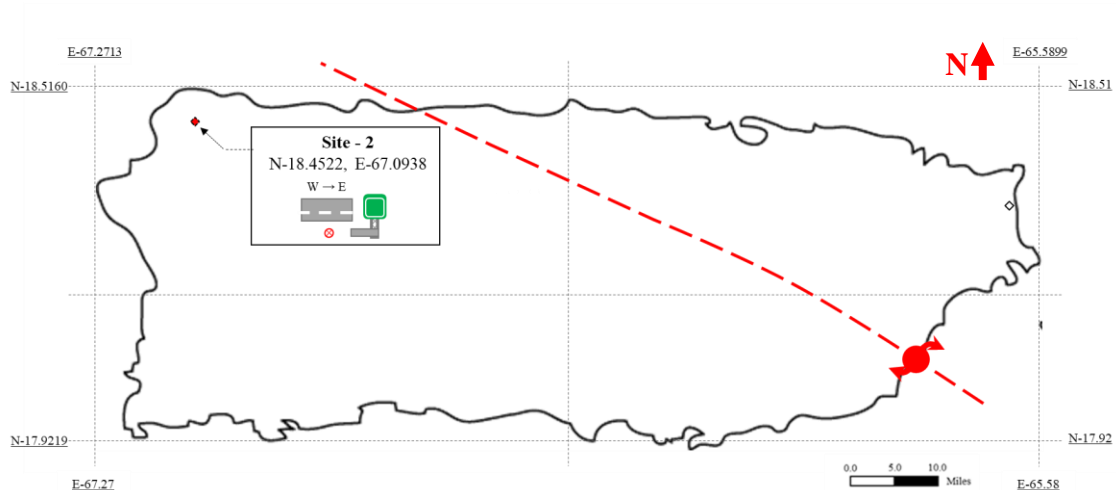


Figure 6-16: Location of the geotechnical failure at Site-2

Figure 6-17 shown frontal and back pictures of the CS structure in this site.



Figure 6-17: Front and back photos of CS structure at Site-2 before Hurricane Maria.
(from Google earth)

Figure 6-18 shows photos of the CS structure at Site-2 after the passing of Hurricane Maria. The photos show a significant rotation of the structure due to high wind pressure associated with Hurricane Maria. The photos in this figure show the inverted L-shaped structure after the event, the final position of the mast arm was rotated about 45 degrees clockwise with respect to the original installation position, and vertical tilt of approximately 9° with respect to the original vertical position.



Figure 6-18: Photos of CS structure at Site-2 after Hurricane Maria

Figure 6-19 is showing a graphical representation, using a photo before hurricane from google maps, combined with photos after the event is shown in Figure 6-19. The final position of the CS structure shown in this figure indicates a substantial rotation and tilted failure about the vertical and horizontal axis.



Figure 6-19: Photo of the initial CS structure position and graphical representation of rotate CS structure at Site-2. (Adapted from Google earth)

A similar figure shown a top view of the failure is shown in Figure 6-20.

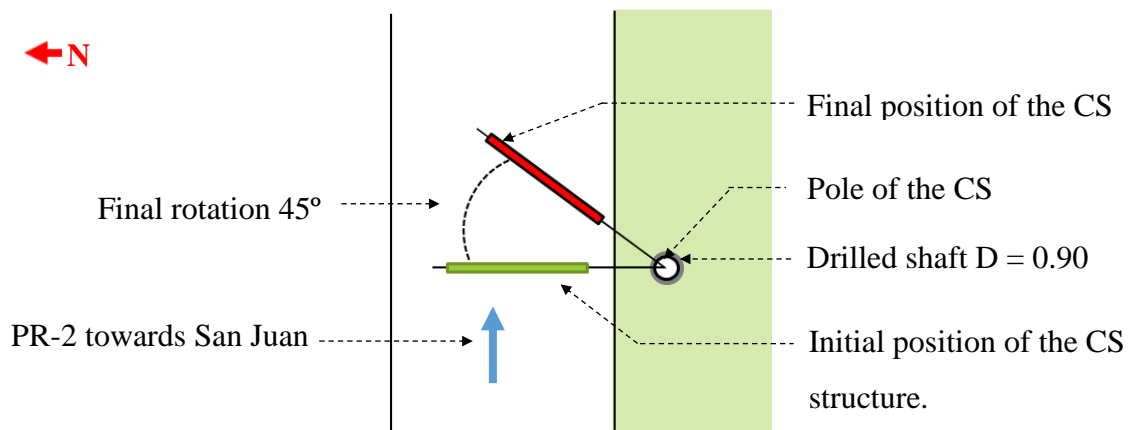


Figure 6-20: Graphical representation of the failure top view at Site-2

6.2.2.2. Geotechnical properties of the soil at Site-2

In order to obtain in-situ soil information in this site, a hand boring of 1.10 meters deep, 0.05 meters diameter, was performed. A grass and organic black soil layer of 0.10 meters was found and removed, then the soil in Site-2 was classified as sandy clay with some gravels, light yellowish, and has with high initial apparent moisture content. A full boring log of Site-2 is provided in Appendix A. Using two disturbed samples located at

0.30 m (Sample-2.1) and 0.60 m (Sample-2.2), the tests listed in column 1 of Table 6-5 were performed.

Table 6-5: Summary of Index test results at Site-2

Test	Sample-2.1	Sample-2.2	Standard
Initial moisture content	30.6 %	32.1 %	ASTM D2216 - 98
Specific gravity	2.69	2.68	ASTM D854-14
Organic matter content	0.61 %	0.71	ASTM D2974-14
Plasticity index	13.3 %	13.5 %	ASTM D4318-17e1
Gravel	4 %		ASTM D7928-17
Sand	32 %		
Fines	64%		

At this site, the vane shear test was not performed, and as no undisturbed samples were collected. The shear soil shear strength was assumed as the one found in Site-1 because the soil properties are very similar i.e., particle size distribution, specific gravity, plasticity index, among others. The approximate distance between both sites is only 500 meters and the elevations of the two sites are 150 and 149 m above sea level for Site-1 and Site-2, respectively. Table 6-6 shows a comparison between the results obtained from geotechnical investigation in each site, as well as, its difference expressed in percentage.

Table 6-6: Summary of comparison between geotechnical parameters in Sites-1 & 2

Test	Site-2	Site-1	Difference <small>Lower result/Greater result</small>
Initial moisture content %	31.3	25.5	0.81
Specific gravity	2.68	2.71	0.99
Organic matter content %	0.305	0.24	0.79
Plasticity index %	13.4	13.80	0.97
Gravel %	4	7	0.57
Sand %	32	34	0.94
Fines %	64	59	0.92

Figure 6-21 is showing a schematic representation of the soil profile in Site-2.

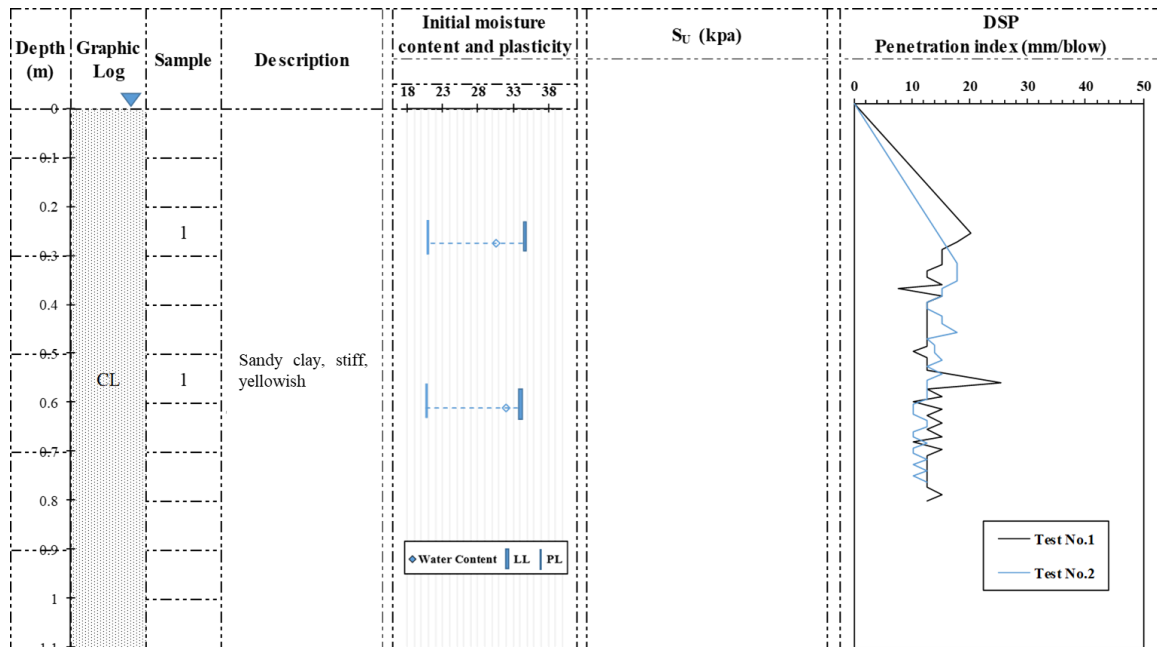


Figure 6-21: Generalized soil profile at Site-2

Table 6-7 lists the geotechnical parameters selected in order calculate the ultimate lateral and torsional soil capacity using different design methods.

Table 6-7: Geotechnical parameters used in lateral and torsional analysis at Site-2

Test	Site-2	Source
Unit total weight kN/m^3	20.0	Assumed as same than Site-1
Undrained shear strength kPa	155	Assumed as same than Site-1
Type of soil/Soil classification	CL	By results from plasticity and size grain distribution

6.2.2.3. Characteristics of the drilled shaft foundation at Site-2

As was described in section 6.2.1.3, in order to predict the DS embedment depth at Site 2, 12 ultrasonic pulse velocity tests were performed following the same configuration shown in Figure 6-8. The pulse velocity results, their average, and the standard deviation are shown in Figure 6-22.

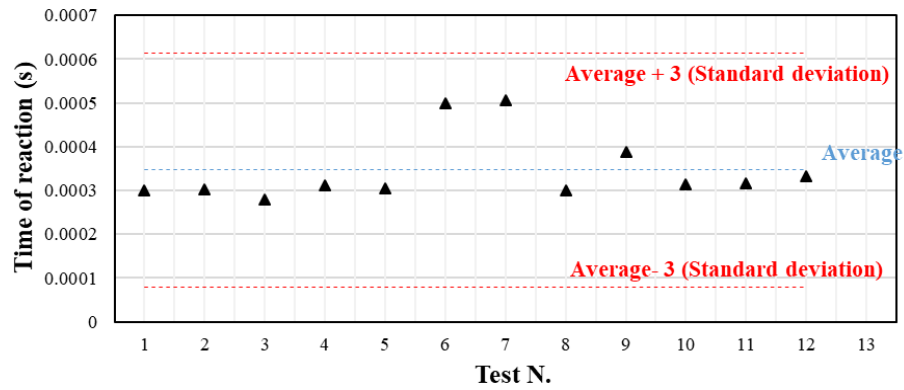


Figure 6-22: Ultrasonic pulse velocity results at Site-1

After performing UPVT, 21 PITs were performed following configurations 1 and 2 shown in Figure 6-11. One of the results obtained from PITs at this site is shown in Figure 6-23, while the rest of the results are shown in Appendix H.

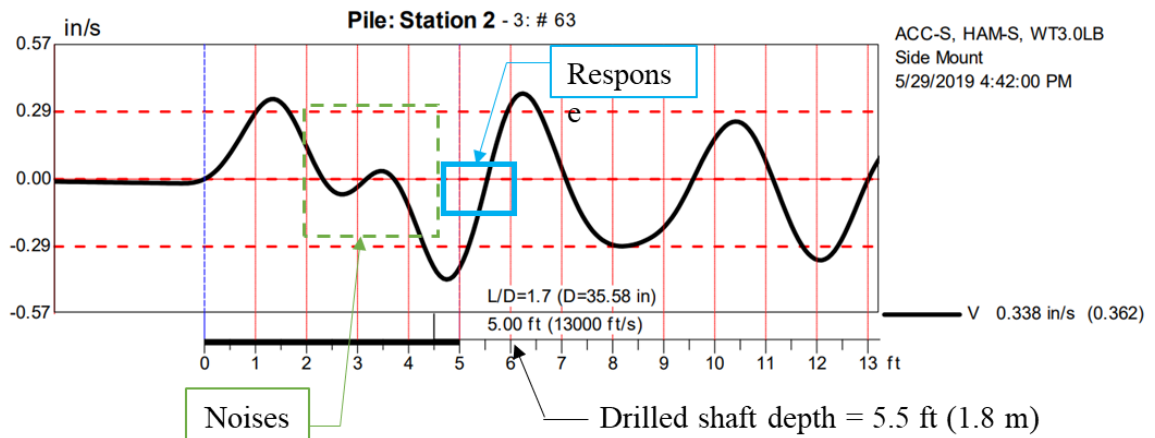


Figure 6-23: Ultrasonic pulse velocity results at Site-1

Figure 6-24 shows a graphical representation of the dimensions of the drilled shaft encountered in Site-2. During the June 2019 visit, the CS structure was still fixed to the drilled shaft.

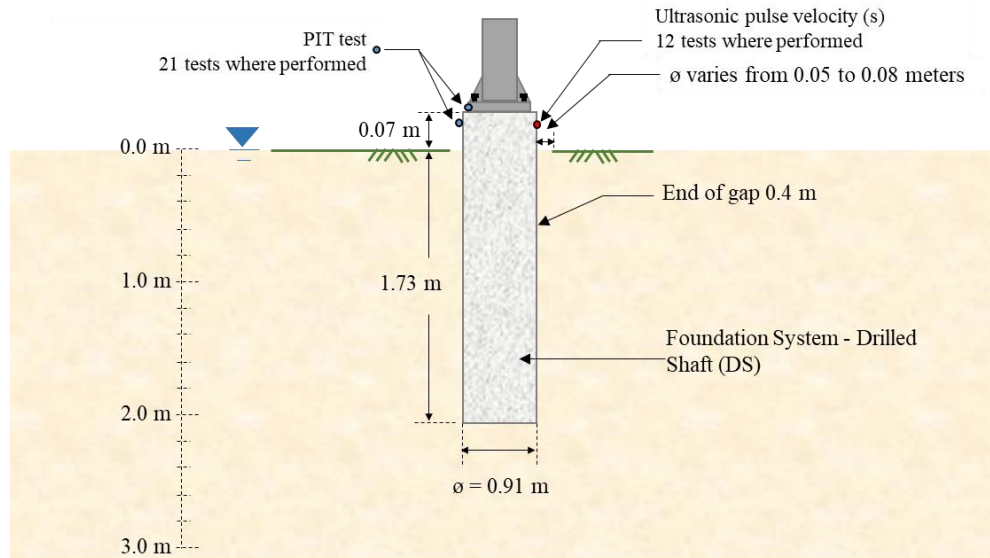


Figure 6-24: Characteristics and dimension of foundation system (Drilled shaft) at Site-2

6.2.2.4. Soil-structure interaction after Hurricane Maria at Site-2

A gap around the drilled shaft was formed as result of the soil deformations caused by the drilled shaft movements. In this structure, the gap was full of organic soil, branches, and grass. However, during the field visit, it was possible to identify the new material that covered the gap Figure 6-25.

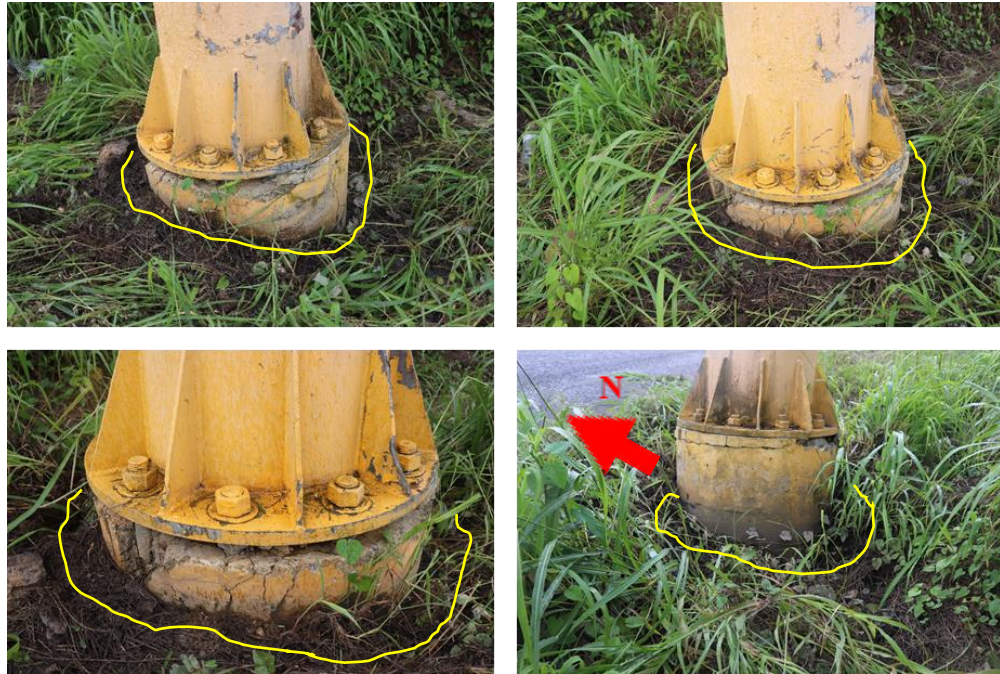


Figure 6-25: Photos of the gap between soil and DS at Site-2

Figure 6-26 shown a schematic representation of the gap top view performed with the measurements taken in field.

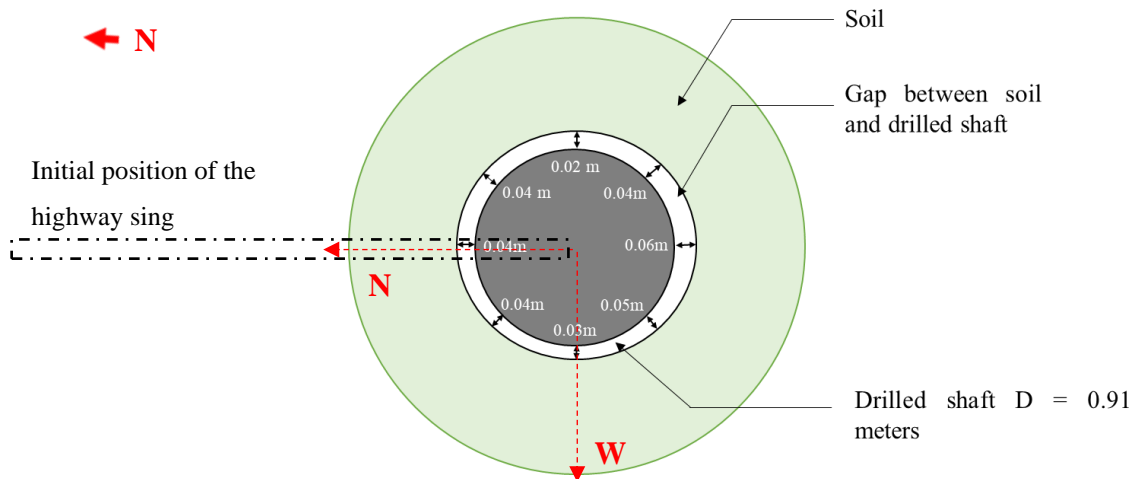


Figure 6-26: Schematic of the gap top view between soil and DS at Site-2

6.2.2.5. Summary of findings at Site-2

Figure 6-27 shown a schematic summary of soil, drilled shaft and inverted L-Shape characteristics found during the in this site. Most of the results shown this figure were obtained from the test performed in the field visit as well as in the geotechnical lab.

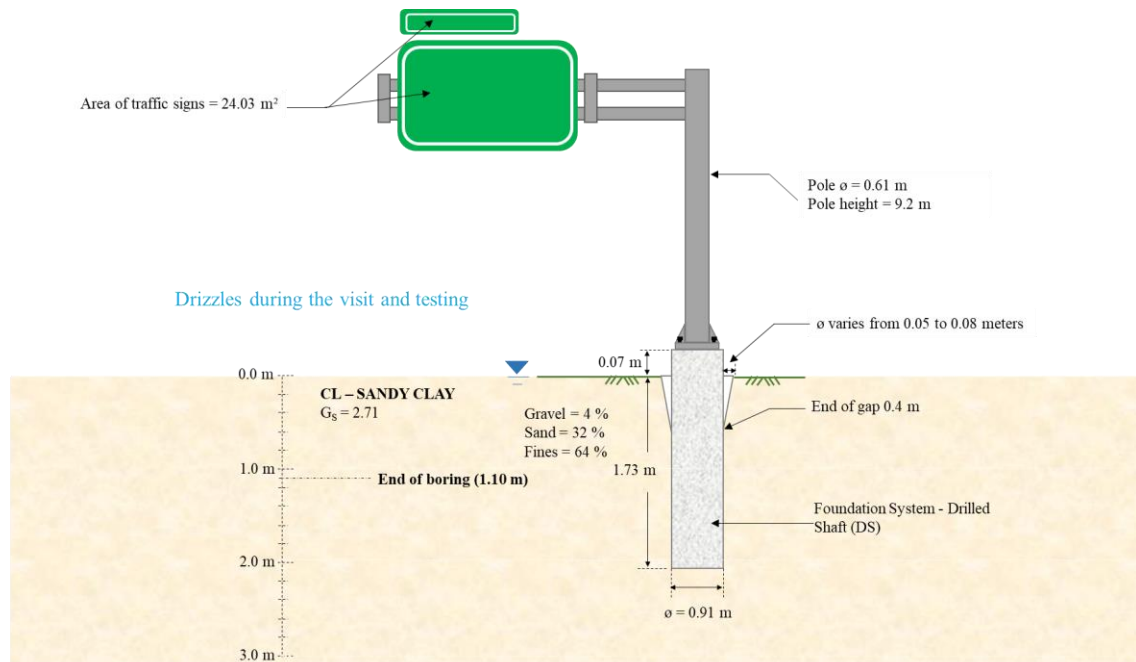


Figure 6-27: Summary of geotechnical and structural information at Site-2

6.2.3. Failure at Site-3

6.2.3.1. Description of the failure at Site-3

Figure 6-28 shows the exact geographic location of the structure. As can be observed in this figure, the failure occurred in the northwest of the Island, in front of Estadio Luis A. Canena Marquez.

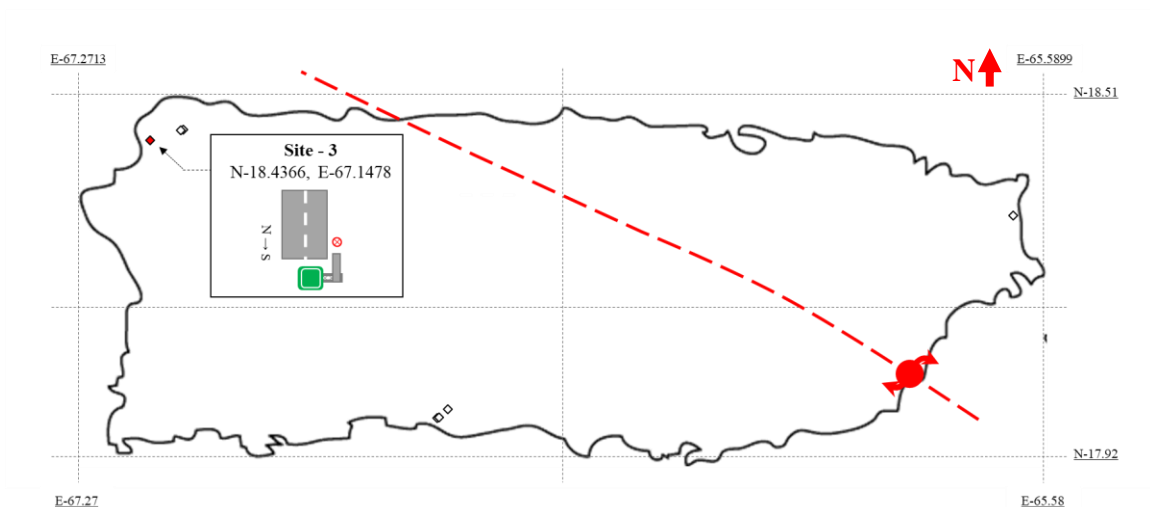


Figure 6-28: Location of the geotechnical failure at Site 3

Figure 6-29 shown front and back pictures of the CS structure in this site. The inverted L-shape structure is composed of a vertical pole, a horizontal truss with two chords and diagonals, and two highway signs.



Figure 6-29: Front and back photos of CS structure at Site-3 before Hurricane Maria.
(From Google Earth)

Figure 6-30 shows photos of the CS structure at Site-3 after the passing of Hurricane Maria. The photos show a significant rotation of the structure due to high wind pressure associated with Hurricane Maria. The photos in this figure show the inverted L-shaped

structure after the event, the final position of the truss was rotated about 115 degrees clockwise with respect to the original installation position, and vertical tilt of approximate 7° with respect to the original vertical position.



Figure 6-30: Photos of CS structure at Site-3. Figure 6-30 (b) (Silva-Tulla et al. 2018)

A graphical representation, using a photo before hurricane from google maps, combined with photos after the event is shown in Figure 6-31. The final position of the CS structure shown in this figure indicates a substantial rotation and tilted failure about the vertical and horizontal axis.



Figure 6-31: Photo of the initial CS structure position and graphical representation of rotate CS structure Site-3. (Adapted from Google Earth)

A similar figure shown a top view of the failure is shown in Figure 6-32. The final rotation showed in this figure is representing a counterclockwise rotation of about 115° . A considerable tilt of about 7° degrees of the pole with respect to the Zenith was also observed in its final failed position.

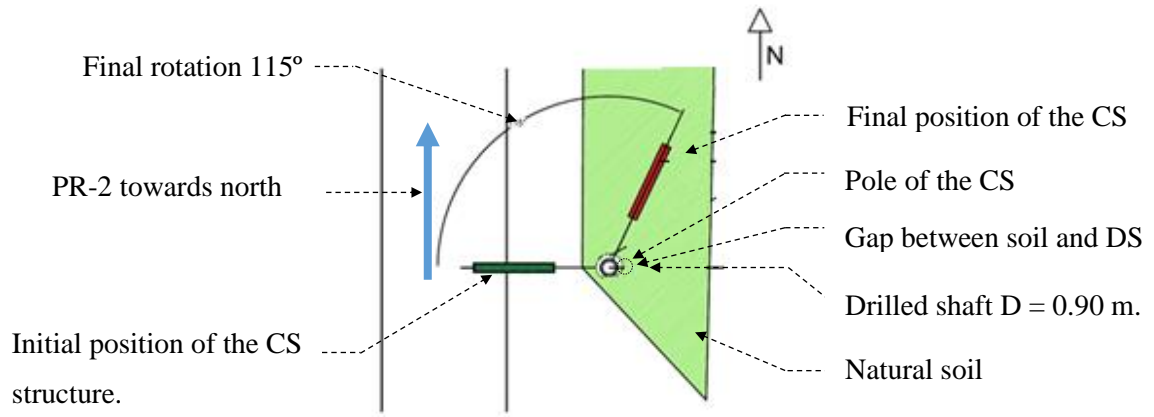


Figure 6-32: Graphical representation of failure top view at Site-3

6.2.3.2. Geotechnical properties of the soil at Site-3

In order to obtain geotechnical information in this site, a hand boring of 1.10 meters deep and 0.05 meters diameter was performed in Site-3. A grass and organic black soil

layer of 0.10 meters was found, then the soil in Site-3 was classified as silty sand with gravels, color very yellowish. A full boring-log of Site-3 is provided in APPENDIX A.

Using two disturbed samples located at 0.45 m (Sample-3.1) and 0.80 m (Sample-3.2), the tests listed in column 1 of Table 6-8 were performed.

Table 6-8: Soil classification summary

Test	Sample-3.1	Sample-3.2	Standard
Initial moisture content (ω)	8.2 %	9.0 %	ASTM D2216 - 98
Specific gravity	2.61	2.60	ASTM D854-14
Organic matter content	0.23 %	0.26	ASTM D2974-14
Plasticity index	1.8 %	1.3 %	ASTM D4318-17e1
Gravel	28 %		ASTM D7928-17
Sand	30 %		
Fines	42%-		

The soil shear strength was obtained based on two Vane Shear Tests located at 0.45 and 0.80 meters, Table 6-9 shown the results obtained.

Table 6-9: Summary of undrained shear strength results

Depth	Sample-3.1	Sample-3.2	Standard
Undrained shear strength by Vane shear test (Peak)	135 kPa	147.5 kPa	ASTM D2573 / D2573M
Undrained shear strength by Vane shear test (Residual)	81.5 kPa	92 kPa	

Figure 6-33 shown a schematic representation of the soil profile in Site-3, this profile includes soil properties obtained from the geotechnical investigation. Properties displayed in this figure will be used in order to classify the soil, as well as correlate it with other properties needed in analysis design.

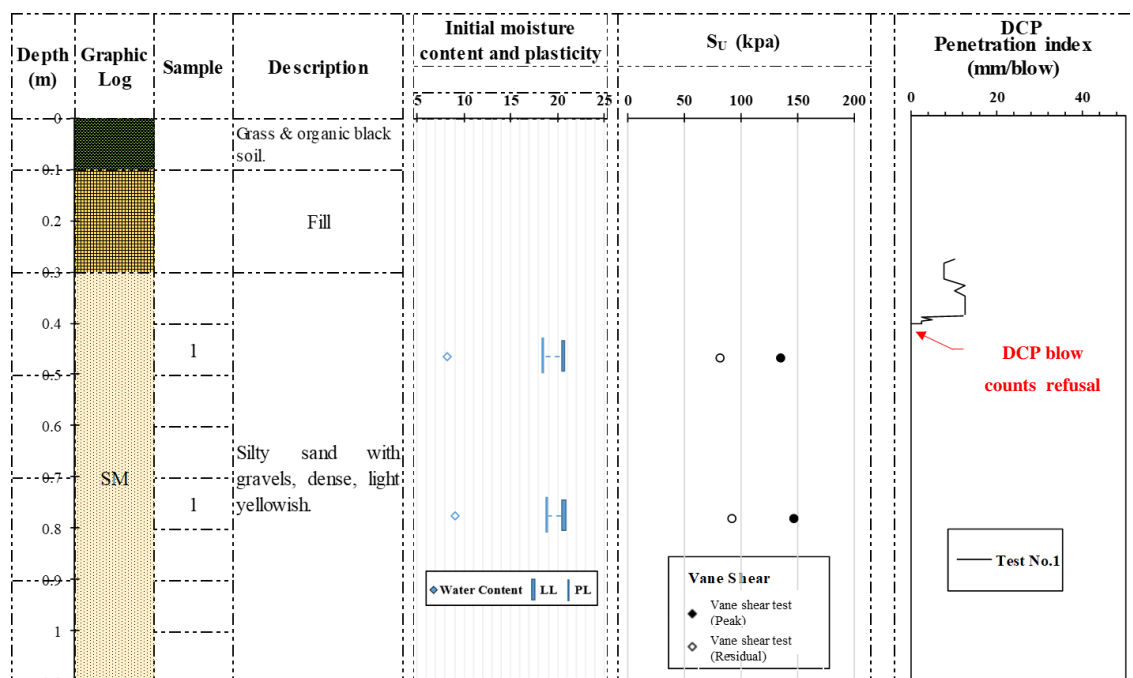


Figure 6-33: Generalized soil profile at Site-3

Table 6-10 and Table 6-11 listed the geotechnical parameters found in this site and the correlated parameters based on these geotechnical parameters.

Table 6-10: Summary of undrained shear strength results at Site-3

Test	Site-3	Source
Unit total weight kN/m ³	18.0	Based on results from grain size distributions, plasticity index, and specific gravity
Undrained shear strength kPa	140	Average of results obtained by shear vane test (Peaks)
Type of soil/Soil classification	SM	By results from plasticity and size grain distribution

Table 6-11: Summary of geotechnical correlations at Site-3

Soil parameter		Source
Friction angle	32°	(Terzhagi et al. 1967)
SPT blow counts N_{value}	22	(Karol, 1960)

6.2.3.3. Characteristics of the drilled shaft foundation at Site-3

Figure 6-34 shown a graphical representation with the dimensions of the drilled shaft encountered in Site-3. The diameter was measured using a flexible tape measure, however, during the last visit to Puerto Rico the DS and the CS structure have been removed by the Puerto Rico Department of Transportation.

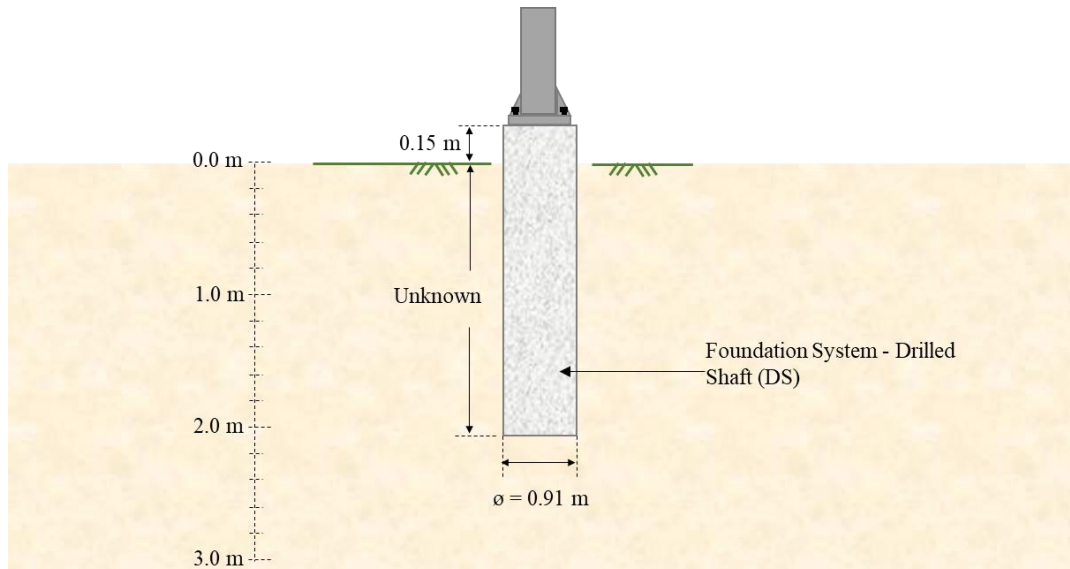


Figure 6-34: Characteristics and dimension of foundation system (Drilled shaft) at Site-3

6.2.3.4. Soil-structure interaction after Hurricane Maria at Site-3

A gap around the drilled shaft was formed as result of the soil deformations caused by the drilled shaft movements. In this site, the gap was only formed in one of the sides of the drilled shaft; more exactly were the lateral pressure of the soil was weaker because the DS was less embedded due to the levels differences Figure 6-35.

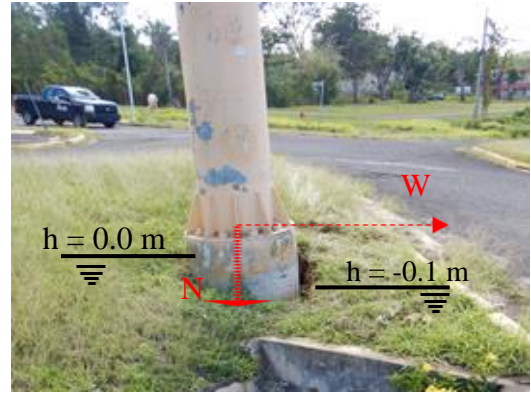


Figure 6-35: Photos of the gap between soil and DS at Site-3. FIGURE28 left (Silva-Tulla et al. 2018)

Figure 6-36 shown a schematic representation of the gap top view performed with the measurements taken in field.

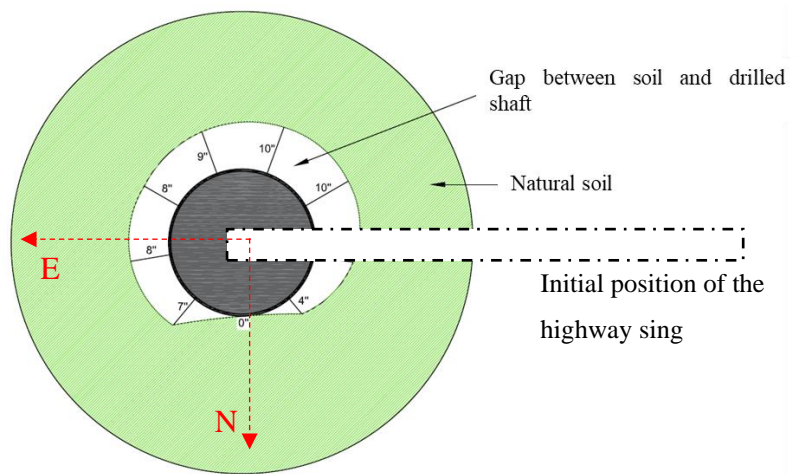


Figure 6-36: Schematic of the gap top view between soil and DS at Site-3

6.2.3.5. Summary of findings at Site-3

Figure 6-37 shown a schematic summary of soil, drilled shaft and inverted L-Shape characteristics found during the in this site.

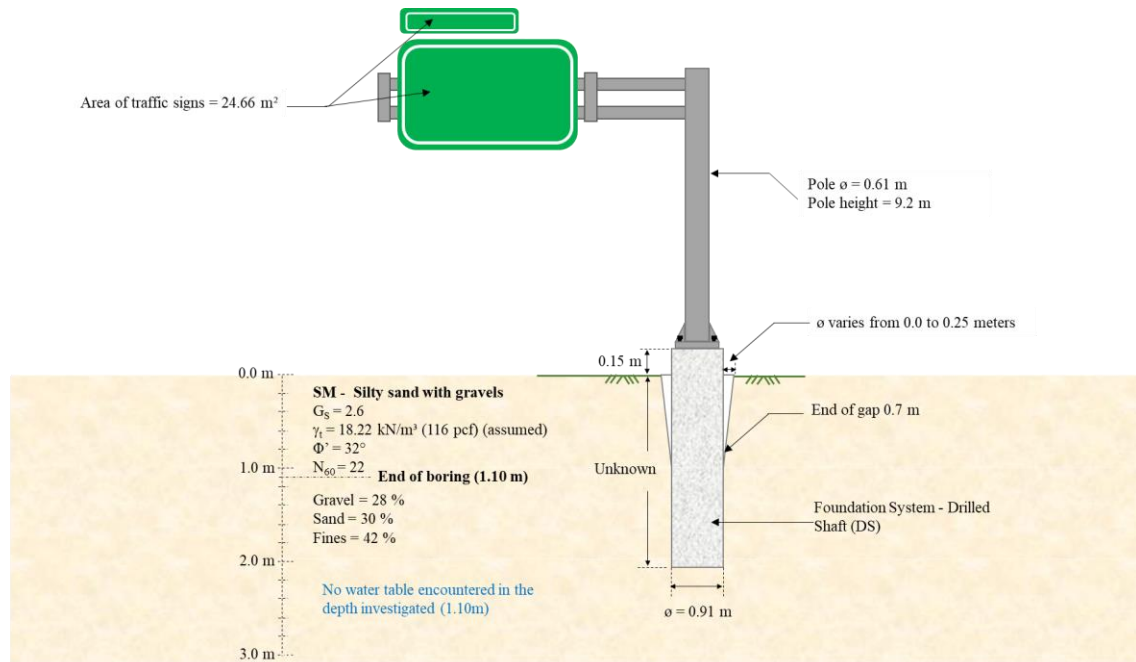


Figure 6-37: Summary of geotechnical and structural information at Site-3

6.3. Summary

This chapter summarizes the findings of three Sites during two visits to Puerto Rico. For each site, the failure, geotechnical soil properties and characteristics of the foundation system were described.

CHAPTER 7: ANALYSIS

7.1. Introduction

This chapter summarizes the loading demand resultants for three inverted L-shape CS structures described previously in chapter 6. In Sites where the cohesive soils governed, the maximum lateral load and torsional moment were calculated following the approaches described in APPENDIX B. For Site-2 where granular soils governed and the embedment depth of the drilled shaft was unknown, the required embedment depth was estimated following approaches for lateral load, torsional moment and coupled load and moment.

7.2. Methodology

The methodology in this chapter was addressed in two ways, *i*) in Sites-1 and 2 the soils loads and moments produced by the foundation was predicted using different approaches, and then compared with the loading demand produced by the inverted L-shaped structure. Whilst, *ii*) in Site-3 the required embedment drilled shaft to withstand the loading demands produced by the inverted L-shaped structure was predicted using different approaches.

The main methods for cohesive and cohesionless soils using in this chapter are listed in Table 7-1 and Table 7-2 respectively.

Table 7-1: Summary of analytical methods for cohesive soils considered

Method	Failure mode	Reference	Type of analysis	Comments
Broms	Lateral	(Broms, 1964a)	Ultimate capacity	Failure of short and long piles
P-y Curves	Lateral	(FB-Multipier, 2000)	Computational	Nonlinear finite element analysis program
β -Method	Torsional	(O'Neill and Reese 1999)	Ultimate capacity	Based on load transfer ratio β
Florida district 7 method	Torsional	(Hu, 2003)	Ultimate capacity	Based on load transfer ratio β
Colorado DOT	Torsional	(Nusairat et al. 2004)	Ultimate capacity	Based on load transfer ratio β

Table 7-2: Summary of analytical methods for cohesionless soils considered

Method	Failure mode	Reference	Type of analysis	Comments
Broms	Lateral	(Broms, 1964b)	Ultimate capacity	Failure of short and long piles
P-y Curves	Lateral	(FB-Multipier, 2000)	Computational	Nonlinear finite element analysis program
FHWA-10 Brown et al. (2010)	Torsional	(O'Neill and Reese 1999)	Ultimate capacity	Based on load transfer ratio β (Depth dependent)
FDOT manual (ω)	Torsional	FDOT Manual (modification of (O'Neill and Reese 1999))	Ultimate capacity	$\omega = \beta$ Failure defined if shaft rotation exceeds 10 degrees. FDOT removed depth (z) dependency. (Depth independent)
Colorado DOT	Torsional	(Nusairat et al. 2004)	Ultimate capacity	(Depth independent)
Tawfiq-Mtenga method	Coupled	(Duncan et al. 1995)	Ultimate capacity	Torsional and lateral loading combined

A description of methods and formulas is provided in APPENDIX C.

7.3. Analysis of failure sites

Figure 7-1 shown a schematic representation of the moments and shear applied on the top of the drilled shaft supporting an inverted-L structure. Bending moment, torsion moment and shear load are acting about xz-axis, y-axis, and x-axis respectively.

Y

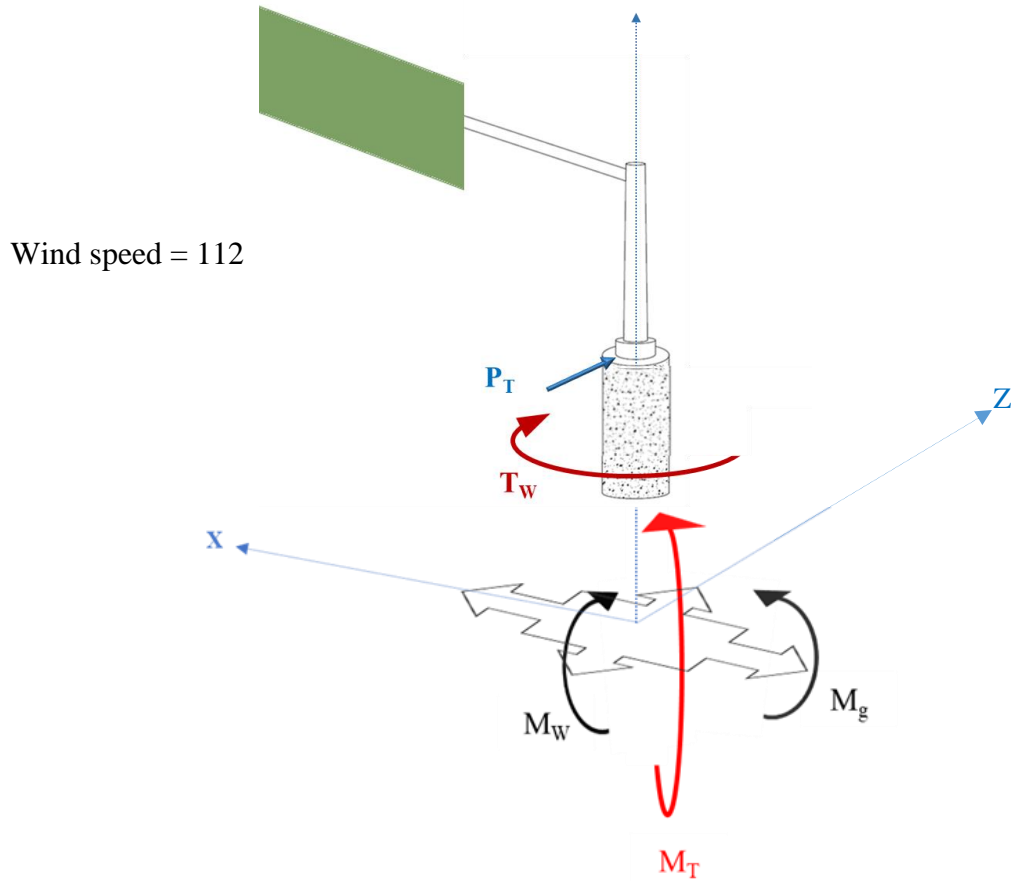


Figure 7-1: Schematic loading demand of an inverted L-shape CS structure

7.3.1. Failure study of Site-1

Table 7-3 shown the resultant reactions and moments calculated with the approach described in chapter 2 section 2.3 loading demand of inverted L-shape structures. This procedure was based on AASHTO 2009 LTS-5.

Table 7-3: Resultant moments, bending moment and shear

SITE-N.	P_t (kN)	M_w (kN·m)	M_g (kN·m)	M_t (kN·m)	T_w (kN·m)
1	61.6	453.6	53.8	456.8	271.5

7.3.1.1. Predicted lateral loads

Brom's method (1964a)

As was described above, the drilled shaft length in this Site-1 is 2.44 m, the diameter 0.91 m, and the ratio $L/D = 2.7$, i.e. very short shaft (UNISING, 2019). For this drilled shaft the required undrained shear strength to withstand the loading demand of the inverted L-shaped structure was predicted using Brom's assumption. The assumptions and diagrams of this method are described in APPENDIX C of this document.

Broms indicates that at the point of M_{\max} can be computed with Eq. 7-1.

$$M_{\max} = M_T \cdot P_T \cdot (f + 1.5 D) - \frac{9 \cdot S_u \cdot D \cdot f^2}{2} \quad (7.1)$$

where, the distance f is shown in figure C-1, M_T and P_T are the total moment (M_W) and shear load (P_T) acting in the foundation, D is the diameter of drilled shaft and S_u is the undrained shear strength. According to Broms the point of M_{\max} occurs at $V = 0$, at a distance of $1.5D + f$ and can be computed as shown in Eq. 7-2.

$$f = \frac{P_T}{9 \cdot S_u \cdot D} \quad (7.2)$$

If Eq. 7-1 is replaced in Eq. 7.2, the M_{\max} can be computed as shown below:

$$M_{\max} = P_T \cdot (e + 1.5D + 0.5 \cdot f) \quad (7.3)$$

As well as, the distance g can be computed knowing the drilled shaft length as is shown in E.q. 7.4. At this point important to bear in mind that Brom's makes an exclusion zone in the drilled shaft top of $1.5 D$ shaft diameters.

$$g = L - f - 1.5D \quad (7.4)$$

The ratio of length and diameter suggests that shaft in this Site, is very short L/D , therefor, the S_u required to withstand the loading demand produced by the inverted L-shaped structure in this site was computed for two cases; considering the total shaft length,

in others words as $g = L + f$ (Brom's modified), as well as, original method proposed by Broms, where g can be calculated as shown in Eq. 7.4.

Table 7-4 shown the predicted S_u resulted from both methods, as well as, the factor of safety resulted from the ratio of the S_u predicted and S_u in site.

Table 7-4: Required S_u and FS computed following (Broms, 1964a) assumptions

	(Brom's, 1964,a) $g = L - f - 1.5D$	(Brom's modified) $g = L - f$
$S_{U \text{ required}} \text{ (kPa)}$	209.4	38.88
F.S	0.74	3.99

As could be observed in results shown in Table 7-4 following the standard approach by (Broms, 1964a), i.e. ignoring the 1.5D zone , the factor of safety is less than 1, which means that loading demand produced by inverted L-shaped structure is greater than the foundation predicted by this method. With this in mind, the minimum embedment depth to withstand the structure and the factor of safety were computed and plotted in Figure 7-2.

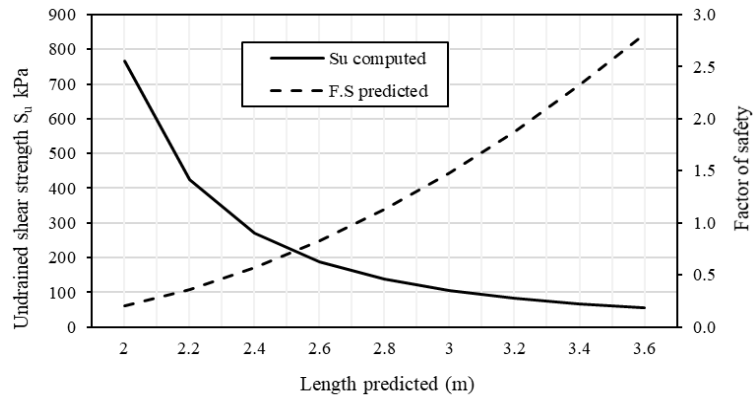


Figure 7-2: Predicted undrained shear strength and factor of safety using (Broms, 1964a) P-y curve method

The p-y curves were modeled using approaches proposed by Reese and Welch's (1975) and (API) Clay model. Both models and respective curves are summarized in

APPENDIX C. The computed relationship between applied load and pile head lateral displacement for a drilled shaft with a diameter of 0.91 m and embedment length of 2.44 m is presented in Figure 7-3 and Figure 7-4 for Reese and Welch's and API models respectively.

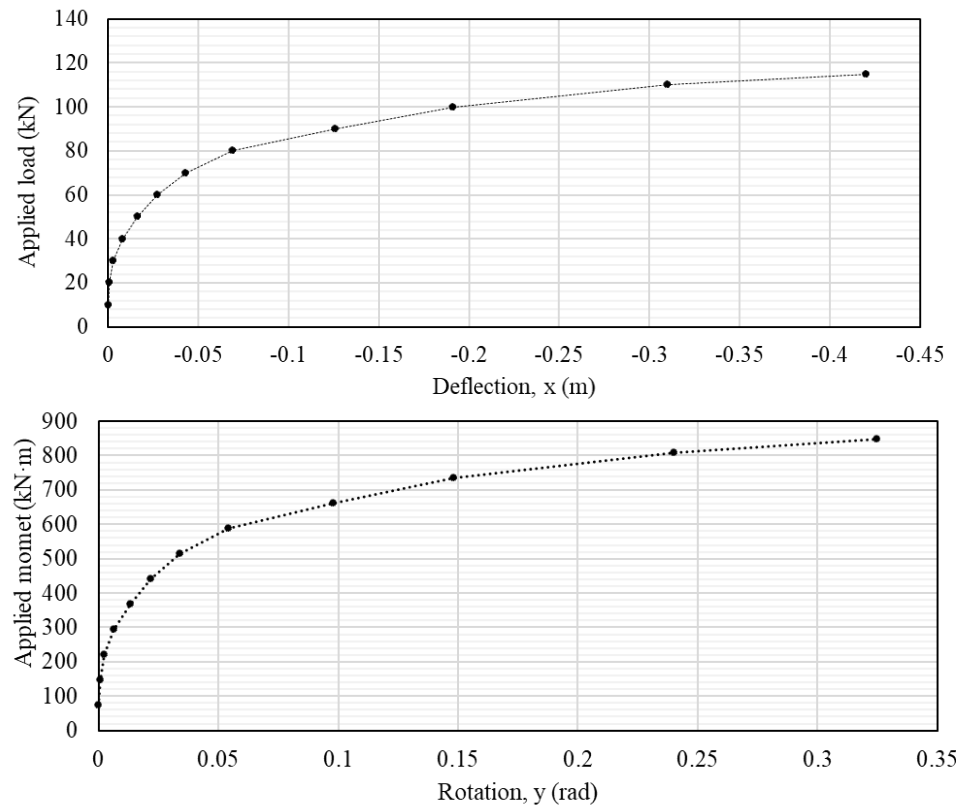


Figure 7-3: Predicted deflection of a drilled shaft with length of 2.44 m and diameter of 0.91 m using Reese and Welch's (1975) model

The nominal lateral load resistance and the nominal moment resistance for this drilled shaft dimensions are 116 kN and 950 kN·m respectively.

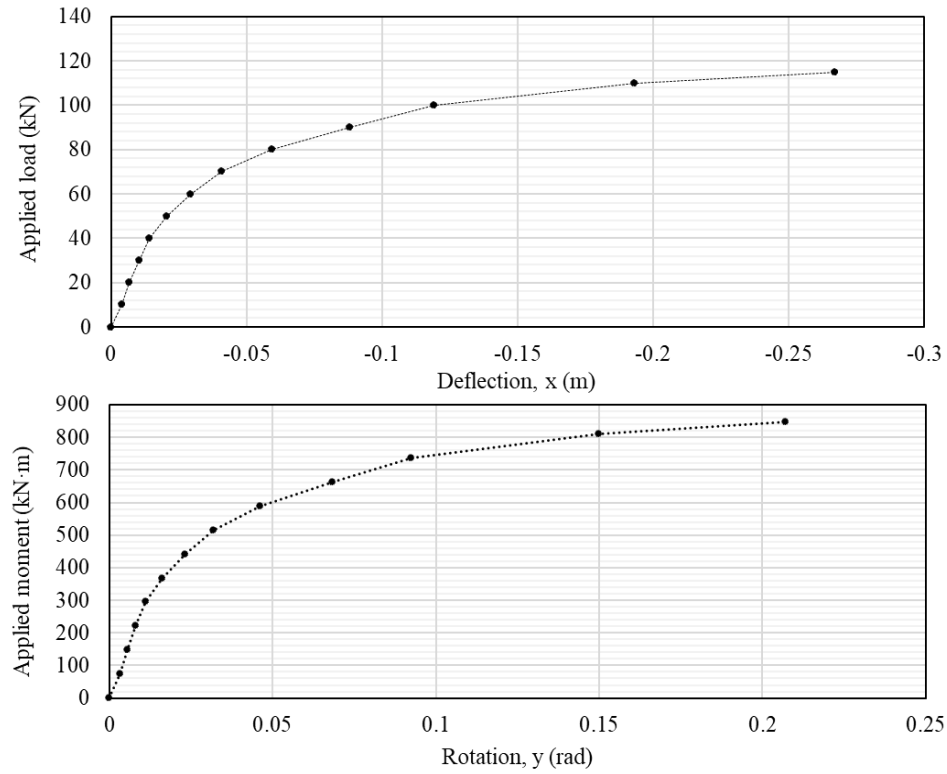


Figure 7-4: Predicted deflection of a drilled shaft with length of 2.44 m and diameter of 0.91 m using API model

The nominal lateral load resistance and the nominal moment resistance for this drilled shaft dimensions are 118 kN and 850 kN·m respectively. Table 7-5 shown a summary of results obtained using p-y curve models and the respective factor of safety.

Table 7-5: Summary of loads and moments predicted using p-y curves

Model	Predicted load kN	Predicted moment kN·m	Factor of safety
Reese and Welch's (1975)	116	950	1.99
(API) Clay model	118	850	1.89

7.3.1.2. Predicted torsional moments

Methods based on side shear resistance

The results provided in this subsection were obtained based on unit shaft resistance in cohesive soils that were calculated considering the undrained shear strength. The predicted torsional moments computed with the different design methods are summarized in Table 7-6; this table also shows the factor of safety computed for the loading demand presented in this site.

Table 7-6: Summary of predicted torsional moments results

Method	Predicted Torsional moment kN·m	Factor of safety
α method	252.57	0.93
(Hu, 2003)	87.13	0.32
(Nusairat et al. 2004)	217.08	0.79

As can be observed, the computed factor of safety does not exceed a unit in any method. As well, as, this table is showing a very small factor of safety computed by (FHWA, 2010) method, which occurs because this method does not consider 1.5 meters from the drilled shaft length.

Using similar approach for other embedment depths, the results in Figure 7-5 were obtained. This figure shows 3 curves corresponding to methods listed in column 1 of Table 7-6.

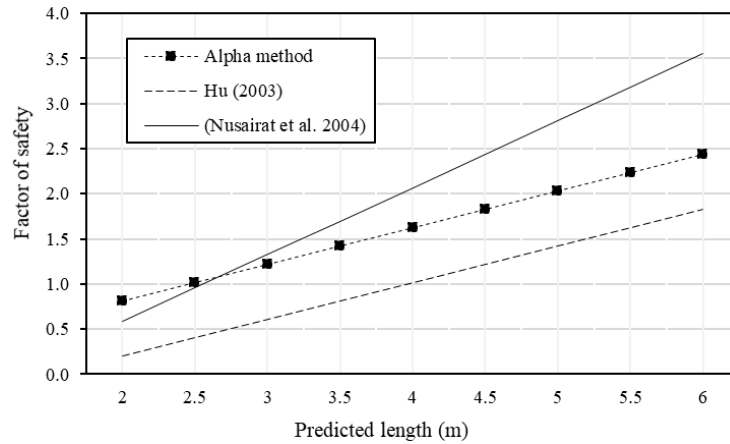


Figure 7-5: Relationship between the embedment depth and factor of safety

7.3.1.3. Summary of results

A summary of predicted maximum loads and moments obtained with lateral and torsional design methods is shown in Table 7-7.

Table 7-7: Summary of FS computed for different prediction failures

Failure mode	Method		F.S
Lateral	Broms	Broms, (1964a)	0.6
Lateral		Broms modified	3.4
Lateral	P-Y (FB-Multiplier)	Reese, 1975	2.0
Lateral		API	1.9
Torsional	Frictional method	α method	0.9
Torsional	Frictional method	Hu (2003)	0.3
Torsional	Frictional method	(Nusairat et al. 2004)	0.8

7.3.1.4. Discussion of results

Figure 7-6 shown the minimum predicted embedment depths required to withstand the lateral and torsional loading demand with a factor of safety of 2 using the methodologies described above. From this table, it can be seen that the required embedment lengths to withstand torsion loading are considerably higher than those required to resist

lateral loading. As can be observed in this figure, in almost all the cases the predicted embedment depths computed with torsional approaches are the double than those depths computed with lateral approaches. The results are supported the field visit in which it could observe that final position of the CS structure shown a failure due to torsional loading.

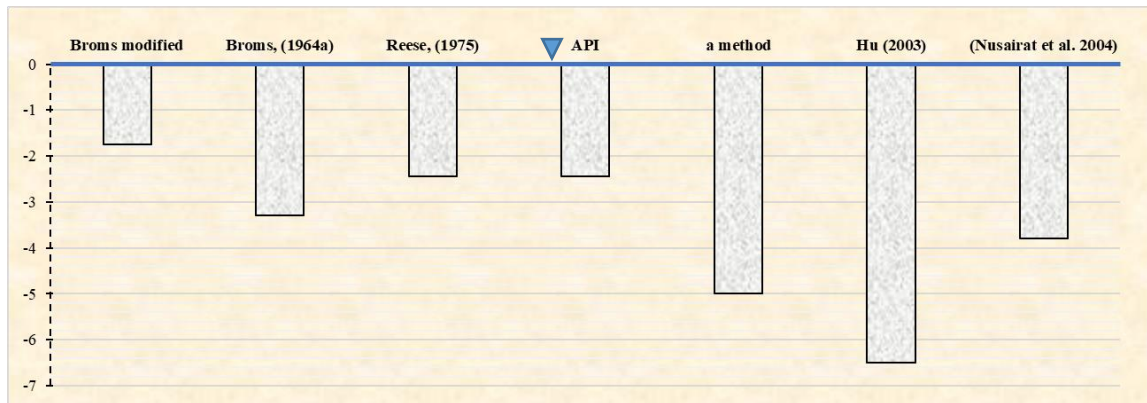


Figure 7-6: Schematic of the comparison of minimum embedment depths required to carry lateral and torsional load demand

The condition described above i.e., failure due to torsion, makes think that torsional loading is greater than lateral loading; nevertheless, it was found that for a CS structure of ratio pole height to arm length of 0.64 as the structure in this Site, the torsion loading never exceeds the lateral loading. The performance described above can be observed in Figure 7-7, which in the horizontal axis the lateral and torsional predicted loading is shown while the vertical axis is showing the wind speed used to calculate the loadings.

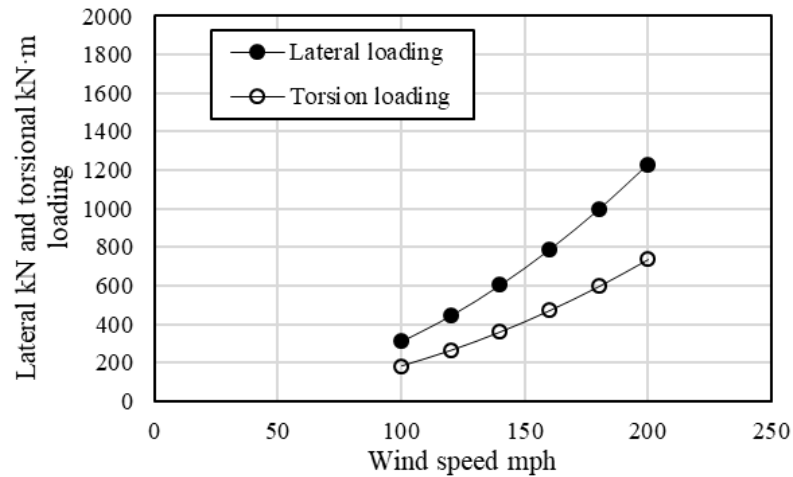


Figure 7-7: Lateral and torsional loadings in a CS with ratio pole height to arm length of 0.64

7.3.2. Failure study of Site-2

Table 7-8 shown the resultant reactions and moments calculated with the approach described in chapter 2 section 2.3 loading demand of inverted L-shape structures. This procedure was based on AASHTO 2009 LTS-5.

Table 7-8: Resultant moments, bending moment and shear

SITE-N	P_t (kN)	M_w (kN·m)	M_g (kN·m)	M_t (kN·m)	T_w (kN·m)
2	68.3	507.1	60.2	510.6	310.9

7.3.2.1. Predicted lateral loads

Brom's method (1964a)

Using the same procedure that Site-1, the minimum required undrained shear strength to withstand the loading demand of the inverted L-shaped structure was predicted using Brom's assumption. In this Site, the drilled shaft length is 1.80 m, the diameter 0.91 m, and the ratio $L/D = 2.$, i.e. very short shaft (UNISING, 2019). As was explained above, by geometry the shaft total length can be calculated as $L = g + f + 1.5D$, nevertheless, for

very short shafts this method results very conservative, therefore, for this analysis the Brom's approach will be used considering and ignoring 1.5D. Table 7-9 shown the predicted S_u resulted from both methods (i.e., with and without modifications), as well as, the factor of safety resulted from the ratio of the S_u predicted and S_u in site.

Table 7-9: Required S_u and FS computed following (Broms, 1964a) assumptions

	(Brom's, 1964,a) $g = L - f - 1.5D$	Brom's modified $g = L - f$
$S_{U \text{ required}}$ (kPa)	2023	38.88
F.S	0.1	3.99

As could be observed in results showed in Table 7-9 following the approach by (Broms, 1964a), i.e. ignoring the 1.5D zone , the factor of safety is less than 1, which means that loading demand produced by inverted L-shaped structure is greater than the foundation resistance predicted by this method. With this in mind, the minimum embedment depth to withstand the structure and the factor of safety were computed and plotted in Figure 7-8.

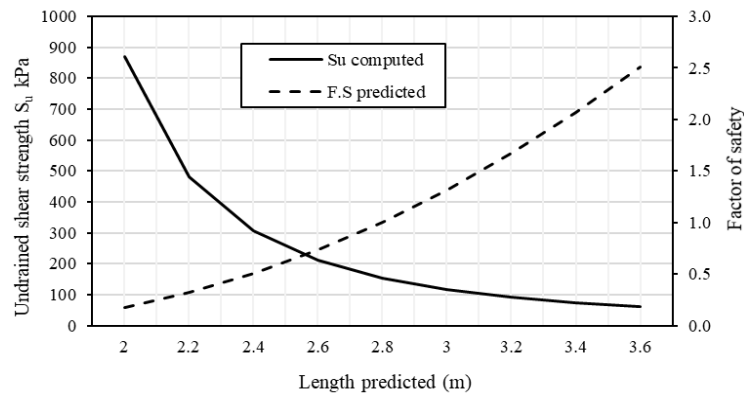


Figure 7-8: Predicted undrained shear strength and factor of safety using (Broms, 1964a) P-y curve method

The p-y curves were modeled using approaches proposed by Reese and Welch's (1975) and (API) Clay model. Both models and respective curves are summarized in APPENDIX C. The computed relationship between applied load and pile head lateral

displacement for a drilled shaft with a diameter of 0.91 m and embedment length of 1.8 m is presented in Figure 7-9 and Figure 7-10 for Reese and Welch's and API models respectively.

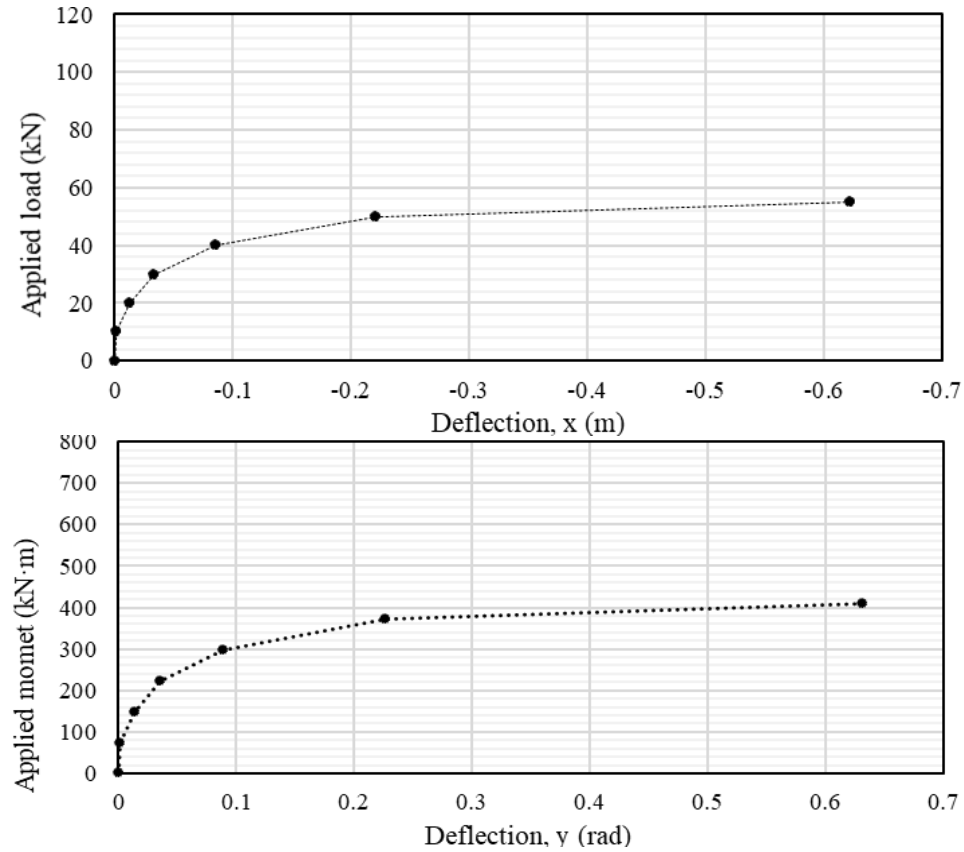


Figure 7-9: Predicted deflection of a drilled shaft with length of 1.8 m and diameter of 0.91 m using Reese and Welch's (1975) model

The nominal lateral load resistance and the nominal moment resistance for this drilled shaft dimensions are 54 kN and 400 kN·m respectively.

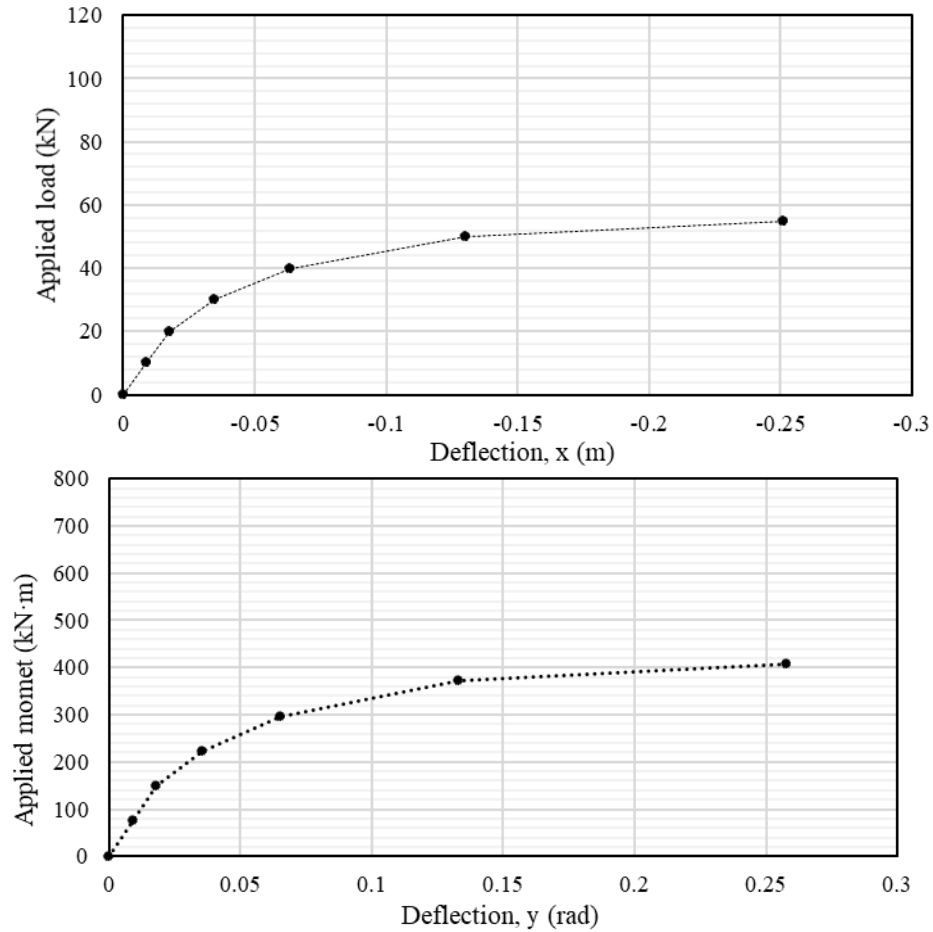


Figure 7-10: Predicted deflection of a drilled shaft with length of 1.8 m and diameter of 0.91 m using API model

The nominal lateral load resistance and the nominal moment resistance for this drilled shaft dimensions are 52 kN and 400 kN·m respectively.

Table 7-10 shown a summary of results obtained using p-y curve models and the respective factor of safety.

Table 7-10: Summary of loads and moments predicted using p-y curves

Model	Predicted load kN	Predicted moment kN·m	Factor of safety
Reese and Welch's (1975)	54	400	0.9
(API) Clay model	52	400	0.9

7.3.2.2. Predicted torsional moments

Methods based on side shear resistance

The results provided in this subsection were obtained based on unit shaft resistance in cohesive soils that were calculated considering the undrained shear strength. The predicted torsional moments computed with the different design methods are summarized in Table 7-11; this table also shows the factor of safety computed for the loading demand presented in this site.

Table 7-11: Summary of predicted torsional moments results

Method	Predicted Torsional moment kN·m	Factor of safety
α method	197	0.6
(Hu, 2003)	26	0.1
(Nusairat et al. 2004)	104	0.3

As can be observed, the computed factor of safety does not exceed a unit in any method. As well, as, this table is showing a very small factor of safety computed by (FHWA, 2010) method, which occurs because this method does not consider 1.5 meters from the drilled shaft length.

Using similar approach for other embedment depths, the results in Figure 7-13 were obtained. This figure shows 3 curves corresponding to methods listed in column 1 of Table 7-11.

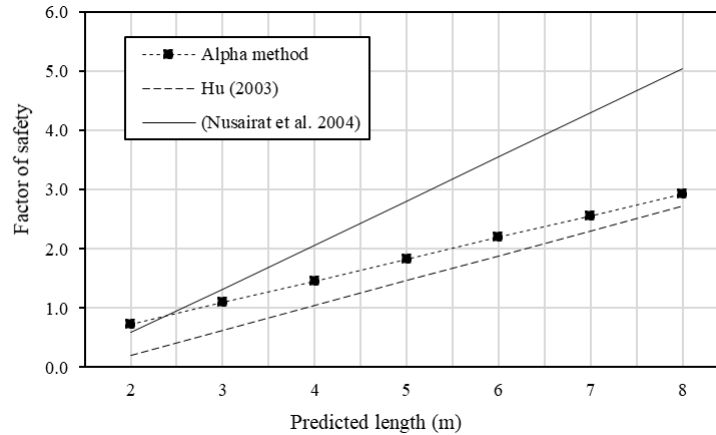


Figure 7-11: Relationship between the embedment depth and factor of safety

7.3.2.3. Summary of results

A summary of predicted maximum loads and moments obtained with lateral and torsional design methods is shown in Table 7-12.

Table 7-12: Summary of FS computed for different prediction failures

Failure mode	Method		F.S
Lateral	Broms	Broms, (1964a)	0.1
Lateral		Broms modified	1.6
Lateral	P-Y (FB-Multiplier)	Reese, 1975	0.9
Lateral		API	0.9
Torsional	Frictional method	α method	0.6
Torsional	Frictional method	Hu (2003)	0.1
Torsional	Frictional method	(Nusairat et al. 2004)	0.3

7.3.2.4. Discussion of results

As in Site-1, it can be seen that the required embedment lengths to withstand torsion loading are considerably higher than those required to resist lateral loading, nevertheless, this study Site allows to observe how the foundation resistance directly depends of the foundation embedment depth. The embedment depth difference between Site-1 and Site 2

is 0.6 meters, therefore, in all the cases a factor of safety is having a reduction of almost half unit as shown in Figure 7-12.

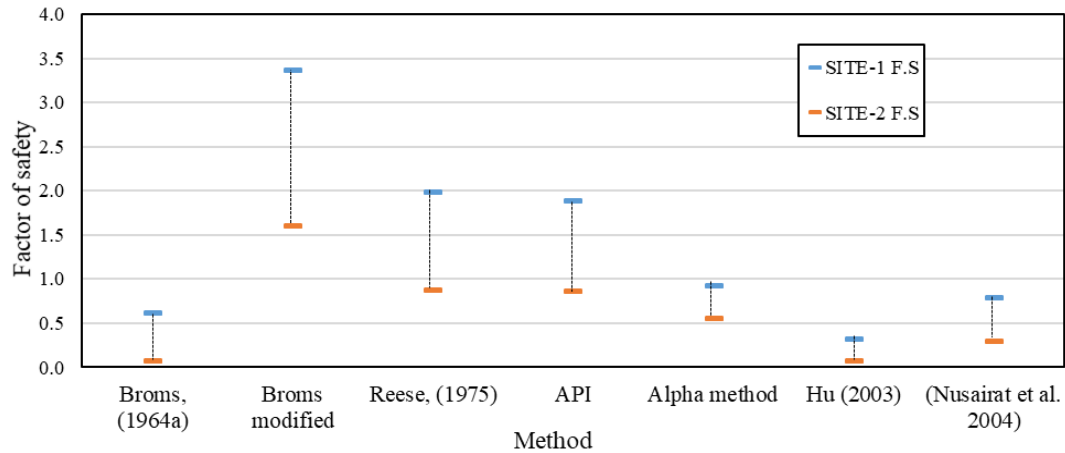


Figure 7-12: FS comparison between shaft resistance in SITE-1 and SITE-2

Figure 7-13 shown the minimum predicted embedment depths required to withstand the lateral and torsional load demand with a factor of safety of 2, computed with the methodologies described above. As can be observed in this figure, in almost all the cases the predicted embedment depths computed with torsional approaches are the double than those depths computed with lateral approaches. The results are supporting the field visit in which it could observe that final position of the CS structure shown a failure due to torsional loading.

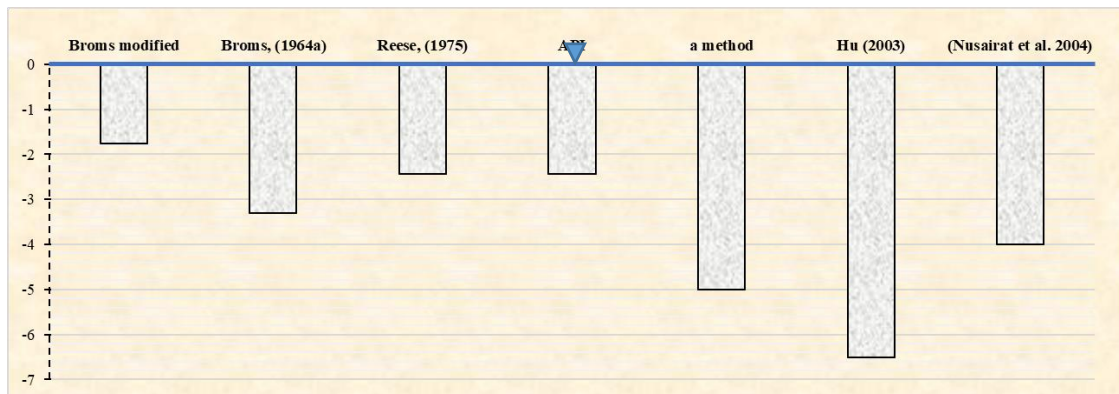


Figure 7-13: Computed factors of safety using predicted results

7.3.3. Failure study of Site-3

Table 7-13 shown the resultant reactions and moments calculated with the approach described in chapter 2 section 2.3 loading demand of inverted L-shape structures. This procedure was based on AASHTO 2009 LTS-5.

Table 7-13: Resultant moments, bending moment and shear

SITE-N	P_t (kN)	M_w (kN·m)	M_g (kN·m)	M_t (kN·m)	T_w (kN·m)
3	69.6	517.4	61.7	521.1	319.8

The drilled shaft embedment depth was predicted using charts that in the horizontal axis show the embedment length while the vertical axis shown either the maximum load or moment calculated with the different approaches listed in Table 7-1.

7.3.3.1. Predicted embedment depth due to lateral loads

Brom's method (1964b)

As was mentioned above, the embedment depths required to withstand the bending moment and lateral load demand for the CS structure were calculated using (Brom's 1964b) and the p-y curves proposed by (Reese et al. 1964), Figure 7-14 and Figure 7-15 respectively. The results are shown in a biaxial chart that in the horizontal axis represents the embedment depth while in the vertical axis either the maximum lateral moment or load are represented. Figure 7-14 shows that the required minimum embedment lengths are approximately 3.0 m and 4.0 m for loading demands with a factor of safeties of 1 and 1.5 respectively.

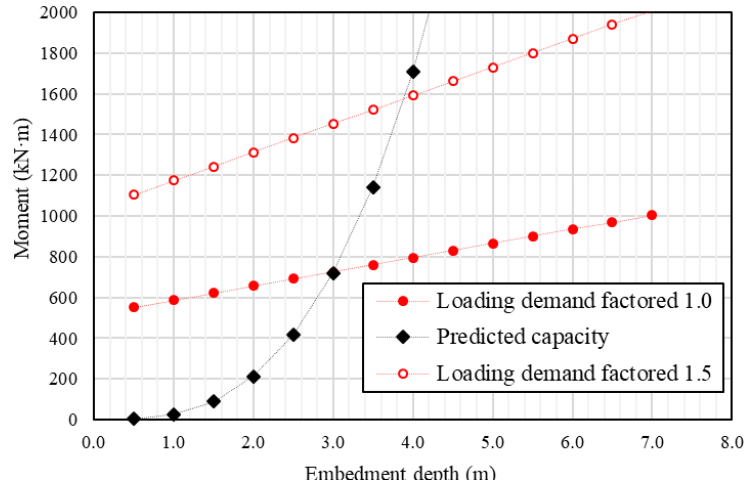


Figure 7-14: Required embedment depth as a function of bending moment according to (Broms, 1964)

For drilled shafts of 091 m diameter, the DTOP have standardized 4 drilled shaft lengths i.e. 2.7 m, 3 m, 3.75 m, and 4.35 m (DTOP, 2000). For these drilled shaft dimensions, the soil resistance was verified using the p-y curves models of (Sand O'Neill, 1984) and (API). According to the results obtained using API model, the minimum standard embedment depth required to withstand a factored loading demand are 3.75 m, and, 4.35 m for a factor of safety of 1 and 2 respectively. Figure 7-15 shows the p-y curves obtained using FB-Multiplier software.

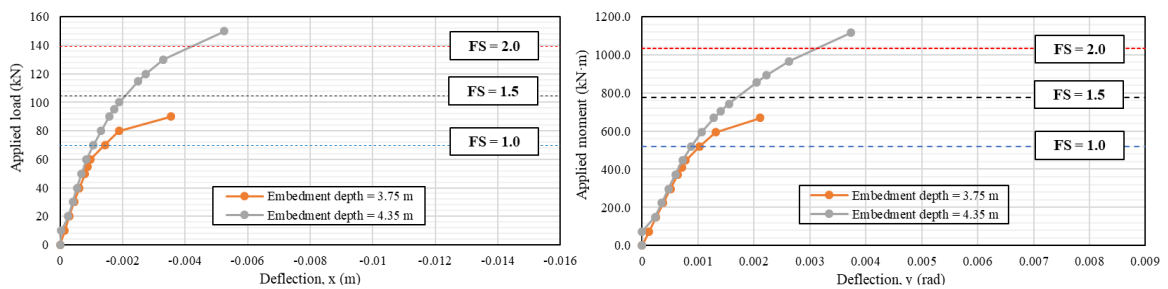


Figure 7-15: Required embedment depth as a function of lateral loading and bending moment according to (API)

As was mentioned above, the model proposed by (Sand O'Neill, 1984) also was used in order to predict the minimum embedment depth required to withstand the loading

demand in CS-3 factored 1 and 2 units. figure shows the results for a lateral load at left and bending moment at right.

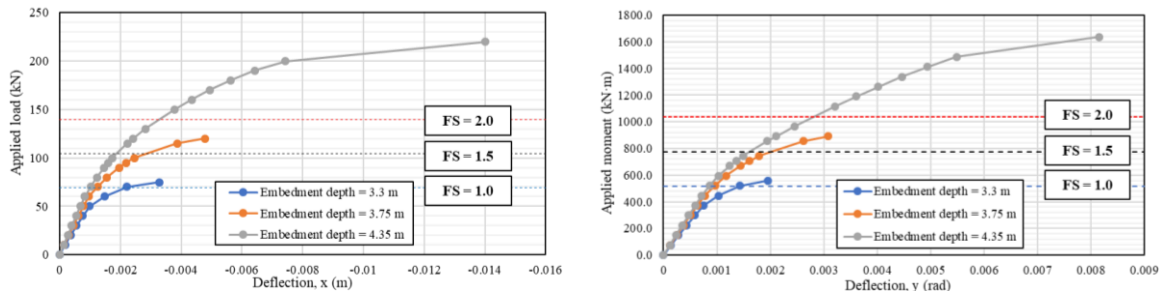


Figure 7-16: Required embedment depth as a function of lateral loading and bending moment according to (Sand O'Neill, 1984)

7.3.3.2. Predicted embedment depth due to torsional loads

The minimum drilled shaft embedment depth required to withstand torsion loading using the design procedures shown in Table 7-2 are shown in Figure 7-17. This figure shows minimum embedment depths for factored loading demands of 1, 1.5, and 2.

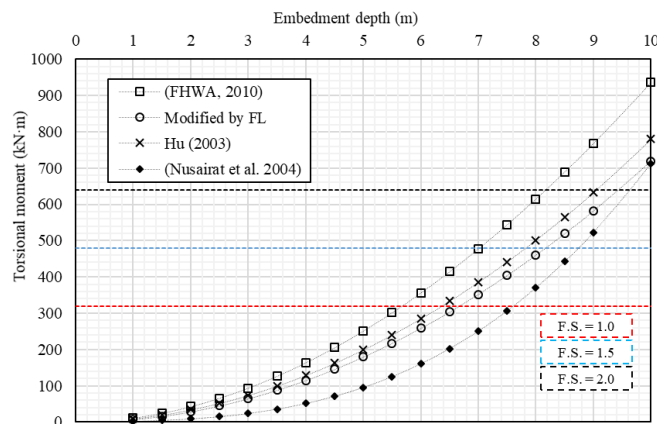


Figure 7-17: Required embedment depth as a function of torsion moment

7.3.3.3. Predicted embedment depth due to combined loading

The minimum drilled shaft embedment depth required to withstand torsion loading using the design procedures following (Duncan et al. 1995). Figure 7-18 shown that the minimum embedment depth obtained corresponds to 8 m for a factor of safety equal to 1.

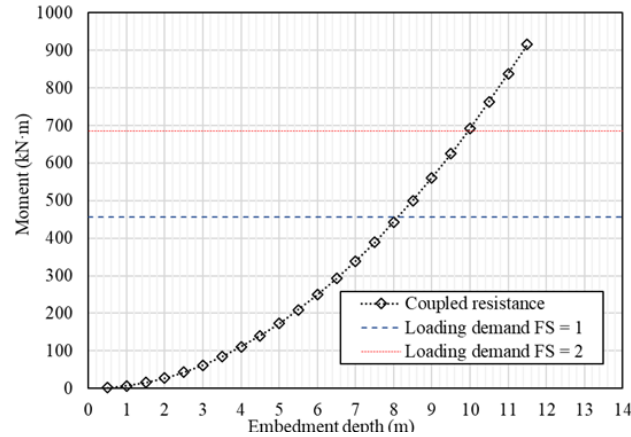


Figure 7-18: Required embedment depth as a function of coupled loading demand

7.3.3.4. Summary of predicted embedment depth

Figure 7-19 shown a summary of required embedment depth of the drilled shafts calculated with different methods and loading demands. The range of embedment depths required to withstand a drilled shaft of 0.91 m diameter is 3 m to 8 m calculated with (Broms, 1964b) and (Duncan et al. 1995) respectively.

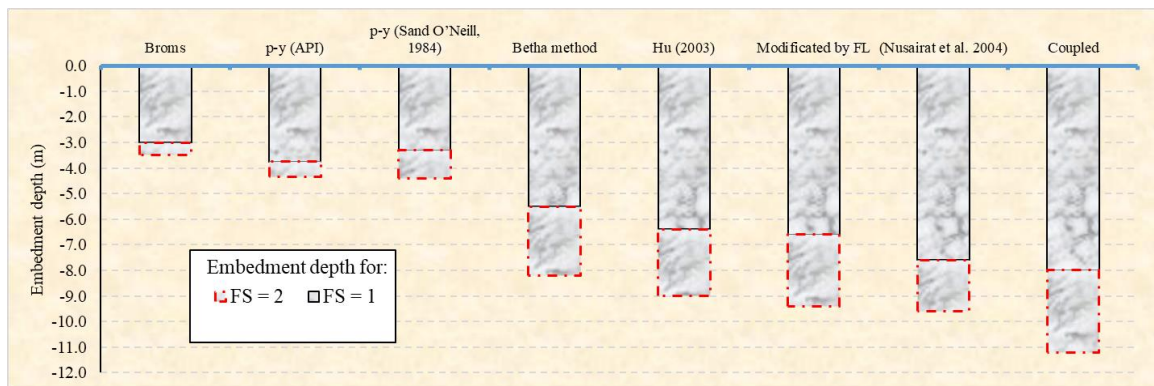


Figure 7-19: Required embedment depth for lateral, torsional and coupled analysis

It also can be seen that the required embedment lengths to withstand coupled loading considerably higher than the values required to torsion loading as well as resist lateral loading reported in Figure 7-19.

7.3.3.5. Discussion of results

As can be observed in this figure, the minimum predicted embedment depth to withstand the structure under a Hurricane corresponds to the obtained using the coupled analysis proposed by (Duncan et al. 1995). This approach consider a coupled (lateral and torsional) loading acting at the same time to the structure. As Site-1 and Site-2, the most conservative design methodology resulted to be those for predicting lateral failures.

7.4. Summary

This chapter provides the results obtained from the analysis of three inverted L-shaped structures due to high wind pressures during Hurricane Maria. In cohesive zones where cohesive soils are governed i.e. Site-1 and Site-2, the soil resistance was calculated using lateral and torsional design methodologies. The results obtained from these analyses where compared with the loading demand produced by the wind in the CS structure and the factor of safety was computed. The minimum predicted embedment depth also was calculated for loading demands factored 1 and 2 times. In Site-3, where cohesive soils predominant, the minimum embedment depth of the Drilled Shaft was predicted using lateral and torsional design methodologies.

In both analysis, lateral approaches turned out much more conservatives than torsional methods, nevertheless, Broms method for cohesive resulted to under predict the loads for ignoring the upper zone of soil equal to $1.5D$.

CHAPTER 8: CONCLUSIONS

8.1. State of practice

The survey found that the most common foundation system used by SOP participants is the conventional drilled shaft without wing walls. The use of wingwalls in drilled shafts is a measure used to increase torsion capacity and involves a conventional drilled shaft with a short wall that is installed in the upper portion that extends beyond the drilled shaft thus referred to as wing walls. Use of wing walls was only reported by NCDOT, VDOT and ALDOT, however VDOT and ALDOT indicated in their responses that use of wing walls is phasing out due to construction difficulties with this installation. The SOP study also found that FDOT, a state that has similar wind loading demand and mast arm dimensions than NCDOT, is not requiring the use of wing walls to meet loading demand for their coastal traffic signal mast arm structures.

8.2. Literature review

The literature review study shows that there is a need for more research that investigates the problem of drilled shafts under combined lateral and torsion loading. Most existing studies found focused on prediction of failure loads for lateral load and torsion separately. The few existing studies that involved combined lateral and torsion loading are useful but involved model testing under uniform, homogeneous soil conditions. There is a need for additional testing in particular full-scale field tests that involved combined lateral and torsion loading. Available experimental data shows the lateral load capacity of piles under combined torsion and lateral loading is significantly decreased and thus could become the controlling design consideration.

The literature review also revealed an important gap related to the need for static methods for predicting unit skin friction under torsion loading, or even better for combined torsion with axial and bending. The current methods are based on recent FHWA drilled shaft manuals (FHWA 1999 and 2010) that report different static methods based on axial load testing so their applicability to the complex loading involved in traffic signal mast arms is questionable.

In terms of alternative foundation systems that could be used for supporting coastal traffic signal mast arm structures at sites with poor geotechnical conditions FDOT has reported research looking at driven post-grouted concrete piles. Other alternatives identified in this study include driven pipe piles (open or closed ended) and finned pipe piles.

8.3. Case studies

Figure 7-6 and Figure 7-13 are shown a comparison of embedment depths required to withstand torsional and lateral loadings in cohesive soils, as well as, Figure 7-19 shown a comparison of embedment depths required to withstand lateral, torsional a coupled loading in cohesionless soils.

In all cases, figures show that the required embedment lengths to withstand torsion loading are almost twice than values required to resist lateral loading. The obtained results shows coherence with the field visit findings based on the final position of CS structure with respect to Zenith. The final position of the structures revealed that all the structures had a combined failure composed by vertical tilts due to lateral displacements with respect to Zenith, and torsional failure due to torsional displacements about the same axis of the

DS. Therefore, all sites had a combined failure governed by torsion. Table 8-1 shown an overview of the failure magnitudes due to torsional and lateral loading demands.

Table 8-1: Rotation and tilts measurements after Hurricane Maria

CS structure N.	Rotation		Tiling
	Clockwise	Counterclockwise	
1	225°	135°	2°
2	45°	315°	9°
3	115°	245°	7°

The failure in Site 1 and Site 2 was analyzed using design approaches for cohesive soils and DS dimensions known i.e. diameter and embedment depth. As was mentioned above, the results revealed combined failure supported by findings in field. The results also shown lateral deformations larger for shorter shafts than longer shafts i.e lateral tilt in Site-2 > lateral tilt in Site-1.

Broms method for cohesive soils and short shaft resulted very conservative. This is due to the soil resistance provided by Brom's method does not take in account the soil zone located adjacent to 1.5 times the DS diameter from the soil surface. For academic propose, the results of this theses were obtained considering and ignoring the 1.5D zone ignored by Broms. The results obtained with Brom's modified shown that the minimum predicted embedment depth to withstand the loading demand in Sites 1 and 2 are 2.5 and 2.5 meters.

Soil conditions, type of structure, and characteristics in Site-3 were used as input information in order to perform a comparison of the minimum embedment depths required to withstand the lateral and torsional load demands in this Site. In this Site, the results revealed that the design by torsion and coupled approaches requires deeper embedment

depths compared to axial load and bending/lateral load demands. The main reason for this significant difference in the required minimum embedment lengths needed to withstand torsional load demand is attributed to differences in simplifying assumptions used to estimate unit side resistance used by the different authors.

None of the methods used in order to predict the lateral resistance of the soil i.e., (Broms and p-y curve methods) expected tilt or lateral failures in the CS structures. Even in all the cases, torsion governed the failure; small tilts with respect to the Zenith were identified. Up to 50% reduction of lateral capacity of shaft due to torsion was predicted by (Hu et al, 2003) after perform 91 centrifuge tests in inverted L-shaped structures.

In inverted L-shape structures, the magnitude of lateral and torsional moments during hurricane events depend of the type and area of elements e.g. highway signs and traffic signals. Nevertheless, the greater magnitude is determined mainly by the structure configuration, more precisely for the ratio of arm length (r) and pole height (L). Figure 8-1(a), (b) and (c) shown a schematic representation of the CS structure bending and torsional moments calculated with ratios r/L of 0.64, 1.0 and 1.5.

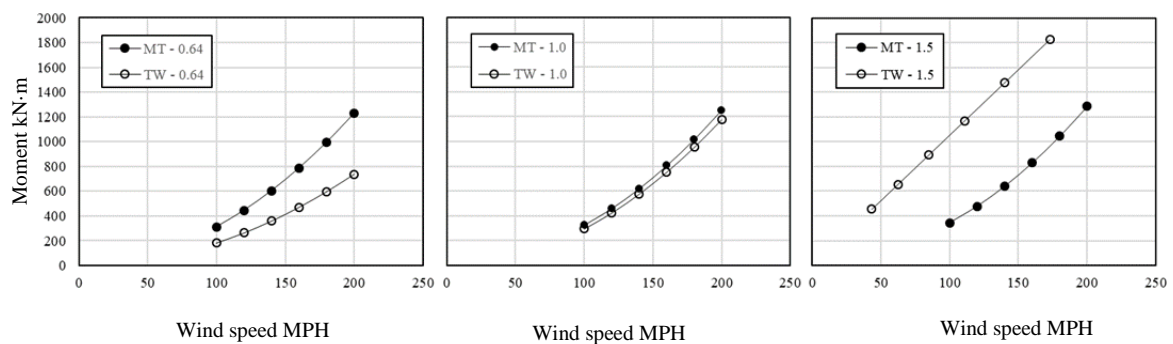


Figure 8-1: Comparison between lateral and torsional loading demand on inverted L-Shape structures varying L/r

The spin direction of Hurricane Maria has been determined to have followed a counterclockwise path due to it is traveling towards northward been pushed toward the

right, however. Nevertheless, this does not indicate what the CS rotation direction was during Hurricane Maria, it could follow a clockwise or counterclockwise rotation depending if the wind hits the front or the back of the structures. Nevertheless, there is a pattern based on the rotation of structures located in Site-1 and Site-2 for which it can be determined that CS structures rotated following a clockwise direction about their Zenith. As mentioned during this research document, Site-1 and Site 2 are located in the same Hurricane zone of affectation, at a distance each other of 300 m, with very similar geotechnical properties. The most important difference between both sites is the predicted DS length, 2.44 and 1.80 for Site-1 and Site-2 respectively, which means that during same loading conditions the rotation of CS structure in Site-2 had to be larger than in Site-1. As can be observed in figure, the condition mentioned above is given when the structures rotate clockwise about its pole.

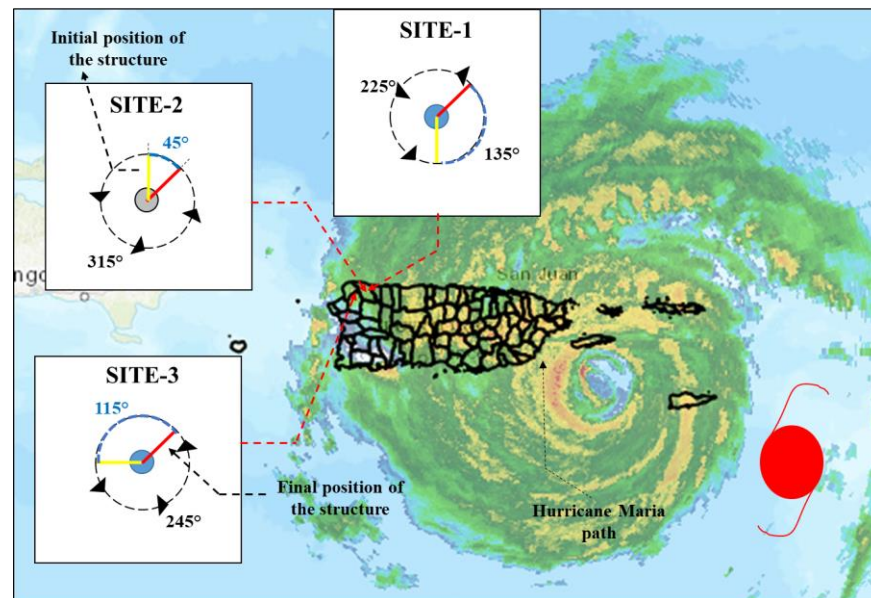


Figure 8-2: Schematic of the failures rotation direction

REFERENCES

- AASHTO (1996). STANDARD SPECIFICATIONS FOR HIGHWAY BRIDGES. FOUNDATIONS, AASHTO.
- AASHTO (2009). STANDARD SPECIFICATIONS FOR STRUCTURAL SUPPORTS FOR HIGHWAY SIGNS, LUMINAIRES, AND TRAFFIC SIGNALS. LOADS., AASHTO: 26.
- AASHTO (2010). AASHTO LRFD BRIDGE DESIGN SPECIFICATIONS FOUNDATIONS, AASHTO.
- AASHTO (2012). AASHTO LRFD BRIDGE DESIGN SPECIFICATIONS. FOUNDATIONS, AASHTO: 10-1.
- AASHTO (2015). LRFD SPECIFICATIONS FOR STRUCTURAL SUPPORTS FOR HIGHWAY SIGNS, LUMINAIRES, AND TRAFFIC SIGNALS. LOADS, AASHTO: 3-1.
- ABU-FARSAKH, M. Y., CHEN, Q., & HAQUE, M. N. (2013). CALIBRATION OF RESISTANCE FACTORS FOR DRILLED SHAFTS FOR THE NEW FHWA DESIGN METHOD. RETRIEVED FROM U.S. DEPARTMENT OF TRANSPORTATION, FEDERAL HIGHWAY ADMINISTRATION
- ASCE. (2010). MINIMUM DESIGN LOADS FOR BUILDINGS AND OTHER STRUCTURES. IN: AMERICAN SOCIETY OF CIVIL ENGINEERS.
- BABOUR, H., (JANUARY 6, 2006). "INFORMATION RELATING TO THE FEDERAL APPROPRIATIONS FOR KATRINA RECOVERY". ACCESSED 09/27/2018.
- BENFIELD, A. (2018). HURRICANE MARIA EVENT RECAP REPORT. RETRIEVED FROM
- BROMS, B.B. (1964A). LATERAL RESISTANCE OF PILES IN COHESIVE SOILS. JOURNAL OF THE SOIL MECHANICS AND FOUNDATIONS DIVISION, ASCE 90(SM2): 27–63.
- BROMS, B.B. (1964B). LATERAL RESISTANCE OF PILES IN COHESIONLESS SOILS. JOURNAL OF THE SOIL MECHANICS AND FOUNDATIONS DIVISION, ASCE 90(SM3): 123–156.
- BROMS, B.B. (1965). DESIGN OF LATERALLY LOADED PILES. JOURNAL OF THE SOIL MECHANICS AND FOUNDATIONS DIVISION, ASCE 91(SM3): 77–99.
- DAS, B. M. (2014). PRINCIPLES OF FOUNDATION ENGINEERING (EIGHTH EDITION ED.): CENGAGE LEARNING.
- DUNCAN, J.M. AND FILZ, G. (1995). CAPACITIES OF DRILLED SHAFTS IN SAND SUBJECTED TO OVERTURNING AND TORSION. BENGT B BROMS SYMPOSIUM ON GEOTECHNICAL ENGINEERING. SINGAPORE: 95-11.
- FDOT (2016). "MAST ARM ASSEMBLIES." ACCESSED 02/28/2018, 2018, FROM [HTTP://WWW.FDOT.GOV/ROADWAY/DS/16/IDx/17745.PDF](http://www.fdot.gov/roadway/DS/16/IDx/17745.pdf).

FDOT (2017). FDOT MODIFICATIONS TO LRFD SPECIFICATIONS FOR STRUCTURAL SUPPORTS FOR HIGHWAY SIGNS, LUMINAIRES AND TRAFFIC SIGNALS (LRFDLTS-1). FDOT: 22.

FDOT (2018). "CANTILEVER SIGN STRUCTURE." ACCESSED 02/28/2018, 2018, FROM [HTTP://WWW.FDOT.GOV/DESIGN/STANDARDPLANS/CURRENT/IDX/700-040.PDF](http://www.fdot.gov/design/standardplans/current/idx/700-040.pdf).

FDOT (2018). "FDOT MODIFICATIONS TO LRFD SPECIFICATIONS FOR STRUCTURAL SUPPORTS FOR HIGHWAY SIGNS, LUMINAIRES AND TRAFFIC SIGNALS (LRFDLTS-1)." ACCESSED 11/20/2017, FROM [HTTP://WWW.FDOT.GOV/STRUCTURES/STRUCTURESMANUAL/CURRENTRELEASE/VOL3LTS.PDF](http://www.fdot.gov/structures/structuresmanual/currentrelease/vol3lts.pdf).

FHWA (1999). DRILLED SHAFTS: CONSTRUCTION PROCEDURES AND LRFD DESIGN METHODS, FHWA.

FHWA (2009). "TRAFFIC CONTROL SIGNALS—GENERAL." ACCESSED 11/11/2017, FROM [HTTPS://MUTCD.FHWA.DOT.GOV/PDFS/2009/PART4.PDF](https://mutcd.fhwa.dot.gov/pdfs/2009/part4.pdf).

FHWA (2010). DRILLED SHAFTS: CONSTRUCTION PROCEDURES AND LRFD DESIGN METHODS. FHWA.

FHWA (2013). "HIGHWAY FUNCTIONAL CLASSIFICATION CONCEPTS, CRITERIA AND PROCEDURES." ACCESSED 12/11/2018, 2018, FROM [HTTPS://WWW.FHWA.DOT.GOV/PLANNING/PROCESSES/STATEWIDE/RELATED/HIGHWAY_FUNCTIONAL_CLASSIFICATIONS/FCAUAB.PDF](https://www.fhwa.dot.gov/planning/processes/statewide/related/highway_functional_classifications/fcauab.pdf).

FHWA (2017). "FREEWAY MANAGEMENT AND OPERATIONS HANDBOOK." ACCESSED 11/11/2017, FROM [HTTPS://OPS.FHWA.DOT.GOV/FREEWAYMGMT/PUBLICATIONS/FRWY_MGMT_HANDBOOK/CHAPTER1_02.HTM](https://ops.fhwa.dot.gov/freewaymgmt/publications/frwy_mgmt_handbook/chapter1_02.htm).

GDOT (2010). "DETAILS OF STRAIN POLE AND MAST ARM FOUNDATIONS." ACCESSED 02/15/2018, FROM [HTTP://MYDOCS.DOT.GA.GOV/INFO/GDOTPUBS/CONSTRUCTIONSTANDARDSANDDETAILS/FORMS/ALLITEMS.ASPX](http://mydocs.dot.ga.gov/info/gdotpubs/constructionstandardsanddetails/forms/allitems.aspx).

GDOT (2013). "STANDARD SPECIFICATIONS CONSTRUCTION OF TRANSPORTATION SYSTEMS." ACCESSED 02/02/2018, FROM [HTTP://WWW.DOT.GA.GOV/PARTNERSMART/BUSINESS/SOURCE/SPECS/2001STANDARDSPECIFICATIONS.PDF](http://www.dot.ga.gov/partnersmart/business/source/specs/2001standardspecifications.pdf).

HALEY BABOUR (JANUARY 6, 2006). "INFORMATION RELATING TO THE FEDERAL APPROPRIATIONS FOR KATRINA RECOVERY". OFFICE OF THE GOVERNOR, MISSISSIPPI. ARCHIVED FROM THE ORIGINAL ON SEPTEMBER 28, 2007.

HERRERA, R. (2001). DETERMINE OPTIMUM DEPTH OF DRILLED SHAFTS SUBJECTED TO COMBINED TORSION AND LATERAL LOADS USING CENTRIFUGE. UNIVERSITY OF FLORIDA.

- HU, Z. (2003). DETERMINING THE OPTIMUM DEPTH OF DRILLED SHAFTS SUBJECT TO COMBINED TORSION AND LATERAL LOADS IN SATURATED SAND FROM CENTRIFUGE TESTING. UNIVERSITY OF FLORIDA, MASTER 160.
- HU, Z., McVAY, M., BLOOMQUIST, D., HERRERA, R., AND LAI, P., (2006). "INFLUENCE OF TORQUE ON LATERAL CAPACITY OF DRILLED SHAFTS IN SANDS." JOURNAL OF GEOTECHNICAL AND GEOENVIRONMENTAL ENGINEERING 132(4): 10.
- HU, Z., McVAY, M., LAI, P., (2006). "INFLUENCE OF DRILLING SLURRY ON DRILLED SHAFTS TORSIONAL & LATERAL CAPACITY." PHYSICAL MODELLING IN GEOTECHNICS: 4.
- LI, Q., (2018). INVESTIGATION OF DRILLED SHAFTS UNDER AXIAL, LATERAL, AND TORSIONAL LOADING. OREGON STATE UNIVERSITY, OREGON STATE UNIVERSITY. DOCTOR OF PHILOSOPHY.
- LI, Q., STUEDLEIN A., BARBOSA, A., (2017). "TORSIONAL LOAD TRANSFER OF DRILLED SHAFT FOUNDATIONS." GEOTECH. GEONVIRON ENG: 13.
- MATLOCK, H. AND REESE, L. C., "GENERALIZED SOLUTIONS FOR LATERALLY LOADED PILES," JOURNAL OF SOIL
- McVAY, M., BLOOMQUIST, D., THIYYAKKANDI, S (2014). FIELD TESTING OF JET-GROUTED PILES AND DRILLED SHAFTS. DEPARTMENT OF CIVIL AND COASTAL ENGINEERING UNIVERSITY OF FLORIDA 314.
- McVAY, M., HERRERA, F., AND HU, Z., (2003). DETERMINE OPTIMUM DEPTH OF DRILLED SHAFTS SUBJECT TO COMBINED TORSION AND LATERAL LOADS USING CENTRIFUGE TESTING DEPARTMENT OF CIVIL AND COASTAL ENGINEERING, COLLEGE OF ENGINEERING UNIVERSITY OF FLORIDA: 387.
- McVAY, M., KUO, C., GUISINGER, A., (2003). CALIBRATING RESISTANCE FACTOR IN THE LOAD AND RESISTANCE FACTOR DESIGN OF STATNOMIC LOADING TEST. DEPARTMENT OF CIVIL AND COASTAL ENGINEERING UNIVERSITY OF FLORIDA. 42.
- McVAY, M., CHUNG, J., NGUYEN, T., THIYYAKKANDI, S., LYU, W., SCHWARTZ III, J., HUANG, L, AND LE, V (2017). EVALUATION OF STATIC RESISTANCE OF DEEP FOUNDATION UNIVERSITY OF FLORIDA UNIVERSITY OF FLORIDA 212.
- MECHANICS AND FOUNDATION DIVISION, ASCE, VOL. 86, No.5, 1960, pp. 63-91.
- MEHTA, K. C. AND P. W. HORN (2010). WIND LOAD HISTORY: ANSI A58.1-1972 TO ASCE 7-05. STRUCTURES CONGRESS 2010. ORLANDO, FLORIDA, UNITED STATES, AMERICAN SOCIETY OF CIVIL ENGINEERS.
- MODULUS ASSUMED PROPORTIONAL TO DEPTH," PROCEEDINGS EIGHTH TEXAS CONFERENCE ON SOIL MECHANICS AND FOUNDATION ENGINEERING, SPECIAL PUBLICATION NO. 29, BUREAU OF ENGINEERING RESEARCH, UNIVERSITY OF TEXAS, AUSTIN, TX, 1956.
- MURAD, A., QIMING, C., AND MD, N., (2013). CALIBRATION OF RESISTANCE FACTORS FOR DRILLED SHAFTS FOR THE NEW FHWA DESIGN METHOD. F. L. 12/495. FHWA.

NCDOT (2010). MAST ARM FOUNDATION DESIGN RECOMMENDATIONS, NCDOT: 3.

NCDOT (2012). DESIGN DRAWINGS FOR PROJECT NO. U-4438.

NCDOT (2016). "NCDOT METAL POLE STANDARD ". ACCESSED 9/22/2017, 2017, FROM [HTTPS://CONNECT.NCDOT.GOV/RESOURCES/SAFETY/PAGES/ITS-DESIGN-RESOURCES.ASPX](https://connect.ncdot.gov/resources/safety/pages/its-design-resources.aspx).

NCDOT (2017). "NCDOT GEOTECHNICAL INVESTIGATION AND RECOMENDATION MANUAL." ACCESSED 9/22/2017, 2018, FROM [HTTPS://CONNECT.NCDOT.GOV/RESOURCES/GEOLOGICAL/DOCUMENTS/16-03-29_GEOTECHNICAL%20INVESTIGATION%20AND%20RECOMMENDATIONS%20MANUAL.PDF](https://connect.ncdot.gov/resources/geological/documents/16-03-29_Geotechnical%20Investigation%20and%20Recommendations%20Manual.pdf).

NCDOT ITC (2011). "RANGE OF LOADING AS A FUNCTION OF MAST ARM LENGTH FOR NCDOT-CR-CHECK-WITH NCDOT-LOAD-VALUES". (ACCESSED 07/15/18).

ODOT (2017). "TRAFFIC 600 - SIGN, ILLUMINATION, AND SIGNAL SUPPORT STRUCTURES." ACCESSED 4/4/2018, 2018, FROM [HTTP://WWW.OREGON.GOV/ODOT/ENGINEERING/PAGES/DRAWINGS-TRAFFIC.ASPX](http://www.oregon.gov/odot/engineering/pages/drawings-traffic.aspx).

PASCH, R., PENNY, A., & BERG, R. (2019). HURRICANE MARIA. RETRIEVED FROM NATIONAL WEATHER SERVICES: [HTTPS://WWW.NHC.NOAA.GOV/DATA/TCR/AL152017_MARIA.PDF](https://www.nhc.noaa.gov/data/tcr/AL152017_MARIA.pdf)

PND ENGINEERS (2018) "SPIN FIN PILES", [HTTP://WWW.PNDENGINEERS.COM/RESEARCH-AND-DEVELOPMENT/APPLIED-RESEARCH-DEVELOPMENT/SPIN-FIN-PILES](http://www.pndengineers.com/research-and-development/applied-research-development/spin-fin-piles) (ACCESSED 11/15/18).

REESE, L. C., AND MATLOCK, H., "NON-DIMENSIONAL SOLUTIONS FOR Laterally LOADED PILES WITH SOIL

RODRIGUEZ, C., PANDO, M., MATTHEW, W., WEGGEL, D., & FANG, H. (2019). STATE OF PRACTICE AND LITERATURE REVIEW ON FOUNDATION FOR COASTAL TRAFFIC SIGNAL MAST ARM STRUCTURES. RETRIEVED FROM

SCDOT (2007). "STANDARD SPECIFICATIONS FOR HIGHWAY CONSTRUCTION ". ACCESSED 05/05/2018, 2018, FROM [HTTPS://WWW.SCDOT.ORG/BUSINESS/STANDARD-SPECIFICATIONS.ASPX](https://www.scdot.org/business/standard-specifications.aspx).

SCDOT (2018). "TRAFFIC CONTROL ". ACCESSED 05/05/2018, 2018, FROM [HTTPS://WWW.SCDOT.ORG/BUSINESS/STANDARD-DRAWINGS.ASPX](https://www.scdot.org/business/standard-drawings.aspx).

SILVA-TULLA, F., PANDO , M., SOTO , A., MORALES, A., PRADEL , D., INCI, G., BERNAL, J., KAYEN, R., HUGHES, S., ADAMS, T., PARK, Y. (2018). GEOTECHNICAL IMPACTS OF HURRICANE MARIA IN PUERTO RICO . GEER.

TAWFIQ, K., "DRILLED SHAFT UNDER TORSIONAL LOADING CONDITIONS," FINAL REPORT TO FLORIDA DEPARTMENT OF TRANSPORTATION, CONTRACT # B-9191, JUNE 2000, 185 PAGES.

THIYYAKKANDI, S. (2013). STUDY OF GROUTED DEEP FOUNDATIONS IN COHESIONLESS SOILS. GRADUATE SCHOOL UNIVERSITY OF FLORIDA, UNIVERSITY OF FLORIDA. DOCTOR OF PHILOSOPHY: 229.

THIYYAKKANDI, S., McVAY, M., LAI, P., HERRERA, R., (2016). "FULL-SCALE COUPLED TORSION AND LATERAL RESPONSE OF MAST ARM DRILLED SHAFT FOUNDATIONS." CANADIAN GEOTECHNICAL JOURNAL 53: 10.

THIYYAKKANDI, S., McVAY, M., LAI, P., HERRERA, R., (2017). "SUITABILITY OF JETTED AND GROUTED PRECAST PILE FOR SUPPORTING MAST ARM STRUCTURES." CANADIAN GEOTECHNICAL JOURNAL 54: 15.

TRANSPORTATION, F. H. O. (2017). "FREEWAY MANAGEMENT AND OPERATIONS HANDBOOK." ACCESSED 11/04/2017, 2017, FROM [HTTPS://OPS.FHWA.DOT.GOV/FREEWAYMGMT/PUBLICATIONS/FRWY_MGMT_HANDBOOK/CHAPTER1_02.HTM](https://ops.fhwa.dot.gov/freewaymgmt/publications/frwy_mgmt_handbook/chapter1_02.htm).

TXDOT (2012). "TRAFFIC SIGNAL POLE STANDARDS." ACCESSED 03/02/2018, 2018, FROM [HTTP://WWW.DOT.STATE.TX.US/INSDTDOT/ORGCHART/CMD/CSERVE/STANDARD/TOC.HTM](http://www.dot.state.tx.us/insdtdot/orgchart/cmd/cserve/standard/toc.htm).

TXDOT (2014). "WIND VELOCITY AND ICE ZONE MAPS." ACCESSED 03/20/2018, 2018, FROM [HTTP://WWW.DOT.STATE.TX.US/INSDTDOT/ORGCHART/CMD/CSERVE/STANDARD/TOC.HTM](http://www.dot.state.tx.us/insdtdot/orgchart/cmd/cserve/standard/toc.htm).

TXDOT (2015). "MONOTUBE SIGN STRUCTURE (CANTILEVER)." ACCESSED 03/20/2018, 2018, FROM [FTP://FTP.DOT.STATE.TX.US/PUB/TXDOT-INFO/CMD/CSERVE/STANDARD/TRAFFIC/MC-15.PDF](ftp://ftp.dot.state.tx.us/pub/txdot-info/cmd/cserve/standard/traffic/mc-15.pdf).

USACE (2006). MISSISSIPPI COASTAL IMPROVEMENT PROJECTS. USACE, USACE. 2018: 371.

USGS. "GEOLOGIC UNITS IN HARRISON COUNTY, MISSISSIPPI." FROM [HTTPS://MRDATA.USGS.GOV/GEOLOGY/STATE/FIPS-UNIT.PHP?CODE=F28047](https://mrdata.usgs.gov/geology/state/fips-unit.php?code=F28047).

VDOT (2016). "INDEX OF SHEETS SECTION 1300-TRAFFIC CONTROL." ACCESSED 01/30/2018, 2016, FROM [HTTP://WWW.EXTRANET.VDOT.STATE.VA.US/LOCDES/ELECTRONIC_PUBS/2008STANDARDS/CSECTION1300.PDF](http://www.extranet.vdot.state.va.us/locdes/electronic_pubs/2008standards/csection1300.pdf).

VDOT (2016). "STRUCTURE AND BRIDGE DIVISION INSTRUCTIONAL AND INFORMATIONAL MEMORANDUM IIM-S&B-90.2-IIM-TE-382.1." ACCESSED 01/24/2018, 2018, FROM [HTTP://WWW.VIRGINIADOT.ORG/BUSINESS/RESOURCES/IIM/TE-382_AASHTO_STANDARD_SPECIFICATIONS.PDF](http://www.virginiadot.org/business/resources/iim/te-382_aashto_standard_specifications.pdf).

WSDOT (2017). "BRIDGE DESIGN MANUAL (LRFD)." Accessed 09/22/2017, 2017, FROM [HTTP://WWW.WSDOT.WA.GOV/PUBLICATIONS/MANUALS/FULLTEXT/M23-50/BDM.PDF](http://www.wsdot.wa.gov/publications/manuals/fulltext/M23-50/BDM.PDF).

WSDOT (2017). "DESIGN MANUAL." Accessed 09/26/2017, 2017, FROM [HTTP://WWW.WSDOT.WA.GOV/PUBLICATIONS/MANUALS/FULLTEXT/M22-01/DESIGN.PDF](http://www.wsdot.wa.gov/publications/manuals/fulltext/M22-01/DESIGN.PDF).

WSDOT (2018). "TRAFFIC SIGNAL STANDARD FOUNDATION." Accessed 09/24/2017, 2017, FROM [HTTP://WWW.WSDOT.WA.GOV/PUBLICATIONS/FULLTEXT/STANDARDS/ENGLISH/PDF/J26.10-03_E.PDF](http://www.wsdot.wa.gov/publications/fulltext/standards/english/pdf/j26.10-03_e.pdf).

ZHANG, L. AND L. G. KONG (2006). "CENTRIFUGE MODELING OF TORSIONAL RESPONSE OF PILES IN SAND "CANADIAN GEOTECHNICAL JOURNAL 43(5).

ZHANG, L., SILVA, F., AND GRISMALA R., (2005). "ULTIMATE LATERAL RESISTANCE TO PILES IN COHESIONLESS SOILS "JOURNAL OF GEOTECHNICAL AND GEOENVIRONMENTAL ENGINEERING 78:

APPENDIX A: GEOTECHNICAL INFORMATION FOUND IN SITES 1, 2 AND 3

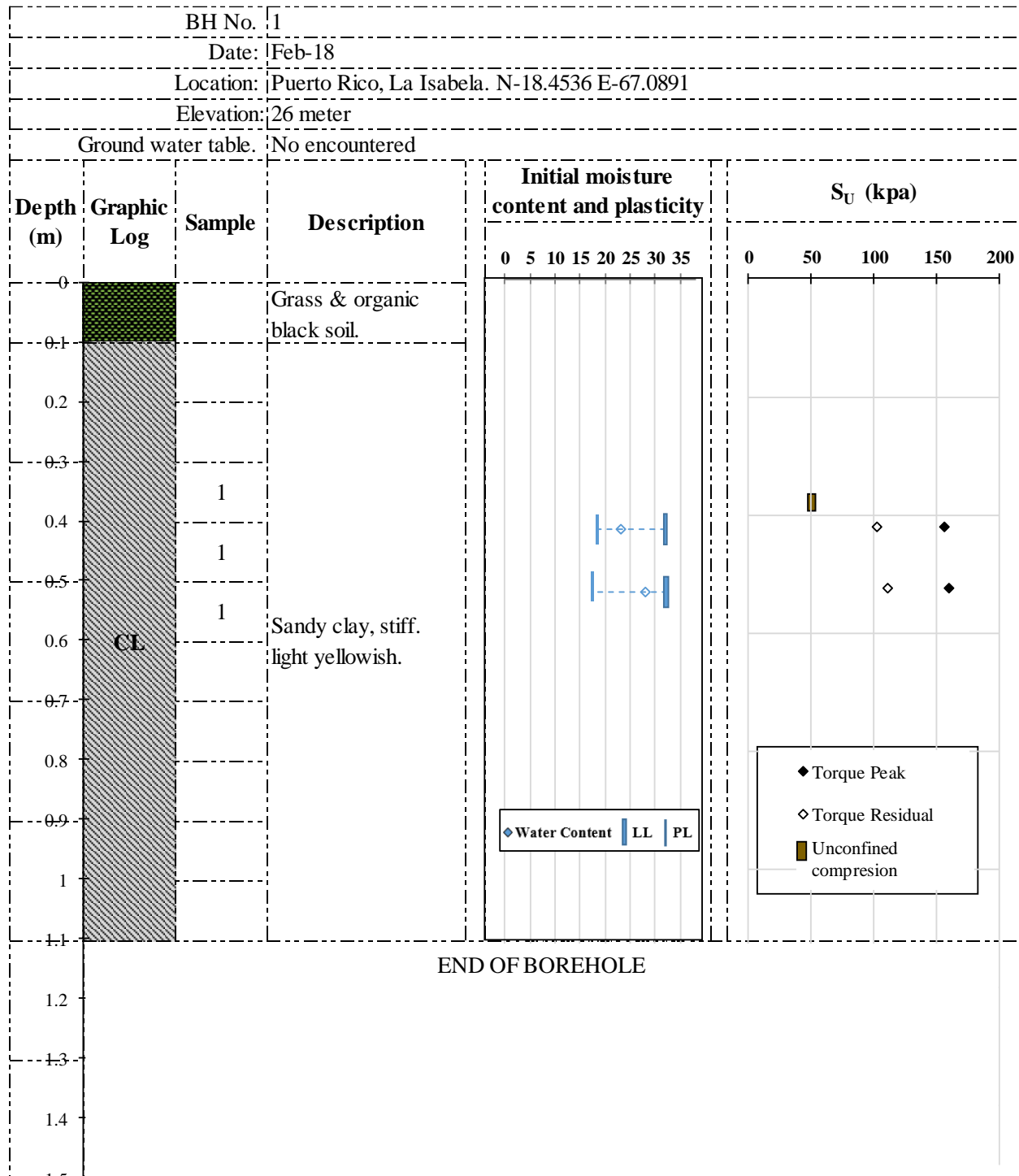


Figure A-1: Summary of geotechnical information at Site-1

Grain size distribution

Test performed to a sample at 0.42 meters, following the D422 – 63 (Standard Test

Method for Particle-Size Analysis of Soils):

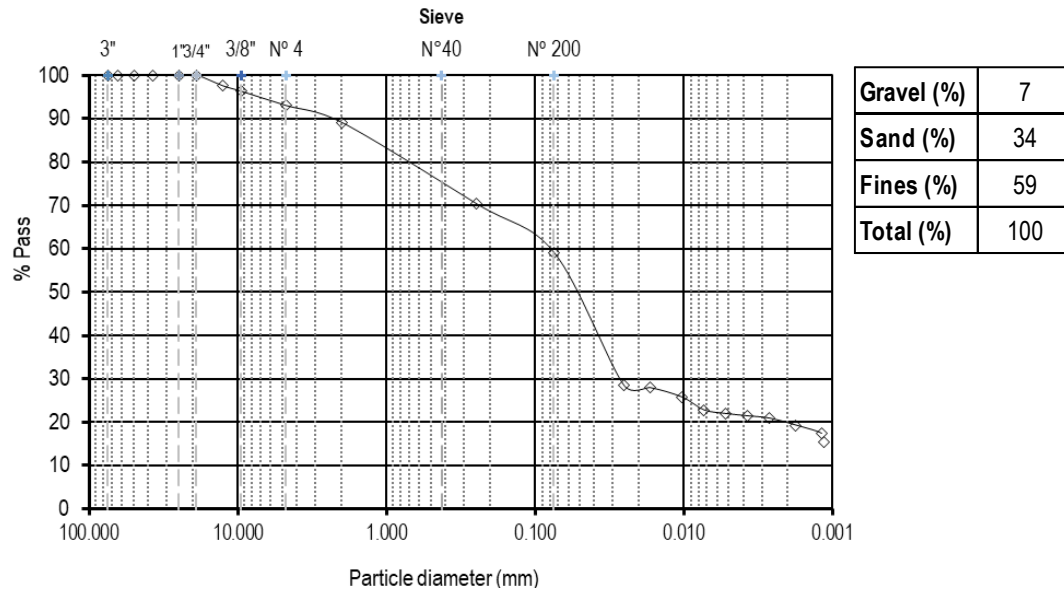


Figure A-2: Grain size distribution at Site-1

Plasticity index chart and Table information

Test performed to a sample at 0.42 meters, following the ASTM D4318-17e1

(Standard Test Methods for Liquid Limit, Plastic Limit, and Plasticity Index of Soils).

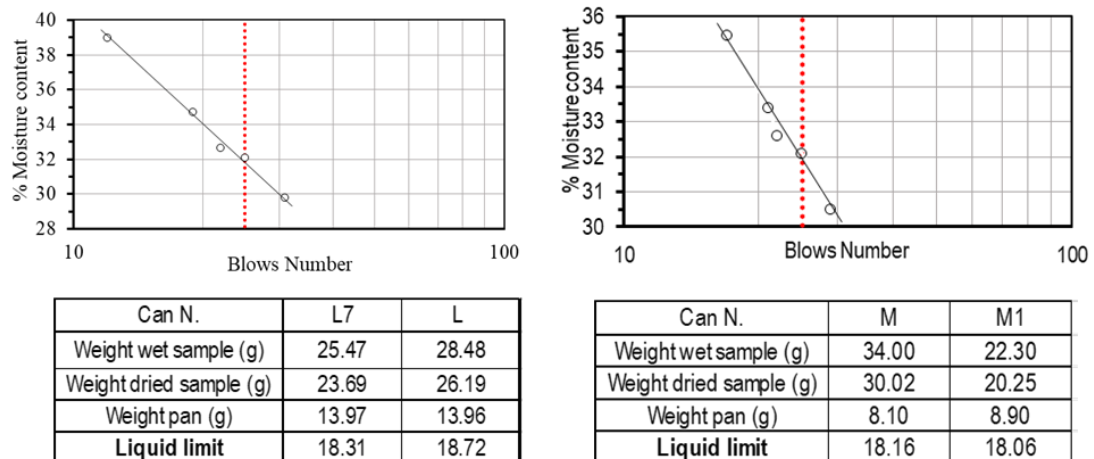


Figure A-3: Plasticity index results at Site-1

Unconfined compression

Curve of a test performed on a sample at 0.38 meters. ASTM D2166/D2166M – 16

(Standard Test Method for Unconfined Compressive Strength of Cohesive Soil).

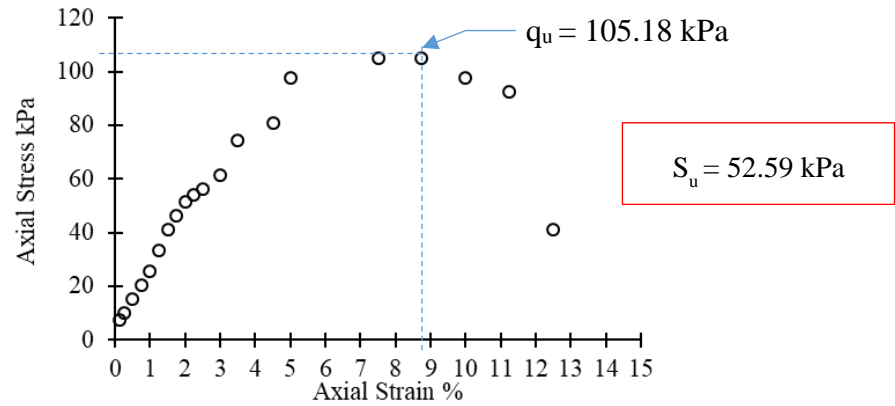


Figure A-4: Unconfined compression results at Site-1

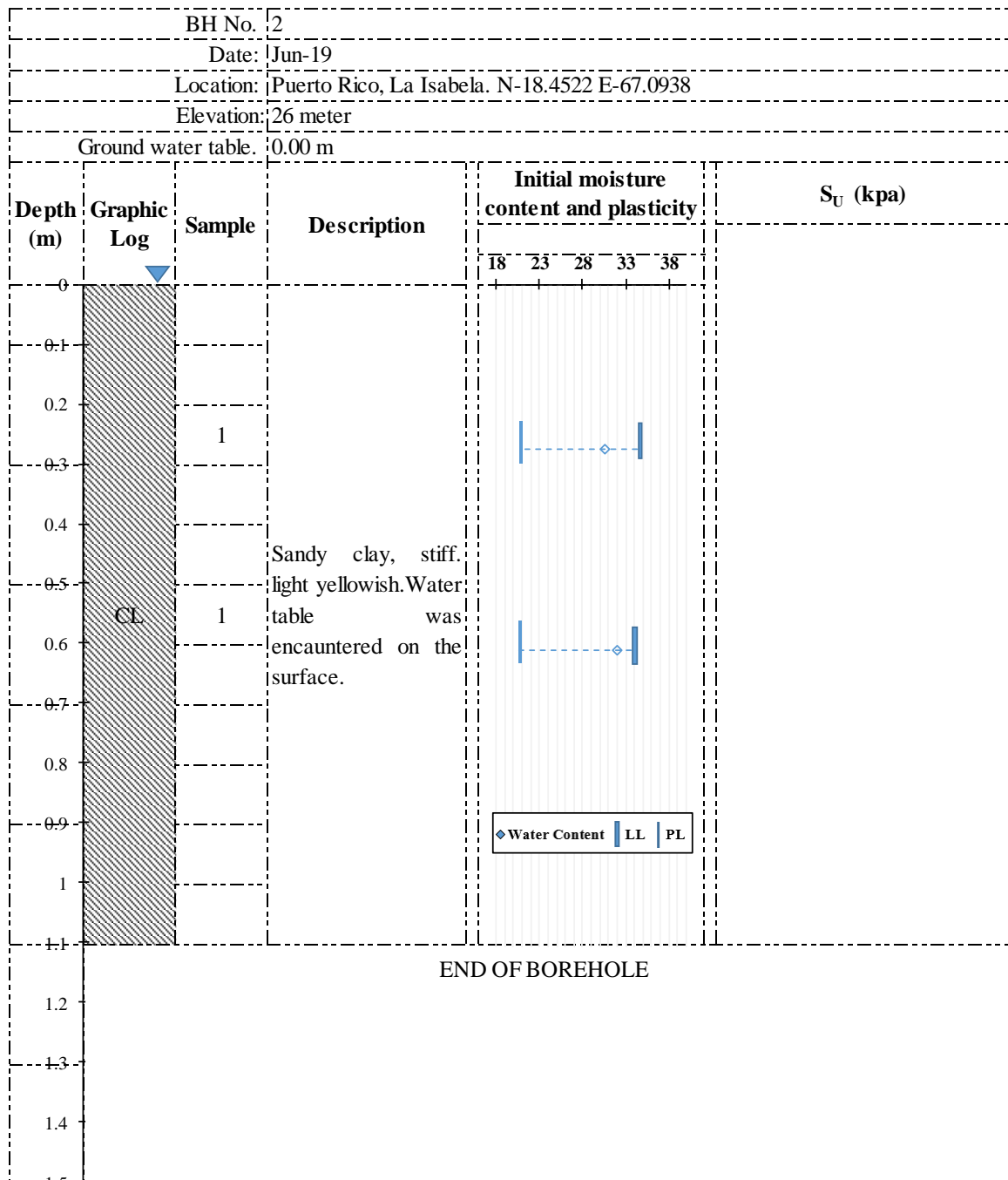


Figure A-5: Summary of geotechnical information at Site-2

Grain size distribution

Test performed on a sample at 0.45 meters. D422 – 63 (Standard Test Method for Particle-Size Analysis of Soils):

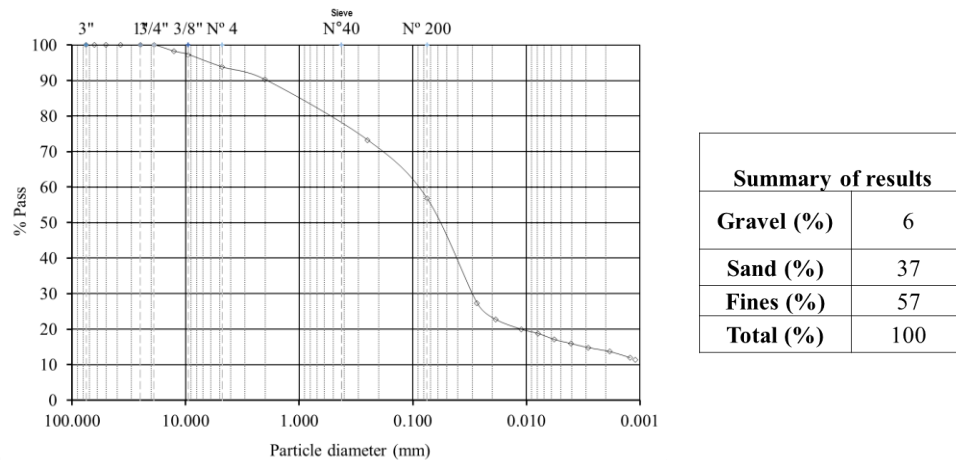


Figure A-6: Grain size distribution Site-2

Plasticity index chart and table information

Test performed on samples at 0.30 and 0.61 meters. ASTM D4318-17e1 (Standard Test Methods for Liquid Limit, Plastic Limit, and Plasticity Index of Soils).

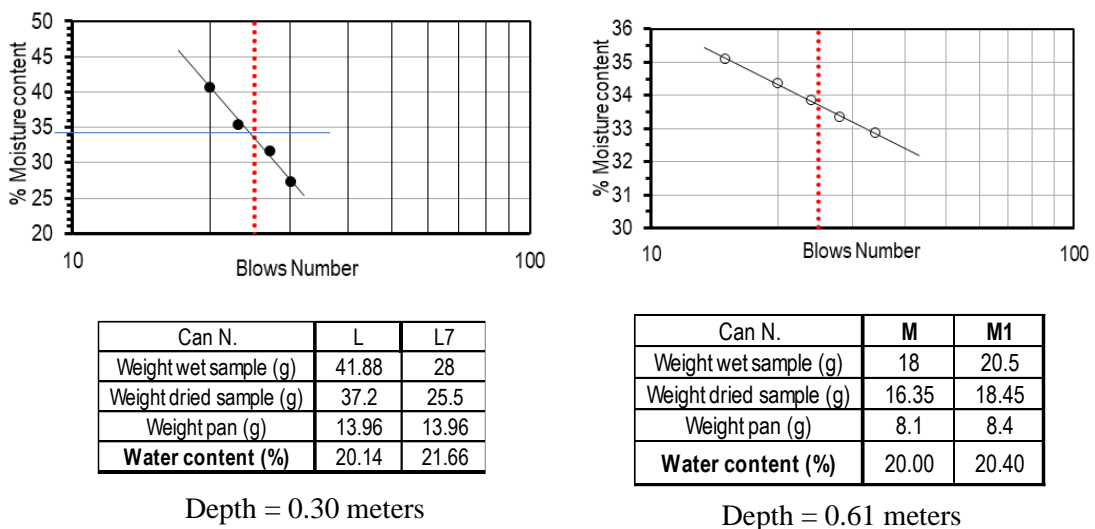


Figure A-7: Plasticity index results at Site-2

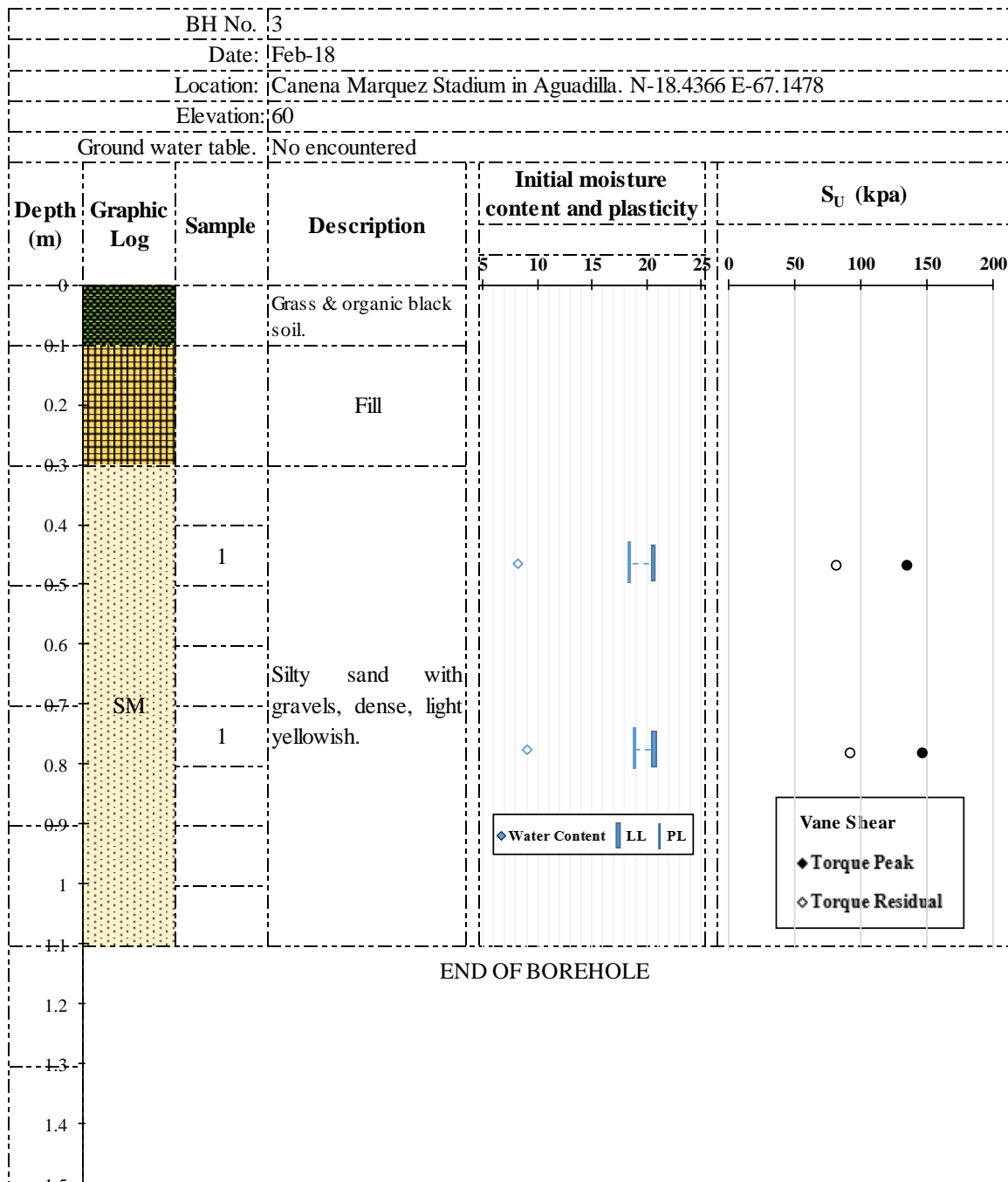


Figure A-8: Summary of geotechnical information at Site-3

Grain size distribution

Test performed in a sample located at 0.60 meters, following the D422-63

(Standard Test Method for Particle-Size Analysis of Soils):

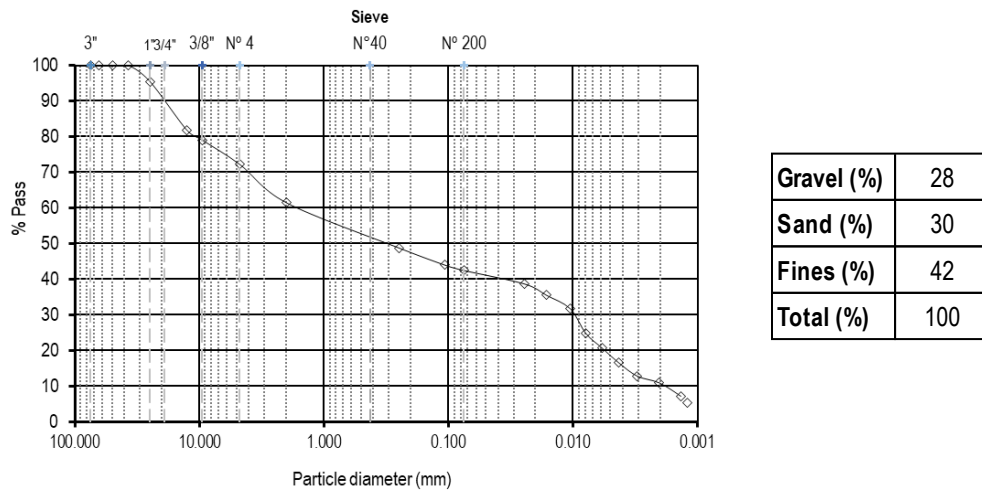
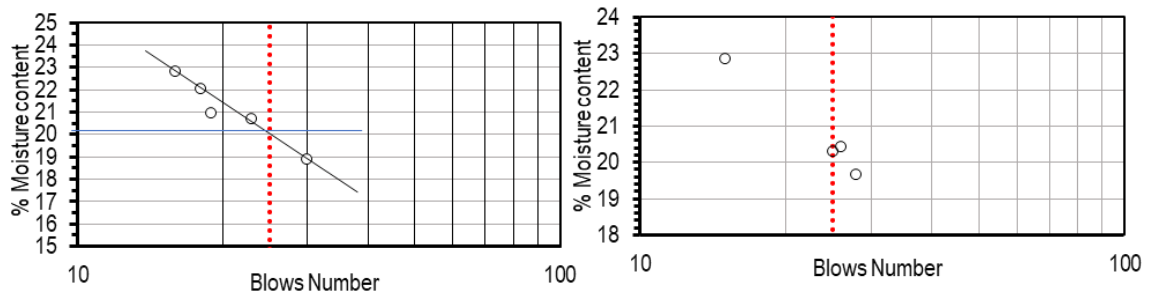


Figure A-9: Grain size distribution at Site-3

Plasticity index chart and table information

Test performed on samples located at 0.30 and 0.61 meters. ASTM D4318-17e1

(Standard Test Methods for Liquid Limit, Plastic Limit, and Plasticity Index of Soils).



Can N.	L	L7
Weight wet sample (g)	27.31	26.99
Weight dried sample (g)	25.18	24.91
Weight pan (g)	13.96	13.97
Water content (%)	18.98	19.01

Figure A-10: Plasticity index results at Site-3

APPENDIX B: LOADING DEMAND OF CS-1, CS-2, AND CS-3 STRUCTURES

B1.1 LOADS & MOMENTS OF THE CANTILEVER STRUCTURE

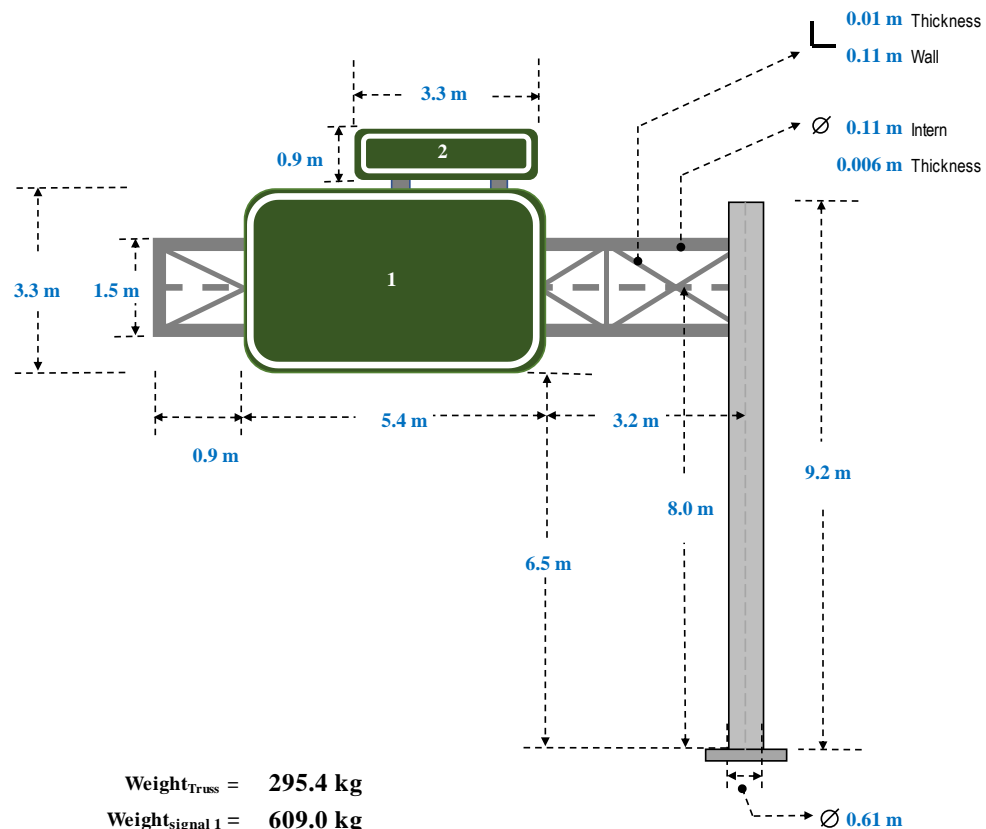
Location: **Site 1, Puerto Rico. (Latitude 18.4536, Longitude -67.0791)**

1. Wind Pressure (Wp)

$V_w =$	112	Basic wind speed (mph)
$K_z =$	0.98	Height and exposure factor
$I_r =$	1	Wind importance factor
$G =$	1.14	Gust effect factor
$C_d =$	1.2	Drag coefficient factor

PW _p =	<u>43.05</u>	<u>PSF</u>	0.00256·K _Z ·G·V _w ² ·I _r ·C _d
	<u>2.06</u>	<u>kPa</u>	

2. Calculation of mast arm loads and moments



Weight_{Truss}	=	295.4 kg
Weight_{signal 1}	=	609.0 kg
Weight_{signal 2}	=	101.5 kg
Area_{truss}	=	8.86 m²
Area_{signal 1}	=	17.82 m²
Area_{signal 2}	=	2.97 m²

Figure A-11: CS structure at Site-1

2.2. Pole base shear and moments:

2.2.1. Bending

2.2.1.1. Shear (q) due to wind:

$P_p =$	11.57 kN	2.60 kip	→ pole shear	
$P_s =$	42.85 kN	9.63 kip	→ signals shear	
$P_{tr} =$	7.20 kN	1.62 kip	→ truss shear	
$P_t =$	<u>61.62 kN</u>	<u>13.85 kip</u>	→ total shear	$P_W = \sum P_{Wi} \quad (2.5)$

2.2.1.2. Moments (M) due to wind:

$MW_p =$	53.21 kN·m	39.25 kip·ft	→ pole moment	
$MW_s =$	342.84 kN·m	252.86 kip·ft	→ signals moment	
$MW_{tr} =$	57.57 kN·m	42.46 kip·ft	→ truss moment	
$M_W =$	<u>453.6 kN·m</u>	<u>334.58 kip·ft</u>	→ total moment	$M_W = \sum_{i=1}^3 P_{Wi} \cdot d_{yi} \quad (2.6)$

2.2.1.3. Moments (M) due to dead loads:

$Mg_p =$	0.0 kN·m	0.0 kN·m	→ pole moment	
$Mg_s =$	40.1 kN·m	29.55 kip·ft	→ signals moment	
$Mg_{tr} =$	13.8 kN·m	10.15 kip·ft	→ truss moment	
$M_g =$	<u>53.8 kN·m</u>	<u>39.70 kip·ft</u>	→ total moment	$M_g = \sum_{i=1}^3 W_{gi} \cdot d_{xi} \quad (2.2)$

$M_T =$ **456.8 kN·m** 336.92 kip·ft

2.2.2. Torsion

$T_W =$ **271.5 kN·m** 200.26 kip·ft → total torsion moment $T_W = \sum_{i=1}^3 P_i \cdot d_{xi} \quad (2.8)$

Summary of Results	
Wind Speed=	112 mph
$P_t =$	61.62 kN
$M_T =$	456.8 kN·m
$T_W =$	271.5 kN·m

Table A-1: Summary of results at Site-1

B1.2

LOADS & MOMENTS OF THE CANTILEVER STRUCTURE

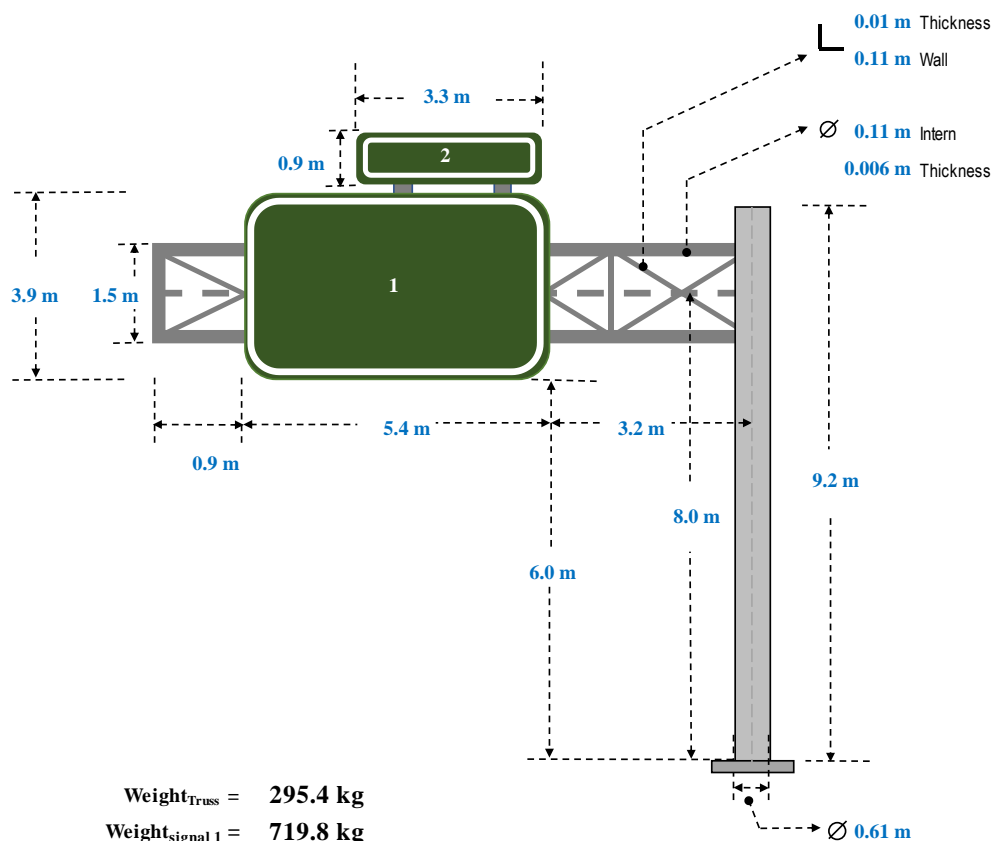
Location: Site 2, Puerto Rico. (Latitude 18.4522, Longitude -67.0938)

1. Wind Pressure (Wp)

$V_w =$	112	Basic wind speed (mph)
$K_z =$	0.98	Height and exposure factor
$I_r =$	1	Wind importance factor
$G_u =$	1.14	Gust effect factor
$C_d =$	1.2	Drag coefficient factor

$$PWp = \frac{43.05}{2.06} \quad \frac{PSF}{kPa} \quad 0.00256 \cdot K_z \cdot G \cdot V_w^2 \cdot I_r \cdot C_d$$

2. Calculation of mast arm loads and moments



Weight _{Truss} =	295.4 kg
Weight _{signal 1} =	719.8 kg
Weight _{signal 2} =	101.5 kg
Area _{truss} =	8.86 m ²
Area _{signal 1} =	21.06 m ²
Area _{signal 2} =	2.97 m ²

Figure A-12: CS structure at Site-2

2.2. Pole base shear and moments:

2.2.1. Bending

2.2.1.1. Shear (q) due to wind:

$P_p =$	11.57 kN	2.60 kip	→ pole shear	
$P_s =$	49.53 kN	11.14 kip	→ signals shear	
$P_{tr} =$	7.20 kN	1.62 kip	→ truss shear	
$P_t =$	<u>68.30 kN</u>	<u>15.35 kip</u>	→ total shear	$P_W = \sum P_{Wi} \quad (2.5)$

2.2.1.2. Moments (M) due to wind:

$MW_p =$	53.21 kN·m	39.25 kip·ft	→ pole moment	
$MW_s =$	396.27 kN·m	292.27 kip·ft	→ signals moment	
$MW_{tr} =$	57.57 kN·m	42.46 kip·ft	→ truss moment	
$M_W =$	<u>507.1 kN·m</u>	<u>373.98 kip·ft</u>	→ total moment	$M_W = \sum_{i=1}^3 P_{wi} \cdot d_{yi} \quad (2.6)$

2.2.1.3. Moments (M) due to dead loads:

$Mg_p =$	0.0 kN·m	0.0 kN·m	→ pole moment	
$Mg_s =$	46.5 kN·m	34.28 kip·ft	→ signals moment	
$Mg_{tr} =$	13.8 kN·m	10.15 kip·ft	→ truss moment	
$Mg =$	<u>60.2 kN·m</u>	<u>44.43 kip·ft</u>	→ total moment	$M_g = \sum_{i=1}^3 W_{gi} \cdot d_{xi} \quad (2.2)$

$M_T =$ **510.6 kN·m** 376.61 kip·ft

2.2.2. Torsion

$T_W =$ **310.9 kN·m** 229.32 kip·ft → total torsion moment $T_W = \sum_{i=1}^3 P_i \cdot d_{xi} \quad (2.8)$

Summary of Results	
Wind Speed	112 mph
$P_t =$	68.30 kN
$M_T =$	510.6 kN·m
$T_W =$	310.9 kN·m

Table A-2: Summary of results at Site-2

B1.3

LOADS & MOMENTS OF THE CANTILEVER STRUCTURE

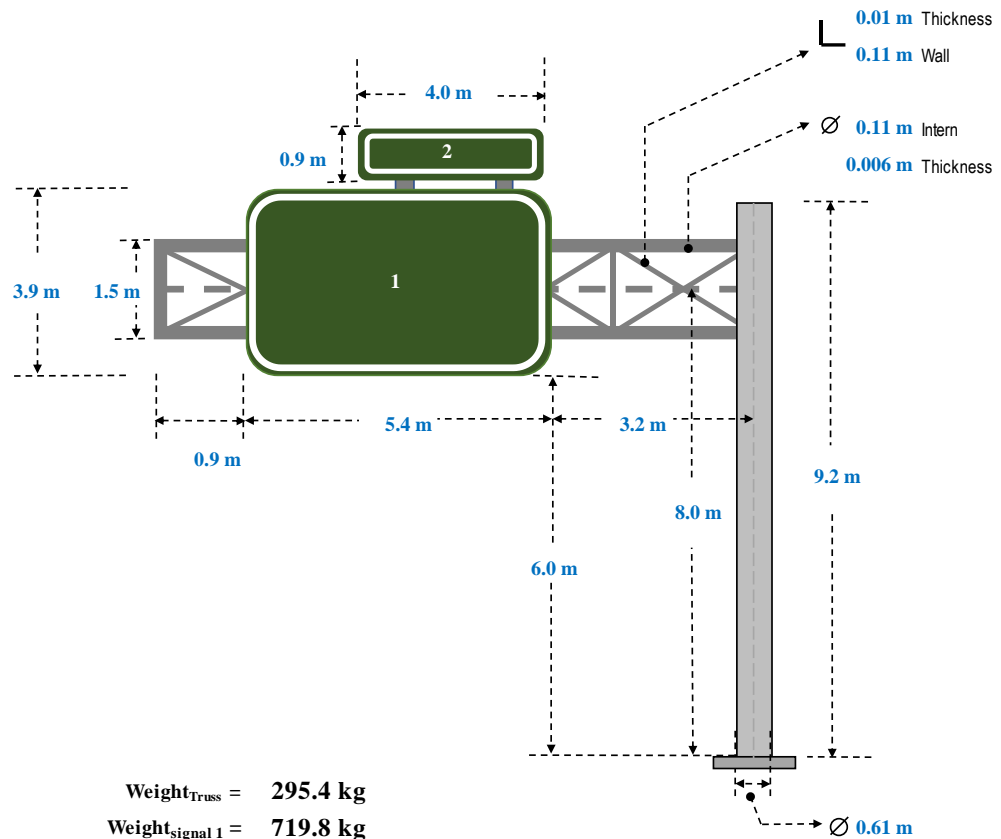
Location: Site 3, Puerto Rico. (Latitude 18.4366, Longitude -67.1478)

1. Wind Pressure (Wp)

$V_w =$	112	Basic wind speed (mph)
$K_z =$	0.98	Height and exposure factor
$I_r =$	1	Wind importance factor
$G_u =$	1.14	Gust effect factor
$C_d =$	1.2	Drag coefficient factor

PWp =	<u>43.05</u>	<u>PSF</u>	0.00256 · Kz · G · Vw ² · Ir · Cd
	<u>2.06</u>	<u>kPa</u>	

2. Calculation of mast arm loads and moments



Weight _{truss} =	295.4 kg
Weight _{signal 1} =	719.8 kg
Weight _{signal 2} =	123.0 kg
Area _{truss} =	8.86 m ²
Area _{signal 1} =	21.06 m ²
Area _{signal 2} =	3.60 m ²

Figure A-13: CS structure at Site-3

2.2. Pole base shear and moments:

2.2.1. Bending

2.2.1.1. Shear (q) due to wind:

$P_p =$	11.57 kN	2.60 kip	→ pole shear	
$P_s =$	50.83 kN	11.43 kip	→ signals shear	
$P_{tr} =$	7.20 kN	1.62 kip	→ truss shear	
$P_t =$	<u>69.60 kN</u>	<u>15.65 kip</u>	→ total shear	$P_W = \sum P_{Wi} \quad (2.5)$

2.2.1.2. Moments (M) due to wind:

$MW_p =$	53.21 kN·m	39.25 kip·ft	→ pole moment	
$MW_s =$	406.66 kN·m	299.93 kip·ft	→ signals moment	
$MW_{tr} =$	57.57 kN·m	42.46 kip·ft	→ truss moment	
$M_W =$	<u>517.4 kN·m</u>	<u>381.65 kip·ft</u>	→ total moment	$M_W = \sum_{i=1}^3 P_{Wi} \cdot d_{yi} \quad (2.6)$

2.2.1.3. Moments (M) due to dead loads:

$Mg_p =$	0.0 kN·m	0.0 kN·m	→ pole moment	
$Mg_s =$	47.9 kN·m	35.34 kip·ft	→ signals moment	
$Mg_{tr} =$	13.8 kN·m	10.15 kip·ft	→ truss moment	
$M_g =$	<u>61.7 kN·m</u>	<u>45.49 kip·ft</u>	→ total moment	$M_g = \sum_{i=1}^3 W_{gi} \cdot d_{xi} \quad (2.2)$

$M_T =$ **521.1 kN·m** 384.35 kip·ft

2.2.2. Torsion

$T_W =$ **319.8 kN·m** 235.88 kip·ft → total torsion moment $T_W = \sum_{i=1}^3 P_i \cdot d_{xi} \quad (2.8)$

Summary of Results	
Wind Speed	112 mph
$P_t =$	69.60 kN
$M_T =$	521.1 kN·m
$T_W =$	319.8 kN·m

Table A-3: Summary of results at Site-3

APPENDIX C: DESCRIPTION OF METHODS FOR PREDICT LATERAL, TORSIONAL AND COUPLED RESISTANCES

C.1. Lateral load and bending capacity

C.1.1. Cohesive soils

C.1.1.1. Ultimate load capacity by Broms

Figure A-14 shows the stress distributions proposed by Broms for cohesive soils. With the method proposed by Broms (1964a) the embedment depth for drilled shaft foundation with a specific diameter and certain soil conditions can be obtained.

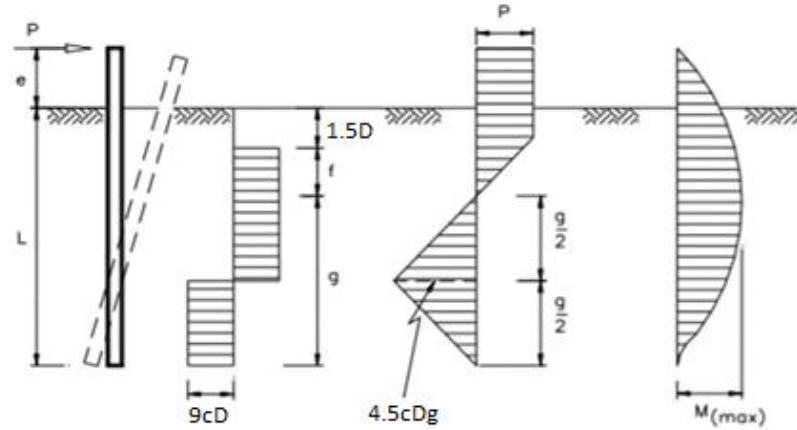


Figure A-14: Schematic of foundation in cohesive soils Brom's method

Where the maximum lateral load (P_T) and the maximum moment (M_{max}) in the drilled shaft could be compute as shown in Eq. C.1 and Eq. C.2 respectively.

$$P_T = 9 \cdot S_U \cdot D \cdot f \quad (C.1)$$

$$M_{max} = P_T \cdot (f + 1.5 D) - \frac{9 \cdot S_U \cdot D \cdot f^2}{2} \quad (C.2)$$

$$L_{req} = 1.5 D + f + g \quad (C.3)$$

where,

$M_{max} \rightarrow$ maximum moment produced on top of the drilled shaft

$P_T \rightarrow$ maximum load produced on top of the drilled shaft

- $S_U \rightarrow$ average shear strength
 $D \rightarrow$ diameter of the shaft
 $L_{req} \rightarrow$ required depth of the shaft

C.1.1.2. P-y model for stiff clay soils below water proposed by (Reese, et al. 1975)

Figure A-15 presents the drilled shaft resistance for specific drilled shaft geometry and soil conditions modeled as nonlinear springs distributed along a drilled shaft. The p and y represent the pile soil pressure per unit length and the deflection respectively. In the model stiff clay below water proposed by (Reese, et al. 1975), maximum load P_u is a function of the undrained shear strength, the diameter of the shaft, and the deflection Y is function of 50% of the shear strain ϵ_{50} and the diameter of the shaft.

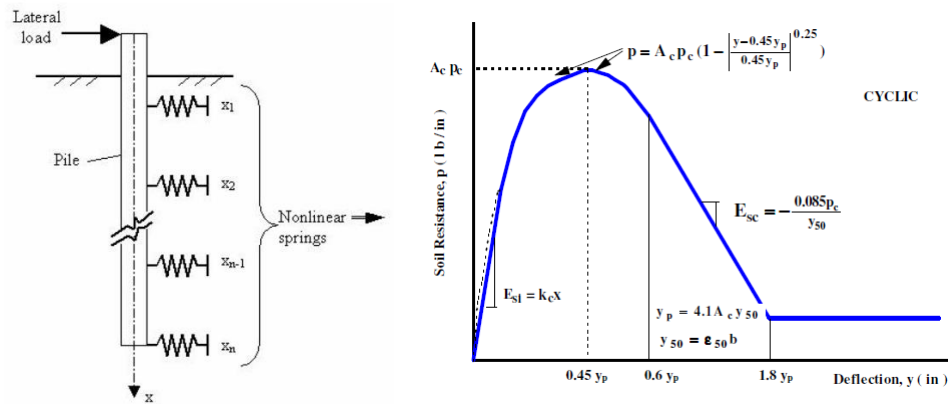


Figure A-15: Schematic showing p-y model used for lateral analysis
(FHWA-HRT-04-043, 2006) and (Reese, et al. 1975)

C.1.2. Cohesionless soils

C.1.2.1. Ultimate load capacity by Broms

Figure A-16 shows the stress distributions proposed by Broms for cohesive soils. With the method proposed by Broms (1964b) the embedment depth for drilled shaft foundation with a specific diameter and certain soil conditions can be obtained.

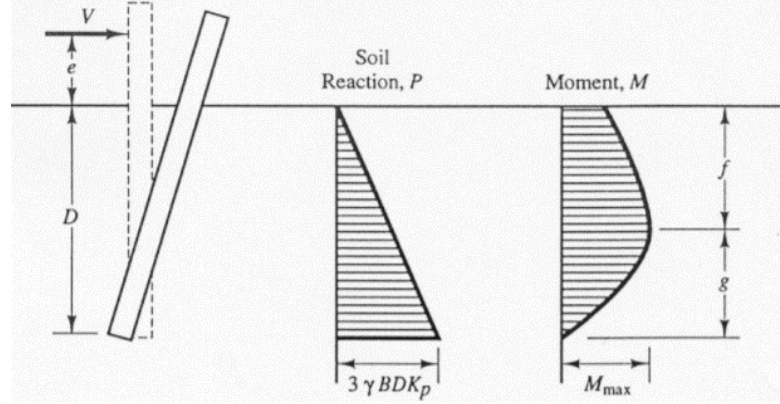


Figure A-16: Schematic of foundation in cohesive soils Brom's method

where the maximum moment (M_{\max}) in the drilled shaft could be computed as shown in Eq.7.4.

$$M_{\max} = \frac{\gamma \cdot D \cdot L \cdot K_p}{2} \quad (C.4)$$

where,

- σ'_{vz} → effective vertical stress at depth
- γ → unit weight of soil
- K_p → Rankine coefficient of passive earth pressure, $K_p = \tan^2(45 + \phi'/2)$
- ϕ' → angle of internal friction of soil

C.1.2.2. P-y model for cohesionless proposed by (Reese, et al. 1975)

FB-Multiplier uses a numerical non-linear analysis that represents the soil resistance with non-linear springs based on p-y curves as shown in Figure A-18. In order to find the relationship between applied load and pile head lateral displacement for a drilled shaft with a diameter of 0.91 a model proposed by (Reese, et al. 1975) was used. In this model, the maximum load P_u is a function of soil friction angle ϕ , soil unit total weight γ and diameter

of the shaft D , while the deflection Y is function of the shaft diameter as shown in Figure A-17.

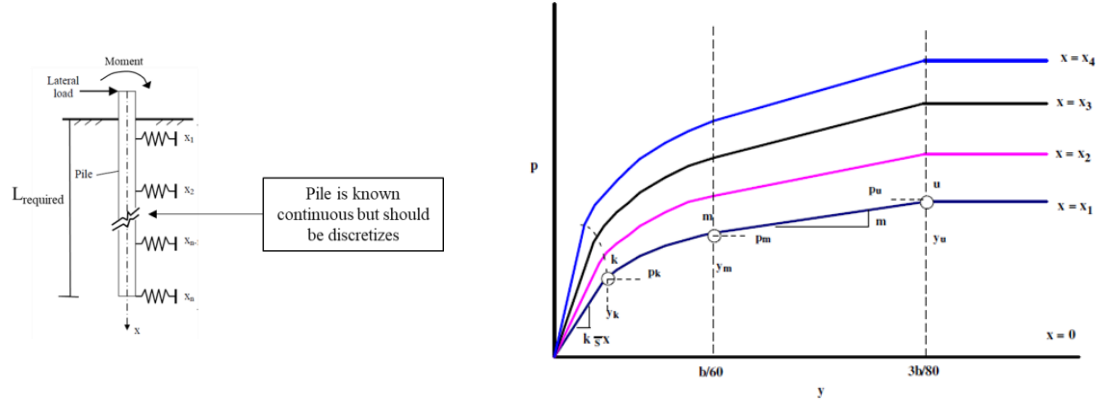


Figure A-17: Schematic showing p-y model used for lateral analysis (FHWA-HRT-04-043, 2006) and (Reese, et al. 1975)

C.2. Torsion capacity

The torsion capacity is computed as shown in Eq. 7.5.

$$T = T_T + T_S \quad (C.5)$$

where the total torsion resistance (T) is equal to the sum of side resistance (T_S) and base resistance (T_T) of the pile.

C.2.1. Cohesive soils

C.2.1.1. Ultimate capacity based on unit resistance α method (O'Neill and Reese, 1999)

$$T_S = \pi \cdot L \cdot D \cdot S_U \cdot \alpha \cdot \frac{D}{2} \quad (C.6)$$

where α could be computed depending the ratio between the undrained shear strength and the atmospheric pressure as shown below:

$$\alpha = 0.55 \text{ when } \frac{S_U}{P_a} \leq 1.5$$

$$\alpha = 0.55 - 0.1 \left(\frac{S_U}{P_a} - 1.5 \right) \text{ when } 1.5 \leq \frac{S_U}{P_a} \leq 2.5$$

$$\alpha = 0.45 \text{ when } \frac{S_U}{P_a} > 2.5$$

$$T_T = N'_C \cdot S_U \quad (C.7)$$

$P_a \rightarrow$ atmospheric pressure (101.325 kPa)

$\alpha \rightarrow$ load transfer ratio

C.2.1.2. Ultimate capacity based on unit resistance α method by (Hu, 2003) based on (O'Neill and Reese, 1999)

$$T_S = \frac{\pi \cdot D^2}{2} \cdot (L - 1.5) \cdot r_s \quad (C.8)$$

$$T_T = \frac{4D}{9} \cdot (W + Q_a) \cdot \tan \delta \quad (C.9)$$

where r_s must be computed as $r_s = \alpha \cdot S_U + K_o \cdot \sigma'_{vz} \cdot \tan \delta$, and α should be calculated as was shown in previous method and,

$\delta \rightarrow$ effective soil-shaft interface friction angle

$W \rightarrow$ weight of the deep drilled shaft

$Q_a \rightarrow$ vertical loading upon the drilled shaft

C.2.1.3. Ultimate capacity based on unit resistance by (Nusairat, 2004)

This design method also is used by CDOT and is based on shaft resistance is equal to the undrained shear strength over the depth of interest.

$$T_S = \frac{\pi \cdot D^2}{2} \cdot (L - 1.5D) \cdot S_U \quad (C.10)$$

$$T_T = \frac{\pi \cdot D^3}{12} \cdot S_U \quad (C.11)$$

C.2.2. Cohesionless soils

C.2.2.1. Ultimate capacity based on unit resistance β method (O'Neill and Reese, 1999)

$$T_S = \pi \cdot L \cdot D \cdot f_s \cdot \frac{D}{2} \quad (C.12)$$

$$T_T = 0.67 \cdot (W \cdot A_y) \cdot \tan(0.67\phi) \cdot \frac{D}{2} \text{ or } 0.67 \cdot (W \cdot A_y) \cdot \tan(\delta) \cdot \frac{D}{2} \quad (C.13)$$

where f_s and β can be computed using Eq 7.13 and 7.14.

$$f_s = \beta \cdot \sigma'_{vz} \quad (C.14)$$

$$\beta = 1.5 - 0.135 \cdot \sqrt{z} \text{ for } N_{60\text{-uncorrected}} \geq 15 \text{ or } \beta = \left(\frac{N}{15}\right) \cdot 1.5 - 0.135 \cdot \sqrt{z} \text{ for } N_{60\text{-uncorrected}} < 15 \quad (C.15)$$

where,

β, ω	\rightarrow	load transfer ratio
k_o	\rightarrow	at rest lateral earth pressure coefficient
σ'_{vz}	\rightarrow	effective vertical stress at the mid-point of the layer of interest
z	\rightarrow	depth from ground surface to the mid-layer
δ	\rightarrow	effective soil-shaft interface friction angle
ϕ'	\rightarrow	effective friction angle
W	\rightarrow	weight of the deep drilled shaft
A_y	\rightarrow	vertical loading upon the drilled shaft

C.2.1.2. Ultimate capacity based on FDOT modifications to LRFD specifications (FDOT, 2019)

$$\phi \cdot T_T = \pi \cdot L \cdot D \cdot f_s \cdot \frac{D}{2} \quad (C.16)$$

where ϕ is the resistance factor for torsion (0.9) for CS structure and f_s is calculated using a load transfer ratio depth independent ω_{fdot} shown in Eq. C.17.

$$f_s = \omega \cdot \sigma'_{vz} \quad (C.17)$$

and ω is computed as shown in Eq. 7.18.

$$\omega = 1.5 \text{ for } N_{60\text{-uncorrected}} \geq 15 \text{ or } \omega = 1.5 - \left(\frac{N_{60}}{15}\right) \text{ for } N_{60\text{-uncorrected}} < 15 \quad (C.18)$$

C.2.1.3. Ultimate capacity based on Florida structure design office method (HU, 2003)

$$T_S = \frac{\pi \cdot D^2}{2} \cdot L \cdot r_s \quad (C.19)$$

$$T_T = \frac{D}{3} \cdot W \cdot \tan \delta \quad (C.20)$$

where r_s is computed as shown in Eq. 7.21.

$$r_s = k_o \cdot \sigma'_{vz} \cdot \tan \delta \quad (C.21)$$

C.2.1.4. Ultimate capacity based on (Nusairat et al. 2004)

$$T_s = \frac{\pi \cdot D^2}{2} \cdot L \cdot r_s \quad (C.22)$$

$$T_T = \frac{D}{3} \cdot W \cdot \tan \delta \quad (C.23)$$

where r_s and k are computed as shown in Eq. C.24 and Eq. C.25 respectively.

$$r_s = k \cdot \sigma'_{vz} \cdot \tan \delta \quad (C.24)$$

$$k = \frac{2L}{3D} (1 - \sin \phi) \quad (C.25)$$

C.3. Coupled analysis lateral loading and torsion

C.3.1. Cohesionless soils

C.3.1.1. Ultimate capacity based on coupled loading (Filz et al., 1995)

Filz (1995) establish his theory on the interaction between the at-rest resistance to torsion, and the additional resistance to torsion from the passive reactions to overturning.

The maximum load could be computed as shown in Eq. C.26.

$$P_{ult} = \frac{\alpha_o \cdot \frac{\pi}{2} \cdot K_o \cdot \gamma \cdot L^2 \cdot D \cdot \tan(\delta_o)}{\left[\frac{r}{D} - \beta_o \cdot \left(2.5 + 3 \frac{e}{L} \right) \cdot \tan(\delta_o) \right]} \quad (C.26)$$

where,

α_o → fraction of the component of torsion capacity due to at-rest earth pressures

β_o → fraction of the component of torsion capacity due to passive ground reactions

δ_o → effective stress angle of friction for the shaft-soil interface

r → radial distance from axis of shaft to load application

e → vertical distance from ground surface to point of load application

APPENDIX D: WEBSITES USED TO COMPILE DESIGN AND CONSTRUCTION INFORMATION

Table A-4: Summary design and construction information

State DOT	Website address	Description
Alabama	https://www.dot.state.al.us/conweb/specifications.html	2018 standard specifications
	https://alletting.dot.state.al.us/Docs/Standard_Drawings/2017%20English/STDUS17_1000.pdf	Standard drawings
	https://alletting.dot.state.al.us/Docs/Standard_Drawings/2016%20English/STDUS16_1200.pdf	Standard drawings wind speed
Florida	http://www.fdot.gov/structures/StructuresManual/CurrentRelease/Vol3LTS.pdf	FdOT modifications to lrfd specifications for structural supports for highway signs, luminaires and traffic signals (lrfdlts-1)
	http://www.fdot.gov/structures/proglib.shtm	Excel Spreadsheet Mastarm-Index17743-v1.1
	http://www.fdot.gov/roadway/DS/18/IDX/17743.pdf	Standard mast arm assemblies 17743
	http://www.fdot.gov/roadway/ds/12/ids/ids-17743.pdf	Index 17743 standard mast arm "d" & "e" assemblies
	http://www.fdot.gov/structures/ProgLib.shtm	Mathcad Drilled Shaft- LRFD v1.0
	http://www.fdot.gov/roadway/DS/16/IDX/17745.pdf	Mast arms drawings
Georgia	http://mydocs.dot.ga.gov/info/gdotpubs/ConstructionStandardsAndDetails/Forms/AllItems.aspx	Standard drawings
	http://www.dot.ga.gov/PartnerSmart/Business/Source/specs/2001StandardSpecifications.pdf	Standard Specifications Construction of Transportation Systems
	http://www.dot.ga.gov/PartnerSmart/DesignManuals/SignalDesignManual/Traffic%20Signal%20Design%20Guidelines-2016.pdf	Traffic signal design guidelines
Louisiana	http://wwwsp.dotd.la.gov/Inside_LaDOTD/Divisions/Engineering/Standard_Plans/Pages/default.aspx	Standard plans / special details

	http://wwwsp.dotd.la.gov/Inside_LaDOTD/Divisions/Engineering/Design-Build/AmiteBridge_Juban/RFP/I-12%20PS-08%20Geotechnical%20PS%20(11-20-09).pdf	Geotechnical performance specification
State DOT	Website address	Description
Mississippi	http://sp.mdot.ms.gov/Construction/Standard%20Specifications/2017%20Standard%20Specifications.pdf	Mississippi Standard Specifications for Road and bridge construction
	http://mdot.ms.gov/documents/lpa/checklist/722-1.pdf	Materials for Traffic Signal Installation
	http://mdot.ms.gov/bidsystem_data/20180123/PLANDATA/107241302.pdf	Standard drawings
North Carolina	https://connect.ncdot.gov/resources/safety/Pages/ITS-Design-Resources.aspx	ITS and Signals Unit Design Resources
	https://connect.ncdot.gov/resources/Geological/Documents/16-03-29_Geotechnical%20Investigation%20and%20Recommendations%20Manual.pdf	Geotechnical investigation and recommendations manual
	https://www.scdot.org/business/standard-specifications.aspx	Standard specifications for highway construction
Oregon	https://www.oregon.gov/ODOT/Engineering/Pages/Drawings-Traffic.aspx	Standard drawings - Traffic
	ftp://ftp.odot.state.or.us/techserv/roadway/web_drawings/2018_STD_July_2017_Update.pdf	Oregon standard drawings 2018 numbers and revision dates
	http://library.state.or.us/repository/2015/201512030819134/ODOT_HWY_GEOENVIRONMENTAL_docs_Geology_Geology_GDM_Chptr16.pdf	Foundation Design for Signs Signals, Luminaires, Sound Walls and Buildings
	https://www.iccsafe.org/	https://www.iccsafe.org/
South Carolina	https://www.scdot.org/business/standard-specifications.aspx	Standard specifications for highway construction
	https://www.scdot.org/business/traffic-signals.aspx	Traffic signal design guidelines sc
	https://www.scdot.org/business/geotech.aspx	Geotechnical design manual
Texas	http://www.dot.state.tx.us/insdtdot/orgchart/cmd/cserve/standard/toc.htm	Traffic standards (english)
	https://library.ctr.utexas.edu/digitized/texasarchive/phase1/244-1-ctr.pdf	Analysis of single piles under lateral loading

	http://onlinemanuals.txdot.gov/txdotmanuals/geo/geo.pdf	Geotechnical manual
	ftp://ftp.dot.state.tx.us/pub/txdot-info/dal/specinfo/trfstds/traffic-signal-pole-foundation.pdf	Traffic signal pole foundation standard drawing
State DOT	Website address	Description
Virginia	http://www.extranet.vdot.state.va.us/LocDes/Electronic_Pubs/2008Standards/CSection1300.pdf	Index of sheets section 1300-traffic control
	http://www.virginiadot.org/business/resources/const/VDOT_2016_RB_Specs.pdf	Road and Bridge Specifications
	http://www.virginiadot.org/business/resources/IIM/TE-382_AASHTO_Standard_Specifications.pdf	VDOT Guidelines to AASHTO Standard Specifications for Structural Supports for Highway Signs, Luminaries, and Traffic Signals, 6th Edition, 2013 with 2015 interims
Washington	http://www.wsdot.wa.gov/publications/fulltext/Standards/english/PDF/j26.15-01_e.pdf	Standard drawings
	http://www.wsdot.wa.gov/publications/fulltext/Standards/english/PDF/j26.10-03_e.pdf	Standard drawings
	http://www.wsdot.wa.gov/Bridge/Structures/StandardDrawings.htm#10	General standard drawings
	http://www.wsdot.wa.gov/publications/manuals/fulltext/M23-50/BDM.pdf	Bridge design manual
	http://www.wsdot.wa.gov/publications/manuals/fulltext/M22-01/design.pdf	Design manual

APPENDIX E: SUMMARY TABLES WITH SUMMARY OF SURVEY QUESTIONNAIRE AND FOLLOW-UP CONFERENCE

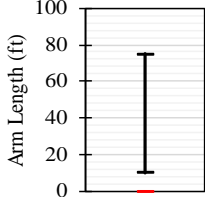
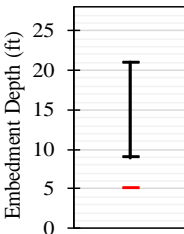
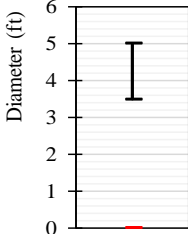

SUMMARY FOR NCDOT			
	Yes/No	Date	Contact-Person
Questionnaire	-	-	Debesh Sarkar dcsarkar@ncdot.gov
Follow-up conference	-	-	
<div style="display: flex; justify-content: space-between;"> <div style="width: 30%;"> <p>a) Mast arm length:</p>  </div> <div style="width: 65%;"> <div style="border: 1px solid black; padding: 5px; margin-top: 10px;"> <p>Notes/Comments:</p> <ul style="list-style-type: none"> - 10 mast arms with different lengths. </div> </div> </div>			
<div style="display: flex; justify-content: space-between;"> <div style="width: 30%;"> <p>b) Most commonly used foundation system: Drilled Shafts</p> <div style="display: flex; justify-content: space-around;">   </div> </div> <div style="width: 65%;"> <div style="border: 1px solid black; padding: 5px; margin-top: 10px;"> <p>Notes/Comments:</p> <ul style="list-style-type: none"> - L-Pile 2016.9.07 for overturning and methods α or β for torsion and axial loading. - Spreadsheet Drilled Shaft Foundation Program_V3.4 - One case of pile cap foundation. </div> </div> </div>			
<div style="display: flex; justify-content: space-between;"> <div style="width: 30%;"> <p>c) Geotechnical exploration:</p> <p>Requirements:</p> </div> <div style="width: 30%;"> <p>Min. Number of borings:</p> <p>SPT Yes</p> <p>Other:</p> </div> <div style="width: 35%;"> <div style="border: 1px solid black; padding: 5px; margin-top: 10px;"> <p>- Standard designs based on soil type, SPT, wind zone, and mast arm length.</p> </div> </div> </div>			
<div style="display: flex; justify-content: space-between;"> <div style="width: 30%;"> <p>d) Design standard used:</p> <p><u>Wind speed in the coastal area:</u></p> <p><u>MRI:</u></p> <p><u>Wind map:</u></p> </div> <div style="width: 30%;"> <p>AASHTO 2009 - LTS 5</p> <p>140 mph</p> <p>50</p> </div> <div style="width: 35%;"> <div style="border: 1px solid black; padding: 5px; margin-top: 10px;"> <p>Notes/Comments:</p> <ul style="list-style-type: none"> - 5 wind zones </div> </div> </div>			
			
<p>d2) Foundation Design Standards: See appendix C-a</p>			
<p>e) Reported Failures: No Comments:</p>			

Table A-5: NCDOT survey summary

SUMMARY FOR FDOT			
	Yes/No	Date	Contact-Person
Questionnaire	Yes	5/29/2018	Larry Jones
Follow-up conference	Yes	8/22/2018	larry.jones@dot.state.fl.us
<div style="display: flex; justify-content: space-between; align-items: flex-start;"> <div style="width: 30%;"> <p>a) Mast arm length:</p> </div> <div style="width: 30%; text-align: center;"> </div> <div style="width: 35%; border: 1px solid black; padding: 5px;"> <p>Notes/Comments:</p> <ul style="list-style-type: none"> - INDEX 17743 STANDARD MAST ARM "D" & "E" ASSEMBLIES <li style="color: red;">- See survey questionnaire in Appendix D-a. </div> </div>			
<p>b) Most commonly used foundation system: Drilled Shafts</p> <div style="display: flex; justify-content: space-between; align-items: flex-start;"> <div style="width: 30%;"> </div> <div style="width: 30%;"> </div> <div style="width: 35%; border: 1px solid black; padding: 5px;"> <p>Notes/Comments:</p> <ul style="list-style-type: none"> Design tools of FDOT - Excel Spreadsheet Mastarm-Index17743-v1.1 - Mathcad Drilled Shaft- LRFD v1.0 </div> </div>			
<div style="display: flex; justify-content: space-between;"> <div style="width: 35%;"> <p>c) Geotechnical Exploration:</p> <p>Requirements:</p> </div> <div style="width: 30%;"> <p>Min. Number of borings: 1*</p> <p>SPT Yes</p> <p>Other:</p> </div> <div style="width: 30%; border: 1px solid black; padding: 5px;"> <p>Notes/Comments: One SPT boring to 25 ft in soil or 10 ft in competent rock with 15 ft min.</p> </div> </div>			
<div style="display: flex; justify-content: space-between;"> <div style="width: 35%;"> <p>d) Design standard used:</p> <p><u>Wind Speed in the coastal are:</u> 170 mph</p> <p><u>MRI:</u> 300</p> <p><u>Wind Map:</u></p> </div> <div style="width: 30%;"> <p>AASHTO LRFD, First Edition 2015 – LRFDLTS 1*</p> </div> <div style="width: 30%; border: 1px solid black; padding: 5px;"> <p>Notes/Comments:</p> <p>* Vol3LTS-19 modifications to LRFDLTS 1</p> </div> </div> <div style="text-align: center; margin-top: 20px;"> </div>			
<p>d2) Foundation Design Standards: See appendix C-b</p>			
<p>e) Reported Failures: NO Comments:</p>			

Table A-6: FDOT survey summary

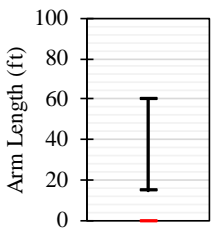
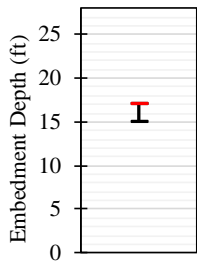
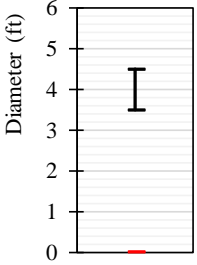
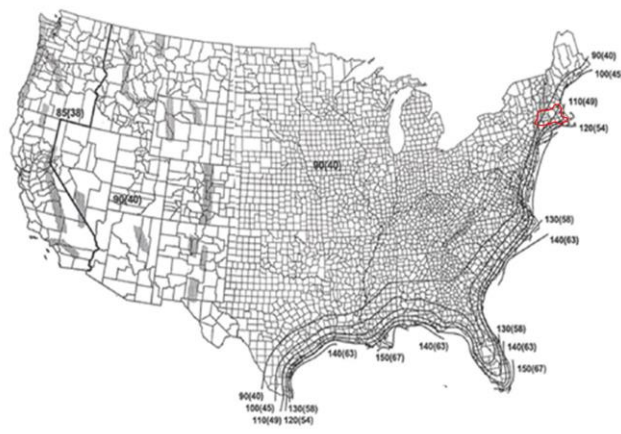
SUMMARY FOR MassDOT			
	Yes/No	Date	Contact-Person
Questionnaire	Yes	5/22/2018	Peter Connors
Follow-up conference	No		peter.connors@state.ma.us
<div style="display: flex; justify-content: space-between; align-items: flex-start;"> <div style="width: 30%;"> <p>a) Mast arm length:</p>  </div> <div style="width: 65%; border: 1px solid black; padding: 10px; min-height: 100px;"> <p style="text-align: center;">Notes/Comments:</p> </div> </div>			
<p>b) Most commonly used foundation system: Drilled Shafts</p> <div style="display: flex; justify-content: space-between; align-items: flex-start;"> <div style="width: 30%;">   </div> <div style="width: 65%; border: 1px solid black; padding: 10px; min-height: 100px;"> <p style="text-align: center;">Notes/Comments:</p> </div> </div>			
<p>c) Geotechnical exploration: Min. Number of borings: 1</p> <p>Requirements: SPT Yes</p> <p>Other:</p>			
<p>d) Design standard used: AASHTO 2013 - LTS 6</p> <div style="display: flex; justify-content: space-between; align-items: flex-start;"> <div style="width: 60%;"> <p>Wind speed in the coastal area: 130 mph</p> <p>MRI: 50</p> <p>Wind map:</p>  </div> <div style="width: 35%; border: 1px solid black; padding: 10px; min-height: 100px;"> <p>- Wind speed AASHTO 2013 - LTS 6.</p> </div> </div>			
<p>d2) Foundation design standards: See appendix N-A</p>			
<p>e) Reported failures: NO Comments:</p>			

Table A-7: MassDOT survey summary

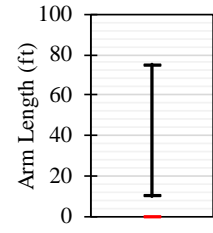
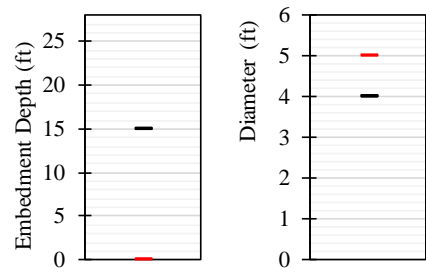

SUMMARY FOR VDOT				
	Yes/No	Date	Contact-Person	
Questionnaire	Yes	6/26/2018	John Hall	john.hall@vdot.virginia.gov
Follow-up conference	Yes	9/21/2018		
<div style="display: flex; justify-content: space-between; align-items: flex-start;"> <div style="width: 30%;"> <p>a) Mast arm length:</p>  </div> <div style="width: 65%; border: 1px solid black; padding: 5px;"> <p>Notes/Comments:</p> <p style="color: red;">- See survey questionnaire in Appendix D-c.</p> </div> </div>				
<p>b) Most commonly used foundation system: Drilled Shafts</p> <div style="display: flex; justify-content: space-around; align-items: flex-start;"> <div style="width: 30%;">  </div> <div style="width: 65%; border: 1px solid black; padding: 5px;"> <p>Notes/Comments:</p> <p>- Notes/Comments: Drilled Shafts. We used to have a foundation that consisted on drilled shaft with "wings" for torsional resistance, but we no longer use the wings. Brom's for preliminary calculations, COM624P or L-Pile</p> </div> </div>				
<div style="display: flex; justify-content: space-between;"> <div style="width: 40%;"> <p>c) Geotechnical Exploration:</p> <p>Requirements:</p> </div> <div style="width: 40%;"> <p>Min. Number of borings:</p> <p>SPT Yes</p> <p>Other:</p> </div> <div style="width: 20%; border: 1px solid black; padding: 5px;"> <p>The testing general consists of simple indices tests (gradations, Atterberg limits and moisture contents).</p> </div> </div>				
<p>d) Design standard used: AASHTO 2013 - LTS 6 - with 2015 interims</p> <div style="display: flex; justify-content: space-between;"> <div style="width: 40%;"> <p>Wind Speed in the coastal are: 90 mph</p> <p>MRI: 50</p> <p>Wind Map:</p> </div> <div style="width: 55%; border: 1px solid black; height: 100px;"></div> </div> <div style="text-align: center; margin-top: 20px;">  </div>				
<p>d2) Foundation Design Standards: See appendix C-c</p>				
<p>e) Reported Failures: NO Comments:</p>				

Table A-8: VDOT survey summary

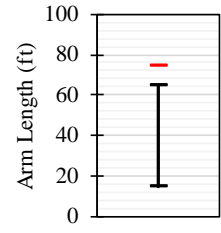
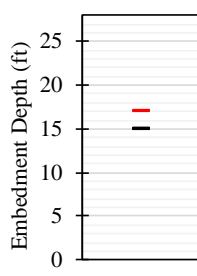
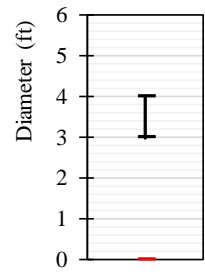

SUMMARY FOR SCDOT				
	Yes/No	Date	Contact-Person	
Questionnaire	Yes	5/22/2018	Carol Jones	JonesVC@scdot.org
Follow-up conference	Yes	9/21/2018		
<div style="display: flex; justify-content: space-between; align-items: flex-start;"> <div style="width: 35%;"> <p>a) Mast arm length:</p>  </div> <div style="width: 60%; border: 1px solid black; padding: 10px; margin-top: 20px;"> <p>Notes/Comments:</p> <p style="color: red;">- See survey questionnaire in Appendix D-d.</p> </div> </div>				
<p>b) Most commonly used foundation system: Drilled Shafts</p> <div style="display: flex; justify-content: space-around; align-items: flex-start;"> <div style="width: 30%;">  </div> <div style="width: 30%;">  </div> <div style="width: 35%; border: 1px solid black; padding: 10px; margin-top: 20px;"> <p>Notes/Comments:</p> <p>- Structure & Foundation AASHTO LRFD Specifications for Structural Supports for Highway Signs, Luminaires and Traffic Signals, 1st Edition (LRFDLTS-1).</p> </div> </div>				
<div style="display: flex; justify-content: space-between;"> <div style="width: 35%;"> <p>c) Geotechnical exploration:</p> <p>Requirements:</p> </div> <div style="width: 35%;"> <p>Min. Number of borings:</p> <p>SPT Yes</p> <p>Other:</p> </div> <div style="width: 30%; border: 1px solid black; padding: 10px;"> <p>Geotechnical exploration: Borehole of 15 ft minimum required. Undisturbed samples if is possible.</p> </div> </div>				
<div style="display: flex; justify-content: space-between;"> <div style="width: 35%;"> <p>d) Design standard used:</p> <p><u>Wind speed in the coastal are:</u></p> <p><u>MRI:</u></p> <p><u>Wind map:</u></p> </div> <div style="width: 35%;"> <p>AASHTO 2013 - LTS 6</p> <p>110 mph</p> <p>50</p> </div> <div style="width: 30%; border: 1px solid black; padding: 10px;"> <p>- Wind speed AASHTO 2013 - LTS 6.</p> </div> </div> <div style="text-align: center; margin-top: 20px;">  </div>				
<p>d2) Foundation design standards: See appendix N-A</p>				
<p>e) Reported failures: NO Comments:</p>				

Table A-9: SCDOT survey summary

SUMMARY FOR GDOT			
	Yes/No	Date	Contact-Person
Questionnaire	Yes	5/22/2018	Glen Foster
Follow-up conference	Yes	9/6/2018	glon_gfoster@dot.ga.gov
<p>a) Mast arm length:</p> <div style="display: flex; align-items: center;"> <div style="flex: 1;"> </div> <div style="flex: 1; border: 1px solid black; padding: 5px; margin-left: 10px;"> <p>Notes/Comments:</p> <p><i>- See survey questionnaire in Appendix D-e.</i></p> </div> </div>			
<p>b) Most commonly used foundation system: Drilled Shafts</p> <div style="display: flex; align-items: center;"> <div style="flex: 1;"> </div> <div style="flex: 1;"> </div> <div style="flex: 1; border: 1px solid black; padding: 5px; margin-left: 10px;"> <p>Notes/Comments:</p> </div> </div>			
<p>c) Geotechnical Exploration:</p> <div style="display: flex; align-items: center;"> <div style="flex: 1;"> <p>Requirements:</p> <p>Min. Number of borings: 1</p> <p>SPT YES</p> <p>Other:</p> </div> <div style="flex: 1; border: 1px solid black; padding: 5px; margin-left: 10px;"> <p>Notes/Comments:</p> </div> </div>			
<p>d) Design standard used: AASHTO 1994 - LTS 3</p> <div style="display: flex; align-items: center;"> <div style="flex: 1;"> <p>Wind Speed: 90 mph</p> <p>MRI: 50</p> <p>Wind Map:</p> </div> <div style="flex: 1; border: 1px solid black; padding: 5px; margin-left: 10px;"> <p>Notes/Comments:</p> <p>Updating from AASHTO 1994 to LRFD 2015</p> </div> </div> <div style="text-align: center; margin-top: 10px;"> </div>			
<p>d2) Foundation Design Standards: See appendix C-d</p>			
<p>e) Reported Failures: NO Comments:</p>			

Table A-10: GDOT survey summary

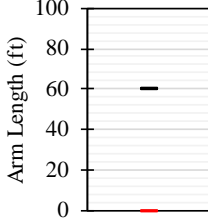
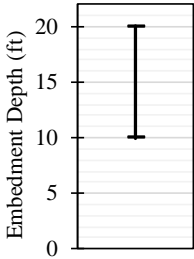
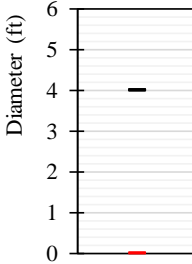
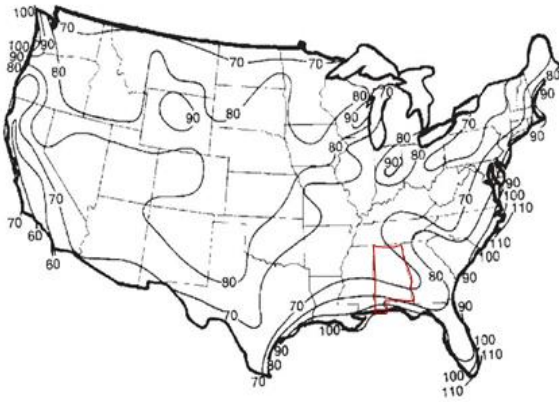
SUMMARY FOR ALDOT			
	Yes/No	Date	Contact-Person
Questionnaire	Yes	6/29/2018	Kate Chancellor zellers@wsdot.wa.gov
Follow-up conference	Yes	8/31/2018	
<div style="display: flex; justify-content: space-between;"> <div style="width: 30%;"> <p>a) Mast arm length:</p> </div> <div style="width: 30%;">  </div> <div style="width: 35%; border: 1px solid black; padding: 5px;"> <p>Notes/Comments:</p> <p>In the past almost exclusively strain poles but now almost exclusively mast arm.</p> <p style="color: red;">- See survey questionnaire in</p> </div> </div>			
<p>b) Most commonly used foundation system: Drilled Shafts</p> <div style="display: flex; justify-content: space-around; align-items: flex-start;"> <div style="width: 30%;">  </div> <div style="width: 30%;">  </div> <div style="width: 35%; border: 1px solid black; padding: 5px;"> <p>Notes/Comments:</p> <p>- Some units have been required to have <u>wing walls</u> attached to the drilled shafts, but we are <u>looking</u> at reevaluating the factor of safety used in our design to <u>eliminate</u> the use of the wings for our pole foundations.</p> </div> </div>			
<div style="display: flex; justify-content: space-between;"> <div style="width: 35%;"> <p>c) Geotechnical Exploration:</p> <p>Requirements:</p> </div> <div style="width: 35%;"> <p>Min. Number of borings: 1*</p> <p>SPT Yes</p> <p>Other:</p> </div> <div style="width: 30%; border: 1px solid black; padding: 5px;"> <p>Notes/Comments: borings for each pole location, unless there are a lot of poles in a close area and the geology is such that we can extrapolate information.</p> </div> </div>			
<p>d) Design standard used: AASHTO 1994 - LTS 3</p> <p>Wind Speed in the coastal are: 100 mph</p> <p><u>MRI:</u> 50</p> <p><u>Wind Map:</u></p> <div style="text-align: center;">  </div>			
<p>d2) Foundation Design Standards: See appendix N-A</p>			
<p>e) Reported Failures: NO Comments:</p>			

Table A-11: ALDOT survey summary

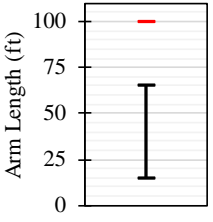
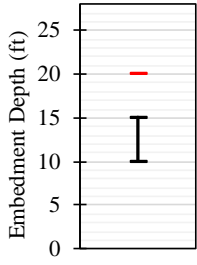
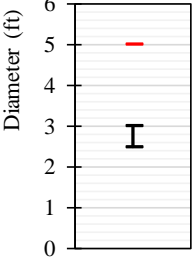
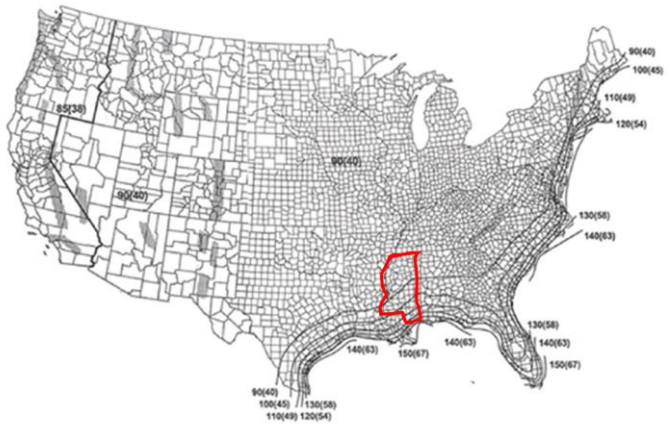
SUMMARY FOR MDOT			
	Yes/No	Date	Contact-Person
Questionnaire	Yes	10/2/2018	James Sullivan
Follow-up conference	Yes	11/6/2018	jssullivan@mdot.ms.gov
<p>a) Mast arm length:</p> <div style="display: flex; align-items: center; justify-content: space-around;"> <div style="text-align: center;">  </div> <div style="border: 1px solid black; padding: 5px; width: 250px;"> <p>Notes/Comments:</p> <ul style="list-style-type: none"> - Longest mast arm mentioned. - See survey questionnaire in Appendix D-g </div> </div>			
<p>b) Most commonly used foundation system: Drilled Shafts</p> <div style="display: flex; align-items: center; justify-content: space-around;"> <div style="text-align: center;">  </div> <div style="text-align: center;">  </div> <div style="border: 1px solid black; padding: 5px; width: 250px;"> <p>Notes/Comments:</p> <ul style="list-style-type: none"> - Design based on Broms for lateral loading and skin friction for torsion loading. </div> </div> <div style="border: 1px solid black; padding: 5px; margin-top: 10px; width: 250px;"> <p>* This will depend on several factors including the type, length, complexity, and scope of the project and whether it's known there are expansive clays in the profile and whether the profile is known to be fairly consistent or varied.</p> </div>			
<p>c) Geotechnical Exploration: Min. Number of borings: 1*</p> <p>Requirements: SPT Depends*</p> <p>Other:</p>			
<p>d) Design standard used: AASHTO 2001 - LTS 4</p> <p>Wind Speed in the coastal are: 140 mph</p> <p>MRI: 50</p> <p>Wind Map:</p> <div style="text-align: center; margin-top: 20px;">  </div> <div style="border: 1px solid black; padding: 5px; margin-top: 10px; width: 250px;"> <p>Notes/Comments:</p> <ul style="list-style-type: none"> * Vol3LTS-19 modifications to LRFDLTS 1 </div>			
<p>d2) Foundation Design Standards: See appendix C-e</p>			
<p>e) Reported Failures: Yes Comments: Mast arm that have rotatet up to 90°</p>			

Table A-12: MDOT survey summary

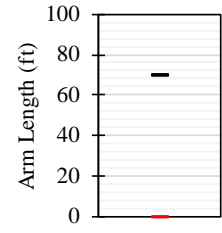
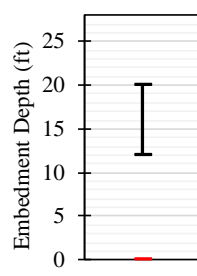
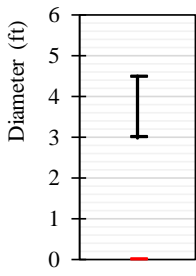
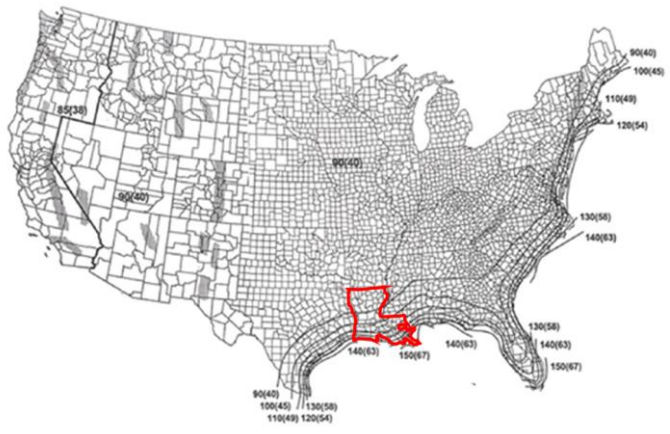
SUMMARY FOR LaDOT				
	Yes/No	Date	Contact-Person	
Questionnaire	Yes	9/21/2018	Chris Nickel	Chris.Nickel@la.gov
Follow-up conference	Yes	10/4/2018		
<div style="display: flex; justify-content: space-between; align-items: flex-start;"> <div style="width: 30%;"> <p>a) Mast arm length:</p>  </div> <div style="width: 65%; border: 1px solid black; padding: 10px;"> <p>Notes/Comments:</p> <p style="color: red;">- See survey questionnaire in Appendix D-h</p> </div> </div>				
<p>b) Most commonly used foundation system: Drilled Shafts</p> <div style="display: flex; justify-content: space-around; align-items: flex-start;"> <div style="width: 30%;">  </div> <div style="width: 30%;">  </div> <div style="width: 35%; border: 1px solid black; padding: 10px;"> <p>Notes/Comments:</p> </div> </div>				
<div style="display: flex; justify-content: space-between;"> <div style="width: 35%;"> <p>c) Geotechnical Exploration:</p> <p>Requirements:</p> </div> <div style="width: 30%;"> <p>Min. Number of borings:</p> <p>SPT</p> <p>Other:</p> </div> <div style="width: 30%; border: 1px solid black; padding: 10px;"> <p>Notes/Comments: Soil maps for Louisiana for types of soils in different areas of the site</p> </div> </div>				
<div style="display: flex; justify-content: space-between;"> <div style="width: 35%;"> <p>d) Design standard used:</p> <p>Wind Speed in the coastal are:</p> <p>MRI:</p> <p>Wind Map:</p> </div> <div style="width: 30%;"> <p>AASHTO 2001 - LTS 4</p> <p>130 mph</p> <p>50</p> </div> <div style="width: 30%; border: 1px solid black; padding: 10px;"> <p>Notes/Comments:</p> </div> </div> <div style="text-align: center; margin-top: 20px;">  </div>				
<p>d2) Foundation Design Standards: See appendix C-f</p>				
<p>e) Reported Failures: NO Comments:</p>				

Table A-13: LaDOT survey summary

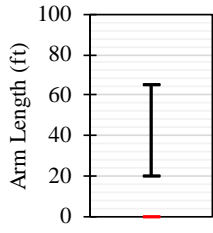
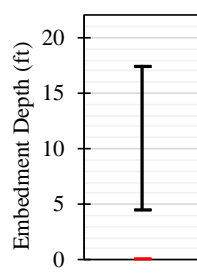
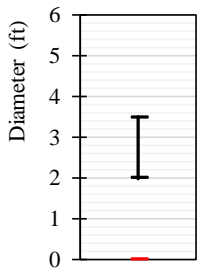
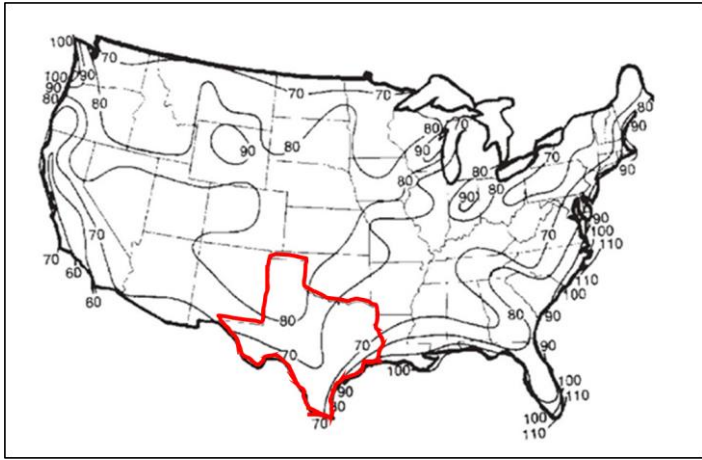
SUMMARY FOR TxDOT			
	Yes/No	Date	Contact-Person
Questionnaire	Yes	6/14/2018	Steven Austin
Follow-up conference	Yes	8/31/2018	Steven.Austin@txdot.gov
<p>a) Mast arm length:</p> <div style="display: flex; align-items: center;"> <div style="flex: 1;">  </div> <div style="flex: 1; border: 1px solid black; padding: 5px;"> <p>Notes/Comments:</p> <p><i>- See survey questionnaire in Appendix D-i</i></p> </div> </div>			
<p>b) Most commonly used foundation system: Drilled Shafts</p> <div style="display: flex; align-items: center;"> <div style="flex: 1;">   </div> <div style="flex: 1; border: 1px solid black; padding: 5px;"> <p>Notes/Comments:</p> </div> </div>			
<p>c) Geotechnical Exploration:</p> <div style="display: flex; align-items: center;"> <div style="flex: 1;"> <p>Requirements:</p> <p>Min. Number of borings: 1</p> <p>SPT -</p> <p>Other: TCP*</p> </div> <div style="flex: 1; border: 1px solid black; padding: 5px;"> <p>Notes/Comments: Texas Cone Penetrometer is using steady SPT</p> </div> </div>			
<p>d) Design standard used: AASHTO 1994 - LTS 3</p> <div style="display: flex; align-items: center;"> <div style="flex: 1;"> <p>Wind Speed in the coastal area: 100 mph</p> <p>MRI: 50</p> <p>Wind Map:</p> </div> <div style="flex: 1; border: 1px solid black; padding: 5px;"> <p>Notes/Comments:</p> </div> </div>			
			
<p>d2) Foundation Design Standards: See appendix C-g</p>			
<p>e) Reported Failures: NO Comments: 0</p>			

Table A-14: TxDOT survey summary

SUMMARY FOR ODOT				
	Yes/No	Date	Contact-Person	
Questionnaire	Yes	5/29/2018	Scott JOLLO	Scott.U.JOLLO@odot.state.or.us
Follow-up conferenc	Yes	8/22/2018		
<p>a) Mast arm length:</p> <div style="display: flex; align-items: center;"> <div style="flex: 1;"> </div> <div style="flex: 1; border: 1px solid black; padding: 5px;"> <p>Notes/Comments:</p> <p><i>- See questionnaire in Appendix D-j</i></p> </div> </div>				
<p>b) Most commonly used foundation system: Drilled Shafts</p> <div style="display: flex; align-items: center;"> <div style="flex: 1;"> </div> <div style="flex: 1; border: 1px solid black; padding: 5px;"> <p>Notes/Comments:</p> <ul style="list-style-type: none"> - Design is based in L-Pile and skin friction. - The foundation conditions at the signal pole site should be investigated and characterized in terms of soil type, soil unit weight, and soil friction angle </div> </div>				
<p>c) Geotechnical Exploration: Min. Number of borings: 1* Requirements: SPT Yes Other:</p> <div style="border: 1px solid black; padding: 5px; margin-top: 10px;"> <p>Notes/Comments: Foundation within 75' with uniform soil have one boring wit SPT.</p> </div>				
<p>d) Design standard used: AASHTO 2001 - LTS 4 & for wind speed AASHTO 2013 -LTS 6</p> <div style="display: flex; align-items: center;"> <div style="flex: 1;"> <p>Wind Speed in the coastal are: 110 mph</p> <p>MRI: 50</p> <p>Wind Map:</p> </div> <div style="flex: 1; border: 1px solid black; padding: 5px; margin-top: 10px;"> <p>Notes/Comments:</p> </div> </div> <div style="text-align: center; margin-top: 20px;"> </div>				
<p>d2) Foundation Design Standards: See appendix</p>				
<p>e) Reported Failures: NO Comments:</p>				

Table A-15: ODOT survey summary

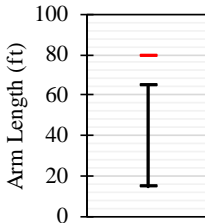
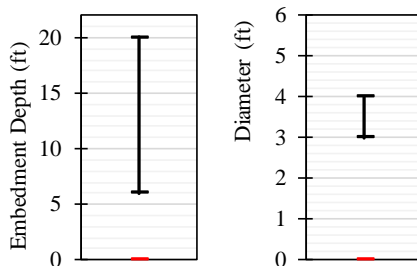
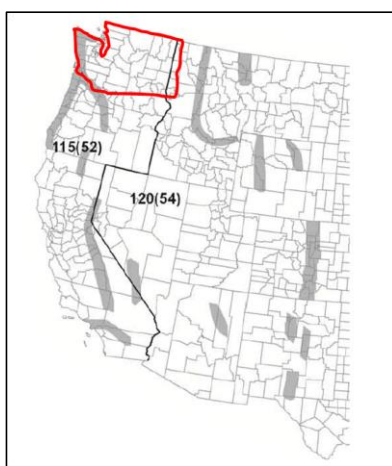
SUMMARY FOR WSDOT			
	Yes/No	Date	Contact-Person
Questionnaire	Yes	6/24/2018	Scot Zeller
Follow-up conference	Yes	8/28/2018	zellers@wsdot.wa.gov
<div style="display: flex; justify-content: space-between; align-items: flex-start;"> <div style="width: 30%;"> <p>a) Mast arm length:</p> </div> <div style="width: 30%; text-align: center;">  </div> <div style="width: 35%; border: 1px solid black; padding: 5px;"> <p>Notes/Comments:</p> <p style="color: red;">- See questionnaire in Appendix D-k</p> </div> </div>			
<div style="display: flex; justify-content: space-between; align-items: flex-start;"> <div style="width: 30%;"> <p>b) Most commonly used foundation system: Drilled Shafts</p> </div> <div style="width: 30%;">  </div> <div style="width: 35%; border: 1px solid black; padding: 5px;"> <p>Notes/Comments:</p> <ul style="list-style-type: none"> - Broms approximate method & torsion in WSDOT bridge design manual 10.1.5C - Foundations that instead of wing have trench. </div> </div>			
<div style="display: flex; justify-content: space-between; align-items: flex-start;"> <div style="width: 30%;"> <p>c) Geotechnical Exploration:</p> <p>Requirements:</p> </div> <div style="width: 30%;"> <p>Min. Number of borings: 1*</p> <p>SPT Yes</p> <p>Other:</p> </div> <div style="width: 35%; border: 1px solid black; padding: 5px;"> <p>Notes/Comments: Bore hole or test pit for each location. Some cases consistency in subsurface.</p> </div> </div>			
<div style="display: flex; justify-content: space-between; align-items: flex-start;"> <div style="width: 30%;"> <p>d) Design standard used:</p> <p><u>Wind Speed in the coastal area:</u></p> <p><u>MRI:</u></p> <p><u>Wind Map:</u></p> </div> <div style="width: 30%;"> <p>AASHTO LRFD, First Edition 2015 – LRFDLTS 1</p> <p>115 mph</p> <p>1700</p> </div> <div style="width: 35%; border: 1px solid black; padding: 5px;"> <p>Notes/Comments:</p> </div> </div> <div style="text-align: center; margin-top: 20px;">  </div>			
<p>d2) Foundation Design Standards: See appendix C-h Based in older standard plan</p>			
<p>e) Reported Failures: NO Comments:</p>			

Table A-16: WSDOT survey summary

APPENDIX F: SUMMARY OF STANDARD DESIGNS

Summary of standard design for North Carolina:

The State of North Carolina have divided the state in 5 wind zones, Figure A-18.

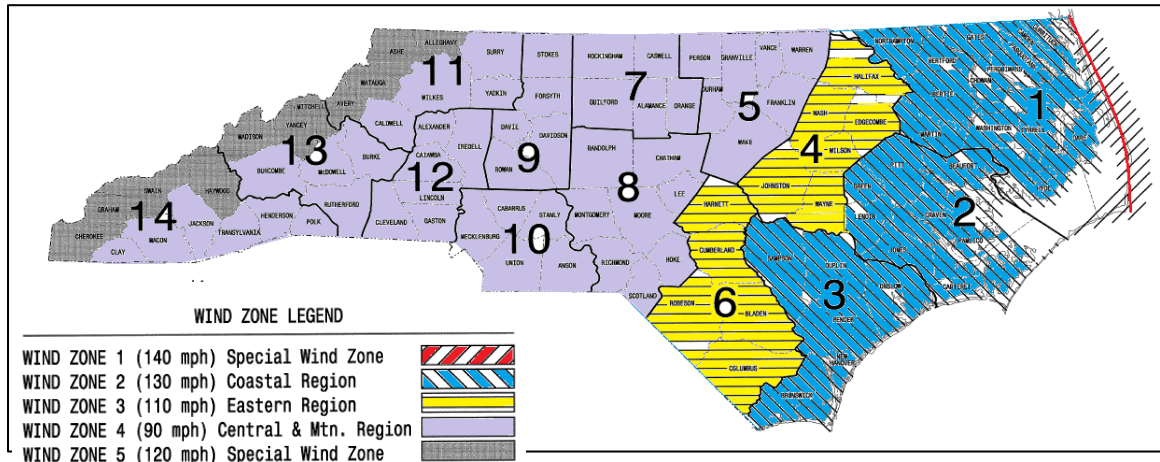


Figure A-18: Wind speed zone in North Carolina (NCDOT)

The procedure to select the drilled shaft embedment depth is: first, from Figure A-19 a wind zone should be selected; second, from A-13 a mast arm number (red Square), then, the third step is to define a type of soil (blue square), the options are cohesive and cohesionless, and by last, a SPT blow counter will be determine the embedment depth (green square). Each load case have assigned a drilled shaft diameter (Purple Square).

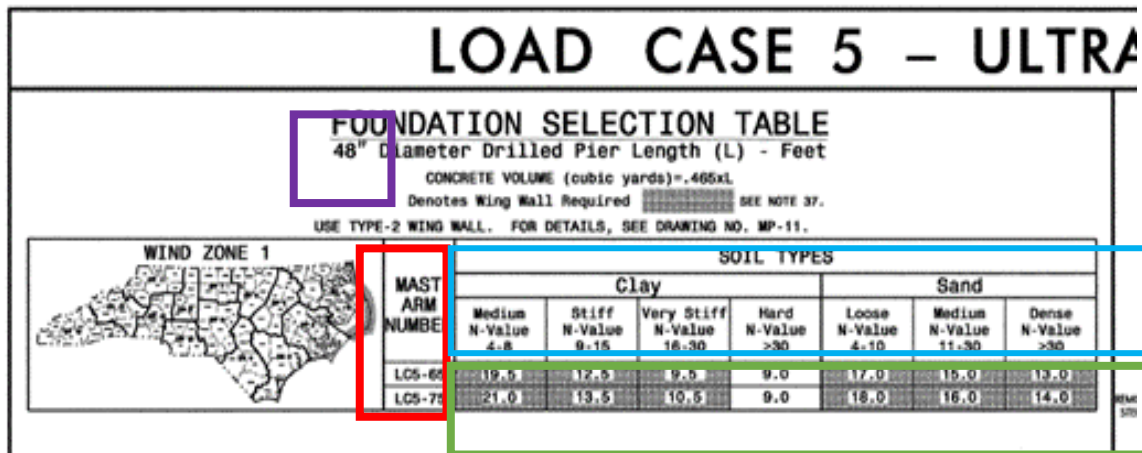
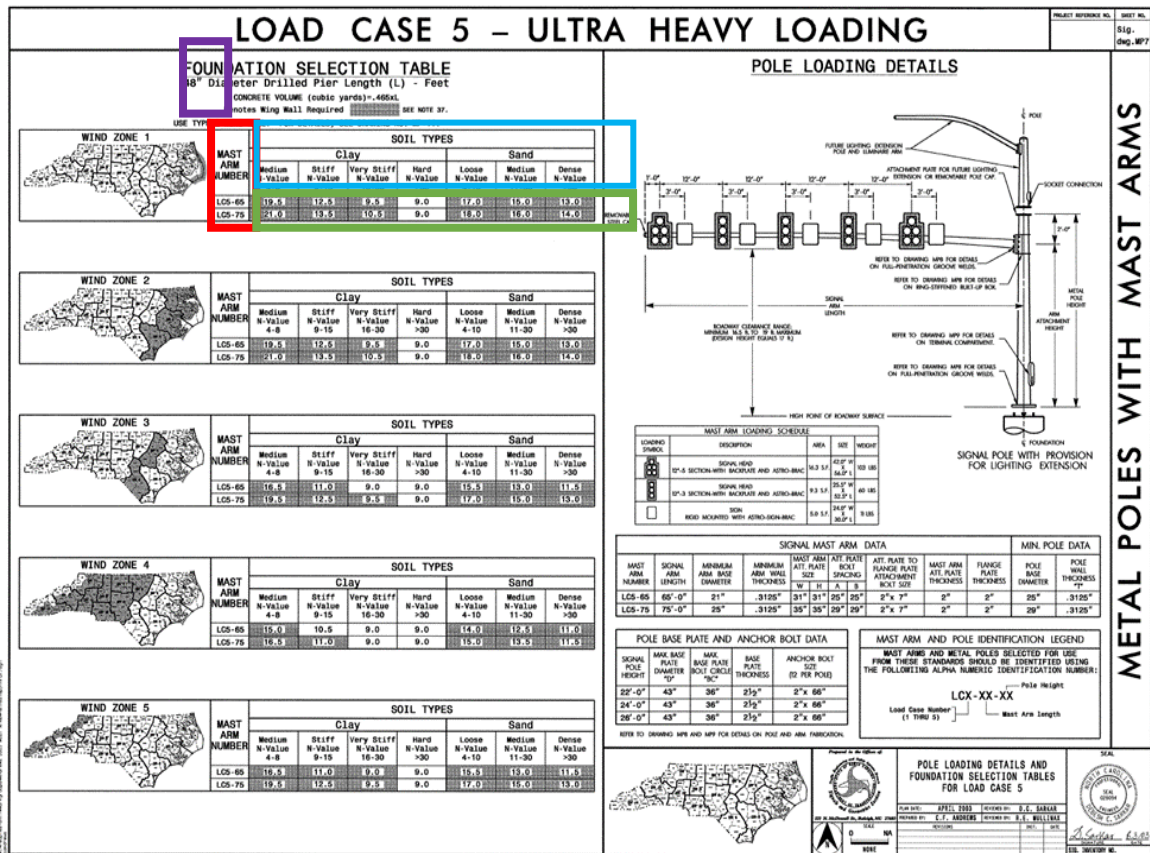


Figure A-19: North Carolina embedment depth and diameter selection
NCDOT)

Summary of standard design for Florida:

Below, expresses the mast arm foundation procedure found in FDOT's website.

The first step corresponds to choose the mast arm elements (arm and pole). The possible combinations could be found in Table 1 and 2 in the STANDARD MAST ARM ASSEMBLIES, Index No. 17743. The arm length depend of the number of lanes, the route configuration and the number of intersections, while, the pole is going to depend of the type of cars traveling on it. The arm and the pole characteristics could be pick up from tables 1 and 2 in STANDARD MAST ARM ASSEMBLIES, Index No.17743 and No.17745 as seen in Figure A-20.

STANDARD MAST ARM ASSEMBLIES														STANDARD MAST ARM ASSEMBLIES													
Arm ID	Total Arm Length (ft)	Arm				Base Plate				Arm ID	Total Arm Length (ft)	Arm				Base Plate											
		F1/S1 (ft)	F2/S2 (ft)	F3/S3 (ft)	F4/S4 (ft)	F5/S5 (ft)	F6/S6 (ft)	F7/S7 (ft)	F8/S8 (ft)			F1/S1 (ft)	F2/S2 (ft)	F3/S3 (ft)	F4/S4 (ft)	F5/S5 (ft)	F6/S6 (ft)	F7/S7 (ft)	F8/S8 (ft)								
A30/S	30	12	0.250							A30/S	30	12	0.250														
A30/S/W	30	12	0.250							A30/S/W	30	12	0.250														
A30/D	30	12	0.250							A30/D	30	12	0.250														
A30/D/W	30	12	0.250							A30/D/W	30	12	0.250														
A40/S	40	14	0.250							A40/S	40	14	0.250														
A40/S/W	40	14	0.250							A40/S/W	40	14	0.250														
A40/D	40	14	0.250							A40/D	40	14	0.250														
A40/D/W	40	14	0.250							A40/D/W	40	14	0.250														
A50/S	50	16	0.250	20.5	14					A50/S	50	16	0.250	20.5	14												
A50/S/W	50	16	0.250	20.5	14	0.375				A50/S/W	50	16	0.250	20.5	14	0.375											
A50/D	50	16	0.250	20.5	14					A50/D	50	16	0.250	20.5	14												
A50/D/W	50	16	0.250	20.5	14					A50/D/W	50	16	0.250	20.5	14												
A60/S	60	18	0.250	27.5	15					A60/S	60	18	0.250	27.5	15												
A60/S/W	60	18	0.250	27.5	15	0.375				A60/S/W	60	18	0.250	27.5	15	0.375											
A60/D	60	18	0.250	27.5	15					A60/D	60	18	0.250	27.5	15												
A60/D/W	60	18	0.250	27.5	15					A60/D/W	60	18	0.250	27.5	15												
A70/S	70	20	0.250	35	17					A70/S	70	20	0.250	35	17												
A70/S/W	70	20	0.250	35	17	0.375				A70/S/W	70	20	0.250	35	17	0.375											
A70/D	70	20	0.250	35	17					A70/D	70	20	0.250	35	17												
A70/D/W	70	20	0.250	35	17					A70/D/W	70	20	0.250	35	17												
A78/S	78	22	0.250	42	18					A78/S	78	22	0.250	42	18												
A78/S/W	78	22	0.250	42	18	0.375				A78/S/W	78	22	0.250	42	18	0.375											
A78/D	78	22	0.250	42	18					A78/D	78	22	0.250	42	18												
A78/D/W	78	22	0.250	42	18					A78/D/W	78	22	0.250	42	18												

ARM AND BASE PLATE									
Arm ID	Total Arm Length (ft)	Arm				Base Plate			
		F1/S1 (ft)	F2/S2 (ft)	F3/S3 (ft)	F4/S4 (ft)	F5/S5 (ft)	F6/S6 (ft)	F7/S7 (ft)	F8/S8 (ft)
A30/S	30	12	0.250					22	25
A30/S/W	30	12	0.250					30	36
A30/D	30	12	0.250					30	36
A30/D/W	30	12	0.250					30	36
A40/S	40	14	0.250					22	27
A40/S/W	40	14	0.250					30	36
A40/D	40	14	0.250					30	36
A40/D/W	40	14	0.250					30	36
A50/S	50	16	0.250	20.5	14			22	29
A50/S/W	50	16	0.250	20.5	14	0.375		30	36
A50/D	50	16	0.250	20.5	14			30	36
A50/D/W	50	16	0.250	20.5	14			30	36
A60/S	60	18	0.250	27.5	15			30	36
A60/S/W	60	18	0.250	27.5	15	0.375		30	36
A60/D	60	18	0.250	27.5	15			30	36
A60/D/W	60	18	0.250	27.5	15			30	36
A70/S	70	20	0.250	35	17			30	36
A70/S/W	70	20	0.250	35	17	0.375		30	36
A70/D	70	20	0.250	35	17			30	36
A70/D/W	70	20	0.250	35	17			30	36
A78/S	78	22	0.250	42	18			30	36
A78/S/W	78	22	0.250	42	18	0.375		30	36
A78/D	78	22	0.250	42	18			30	36
A78/D/W	78	22	0.250	42	18			30	36

POLE, BASE PLATE AND ARM CONNECTION															
Pole ID	Pole Height (ft)	Base Plate				Arm-to-right Connection									
		F1/S1 (ft)	F2/S2 (ft)	F3/S3 (ft)	F4/S4 (ft)	F1/S1 (ft)	F2/S2 (ft)	F3/S3 (ft)	F4/S4 (ft)	F5/S5 (ft)	F6/S6 (ft)	F7/S7 (ft)	F8/S8 (ft)		
P1/S	25														
P1/S/W	25														
P1/D	25														
P1/D/W	25														
P2/S	30														
P2/S/W	30														
P2/D	30														
P2/D/W	30														
P3/S	35														
P3/S/W	35														
P3/D	35														
P3/D/W	35														
P4/S	40														
P4/S/W	40														
P4/D	40														
P4/D/W	40														
P5/S	45														
P5/S/W	45														
P5/D	45														
P5/D/W	45														
P6/S	50														
P6/S/W	50														
P6/D	50														
P6/D/W	50														
P7/S	55														
P7/S/W	55														
P7/D	55														
P7/D/W	55														

Figure A-20: Standard Mast Arm Assemblies Document (FDOT 2016)

The lateral moment should be calculate and it must satisfy the relation given in the spreadsheet, which can be expressed in Figure A-21.

$$\phi \cdot \frac{\gamma_{\text{soil}} \cdot b_{\text{shaft}} \cdot L_{\text{shaft}}^3 \cdot K_p}{2} \geq M_u + P_u \cdot L_{\text{shaft}}$$

Figure A-21: Lateral Moment Equation (FDOT 2016)

As mentioned above, the result obtained with $M_u + P_u \cdot L_{\text{shaft}}$ should be compared with the result of the left side of the equation above in Figure A-22. Florida DOT provides eight drilled shafts with different geometries (depth and diameter), for these geometries, the lateral capacity was calculated following Brom's theory (1964). These values are provided by Florida DOT in its spreadsheet Mastarm-Index17743-v1.1 – Sheet CFI&Designation – TABLE DRILLED SHAFT – Column 7, seen below in Figure A-22.

Drilled Shaft																
Index 17743 Drilled Shaft Capacities							1 Arm Assembly Loads And Capacity Check				2 Arm Assembly Loads and Capacity Check					
DS Index #	ID	Length	Diameter	ϕM_n	ϕT_n	$M_u + P_u \cdot L_{\text{shaft}}$	T_u	Check Mom. & Min Dia.	Check Torsion	Check	$M_u + P_u \cdot L_{\text{shaft}}$	T_u	Check Mom. & Min Dia.	Check Torsion	Check	
1	DS/20/5	20	5	1800	589	842.8	587.5	Okay	Okay	Okay	0.0	0.0	0	0	0	
2	DS/18/5	18	5	1312	477	804.5		Okay	NoGood	NoGood	0.0		0	0	0	
3	DS/16/5	16	5	922	377	766.2		Okay	NoGood	NoGood	0.0		0	0	0	
4	DS/16/4.5	16	4.5	829	305	766.2		NoGood	NoGood	NoGood	0.0		0	0	0	
5	DS/14/5	14	5	617	289	728.0		NoGood	NoGood	NoGood	0.0		0	0	0	
6	DS/14/4.5	14	4.5	556	234	728.0		NoGood	NoGood	NoGood	0.0		0	0	0	
7	DS/12/4.5	12	4.5	350	172	689.7		NoGood	NoGood	NoGood	0.0		0	0	0	
8	DS/12/4	12	4	311	136	689.7		NoGood	NoGood	NoGood	0.0		0	0	0	

Figure A-22: Spreadsheet of Florida DOT Drilled Shaft Dimensions (FDOT 2016)

The information about drilled shafts geometry used by Florida DOT could be observed in spreadsheet Mastarm-Index17743-v1.1 – Sheet CFI&Designation – TABLE DRILLED SHAFT – Columns 2 and 3, as seen in Figure 2-23.

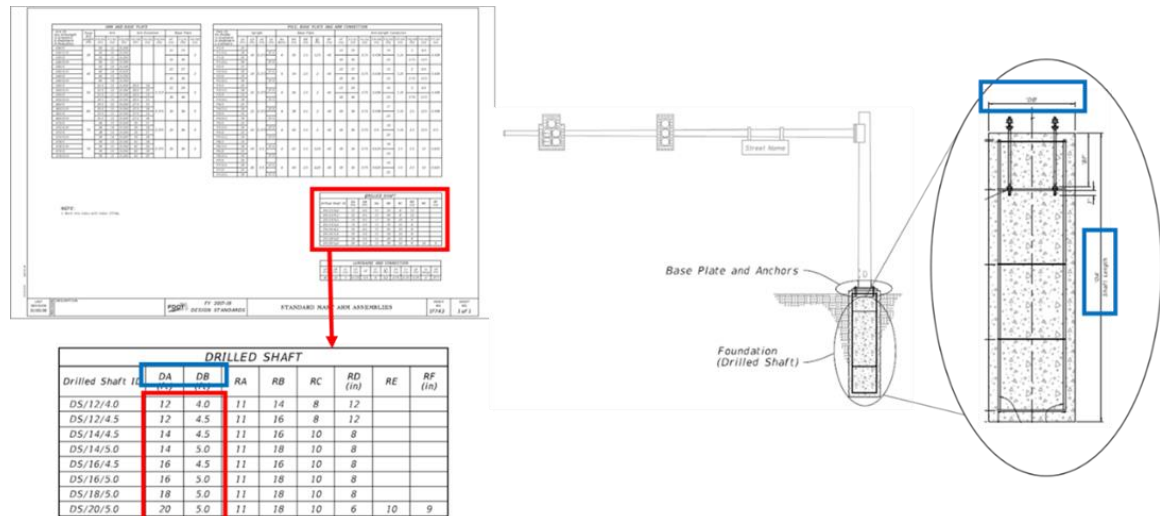
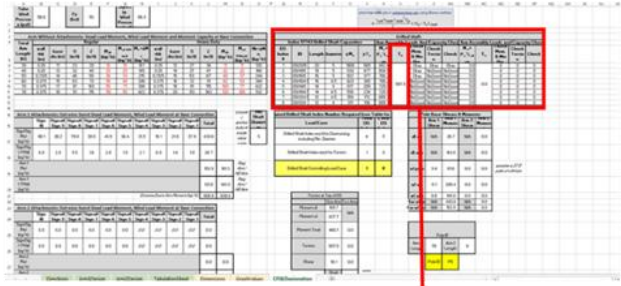


Figure A-23: Florida DOT Drilled Shaft Dimensions (FDOT 2016)

Once the Lateral moment was verified, the torsion parameter should be calculated using the mast arm geometry and the elements selected.

As the lateral moment, the torsion moment should be compared with the value preview calculated using the Beta theory method. In its spreadsheet, Florida DOT provides a set of values calculated with the mentioned theory for different drilled shafts geometries seen in Figure A-24.



The image shows a screenshot of a spreadsheet with various data tables. A red rectangular box highlights a specific section of the spreadsheet, and a red arrow points from this box to a detailed table below. The detailed table is titled "Drilled Shaft" and contains data for "Index 17743 Drilled Shaft Capacities".

Drilled Shaft															
Index 17743 Drilled Shaft Capacities							1 Arm Assembly Loads And Capacity Check			2 Arm Assembly Loads and Capacity Check					
DS Index #	ID	Length	Diameter	ϕM_n	ϕT_n	$M_u + P_u * L_{shaft}$	T_u	Check Mom. & Min Dia.	Check Torsion	Check	$M_u + P_u * L_{shaft}$	T_u	Check Mom. & Min Dia.	Check Torsion	Check
1	DS/20/5	20	5	1800	589	842.8	587.5	Okay	Okay	Okay	0.0	0.0	0	0	0
2	DS/18/5	18	5	1312	477	804.5		Okay	NoGood	NoGood	0.0		0	0	0
3	DS/16/5	16	5	922	377	766.2		Okay	NoGood	NoGood	0.0		0	0	0
4	DS/16/4.5	16	4.5	829	305	766.2		NoGood	NoGood	NoGood	0.0		0	0	0
5	DS/14/5	14	5	617	289	728.0		NoGood	NoGood	NoGood	0.0		0	0	0
6	DS/14/4.5	14	4.5	556	234	728.0		NoGood	NoGood	NoGood	0.0		0	0	0
7	DS/12/4.5	12	4.5	350	172	689.7		NoGood	NoGood	NoGood	0.0		0	0	0
8	DS/12/4	12	4	311	136	689.7		NoGood	NoGood	NoGood	0.0		0	0	0

Figure A-24: Florida DOT Drilled Shaft Dimensions (FDOT 2016)

Summary of standard design for Virginia:

Bearing pressure:

The first Tip resistance/ Bearing pressure parameter is calculated using the Brom's theory for piles, considering the loads shown in Figure A-25; nevertheless, other theory methods or software could be used to estimate shaft deflections. In terms of this parameter the following was defined:

For mast arm signals and span wire signals, the maximum total horizontal deflection shall must be 0.75 inches at ground level and 0.25 inches in the pole tip.

For other structures, the maximum total horizontal deflection shall must be 0.5 inches at ground level and 0.15 inches in the pole tip.

For no reason shall be a loading reduction by the allowable overload/overstress factor.

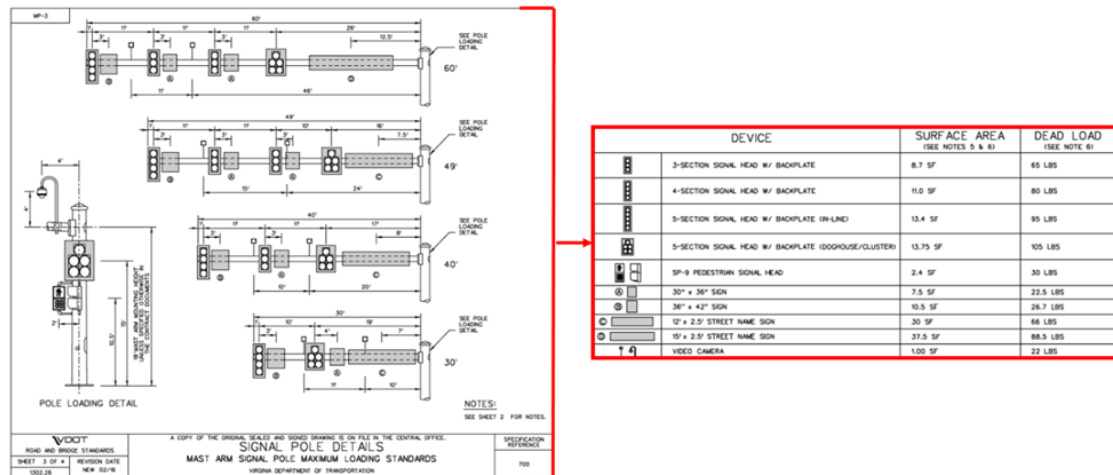


Figure A-25: Virginia Plan MP-3 Document (VDOT 2016a)

Torsion moment:

The second parameter corresponds to Torsion/Sliding/Skin Friction and should be evaluated following the *ASSHTO LRFD Bridge Design Specifications* (AASHTO, 2015).

Section 10.8.3.5- Nominal Axial Compression Resistance of Single Drilled Shafts, nevertheless, the values in Table 10.5.5.2.4-1 should be replaced by 1.

In its standard drawings, the plan PF-8 refers to *Signal Pole Foundation Installation Details*, where the drilled shaft characteristics are defined. In this case, the Virginia's department of transportation does not define a range in terms of drilled shaft diameter and depth, instead they only defined a minimum diameter and depth. Nevertheless, the use of wing walls are specified when required, A layout of typical wing wall structures can be seen below in Figure A-26 (VDOT, 2016a).

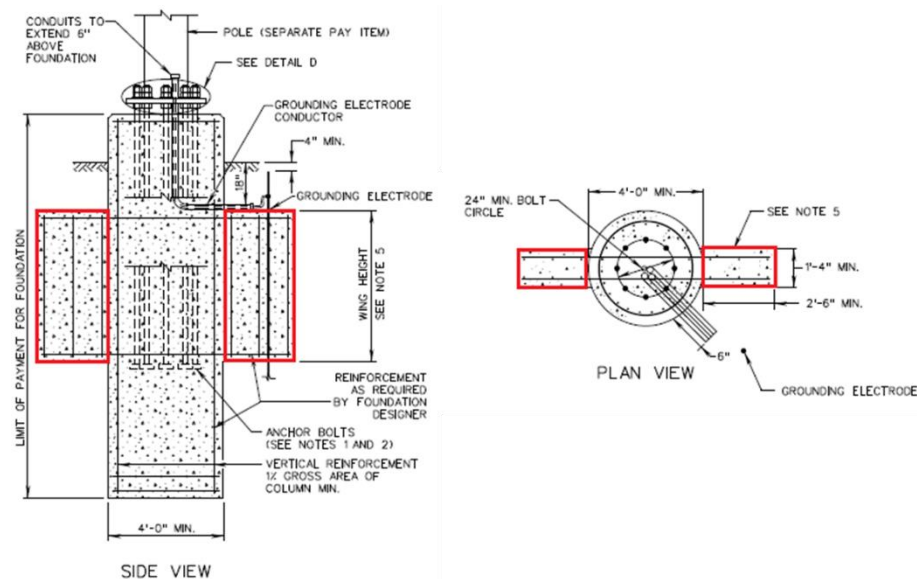


Figure A-26: Virginia Plan PF-8 Document (VDOT 2016a)

Summary of standard design for Georgia:

Each mast arm and Traffic Signal Support requires a minimum a drawing where the location and the foundation design can be observed. Georgia DOT along with other DOT states provides a Standard Drawing where the guidelines for the foundations specified can be observed. In the case of the current state, the foundation recommended corresponds to drilled shaft.

The traffic signal detail, DETAILS OF STRAIN POLE AND MAST ARM FOUNDATIONS T5-06 by The Department of transportation State of Georgia shows the conditions, geometries and specifications for Drilled Shafts. The drawing is divided in three charts for different types of soils; PIEDEMONT, VALLEY & RIDGE and COASTAL PLAN, where for each place, geotechnical parameters are defined in Figure A-27 (GDOT, 2010).

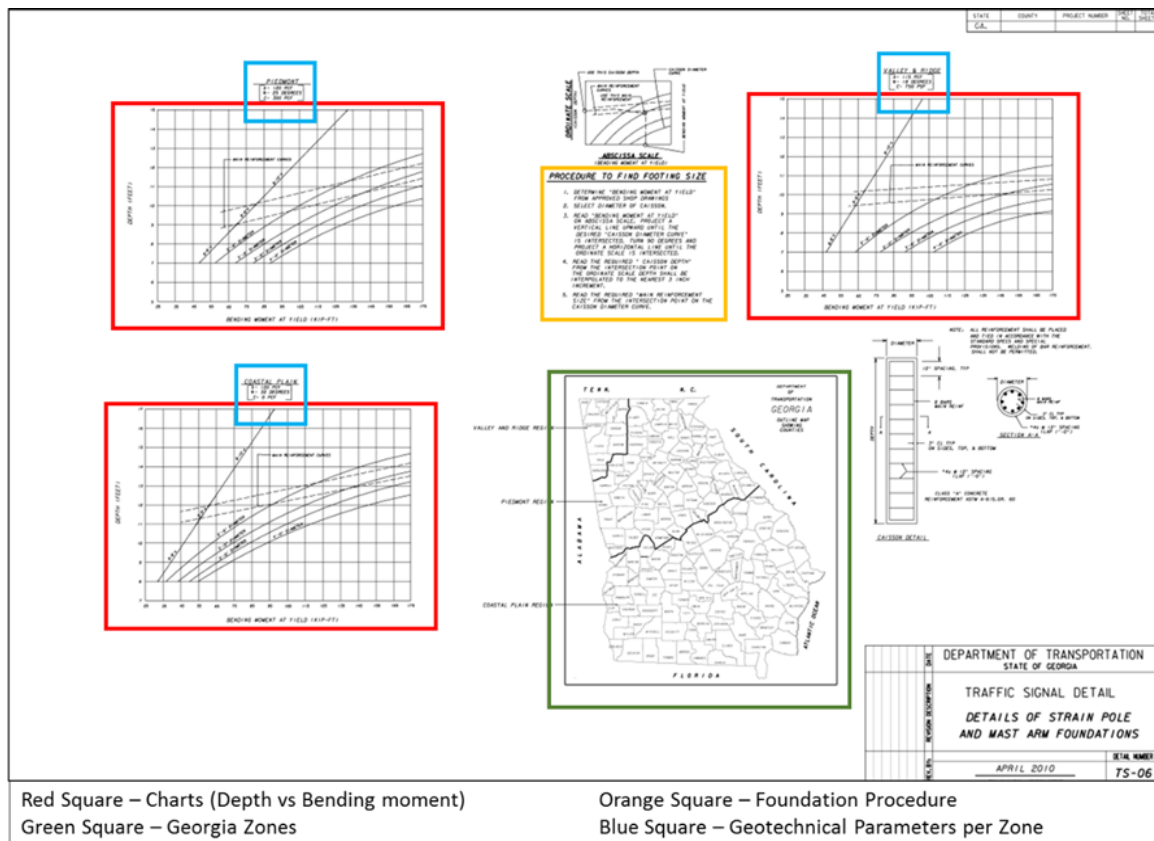


Figure A-27: TS-06 Standard Drawing Modify from (GDOT 2010)

Consider the TS-06 standard drawing, the depth and diameter range of Drilled Shafts is varying as is shown in Figure A-28.

The charts are showing three drilled shaft parameters horizontally, depth, and diameter and ratio h/d vertically. The square represents the minimum and maximum limits for a specific drilled shaft condition. In some cases, two vertical lines displays the maximum and minimum geometries when all the conditions are considered. Once the standard drawing had been identified, Georgia DOT specified the procedure below to determine the most accurate drilled shaft in terms of depth and diameter.

- Identify the zone where the traffic signal or highway signs will be located. This can be seen in the green enclosed area in Figure A-28 above,

- Determine Max. bending moment at yield using an approved theoretical method.
- Select the caisson diameter desired. Lines 1 to 4 in the example from Figure A-28.

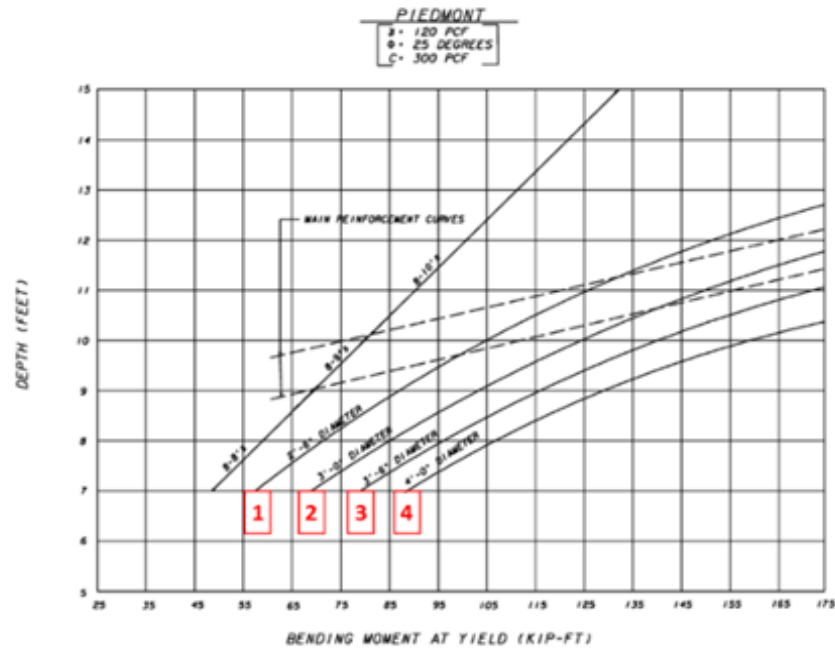


Figure A-28: Georgia Drilled Shafts Diameters (GDOT 2010)

Read the bending moment found in numeral (ii) and draw a vertical line up to intersect the desired diameter line.

From the vertical axis, read the correspondent depth for the point generated by the vertical line and the diameter. The main reinforcement size should be taken at the point where the vertical line intersect the MAIN REINFORCEMENT LINES. Blue lines in Figure A-29. In this way, the depth and diameter of the drilled shaft are selected.

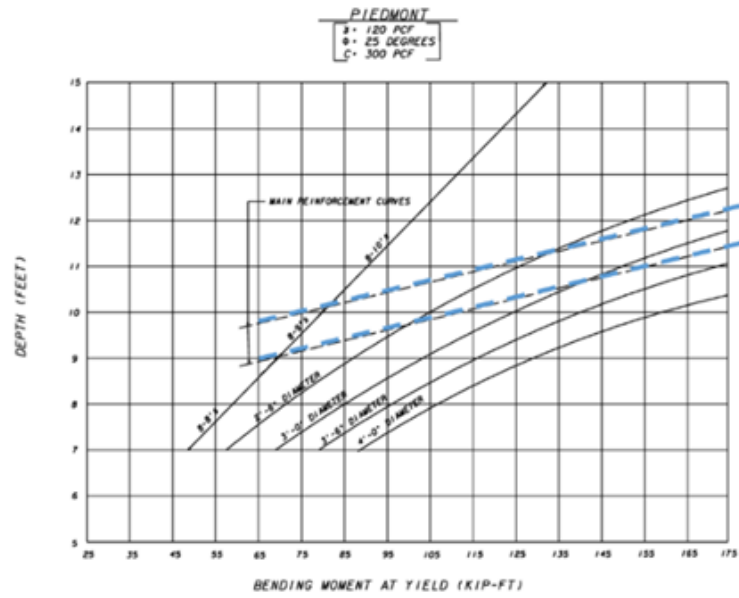


Figure A-29: Georgia reinforcement drilled shafts. (GDOT 2010)

As seen in Figure A-30, Georgia DOT has divided its map in three zones; Piedmont, Valley & Ridge and Coastal Plain. Georgia DOT also has assigned three geotechnical parameters for each zone; unit total weight (γ), friction angle (ϕ°) and cohesion (C). These parameters were used to calculate the drilled shafts depth following Brom's assumption for cohesive and non-cohesive soils Figure A-30.

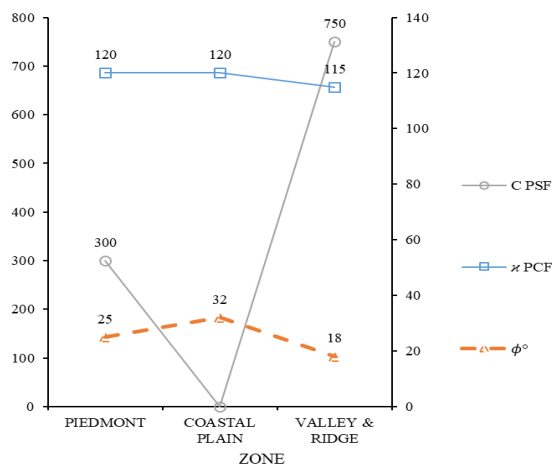


Figure A-30: Zones of Georgia Corresponding to geotechnical parameters (GDOT 2010)

Summary of standard design for Mississippi:

In its TSD-6.DGN standard drawing, MDOT have assigned two standard foundations, which depend of the structure location. There are two options: first for coastal areas (blue square) and second for other areas (red square) shown in Figure A-31.

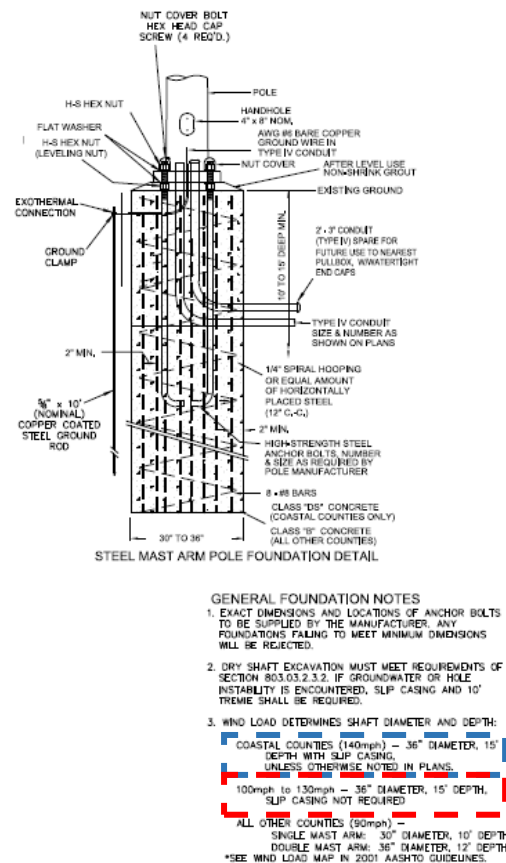


Figure A-31: MDOT Drilled shaft dimensions

Summary of standard design for Louisiana:

Identify the mast arm zone, from zone 1 to 4 in Figure A-32.

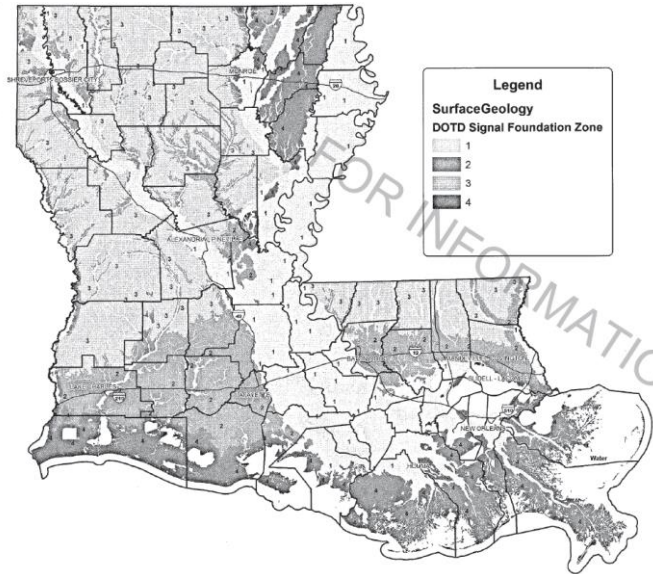


Figure A-32: LaDOT signal foundation zone

In Figure A-33, the red square is showing length in feet for single and double mast arm.

Green square is showing zone from 1 to 4 and blue square the diameter/depth drilled shaft.

FOUNDATION SIZE SELECTION TABLE												
Mast Arm Length(s) (ft)	Bending Moment (ft-lb)	Torsion (ft-lb)	Shear (lb)	Axial Force (lb)	Foundation Size Selection (diameter in inches, depth in feet)							
					Zone 1 (Diameter/Depth)		Zone 2+ (Diameter/Depth)		Zone 3+ (Diameter/Depth)		Zone 4 (Diameter/Depth)	
55	125,120	121,100	5,500	5,862	*	*	42	18	36	14	*	*
60	141,805	128,940	5,930	6,561	*	*	42	19	36	15	*	*
65	161,259	150,480	6,130	6,965	*	*	48	17	36	16	*	*
70	182,103	169,590	6,620	7,377	*	*	48	19	36	17	*	*
50 & 35	142,210	101,630	5,860	7,572	54	18	36	20	36	13	*	*
50 & 40	147,540	101,610	5,860	7,798	54	18	36	20	36	13	*	*
55 & 40	159,408	119,900	5,910	8,195	*	*	42	18	36	14	*	*
55 & 45	165,981	119,870	5,910	8,425	*	*	42	18	36	14	*	*
*: Special Design Foundation Required												

Figure A-33: Foundation size selection table

Summary of standard design for Texas:

Structures as pedestal pole, mast arm, strain pole, among others which include a traffic signal pole in its structure. For this case of structures, the foundation proposed also correspond to DRILLED SHAFT. It have been defined five types of drilled shafts; 24-A, 30-A, 36-A, 36-B and 40-A. The geometries, design loads and embedded drilled shaft for each type is define in the plan TS-FD-12. The figures distribution of the plan TS-FD-12 will be shown in Figure A-34. Where the highlighted squares represents:

Blue – All the information related with drilled shafts.

Green – De available drilled shaft depths.

Red – The number of Texas penetrometer blows per feet.

Purple – The foundation design information

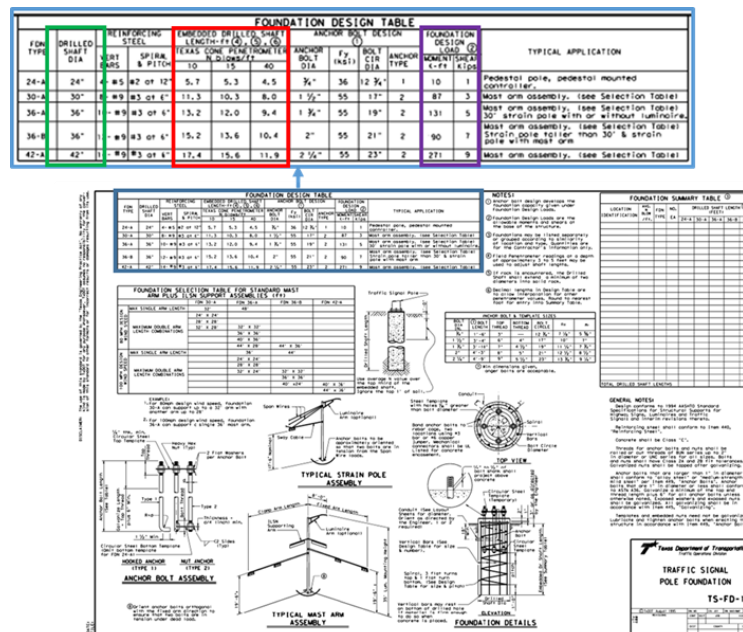


Figure A-34: Texas Plan TS-FD-12 Document (TxDOT 2012)

In Figure A-35, the Drilled Shaft selection could be using two methods; (i) an easy method consider the number of blows/ft from the Texas Penetrometer Test, as seen within the red

square. Here, the depth (ft.) for 10, 15 and 20 blows is provided, (ii) in the same plan, TxDOT also offers the design load considering the drilled shaft diameter, for each standard diameter the moment and the torsion are shown within the square purple. ***Note: “In rock is encountered, the Drilled Shaft shall extend a minimum of two diameters into solid rock”.*** Summary of standard design for Washington:

WSDOT been defined eight load cases, which also depends of the sign area supported by the mast arm. The load cases have been named 700, 900, 1350, 1500, 1900, 2300, 2600 and 3000, which corresponds to the product between XY (sign area) and Z (distance from the centerlines of the pole and sign). (WSDOT, 2018).

Once the XYZ value in numeral has been calculated. The foundation design of Mast Arms will be determined with the aspects listed below:

Friction angle; this value should be taken from geotechnical lab tests or could be correlated from the n-value on Standard Penetration Test.

Allowable lateral bearing pressure; this value could be correlated from the n-value on Standard Penetration Test.

Shape of the drilled shaft diameter (round or square) and its length.

Figure A-35 is showing step by step the method to go through the Standard Plan J-26.10-03, as seen in Figure A-36, and select the most precise drilled shaft depth (WSDOT, 2017b).

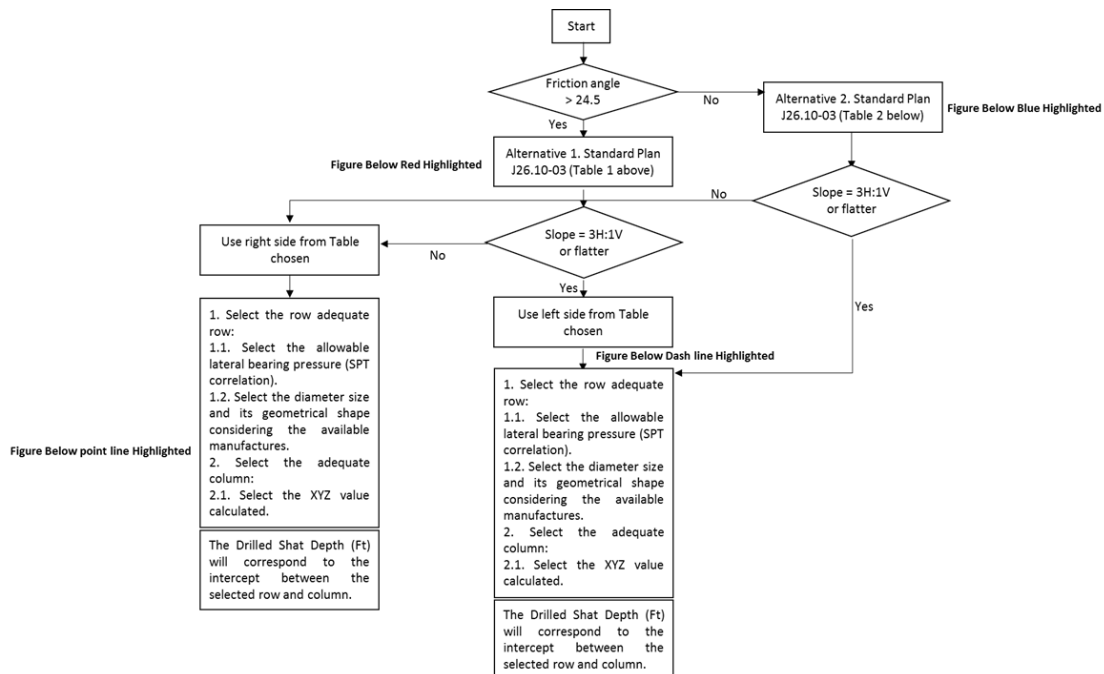
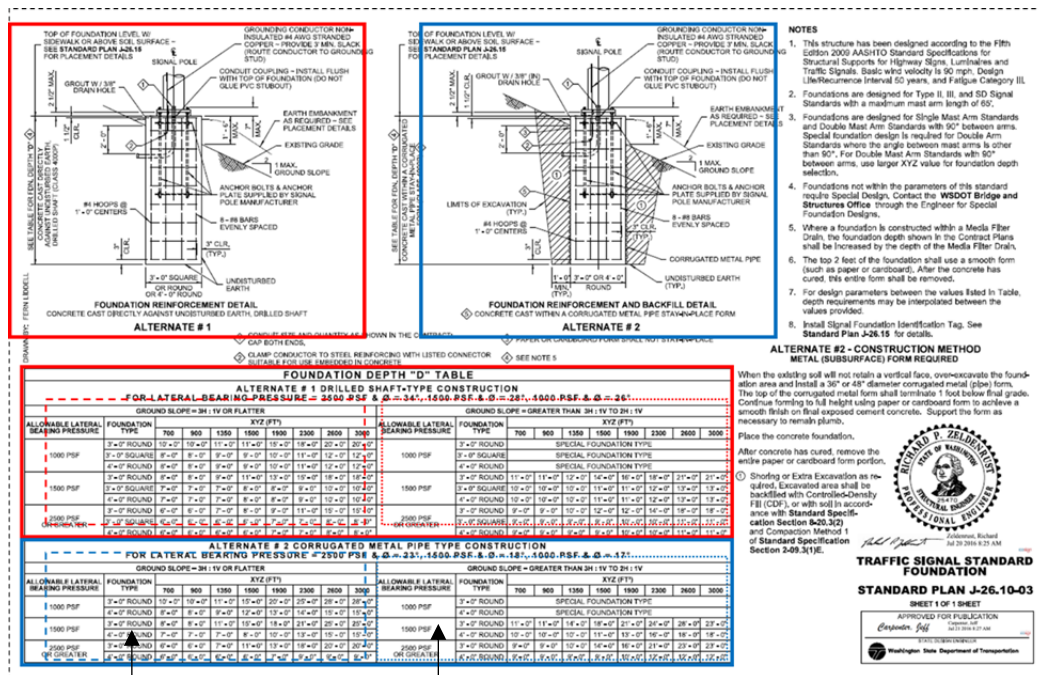


Figure A-35: Washington Plan J-26 Document (WSDOT 2018)



Diameter (ft)

Embedment Depth (ft)

Figure A-36: Washington Plan J-26 Document (WSDOT 2018)

APPENDIX G: COPY OF SURVEY QUESTIONNAIRES RESPONSES FROM COASTAL DOTs

SURVEY QUESTIONNAIRES

NCDOT has an ongoing research project considering alternative foundation designs for traffic signals and highway signs. As part of this project we are summarizing the state of practice for the design of foundation systems of these structures in select states that have similar wind loading and geotechnical conditions as NCDOT. We are compiling information on: design wind speed, wind load considerations, design standards/codes used, foundation systems commonly used by your DOT, design drawings, design aids used by your DOT to select dimensions and design the foundation system, and alternative designs.

1. What are the main structure types used for supporting Traffic Signals and Highway Signs in your state?
2. Please list all of the standard and alternative foundation systems used by your DOT to support highway and traffic signal structures in coastal regions of your state (e.g., drilled shafts, driven piles, shallow foundations, drilled shafts with wing walls, others)?
 - a. Standard:
 - b. Alternative:
3. What separates the use/justification of standard and alternate design systems? Is there an exceptions process required to use an alternate design? If so, what is it?
4. For design of foundation systems of traffic and highway signs, what are the design wind speed ranges typically used? Maximums? What is the basis (design code and edition) for these design wind speeds (e.g., AASHTO or ASCE code, etc.)? What analysis programs are being utilized (if any)?
5. What are the typical mast arm length ranges and maximums allowed?
6. Who has design responsibility for traffic signal and/or sign foundations? State DOT, Private Design Firm, Both?

7. Are there any FHWA requirements/directives on the use of the standard or alternative design systems?
8. In terms of geotechnical subsurface investigations (studies) for the foundation design of these structures, what is the usual scope of the field geotechnical exploration (e.g., number of boreholes, types of field tests required, soil tests performed, etc.)?
9. When the selected foundation system corresponds to a drilled shaft, what design methods or procedures are used to design against lateral, bending, and torsion loading associated to the wind
10. loads acting on the structure (e.g., please indicate methods used or a DOT report or design drawings)?
11. Does the design method listed in Question 5 include lateral loading and bending coupled with the torsion, or is torsion considered separately in the foundation design?
12. What issues does each foundation design present in terms of constructability challenges? What are the installation procedures for each design?
13. Please indicate any other information or comments you consider useful for the scope of this research project involving foundation under lateral, bending and torsion loading in coastal regions: Should we ask the states to discuss what soil conditions exist in their coastal regions? Any Water Table Effects? Any seismic effects?
14. Does your state have a typical/standard cost projections for any of your design alternatives? If so, please list them for each foundation type.
15. Who owns and maintains the signals/signs?

Florida

1. What is the main structure used for supporting both Traffic Signals and Highway Signs?

Cantilever sign YES

Cantilever Sign – Yes

Monotube Sign – Yes

Monotube Signal – Very Rare/No

Mast Arm – Yes

Strain Pole – Yes

Span Truss

2. What are the most commonly used foundation systems used by your DOT to support these highway and traffic signal structures when in coastal regions of your state (e.g., drilled shafts, driven piles, shallow foundations, drilled shafts with wing walls, others) ?

Drilled Shafts

3. For design of foundation systems of traffic and highway signs, what is the basic wind speed(s) is typically used? What is the basis for these design wind speeds (e.g., AASHTO or ASCE code, etc)?

170/150/130- AASHTO LRFD LTS Design Specification

4. In terms of geotechnical studies for the foundation design of these structures, what is the usual scope of the field geotechnical exploration (e.g., number of boreholes, types of field tests required, soil tests performed,etc)?

One SPT Boring to 25 ft in soil or 10 ft in competent rock with 15 ft minimum total boring depth

5. When the selected foundation system corresponds to a drilled shaft, what design methods or procedures are used to design against lateral, bending, and torsion loading associated to the wind loads acting on the structure (e.g., please indicate methods used or a DOT report or design drawings)?

FDOT Sign & Signal Support

Programs See: <http://www.fdot.gov/structures/ProgLib.shtm>

6. Does the design method listed in Question 5 include lateral loading and bending coupled with the torsion, or is torsion considered separately in the foundation design?

Separately

7. Please indicate any other information or comments you consider useful for the scope of this research project involving foundation under lateral, bending and torsion loading in coastal regions:

Unless the foundation is in a high embankment fill, the Design Groundwater Level is always at the ground surface; the Design Windspeed most frequently occurs following 3 to 4 days of continuous heavy rainfall resulting in temporary localized flooding

Massachusetts:

1. What is the main structure used for supporting both Traffic Signals and Highway Signs?

Cantilever, mast arm, strain pole.

2. What are the most commonly used foundation systems used by your DOT to support these highway and traffic signal structures when in coastal regions of your state (e.g., drilled shafts, driven piles, shallow foundations, drilled shafts with wing walls, others) ?

Drilled shafts or spread footings

3. For design of foundation systems of traffic and highway signs, what is the basic wind speed(s) is typically used? What is the basis for these design wind speeds (e.g., AASHTO or ASCE code, etc)?

Please refer to standards, but I think 130 MPH coastal and 110 inland

4. In terms of geotechnical studies for the foundation design of these structures, what is the usual scope of the field geotechnical exploration (e.g., number of boreholes, types of field tests required, soil tests performed, etc)?

One boring per foundation is recommended per the engineering directive.

5. When the selected foundation system corresponds to a drilled shaft, what design methods or procedures are used to design against lateral, bending, and torsion loading associated to the wind loads acting on the structure (e.g., please indicate methods used or a DOT report or design drawings)?

Please refer to standards for reference documents used to develop the standards.

6. Does the design method listed in Question 5 include lateral loading and bending coupled with the torsion, or is torsion considered separately in the foundation design?

For foundation embedment, it appears the embedment depth was based upon the larger of either of the cases mentioned

Virginia:

1. What is the main structure used for supporting both Traffic Signals and Highway Signs?

Traffic Signals – Mast Arms and Strain Poles - Highway Signs – Cantilever and Span

2. What are the most commonly used foundation systems used by your DOT to support these highway and traffic signal structures when in coastal regions of your state (e.g., drilled shafts, driven piles, shallow foundations, drilled shafts with wing walls, others) ?

Drilled Shafts. We used to have a foundation that consisted on drilled shaft with “wings” for torsional resistance, but we no longer use the wings.

3. For design of foundation systems of traffic and highway signs, what is the basic wind speed(s) is typically used? What is the basis for these design wind speeds (e.g., AASHTO or ASCE code, etc)?

90 MPH (AASHTO Standard Specifications for Structural Supports for Highway Signs, Luminaires, and Traffic Signals, 6th Edition (LTS-6), 2013 with 2015 interims)

4. In terms of geotechnical studies for the foundation design of these structures, what is the usual scope of the field geotechnical exploration (e.g., number of boreholes, types of field tests required, soil tests performed,etc)?

We require one boring (with Standard Penetration Testing) at each pole foundation. The testing general consists of simple indices tests (gradations, Atterberg limits and moisture contents).

5. When the selected foundation system corresponds to a drilled shaft, what design methods or procedures are used to design against lateral, bending, and torsion loading associated to the wind loads acting on the structure (e.g., please indicate methods used or a DOT report or design drawings)?

We currently allow the Broms’ method to determine lateral capacity; however, we are getting ready to revise our procedure to only allow Broms’ for preliminary calculations.

We state COM624P, or any commercially available software, can be used for lateral/bending calculations. Most of our consultant designers use L-PILE.

6. Does the design method listed in Question 9 include lateral loading and bending coupled with the torsion, or is torsion considered separately in the foundation design?

This is a good question. One of the changes we are considering is to add the following sentence, “Concurrent overturning and torsional forces reduce a shaft’s overturning resistance. To account for this effect, the lateral loads should not be reduced by the allowable overstress when analyzing the required shaft length and deflections for overturning.”

7. Please indicate any other information or comments you consider useful for the scope of this research project involving foundation under lateral, bending and torsion lading in coastal regions:

It’s interesting that this research is being performed, because as I mentioned, we in the process of revising our practice (IIM-S&B-90.2) in this area. My former boss (Ashton Lawler) retired, and came back to work with us on a part-time basis. One of his primary duties over the last couple of months has been to complete this revision. I will copy Ashton on this response, in case he has anything he’d like to add. I will also attached IIM-S&B-90.2.

South Carolina:

1. What is the main structure used for supporting both Traffic Signals and Highway Signs?

We use all but monotube

2. What are the most commonly used foundation systems used by your DOT to support these highway and traffic signal structures when in coastal regions of your state (e.g., drilled shafts, driven piles, shallow foundations, drilled shafts with wing walls, others) ?

Shallow foundations, drilled shafts

3. For design of foundation systems of traffic and highway signs, what is the basic wind speed(s) is typically used? What is the basis for these design wind speeds (e.g., AASHTO or ASCE code, etc)?

AASHTO specs for all

4. In terms of geotechnical studies for the foundation design of these structures, what is the usual scope of the field geotechnical exploration (e.g., number of boreholes, types of field tests required, soil tests performed,etc)?

Typically one boring with SPT testing

5. When the selected foundation system corresponds to a drilled shaft, what design methods or procedures are used to design against lateral, bending, and torsion loading associated to the wind loads acting on the structure (e.g., please indicate methods used or a DOT report or design drawings)?

AASHTO methods

6. Does the design method listed in Question 5 include lateral loading and bending coupled with the torsion, or is torsion considered separately in the foundation design?

Not sure- whatever AAHTO requires

7. Please indicate any other information or comments you consider useful for the scope of this research project involving foundation under lateral, bending and torsion lading in coastal regions:

Our Traffic office does all of these foundations through Contractor Design-Build procurement, specifying the use of AASHTO design specs.

Alabama:

1. What is the main structure used for supporting both Traffic Signals and Highway Signs?

Many of our signs are supported by cantilever poles. In the past we used almost exclusively strain poles but now use almost exclusively mast arms. We have not to my knowledge used either of the monotube style structures.

2. What are the most commonly used foundation systems used by your DOT to support these highway and traffic signal structures when in coastal regions of your state (e.g., drilled shafts, driven piles, shallow foundations, drilled shafts with wing walls, others) ?

We use almost exclusively the drilled shaft for our foundations. Some units have been required to have wing walls attached to the drilled shafts, but we are looking at reevaluating the factor of safety used in our design to eliminate the use of the wings for our pole foundations.

3. For design of foundation systems of traffic and highway signs, what is the basic wind speed(s) is typically used? What is the basis for these design wind speeds (e.g., AASHTO or ASCE code, etc)? We use the AASHTO code with, in state modifications, I think. The wind speed varies for different parts of the state.

We use the AASHTO code with, in state modifications, I think. The wind speed varies for different parts of the state.

4. In terms of geotechnical studies for the foundation design of these structures, what is the usual scope of the field geotechnical exploration (e.g., number of boreholes, types of field tests required, soil tests performed,etc)?

Typically we take borings for each pole location, unless there are a lot of poles in a close area and the geology is such that we can extrapolate information. There is also the issue of utility conflicts which requires offset or elimination of some borings. The borings consist of AASHTO T206 borings. Laboratory soil testing is typically not performed for these structures at this time.

5. When the selected foundation system corresponds to a drilled shaft, what design methods or procedures are used to design against lateral, bending, and torsion loading associated to the wind loads acting on the structure (e.g., please indicate methods used or a DOT report or design drawings)?

The lateral load characteristics of the drilled shaft is modeled using LPile, using parameters assigned by our in house staff. The torsion loading is checked by our consultants, so they will have to tell you what they use for this model.

6. Does the design method listed in Question 5 include lateral loading and bending coupled with the torsion, or is torsion considered separately in the foundation design?

I believe the torsion is considered separately but defer to our consultants to confirm how the analysis is performed.

Mississippi:

1. What are the main structure types used for supporting Traffic Signals and Highway Signs in your state?

Shallow Cast-in-Place Concrete Shafts for traffic signals and large guide signs. For smaller signs we use posts (smaller u-channels and smaller square tubes) that are a Direct Drive type – driven into the ground a sufficient length; if larger they are placed on a break-away sign assemblies which are set in concrete.

2. Please list all of the standard and alternative foundation systems used by your DOT to support highway and traffic signal structures in coastal regions of your state (e.g., drilled shafts, driven piles, shallow foundations, drilled shafts with wing walls, others)?

a. Standard:

See above

b. Alternative:

Alternative foundation systems would be evaluated on a case by case basis.

3. What separates the use/justification of standard and alternate design systems? Is there an exceptions process required to use an alternate design? If so, what is it?

An alternative design system would be given consideration on its merits by the appropriate MDOT personnel and then either tested and evaluated in a test bed or in the field on a trial basis.

4. For design of foundation systems of traffic and highway signs, what are the design wind speed ranges typically used? Maximums? What is the basis (design code and edition) for these design wind speeds (e.g., AASHTO or ASCE code, etc.)? What analysis programs are being utilized (if any)?

AASHTO wind loading.

5. What are the typical mast arm length ranges and maximums allowed?

Typically, 40 to 60 feet. The longest mast arm we've built is approximately 100 feet long. Longer mast arms on some jobs have recently been necessary due to accommodating the flashing yellow arrow signal head (which is required to be placed in the center of the left turn lane) where used on certain 4-lane divided highways with offset left turn lanes and where it's desired to keep the signal pole out of the median. Due to their length, these arms were required to be straight arms where otherwise it has been MDOT's preference to use upswept mast arms.

6. Who has design responsibility for traffic signal and/or sign foundations? State DOT, Private Design Firm, Both?

State DOT if constructed by maintenance forces or designed in-house and built by a contractor; private design firm if they prepare the plans.

7. Are there any FHWA requirements/directives on the use of the standard or alternative design systems?

None other than meeting the required design guidelines.

8. In terms of geotechnical subsurface investigations (studies) for the foundation design of these structures, what is the usual scope of the field geotechnical exploration (e.g., number of boreholes, types of field tests required, soil tests performed, etc.)?

This will depend on several factors including the type, length, complexity, and scope of the project and whether it's known there are expansive clays in the profile and whether the profile is known to be fairly consistent or varied.

9. When the selected foundation system corresponds to a drilled shaft, what design methods or procedures are used to design against lateral, bending, and torsion loading associated to the wind loads acting on the structure (e.g., please indicate methods used or a DOT report or design drawings)?

AASHTO Bridge Design standards. MDOT has developed a standard detail for the foundations for its guide signs and signals foundation designs.

10. Does the design method listed in Question 5 include lateral loading and bending coupled with the torsion, or is torsion considered separately in the foundation design?

Yes.

11. What issues does each foundation design present in terms of constructability challenges? What are the installation procedures for each design?

Usually, the foundations for smaller structures such as these do not present constructability challenges

12. Please indicate any other information or comments you consider useful for the scope of this research project involving foundation under lateral, bending and torsion loading in coastal regions: Should we ask the states to discuss what soil conditions exist in their coastal regions? Any Water Table Effects? Any seismic effects?

We have experienced a couple signal mast arms that have rotated up to 90 degrees in place during storm events due to saturated soil and high wind loads. In each case the shaft rotated in its place. A solution to this would be to have a lateral reinforced concrete key built near the upper portion of the shaft.

13. Does your state have a typical/standard cost projections for any of your design alternatives? If so, please list them for each foundation type.

Yes, the MDOT Construction Division maintains cost data as bid by the contractors for each pay item and size. It may be possible to obtain this information by contacting the MDOT Construction Division.

14. Who owns and maintains the signals/signs?

MDOT owns all of the signals on state highways. The cities with a population over 20,000 are responsible to maintain the signals on State routes; however, MDOT maintains operational jurisdiction over these signals

Louisiana:

1. What are the main structure types used for supporting Traffic Signals and Highway Signs in your state?

Refer to our Standards...

2. Please list all of the standard and alternative foundation systems used by your DOT to support highway and traffic signal structures in coastal regions of your state (e.g., drilled shafts, driven piles, shallow foundations, drilled shafts with wing walls, others)?

a. Standard: Traffic Signals: Drilled Shafts are the only option. Overhead Traffic Signs: Timber piles are the standard option. Dynamic Message Signs: Timber piles are the standard option. Highmast Lighting: Drilled shafts are the only option.

b. Alternative: Overhead Traffic Signs: Drilled shafts may be used as an alternate.

3. What separates the use/justification of standard and alternate design systems? Is there an exceptions process required to use an alternate design? If so, what is it?

Overhead Traffic Signs: It is up to the Contractor whether they use timber piles or alternatively, drilled shaft option.

Traffic Signals: A special design is required for the longer mast-arms in the weaker soil zones.

4. For design of foundation systems of traffic and highway signs, what are the design wind speed ranges typically used? Maximums? What is the basis (design code and edition) for these design wind speeds (e.g., AASHTO or ASCE code, etc.)? What analysis programs are being utilized (if any)?

Max wind speed = 130 MPH for Dynamic Message Signs (Wind Load Map AASHTO 2001). For Highmast Lighting and Overhead Traffic Signs, Max wind speed = 130 MPH, using (Wind Zone Map for Louisiana).

6. What are the typical mast arm length ranges and maximums allowed?

Single Mast-Arms (55 ft., 60 ft., 65 ft., 70 ft.)

Dual Mast-Arms (50 & 35 ft., 50 & 40 ft., 55 & 40 ft., 55 & 45 ft.)

7. Who has design responsibility for traffic signal and/or sign foundations? State DOT, Private Design Firm, Both?

Either, depends on who is designing the overall project.

8. Are there any FHWA requirements/directives on the use of the standard or alternative design systems?

9. In terms of geotechnical subsurface investigations (studies) for the foundation design of these structures, what is the usual scope of the field geotechnical exploration (e.g., number of boreholes, types of field tests required, soil tests performed, etc.)?

Soil borings/tests are rarely performed for these types of structures. The standards rely on predefined Soil Zone maps for Louisiana for a general guidance of the types of soils in different areas of the state. Sometimes nearby soil borings can be located and used to analyze proposed sign foundations. When necessary, a deep soil boring similar to what is required for deep foundation design, may be taken for special design cases such as, (weak coastal soil zones, long mast-arm lengths, etc.).

10. When the selected foundation system corresponds to a drilled shaft, what design methods or procedures are used to design against lateral, bending, and torsion loading associated to the wind loads acting on the structure (e.g., please indicate methods used or a DOT report or design drawings)?

LRFD

11. Does the design method listed in Question 5 include lateral loading and bending coupled with the torsion, or is torsion considered separately in the foundation design?

We use Ensoft Shaft and LPILE software to design for lateral loading and bending and axial loading. Torsion is considered separately.

12. What issues does each foundation design present in terms of constructability challenges? What are the installation procedures for each design?

All piles are driven into the ground using a pile driving hammer. A drilled shaft alternative is considered when hard driving is expected for installing piles. On the other hand, drilled shafts are preferred in denser soils and structures that have single mounted poles. In soft soils, it can be difficult to install drilled shafts without the use of steel casing.

13. Please indicate any other information or comments you consider useful for the scope of this research project involving foundation under lateral, bending and torsion loading in coastal regions: Should we ask the states to discuss what soil conditions exist in their coastal regions? Any Water Table Effects? Any seismic effects?

Many of your questions can be answered by reading our standard plans.

14. Does your state have a typical/standard cost projections for any of your design alternatives? If so, please list them for each foundation type.

Currently we do not perform cost projections for signs and light foundation alternatives.

15. Who owns and maintains the signals/signs?

I believe all signals/signs constructed by LADOTD are owned by LADOTD.

Texas:

1. What is the main structure used by TxDOT for supporting both Traffic Signals and Highway Signs?

TxDOT has used all of these structure types. Cantilever signs are the most common structures used for supporting highway signs. Additionally, overhead sign bridges are used when cantilever signs cannot provide the desired arm length. Mast arms are the main structure used for traffic signals.

2. What are the most commonly used foundation systems used by TxDOT to support these highway and traffic signal structures when in coastal regions of your state (e.g., drilled shafts, driven piles, shallow foundations, drilled shafts with wing walls, others) ?

Drilled shafts are the most common foundation system.

3. For design of foundation systems of traffic and highway signs, what is the basic wind speed(s) is typically used?

Designs are based on AASHTO 1994 Standard Specifications for Structural Supports for Highway Signs, Luminaires, and Traffic Signals and Interim Revisions thereto. Designs are based on either 70, 80, 90, or 100 MPH wind speed as defined by the 50 year mean recurrence interval of fastest mile wind velocity at 33 feet height.

4. In terms of requirements for geotechnical studies for the foundation design of these structures, what is the usual scope of the field geotechnical exploration (e.g., number of boreholes, types of field tests required, soil tests performed, etc)?

Soil borings are performed to classify soil type and perform Texas Cone Penetrometer (blow count) testing. Soil classification (cohesionless vs cohesive) is used in conjunction with blow counts on standard foundation embedment charts to determine embedment depth. Boreholes for overhead sign structures are generally 30 to 50 feet in depth and are typically located within 100 feet of the structure.

5. When the selected foundation system corresponds to a drilled shaft, what design methods or procedures are used to design against lateral, bending, and torsion

loading associated to the wind loads acting on the structure (e.g., please indicate methods used or a DOT report or design drawings)?

Design charts with design guidance are provided on standards to aid in the design of the foundation depths for drilled shafts supporting overhead sign structures. This guidance includes both consideration of bending moment and torsional forces. The approach was developed in 1984. The design charts go back to 1984 and are based on Brom's method for moment resistance while torsional resistance is based on soil shear resistance along the side of the shafts. In addition to using the design guidance on the standards, TxDOT also utilizes soil-structure interaction programs (such as LPILE) to determine the appropriate depth of drilled shaft for the required lateral loading condition.

6. Does the design method listed in Question 5 include lateral loading and bending coupled with the torsion, or is torsion considered separately in the foundation design?

Lateral loading and torsion are included on the foundation embedment selection charts. The foundation design is based on evaluation of torsion and bending independently. The design process outlined on our standards specifies that the longer of the length required for bending or torsion be used for the embedment length.

7. Please indicate any other information or comments you consider useful for the scope of this research project involving foundation under lateral, bending and torsion loading in coastal regions:

TxDOT's standards for overhead sign structures are available for download from the TxDOT website:

<https://www.dot.state.tx.us/insdtdot/orgchart/cmd/cserve/standard/toc.htm#CANTILEVEROVERHEADSIGNSSUPPORTSTANDARDS>

Oregon:

1. What is the main structure used for supporting both Traffic Signals and Highway Signs?

Monotube and Mast arm

2. What are the most commonly used foundation systems used by your DOT to support these highway and traffic signal structures when in coastal regions of your state (e.g., drilled shafts, driven piles, shallow foundations, drilled shafts with wing walls, others) ?

Drilled shafts and Spread footings (Pad and Pedestal)

3. For design of foundation systems of traffic and highway signs, what is the basic wind speed(s) is typically used? What is the basis for these design wind speeds (e.g., AASHTO or ASCE code, etc)?

AASHTO 6th Ed. ASD 110 MPH

AASHTO 1st Ed. LRFD 145 MPH Extreme and 91 MPH Service

Oregon Structural Specialty Code State specific wind maps

4. In terms of geotechnical studies for the foundation design of these structures, what is the usual scope of the field geotechnical exploration (e.g., number of boreholes, types of field tests required, soil tests performed,etc)?

Signal poles – Foundations within 75' with uniform soil have one boring with SPT.

Sign Cantilevers and Truss Bridges – One boring at each foundation with SPT.

5. When the selected foundation system corresponds to a drilled shaft, what design methods or procedures are used to design against lateral, bending, and torsion loading associated to the wind loads acting on the structure (e.g., please indicate methods used or a DOT report or design drawings)?

LPile used for overturning moment

Skin friction used for torsion

6. Does the design method listed in Question 5 include lateral loading and bending coupled with the torsion, or is torsion considered separately in the foundation design?

Torsion is considered separately

Washington:

1. What is the main structure used by WSDOT for supporting both Traffic Signals and Highway Signs?

For support of traffic signals, WSDOT uses pole structures with cantilevered mast arms.

Overhead support of highway signs is generally accomplished with sign bridges or cantilever sign structures.

2. What are the most commonly used foundation systems used by your DOT to support these highway and traffic signal structures when in coastal regions of your state (e.g., drilled shafts, driven piles, shallow foundations, drilled shafts with wing walls, others) ?

Signal poles and overhead sign structures are most often supported on drilled shaft foundations.

3. For design of foundation systems of traffic and highway signs, what is the basic wind speed(s) is typically used?

We use the LRFD Specifications for Structural Supports for Highway Signs, Luminaires, and Traffic Signals, First Edition 2015, and Amendments. (AASHTO)

4. What is the basis for these design wind speeds (e.g., AASHTO or ASCE code, etc)?

Basic Wind Speed is 115 MPH, for a 1700 year MRI, per Fig 3.8-2a in the Code.

5. In terms of requirements for geotechnical studies for the foundation design of these structures, what is the usual scope of the field geotechnical exploration (e.g., number of boreholes, types of field tests required, soil tests performed, etc)?

Ideally, we would have a borehole or test pit for each location, but this is rarely the case in practice. If the Geotechs see some consistency in subsurface soil profiles and properties, then we may generate foundation designs based on much more widely-spaced test pits or bore holes, laid out to cover a longer length of highway. We generally ask for soil unit weight, soil phi angles, and allowable lateral bearing pressures (used to reference

some of our older Standard Plan solutions which are based on earlier WSD versions of the Code). The Geotechs will also identify any potential complications anticipated for drilled shaft foundations (high water table, artesian conditions, caving soils, obstructions, rock, etc).5. When the selected foundation system corresponds to a drilled shaft, what design methods or procedures are used to design against lateral, bending, and torsion loading associated to the wind loads acting on the structure (e.g., please indicate methods used or a DOT report or design drawings)?

For drilled shaft foundation design, we use the Broms Approximate Method, described in the Code Commentary 13.6.1.1. Torsional Capacities are not covered in the Code. Please refer to the WSDOT Bridge Design Manual 10.1.5C for torsional considerations.

6. Does the design method listed in Question 5 include lateral loading and bending coupled with the torsion, or is torsion considered separately in the foundation design?

The method described in the WSDOT BDM takes lateral loading into account for the torsional design.

7. Please indicate any other information or comments you consider useful for the scope of this research project involving foundation under lateral, bending and torsion lading in coastal regions:

Please refer to WSDOT Standard Plan J-26.10 for typical Signal Pole Foundation

APPENDIX H: RESULTS OF PILE INTEGRITY TESTS

SITE-1

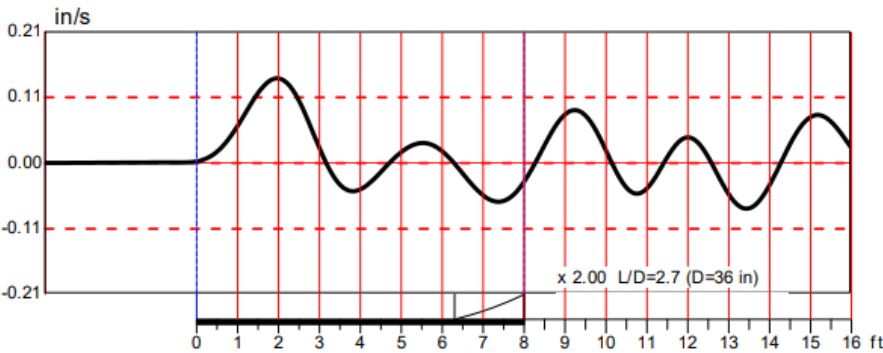


Figure A-37: Test 1 at Site-1

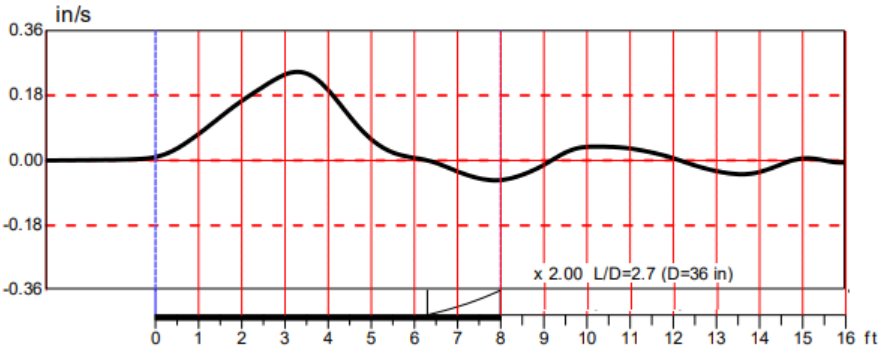


Figure A-38: Test 2 at Site-1

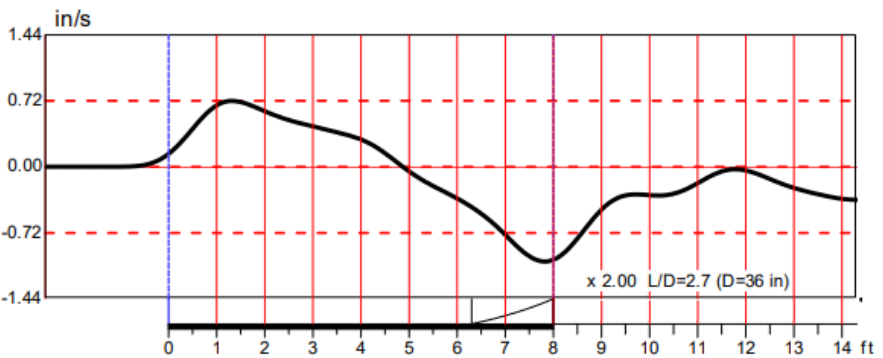


Figure A-39: Test 3 at Site-1

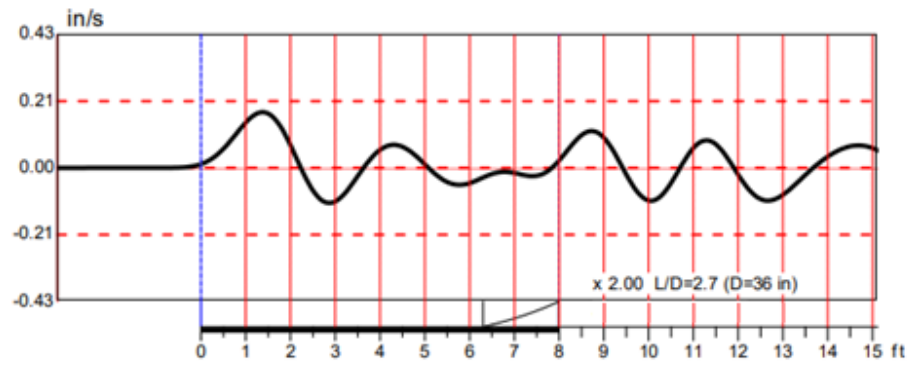


Figure A-40: Test 4 at Site-1

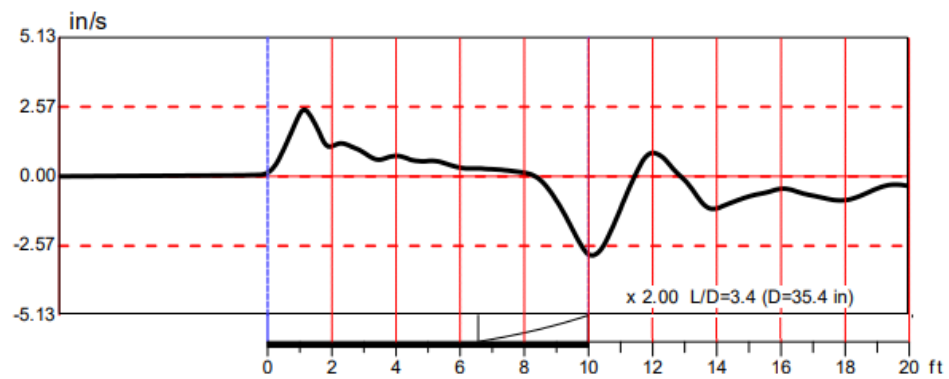


Figure A-41: Test 5 at Site-1

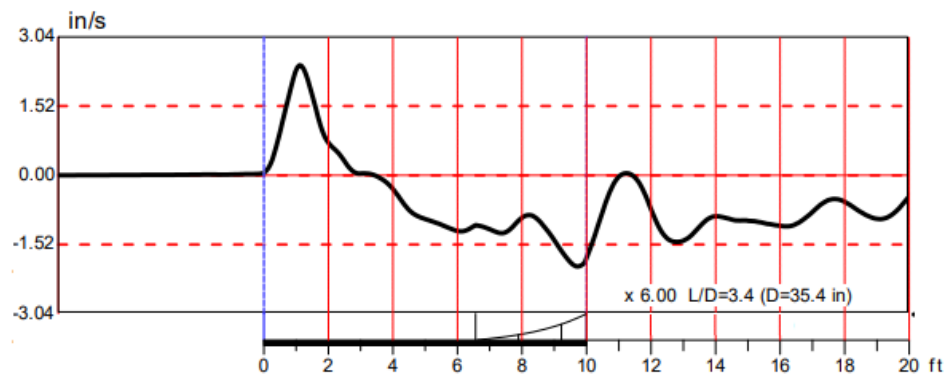


Figure A-42: Test 6 at Site-1

SITE-2

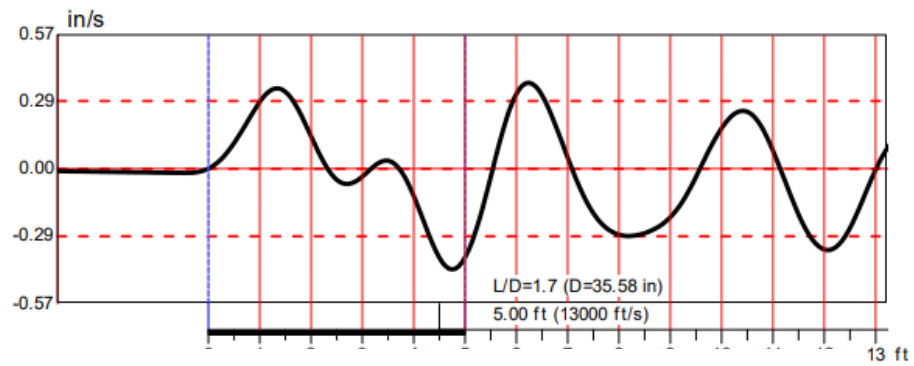


Figure A-43: Test 1 at Site-2

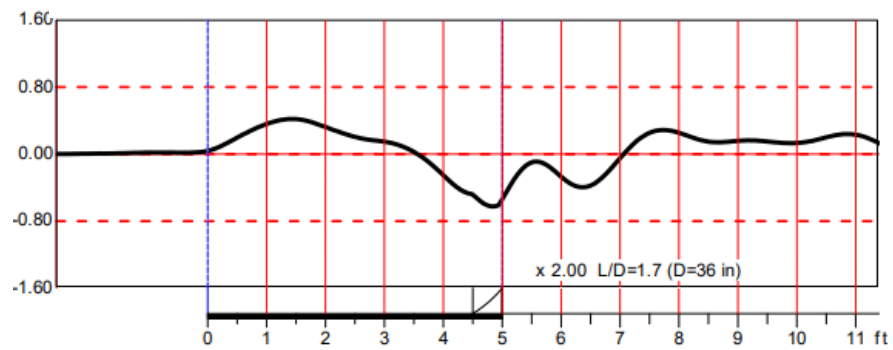


Figure A-44: Test 2 at Site-2

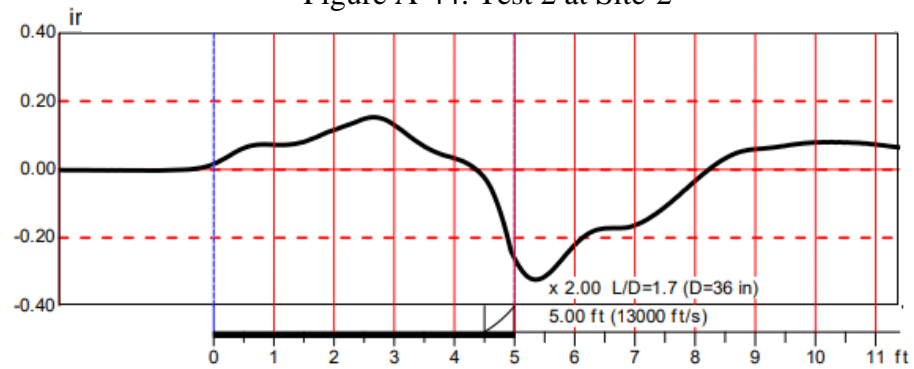


Figure A-45: Test 3 at Site-2

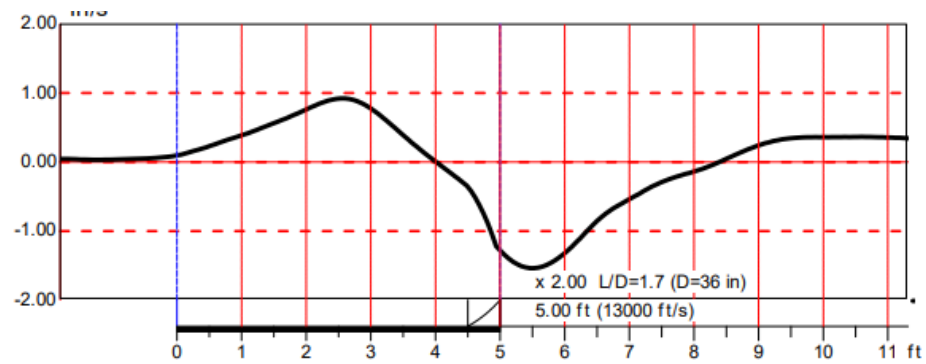


Figure A-46: Test 4 at Site-2

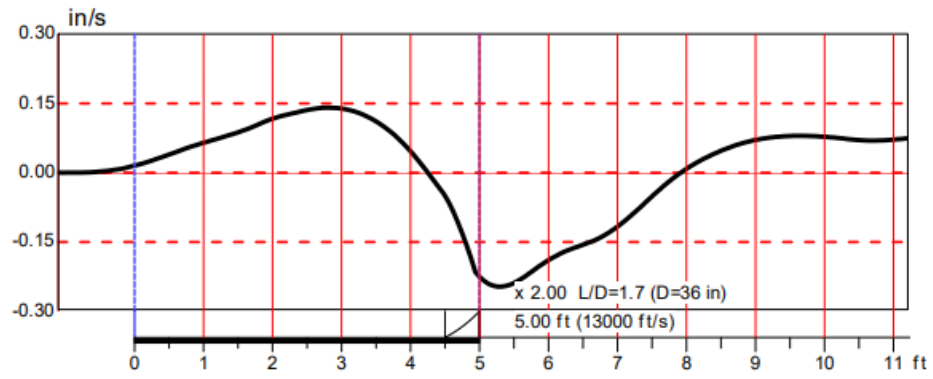


Figure A-47: Test 5 at Site-2

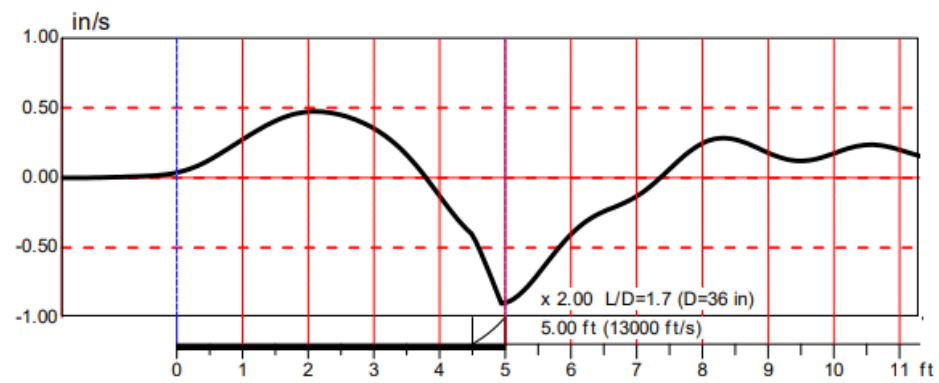


Figure A-48: Test 6 at Site-2